THE ASTROPHYSICAL JOURNAL

AN INTERNATIONAL REVIEW OF SPECTROSCOPY AND ASTRONOMICAL PHYSICS

VOLUME 97 MARCH 1943 NUMBER 2

HENRY GORDON GALE

1874–1942

Professor Henry G. Gale, who for many years had been chairman of the department of physics at the University of Chicago, died on November 16, 1942. He was born at Aurora, Illinois, on September 12, 1874, and registered at the University of Chicago with its first class in the autumn of 1892. The last fifty years of his life were, therefore, practically coincident with that first half-century of achievement which the University recently celebrated—the half-century which has seen the face of the world changed. Many citizens of Chicago have lived here for more than that length of time, but rarely has any one of them been an active participant in the intellectual life of the city for such a period as was Professor Gale.

Among the American colleges of outstanding quality must always be reckoned the one at Middlebury, Vermont. It was here, in the midst of our Civil War, that the father of our subject, Eli Holbrook Gale, graduated in 1862 and at once proceeded to the University of Pennsylvania, where he took his medical degree in 1865. He had enlisted in the 186th Pennsylvania volunteers and was assistant surgeon at the Provost Barracks in Philadelphia. A little later Dr. Gale came to Illinois and settled at Aurora, where, up to the time of his death in 1912, he was known as an able physician, a man of quick sympathy, with a fine sense of humor and a taste for the classics. It was here that he married a vigorous young woman, Miss Adelaide Parker, the mother of our Professor Gale, who was the youngest in a family of two sisters and three brothers.

When the boy was only six weeks old he had the misfortune to lose his best friend—his mother. The result was that his early boyhood was spent on the farm with his maternal grandparents; and, in this kindly atmosphere, he soon learned to know and to love all the animals, plants, trees, fish, and fowl of the countryside in the Mississippi Valley—an interest which remained keen throughout his later years and always manifested itself during his camping and fishing trips in the north woods.

Gale's mother had four brothers in the war between the states. One can imagine, therefore, how eagerly the lad listened to the stories of "the late unpleasantness" from his four uncles and from his father. The devotion to his country thus early acquired never deserted him.

In 1890 he graduated from the Union High School at Lacon, Illinois, where the family had recently moved, and then completed his preparation for college by graduation at the East Aurora High School in 1892. At the University of Chicago this finely proportioned and strikingly handsome young man was a "charter member" along with that outstanding group of productive scholars whom Dr. Harper had called to his staff from twelve or

fifteen leading institutions of the world. These were the days when Cobb Hall was the only building on the campus, and the physical laboratory was housed in a small brick residence just north of Marshall Field. Mr. Stagg deeply appreciated Gale's skill and sense of responsibility as a football player. A little later his election to the captaincy of the team came as a vote of confidence. But of all undergraduate events, none was so full of significance as a chance meeting in Sophomore year with a talented young girl who, after spending her Freshman year at Wellesley, had returned to the West for the remaining three years at the University of Chicago. The home of this young woman, Agnes S. Cook, was at Normal, Illinois. She was the daughter of Dr. John W. Cook, a pioneer in American education. Their friendship, sealed by marriage in 1901, continued a high privilege for both during more than forty years and was broken only by death. Their daughter Beatrice (now Mrs. Kimball Valentine) and her family live only a few steps away from the parental home.

Gale's professional career began in 1899 when he had completed three years of graduate study and had accepted appointment on the staff of the Ryerson Laboratory. In his Doctor's thesis he employed the interferometer to determine the refractive index of air as a function of its density and established the law of Gladstone and Dale ($[n - 1]/d$ = constant) as accurate to one part in a thousand for pressures all the way up to nineteen atmospheres. The cleverly devised gauge which Gale invented for this experiment made the readings directly proportional not to the pressures but to the densities of the air. This device alone would have made the thesis notable.

It was in February of 1906 that Gale first went to Mount Wilson. This visit was at the request of George E. Hale, who was then seeking for an explanation of astrophysical results by the aid of data gathered under controlled conditions in the physical laboratory.

Dr. Walter S. Adams writes, in speaking of Gale's visit:

> It is difficult to realize, at the present, when the theory of ionization and the term analysis of spectra have given us so clear a picture of the origin and behaviour of spectral lines, that thirty years ago almost nothing was known regarding the differentiation of lines according to physical conditions. It is true that "enhanced" lines, which are lines stronger in the electric spark than in the arc, were recognized as a distinct class, but the normal arc lines were classed together and were supposed to behave essentially alike. Accordingly when Gale came to Mt. Wilson his problem was to learn whether the spectroscopic laboratory could devise conditions which would affect lines in the same way in which they are affected in sunspots. The first and most natural hypothesis was that difference of temperature might be the controlling factor since there was considerable reason to believe that spots are considerably cooler than the general solar surface.
>
> Gale used a variety of light sources including a synchronous rotating arc, a direct current arc with widely different currents, but nearly constant difference of potential between the poles, and finally the outer flame and core of a simple arc. All these sources gave definite results of the same type and showed that in passing from higher to lower temperature the spectral lines were affected differently and could be divided into distinct classes according to behavior with temperature. A comparison with sunspot results showed at once that just the lines which were strengthened at low temperatures in the laboratory were strengthened in spots, while unaffected lines remained unchanged. As a final test the comparison was repeated with a somewhat crude electric furnace and gave identical results. These relatively simple investigations have proved of great value both to astrophysical and physical research and helped to lay the observational basis for the theory of ionization. Similarly the temperature classification of spectral lines has proved to be one of the most valuable tools which the physicist can use in undertaking the analysis, according to energy level, of complex spectra of most of the elements. In much of the work which was undertaken Hale and Adams collaborated with Gale, but chiefly on the astrophysical side.

Some six years later Gale and Adams collaborated on the displacements produced in spectral lines by pressure applied at the source. Their report (*Ap. J.*, **35**, 10, 1912) contains a large amount of accurate experimental detail, confirming and extending earlier work by Humphreys, Duffield, and Rossi. Since this work antedated by one year the

discovery of the "pole effect" by F. Goos, it is interesting to note that Gale and Adams had already encountered this phenomenon when they surrounded their arc with an atmosphere of hydrogen and found that the arc worked badly, so that they had to bring the poles closer together and were thus introducing the exact conditions required for the pole effect. They describe the result by saying that a hydrogen atmosphere "affects not only the intensities but the displacements of the enhanced lines in the same way as does a change from arc to spark."

It was about this same time that Gale and Adams published a series of important papers dealing with the effect of pressure upon the character and displacement of lines in several of the more important elements. Dr. Adams writes:

> The fact was well known that reduction of pressure around a light source in the laboratory favored the appearance of the enhanced lines and Gale offered the suggestion that their prominence in the chromosphere might be due to the very low density of the gases at this high level in the sun's atmosphere. Later the theory of ionization fully bore out this suggestion and conspicuous enhanced lines in any stellar spectrum are now recognized as a criterion and measure of low density.

A little later a group of important experimental results were published by Gale and Whitney describing the change of wave length which takes place in passing from the positive to the negative pole through the middle of the arc. The explanation of the pole effect, as well as of the pressure effect, was still a matter of speculation. In commenting later upon various possible causes, such as temperature, vapor density, modification of dielectric constant, magnetic influence of neighboring atoms, and potential gradients, Gale closes with the following characteristic remark:

> Certainly I have no favorite theory to defend and shall be quite as pleased if the final outcome points to vapor density as I shall if it points to any other factor; but I doubt if the explanation will be a simple one or the same for all lines. In the final solution of these questions I am sure the interesting and valuable contributions of Dr. Royds will have great weight.

The two well-known experiments, by which Michelson and Gale established the fact that "the tides in the actual earth are 0.310 of what they would be if the earth were fluid," were performed on the grounds of the Yerkes Observatory. All the observations, the photographic records, and the meticulous adjustments were made by Professor Gale.

Another experiment in which Gale also played a large role was that in which he and Michelson divided a beam of light into two parts and sent one of them around a city block in the clockwise sense and the other in the opposite sense. When these two beams, traveling through a 12-inch pipe from which the air had been removed, reunited at the original mirror, the interference fringes showed that the counterclockwise beam (that is, the one which had made the circuit in the same sense in which the earth is rotating) had been slightly retarded over the other. The amount of the retardation was very nearly a quarter of a fringe. This, as Gale playfully and truthfully remarked, demonstrated that the earth is rotating about an axis which passes through the town of Clearing, Illinois. In his memorial address, Professor A. J. Dempster commented upon this result as follows: "This added one more phenomenon to the comparatively few critical ones, such as the aberration of light from the stars, the Doppler effect, the aether-drift experiment and the bending of light rays passing the sun, for which our theories of light in moving media must account." Here again the laborious and difficult observations were practically all made by Professor Gale, assisted by the skilful Mr. Fred Pearson.

Colleagues always found Gale such good company that they were delighted to work with him. The studies which he and Dr. Monk made upon that aggressive element, fluorine, and those upon ionized lithium made by him and Dr. Hoag illustrate this genial laboratory companionship.

Among the last and best of Gale's researches must be reckoned the improvements

which he added to the engine for ruling diffraction gratings. This instrument, first brought to a marvelous degree of perfection by H. A. Rowland, in 1882, received various refinements at the hands of Michelson immediately following Rowland's death in 1901. Then, shortly after Michelson's death in 1931, Gale took up the succession and improved the engine by the addition of a "work screw" to drive the heavy carriage, while a "precision screw" of the same nominal pitch drives a superposed lighter carriage upon which rests the speculum plate about to be ruled. The irregularity of friction between nut and screw Gale eliminated by immersing both of them in an oil bath. In all this work he acknowledges with characteristic grace the help of three skilful assistants, Messrs. Pearson, O'Donnell, and Getzholz.

No sketch of Henry Gale can be so brief as not to mention the *First Course in Physics* which he and Dr. Millikan wrote, first as a text for high schools and afterward enlarged for use in colleges. Here they accomplish the rare and difficult feat of maintaining a high standard of scientific accuracy while keeping the subject matter really entertaining.

The company and counsel of such a man was, of course, constantly in demand. Thus we find him, of course, an early member of the Quadrangle Club and a most acceptable member of that informal group of research men known as the Chaos Club. His response to the call of military duty in 1917 was prompt and generous. As captain of infantry he was sent from Fort Sheridan to Camp Grant, where he assisted in organizing the Third Officers' Training Camp. After the completion of this work, he was transferred from the infantry to the signal corps, with the rank of major, and was ordered overseas. In France he was placed in charge of a special service division at Tours and, at the end of the war, having been promoted to the rank of lieutenant colonel, he was cited by General Pershing for "especially meritorious and conspicuous service" and received the decoration of the Legion of Honor from the French government. The gospel of fresh air and sunshine he practiced with the Lake Zurich Golf Club; also with those genial spirits who call themselves the Wayfarers Club. The governing board of the Crerar Library obtained his advice conveniently by electing him to membership. The *Astrophysical Journal* enjoyed his editorial help for well-nigh a third of a century. The Physics Club of Chicago chose him for their president at their very first meeting, in 1931, and at their decennial meeting, in 1941, elected him to honorary life-membership. Of all Professor Gale's many friends, none will hold his memory in more grateful remembrance than that large group whom he assisted in the laboratory: suggesting research problems to some, solving experimental difficulties for others, finding appropriate appointments for those who had just completed their graduate study. His unfailing interest in the University of Chicago and the deep indebtedness of that institution to him were admirably set forth by his colleagues at the memorial service held in Bond Chapel on November 18, two days after his death.

HENRY CREW

Arthur B. Wyse.

UNIV. OF MICH.

ARTHUR BAMBRIDGE WYSE

1909–1942

On the night of June 8, 1942, there occurred a disastrous accident over the Atlantic Ocean, off the New Jersey coast. Two lighter-than-air navy craft collided during an experimental operation in which they were jointly engaged, and the occupants of both vessels, thirteen in number, were, with a single exception, lost. Besides the crews, there were aboard five scientists, all of whom perished; among them was Arthur Bambridge Wyse. In this swift tragedy the Lick Observatory lost a useful and promising member of its staff. Dr. Wyse was at the time under leave of absence from the Observatory in engagement upon technical developments relating to the war.

Dr. Wyse had been a member of the Lick Observatory staff, with the rank of assistant astronomer, since July 1, 1935. He received the degree of Doctor of Philosophy from the University of California in May of the preceding year and in the interim had held minor positions in the Observatory, as noted elsewhere in this account. At times a good deal of routine labor has been required of the younger members of the Observatory staff, but Wyse and his colleagues were encouraged to find their own leads, and in the beginning he followed that opened by a study of eclipsing variable stars, which had constituted his Doctor's thesis. However, he did not fall into the not uncommon error of narrowing his attention to the field of his maiden effort, and it required little persuasion to interest him in undertaking a description of the large store of photographs of the spectra of novae that the Observatory possesses. The material had been gathered by various members of the staff, and, as I happened to have the discussion of it in hand, Mr. Wyse participated first in the capacity of collaborator. However, interest and aptitude on his part and preoccupation with other matters on my own resulted in his assuming the burden of the work, and publication was correctly made over his own name. His principal papers on this subject are the three that form Parts III, IV, and V of Volume XIV, *Publications of the Lick Observatory*. Of these, the first, dealing with the spectrum of Nova Aquilae (1918), is probably the most noteworthy. These papers are primarily descriptive accounts of the several spectra, written in the light of present-day knowledge of spectral structure. No attempt is made in them to provide a mechanistic theory of temporary stars, but the papers give a great amount of information that undoubtedly will, in time, aid in the understanding of these remarkable objects.

In 1938 Professor Ira S. Bowen, of the California Institute of Technology, accepted an invitation to be the Morrison Research Associate at the Lick Observatory for the year 1938–1939. He naturally chose the gaseous nebulae as the subject of his study. His classical researches on the origin of the known nebula lines suggested to him the desirability of searching for fainter radiations that might indicate the presence of elements not then known to exist in the nebulae. As is well known, nova and nebular spectra are closely related, and Professor Bowen was very hospitable to a suggestion that Wyse, who was interested in the former, should participate in the observation of the nebulae. The research was signally successful and not only revealed the presence in these objects of several elements, including iron, which had not been known to exist in them, but indicated the probability that the chemical composition of the gaseous nebulae does not differ greatly from that of the sun and the stars. The very important paper in which these results were announced[1] was issued jointly by Bowen and Wyse, but it seems fair to say that Professor Bowen's generosity in permitting the participation of the younger man should not be allowed to obscure the fact that his was the outstanding contribution.

[1] *Lick Obs. Bull.*, **19**, 1, 1939.

After the conclusion of Bowen's engagement at the Lick Observatory, the observations were continued by Wyse, who reported upon them in his last published paper.[2]

In Wyse's preoccupation with general spectroscopic studies he did not permit his early interest in eclipsing variable stars to lapse, and in 1939 he developed an accurate method for deriving the elements of an eclipsing binary system from photometric observations.[3] This investigation, which is of a mathematical character, followed upon the circumstance that Wyse's colleague, G. E. Kron, had succeeded in improving the technique of stellar photometry to such a degree that the approximate methods then available for calculating the orbit of an eclipsing variable were not sufficiently exact to conserve the excellencies of the new observations. The critical feature of Wyse's discussion is that he introduced the "coefficient of limb darkening" into the equations of condition of a least squares solution, making this quantity, in effect, one of the elements of the system. There was, of course, nothing new in such a procedure; the fact that it had not been attempted before was due to the mathematical complexities that were feared. These were successfully resolved by Wyse, who thus provided a straightforward method for evaluating the coefficient of limb darkening, a quantity which happens to be an important parameter in stellar theory and one which, except in the case of the sun, is not experimentally determinable in any other known way.

Another of Wyse's mathematical studies was upon the distribution of mass in the great spiral nebulae in Andromeda and in Triangulum.[4] The paper in which this investigation is described was authored jointly with N. U. Mayall. Mayall and his associates had found peculiarities in the rotational motions of these two objects that were unexpected and, in fact, at first sight rather bewildering. On the basis of certain simplifying assumptions regarding the structure of these nebulae the authors were able, after an elaborate analysis, to postulate distributions of mass that would cause rotations of the character of those observed. It should be stated that in this collaboration Wyse was the principal contributor to the dynamical part of the paper and Mayall to the observational part.

I think it not without significance that both of the investigations just mentioned had to do with problems encountered by Wyse's colleagues. He seemed always to take as much interest in the work of his friends as in his own, and his command of such mathematical methods as find ready application in the solution of physical problems enabled him to extend timely aid. One is, in fact, impressed quite as much by the breadth of his scientific interests as by the excellence of his technical performance, and there is little doubt that, had his work been permitted to continue, it would have been characterized by still greater diversity. During the last year of his residence at the Observatory he collaborated in the testing of the lens of the Carnegie astrographic telescope, and it was understood at the time that he would eventually devote himself to the use of that instrument. This would have absorbed most of his attention for many years. The work of this telescope has to do with astrometry, a field rather apart from astrophysics, which had theretofore been Wyse's principal concern, and one harbors no doubt that he would have been as successful in the new activity as in the old. His ability to work to advantage in many fields was, I think, to be ascribed to the clarity of his mind and to his quick recognition of fundamental principles. These qualities explain also his faculty for teaching.

The desire and ability to teach are not always encountered in persons possessing aptitude for research, but they were in Mr. Wyse. I was never quite certain which of these employments gave him the greater pleasure, and I doubt whether he himself was really sure. He frequently expressed regret that at the Lick Observatory the opportunity for teaching was limited, and he would undoubtedly have been better satisfied had his

[2] *Ap. J.*, **95**, 356, 1942; *Lick Obs. Contr.*, Ser. II, No. 4.

[3] *Lick Obs. Bull.*, **19**, 17, 1939.

[4] *Ap. J.*, **95**, 24, 1942; *Lick Obs. Contr.*, Ser. II, No. 2.

position provided the occasion both for research and for the giving of instruction. For a season he conducted a course in astronomy in the neighboring city of San José, as part of a project in adult education sponsored by the city school system. The lectures were given at night, and the fact that to deliver them he had to travel fifty miles over a mountain road, while some of his auditors came from places still more remote, testifies to his own interest in the undertaking and the appreciation by his audience of the quality of the instruction received. Those familiar with his published papers will understand his success as a teacher.

Arthur Wyse was born in Blairstown, Iowa, on June 25, 1909; he was the son of Rev. Charles M. and Celia Wyse. The father was a Presbyterian clergyman, a circumstance which was not without influence during the formative period of his son's character. Of this family there survive the mother, a brother, and a sister.

Arthur entered the College of Wooster at the age of sixteen. He was markedly successful in his study both of the classics and of the natural sciences, his interest apparently going over from the one subject to the other during his college course. He received a prize for excellence in Greek and was graduated with the degree of A.B., *cum laude*, in 1929. After a year spent as accountant for the Bell Telephone Company, Wyse attended the graduate school of the University of Michigan, where he came under the instruction of Heber D. Curtis. At that time he decided to make astronomy the basis of a professional career, and after receiving the M.A. degree at Michigan he enrolled in the graduate division of the University of California, at Berkeley, where the degree of Doctor of Philosophy was conferred upon him in May, 1934. Thereafter he was at the Lick Observatory, first as Martin Kellogg Fellow, then as research assistant. His engagement as assistant astronomer, in 1935, and his later relationship to the Observatory have already been referred to.

In 1934 Dr. Wyse was married to Miss Marylyn Crandell, who had been his classmate at the College of Wooster. They had two sons, Kenneth and Gordon, and lived most happily on Mount Hamilton. The closely knit observatory community was enriched by the presence of these young people. They were cheerful, loyal friends, always ready to put the interests of their neighbors in advance of their own. To know them was to be aware of their profound appreciation of their obligations to society. This was perhaps the dominant quality of Mr. Wyse's character, and it found expression in many ways—in his deportment, in his friendships, and in the fine spirit of self-reliance, which was exemplified alike in his professional work and in the conduct of his daily life. In an era marked by extravagance, he preferred the practice of thrift to the incurrence of obligation, and his manual skill enabled him to make with his hands much that is customarily bought. A happy recollection is of seeing him and his family on a holiday, picnicking on a sunny mountainside with the purpose of laying in their winter supply of firewood. Sped by his supple body and practiced hand, the ax flew swift and sure to the mark in its appointed task of felling an oak or of converting it into neat and even lengths of cordwood. He was fond of the out-of-doors and of its sports. In all such activities his movements were graceful and bespoke a well-balanced muscular development. Above all he possessed that superb quality of sportsmanship that smiles in defeat as well as in victory.

NAVAL SERVICE

Dr. Wyse held a commission as lieutenant, junior grade, in the United States Naval Reserve, and in December, 1941, he was granted leave of absence from the Observatory to permit him to accept civilian service in the United States Navy Radio and Sound Laboratory, at San Diego, a project of the National Defense Research Committee. The tragic termination of this engagement has already been noted.

At this time little is known, except by the Navy Department or its affiliates, of the service rendered the government, but one may be sure that to that service he dedicated

himself without stint. Numerous letters have been received by his widow and by the Lick Observatory in which the value of his contribution to the war effort is attested. These have come from the Secretary of the Navy, from various officers of the service, from the chairman of the National Defense Research Committee, and from others. Inasmuch as it is not possible to provide a circumstantial account of what he was able to do, it seems permissible to quote from the commanding officer's tribute, spoken on the occasion of the memorial services held at the Lakehurst Naval Air Station:

> We are assembled here at the Naval Air Station, Lakehurst, New Jersey, to render tribute to those who lost their lives in an airship accident on Monday night of this week.
>
> A night experimental mission was being conducted. Any air operation is attended by a certain amount of hazard. When it is conducted at night an additional hazard exists.
>
> The officers and men who manned the ships were aware of the circumstances. Nevertheless, they did not hold back—they were eager to make this flight. Those in charge were experienced and with many hours in the air in airships of this type.
>
> Under the conditions existing, no other crew was better fitted to conduct this operation—nor could any other crew have succeeded in conducting it otherwise. Theirs is a great loss to the Airship Organization.
>
> On board these airships were five eminent members of the National Defense Research Council. Some of these scientists had visited this station before and were known and held in high regard here. Some came from distant points of the country to take part. They cannot be replaced.
>
> Their loss is a distinct blow to the war effort of the National Defense Research Council.
>
> The fact that civilians and naval men were working side by side and were lost together is symbolic of the spirit of co-operation between all branches which now exists throughout this country in the determination and effort to win the war.
>
> We are conducting a service in memory of the twelve men who gave up their lives. I speak not only for myself but for every person connected with this station and with the war effort of the entire country when I say that each one of them—whether in the naval service or in part of the civilian organization—gave up his life in this effort just as gallantly and just as much in the line of duty in defense of his country as the man who likewise gives up his life in a naval action at sea or in the front line of battle. . . . .
>
> The most recent disaster will in no way impede our progress. This is no time to quit, and we will carry on to completion the work which these men began and in so doing gave up their lives.

A growing circle of astronomers knew Arthur Wyse as a young scientist of excellent ability and much promise. His immediate associates remember him as, above all, a man of flawless integrity, a sympathetic friend, and a person of great charm. Elegant in body and in mind, he would have gone far in any walk of life he might have elected to follow.

W. H. WRIGHT

THE GALACTIC CLUSTERS NGC 2126 AND NGC 2194

JAMES CUFFEY[1]
Kirkwood Observatory, Indiana University
Received December 28, 1942

ABSTRACT

The galactic clusters NGC 2126 and NGC 2194 are examined photometrically, and the relations between red color indices and apparent magnitude are obtained. In the case of NGC 2126 a well-defined main sequence and a giant branch containing red stars are in evidence. New values for its distance and color excess, estimated from the color-magnitude relation, are 950 parsecs and 0.8 mag. NGC 2194 has a poorly defined main sequence and a group of giants, whose absolute magnitudes appear to be a magnitude fainter than usual. For NGC 2194 the distance and color excess estimates are 1200 parsecs and 0.9 mag. These distances are considerably smaller than those previously given. The average star densities in the two clusters are high (8 stars/parsecs^3) and appear to indicate again that the smaller clusters have somewhat higher average star densities than the larger ones.

A serious deficiency in our knowledge of the galactic clusters still exists because of the fact that very few of the objects with small angular diameters have been thoroughly investigated by either spectrographic or photometric means. For this reason the present work on the colors of stars in two of these clusters is of interest.

NGC 2126 and NGC 2194 are typical galactic clusters having apparent diameters of approximately 6 minutes of arc and located in uniform, moderately rich star fields. The co-ordinates and previous estimates of distance are given in Table 1.

TABLE 1

NGC	1900		l	b	TYPE*	DISTANCE	
	α	δ				Trumpler* (Parsecs)	Shapley† (Kpc)
2126	5^h55^m	49°.9	131°	14°	III2p	2810	.....
2194	6 08	12.8	165	− 0.8	I2r	2520	>3.2 to >5.0

* *Lick. Obs. Bull.*, **14**, 154, 1930. † *Star Clusters*, Appen. B., New York: McGraw-Hill, 1930.

Red color indices ($\lambda\lambda$ 4300–6200) for 282 stars in the two clusters were obtained from plates taken with the 36-inch reflector of the Steward Observatory in Tucson. Magnitude sequences were obtained partly from equal-altitude comparison exposures with Messier 35[2] and partly from polar comparisons made with the 36-inch reflector of the Goethe Link Observatory in Brooklyn, Indiana. Measurements were made with an image scale, and other details are similar to those described in *Harvard Annals*, Volume **106**, No. 2. For the observational material and the probable errors of the magnitudes of cluster stars see Table 2. The probable errors of the red color indices are ± 0.08 in NGC 2126 and ± 0.11 in NGC 2194.

The relations between color and apparent red magnitude (Figs. 1 and 2) show, in NGC 2126, a giant branch and a well-defined main sequence. The absence of stars with

[1] Lieutenant, U.S.N.R., U.S. Naval Academy, Annapolis.

[2] *Harvard Ann.*, Vol. **106**, No. 2.

apparent red magnitudes between 14 and 15 is perhaps worth noticing as a peculiarity. In NGC 2194 the main sequence is poorly defined, and there is an unusual group of giant stars near $m_r = 13.3, C_r = 2.2$. These stars are contributed mainly by the central part of the cluster, and they probably are cluster members. Judging from their position with respect to the cluster's main sequence, their absolute magnitudes are low, and about 1 mag. fainter than normal giants.

In NGC 2126 there are no colors less than 0.65 mag., and in NGC 2194 there is only one star with a color index less than 0.5 mag. The lack of white stars is probably due to selective absorption. If the color-magnitude relations are compared with that of Messier 38, the values shown in Table 3 may be obtained for the color excesses and distances.

TABLE 2

NGC	Number of Comparison Exposures of Cluster		Number of Long Exposures		Probable Errors	
	Red	Blue	Red	Blue	Red	Blue
2126.....	7	9	3	3	±0.050	±0.061
2194.....	8	8	2	3	±0.074	±0.083

TABLE 3

NGC	Color Excess	Distance* (Parsecs)	Linear Diameter (Parsecs)	No. of Cluster Stars
2126.....	$0^m.8$	950	2.8	90
2194.....	0.9	1200	3.0	120

* Corrected for absorption, using $A_{\epsilon 200} = 2x$ (color excess).

The star densities in these clusters, considered as the average over the whole cluster, are high: 7.8 stars/parsecs[3] in NGC 2126 and 8.6 in NGC 2194. These figures may give a somewhat misleading impression as to the richness of the clusters, for the total numbers of cluster stars observed is only 90 in NGC 2126 and 120 in NGC 2194. Inasmuch as the densities are very sensitive to the distances, and therefore to the exact value of the ratio between color excess and general absorption, and also because the boundaries of the clusters are poorly defined, the densities cannot be regarded as more than a rough indication. They do confirm, however, an earlier conclusion that the average stellar densities in these small, relatively poor clusters are higher than the average densities observed in many of the larger and richer objects. In fact, the average density over the whole of a small cluster like NGC 2194 may be compared with the central density in Messier 37[3] (18 stars/parsecs[3]), for example.

A conclusion reached in *Harvard Annals*, Volume **106,** No. 2, that the distances of galactic clusters of small apparent diameter tend to be overestimated, is confirmed by the present material. A great deal more work on these objects must be completed, however, before we may expect to obtain a reliable estimate of the frequencies of linear diameters of the galactic clusters in general.

[3] Shapley, *Star Clusters*, p. 203.

PLATE VI

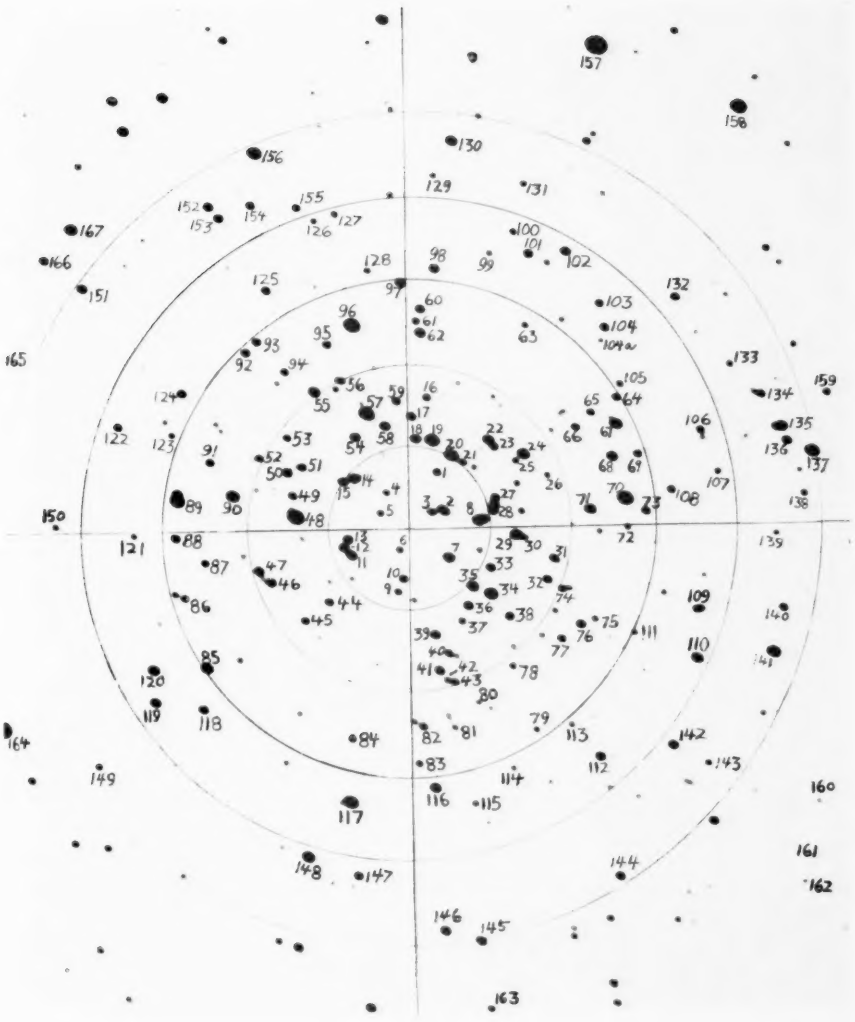

NGC 2194

PLATE VII

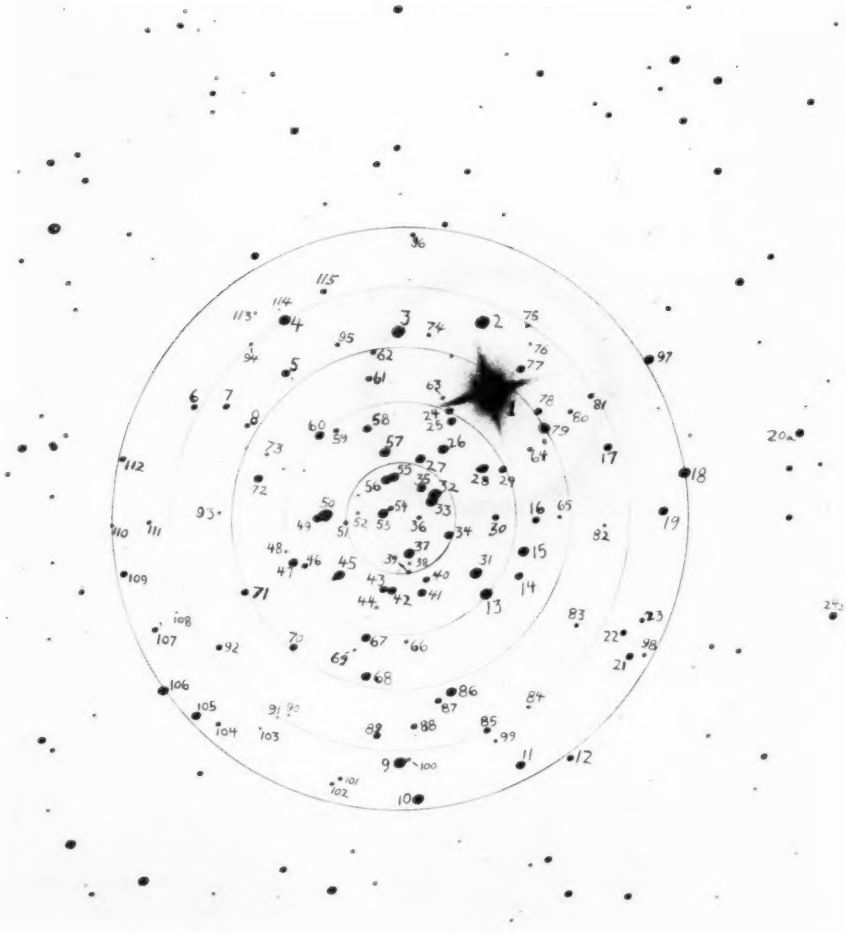

NGC 2126

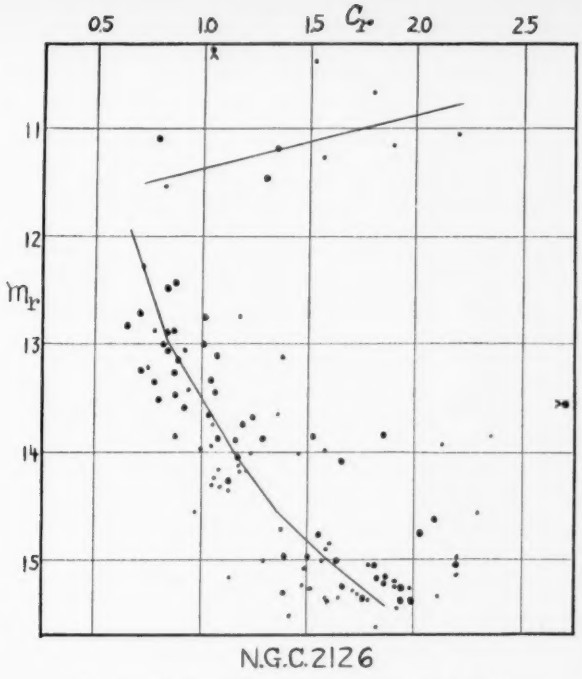

FIG. 1.—Relation between color and magnitude

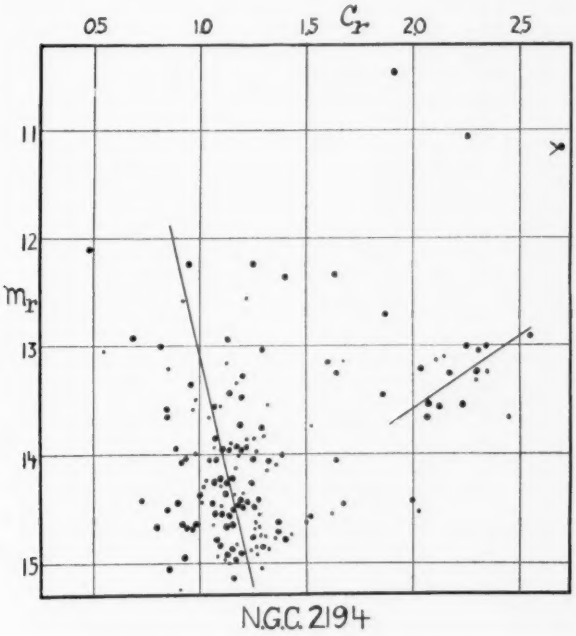

FIG. 2.—Relation between color and magnitude

TABLE 4

STAR CATALOGUES: NGC 2126 AND NGC 2194

NGC 2126*

No.	R†	m_{pg}	m_r	C_r
1	3	6.00::	5.00::	1.00::
2	4	11.89	10.37	1.52
3	4	12.44	10.65	1.79
4	4	12.83	11.27	1.56
5	4	14.35	13.41	0.94
6	5	15.50	14.37	1.13
7	4	15.35	14.30	1.05
8	4	16.21	13.85	2.36
9	5	12.34	11.52	0.82
10	5	13.05	11.16	1.89
11	5	13.98	13.05	0.93
12	6	15.30	14.12	1.18
13	2	12.54	11.19	1.35
14	3	14.97	13.88	1.09
15	3	13.46	12.81	0.65
16	3	15.40	14.27	1.13
17	4	15.00	13.95	1.05
18	5	13.01	12.28	0.73
19	5	13.96	13.23	0.73
20a	6	14.27	13.16	1.11
21	5	14.79	13.74	1.05
22	5	15.39	14.18	1.21
23	5	16.05	13.93	2.12
24s	6	14.41	13.53	0.88
24	3	15.74	14.09	1.65
25	2	14.93	13.69	1.24
26	2	13.75	12.87	0.88
27	2	14.14	13.27	0.87
28	2	14.01	13.00	1.01
29	2	15.37	14.32	1.05
30	2	16.32	14.77	1.55
31	2	12.77	11.47	1.30
32	1	13.29	12.41	0.88
33	1	13.75	12.74	1.01
34	1	14.67	13.64	1.03
35	1	15.17	13.89	1.28
36	1	16.71	14.62	2.09
37	1	13.33	12.48	0.85
38	1	17.24	15.05	2.19
39	1	16.64	15.00	1.64
40	2	15.40	13.87	1.53
41	2	14.53	13.47	1.06
42	2	14.50	13.11	1.39
43	2	15.04	13.88	1.16
44	2	17.02	15.16	1.86
45	2	13.41	12.70	0.71
46	2	15.68	13.83	1.85
47	2	13.92	13.08	0.84
48	3	17.22	15.28	1.94
49	2	14.31	13.51:	0.80 :
50	2	11.88	11.10	0.78
51	1	16.70	13.55	3.15
52	1	17.33	15.39	1.94
53	1	13.75	12.89	0.86
54	1	16.68	15.30:	1.38 :
55	1	14.18	13.10	1.08
56	1	14.02	13.13	0.89
57	2	14.12	13.34	0.78
58	2	15.20	14.03	1.17
59	2	16.48	14.98	1.50
60	2	14.36	13.48	0.88
61	3	16.34	14.95	1.39
62	3	16.76	14.74	2.02
63	3	17.37	15.38:	1.99:
64	3	16.98	15.16	1.82
65	3	17.11	15.35:	1.76:
66	3	16.84	15.03	1.81
67	3	13.96	13.24	0.72
68	3	13.82	13.00	0.82
69	3	16.92	15.26	1.66
70	3	14.74	13.86	0.88
71	3	14.92	13.72	1.20

NGC 2126

No.	R	m_{pg}	m_r	C_r
72	3	14.51	13.58	0.93
73	3	17.06	15.20	1.86
74	4	17.04	15.30	1.74
75	4	17.00	15.29:	1.71:
76	4	17.38	15.46	1.92
77	4	15.25	14.16	1.09
78	4	15.54	14.57	0.97
79	4	.....	ghost	.....
80	4	16.77	15.26	1.51
81	4	16.28	14.99	1.29
82	4	17.11	15.35	1.76
83	4	16.57	15.01	1.56
84	4	16.99	16.34	1.65
85	4	15.25	14.02	1.23
86	4	13.66	12.88	0.78
87	4	15.46	14.01	1.45
88	4	15.36	14.17	1.19
89	4	15.00	13.64	1.36
90	4	17.45	15.63	1.82
91	5	17.32	15.13	2.19
92	4	15.31	14.25	1.06
93	4	17.22	15.25	1.97
94	4	17.18	14.98	2.20
95	4	16.70	15.22	1.48
96	5	16.27	15.14	1.13
97	6	13.81	13.04	0.77
98	5	16.82	15.03	1.79
99	5	16.88	14.58	2.30
100	5	16.91:	15.33	1.58:
101	5	16.49	14.90	1.59
102	5	16.58	15.09	1.49
103	5	17.15	15.23	1.92
104	5	16.08	14.71	1.37
105	5	13.91	12.73	1.18
106	5	13.24	11.04	2.20
107	5	15.55	13.98	1.57
108	5	17.40	.....	.....
109	5	14.97	13.97	1.00
110	5	17.13	15.22	1.91
111	5	16.47	14.87	1.60
112	5	15.39	14.31	1.08
113	5	17.44	15.33	2.11
114	5	17.85:	.....	.....
115	5	15.94:	.....	.....

NGC 2194

No.	R	m_{pg}	m_r	C_r
1	1	15.63	14.56	1.07
2	1	14.89	13.25	1.64
3	1	15.61	14.42	1.19
4	1	16.04	14.89	1.15
5	1	16.11	14.91	1.20
6	1	15.95	14.85	1.10
7	1	14.56	13.42	1.14
8	1	13.76	12.36	1.40d
9	1	15.90	14.81	1.09
10	1	15.36	14.46	0.90
11	1	14.91	13.72	1.19
12	1	15.41	13.24	2.17
13	1	15.25	13.20	2.05
14	1	14.68	13.48	1.20
15	1	15.35	13.00	2.35
16	2	15.61	14.63	0.98
17	2	15.34	13.03	2.31
18	2	15.14	13.92	1.22
19	2	13.61	12.92	0.69
20	2	13.81	13.00	0.81
21	2	16.00	14.62	1.38
22	2	14.82	13.93	0.89
23	2	15.51	14.38	1.13

NGC 2194

No.	R	m_{pg}	m_r	C_r
24	2	14.68:	11.17	3.51:
25	2	16.20	.....	.....
26	2	16.30	15.14	1.16
27	2	15.45	12.90	2.55
28	2	14.57	12.70	1.87d
29	2	14.32	13.36	0.96
30	2	16.11	14.44	1.67
31	2	15.30	13.44	1.86
32	2	15.30	14.05	1.25
33	2	15.11	13.97	1.14
34	2	13.94	12.31	1.63
35	2	14.44	13.59	0.85
36	2	15.00	14.07	0.93
37	2	15.93	15.05	0.88
38	2	15.33	14.25	1.08
39	2	15.07	13.96	1.11
40	2	15.78	13.54	2.24
41	2	15.26	13.00	2.26
42	2	16.17	14.87	1.30
43	2	16.10	14.58	1.52
44	2	15.55	14.63	0.92
45	2	15.66	14.56	1.10
46	2	15.17	13.96	1.21
47	2	15.10	13.93	1.17
48	2	12.58	12.10	0.48
49	2	15.60	13.53	2.07
50	2	15.13	14.05	1.08
51	2	15.40	14.40	1.00
52	3	15.75	14.49	1.26
53	2	15.69	14.49	1.20
54	2	15.03	13.74	1.29
55	3	14.52	13.66	0.86
56	2	15.74	13.67	2.07
57	2	13.32	11.06	2.26
58	2	14.98	14.05	0.93
59	2	15.36	14.51	0.85
60	3	15.13	14.41	0.72
61	3	15.80	14.67	1.13
62	3	15.10	14.05	1.05
63	3	16.04	14.91	1.13
64	3	15.67	14.44	1.23
65	3	15.71	13.58	2.13
66	3	15.48	14.68	0.80
67	3	14.48	13.28	1.20
68	3	14.91	13.84	1.07
69	3	15.57	14.64	0.93
70	3	13.18	12.23	0.95
71	3	14.64	13.56	1.08
72	3	15.87	14.94	0.93
73	3	15.41	14.29	1.12
74	3	15.70	14.55	1.15d
75	3	16.04	14.79	1.25
76	3	15.33	14.24	1.09
77	3	15.53	14.47	1.06
78	3	16.08	14.71	1.37
79	3	16.16	14.99	1.17
80	3	16.20	14.80	1.40
81	3	16.41	14.41	2.00
82	3	15.54	13.24	2.30
83	3	15.81	14.65	1.16
84	3	15.66	14.50	1.16
85	3	14.30	13.01	1.29
86	3	15.70	14.42	1.28
87	3	15.66	14.48	1.18
88	3	15.39	14.07	1.32
89	3	13.48	12.23	1.25d
90	3	14.08	12.95	1.13
91	3	15.70	14.06	1.64
92	3	15.38	14.22	1.16
93	3	15.39	14.00	1.39
94	3	15.62	14.64	0.98

* Abbreviations: d, double; : uncertain; | stars close together. † Ring.

TABLE 4—*Continued*

NGC 2194					NGC 2194					NGC 2194				
No.	R	m_{pg}	m_r	C_r	No.	R	m_{pg}	m_r	C_r	No.	R	m_{pg}	m_r	C_r
95	3	15.52	14.27	1.25	119	4	14.80	13.13	1.67	144	5	15.18	14.00	1.18
96	3	12.35	10.44	1.91	120	4	14.48	13.50	0.98	145	5	15.08	13.85	1.23
97	3	14.77	13.17	1.60	121	4	16.15	14.72	1.43	146	5	14.88	13.56	1.32
98	4	15.00	13.93	1.07	122	4	15.54	14.38	1.16	147	5	15.24	13.72	1.52
99	4	16.36	15.07	1.29	123	4	16.15	14.88	1.27	148	5	14.05	13.20	0.85
100	4	15.97	14.69	1.28	124	4	15.39	14.29	1.10	149	5	15.83	14.55	1.28
101	4	15.49	13.32	2.17	125	4	15.28	14.11	1.17	150	5	16.17	14.55	1.62
102	4	15.13	13.83	1.30	126	4	16.09	13.64	2.45	151	5	15.06	13.84	1.22
103	4	15.65	14.55	1.10	127	4	15.96	14.70	1.26	152	5	15.25	13.12	2.13
104	4	15.45	14.13	1.32	128	4	16.10	14.97	1.13	153	5	15.30	14.28	1.02
104a	4	16.55	14.52	2.03	129	5	16.06	14.75	1.31	154	5	15.59	13.23	2.36
105	4	16.02	14.75	1.27	130	5	14.72	13.68	1.04	155	5	15.72	14.65	1.07
106	4	15.91	14.64	1.27	131	5	16.11	14.60	1.51	156	5	13.76	12.54	1.22
107	4	16.16	15.25	0.91	132	5	15.44	14.10	1.34	157	6	10.72	9.89	0.83
108	4	15.47	14.46	1.01	133	5	16.06	14.97	1.09	158	6	12.91	12.39	0.52
109	4	15.24	13.98	1.26d	134	5	15.60	13.30	2.30d	159	6	15.57	13.94	1.63
110	4	14.62	13.54	1.08	135	5	14.29	13.17	1.12d	160	6	16.40	.....	.....
111	4	16.14	14.87	1.27	136	5	15.25	13.10	2.15	161	6	16.65	.....	.....
112	4	14.98	14.00	0.98	137	5	13.52	12.59	0.93	162	6	16.33	.....	.....
113	4	16.13	14.77	1.36	138	5	16.03	14.85	1.18	163	6	15.57	14.40	1.17
114	4	16.18	14.91	1.27d	139	5	16.18	14.88	1.30	164	6	11.45	10.70	0.75
115	4	16.19	14.00	2.19	140	5	15.54	14.38	1.16	165	6	15.16	13.18	1.98
116	4	14.55	13.58	0.97	141	5	13.58	13.03	0.55	166	6	15.41	13.20	2.21
117	4	13.21	11.55	1.66	142	5	15.10	13.96	1.14	167	6	14.30	13.11	1.19
118	4	15.29	14.25	1.04	143	5	16.08	14.94	1.14					

Acknowledgments are made to Dr. E. F. Carpenter and to the University of Arizona, for the use of plates taken with the reflector at Steward Observatory; to Dr. Goethe Link, for the use of the equipment of the Link Observatory; and to Indiana University, for a fellowship which enabled me to complete the measurements and reductions.

MEASUREMENTS IN THE SPECTRUM OF τ SCORPII*

PAUL W. MERRILL AND WALTER S. ADAMS
Mount Wilson Observatory
Received December 17, 1942

ABSTRACT

Three coudé spectrograms, dispersion 2.9 A/mm, provide the basis for a brief study of the widths and displacements of lines of *H*, *He*, *O*, *Ne*, and other elements. Total widths are approximately as follows: *H*, 23 A; *He*, 1–8 A; *O*, *Ne*, etc., 0.5 A. With a few exceptions, lines of various elements yield accordant values of the radial velocity. Some of the exceptions are possibly to be explained by the instability of certain lines in the laboratory. The profiles and displacements of the *He* lines offer strong evidence of the Stark effect.

Because of its numerous narrow lines, the spectrum of τ Scorpii[1] has received considerable attention, lists of lines having been published by several observers.[2] The presence of lines of ionized neon, discovered by Menzel and Marshall,[3] is the subject of two special articles.[4]

Spectrograms, dispersion 2.9 A/mm, obtained with the coudé spectrograph on Mount Wilson on May 29, June 2, and June 30, 1942, serve as the basis for the following discussion. The emulsion employed was the very fast Eastman 103*a*-O, which is coarse-grained but has fair contrast and gives excellent results for spectra as wide as these (1 mm). The spectral region extends from λ 3300 to λ 4720. Wave lengths of the lines have been measured by Miss Cora G. Burwell. Microphotometer tracings, made by Miss Louise Ware and Miss Dorothy Davis, have been useful in various ways.

WIDTHS OF LINES

The hydrogen lines are diffuse, without marked cores; their profiles appear symmetrical. On the tracings (see Figs. 1 and 2) the series seems to end rather abruptly with *H*15 λ 3712; the line *H*16 λ 3704 is blended with *He* I λ 3705, while the lines following are not recognizable. The widths of various lines in the series are nearly the same (see Table 1), the decreasing intensities of the ultraviolet lines being compensated by greater diffuseness. The widths of the *He* I lines vary decidedly from series to series. The *He* II line λ 4686 is slightly diffuse. Many narrow lines occur throughout the spectrum, a considerable proportion of which may be identified with *O* II or *Ne* II; most of the others are due to *C* II, *C* III, *N* II, *N* III, *O* III, *Mg* II, *Al* III, *Si* III, *Si* IV, *S* III, or *Ca* II.

The total widths (Table 1) of lines of various elements, measured from the tracings, are subject to the usual uncertainty in determining the precise limits to which the wings extend. The uncertainty is considerable for the hydrogen lines, decidedly less for the helium lines. It is numerically very small for the narrow lines but, nevertheless, for any given line is a considerable fraction of the whole width. The values in Table 1 for *O*, *Ne*, *C*, *N*, and *Si* are means for a group of the stronger lines of each element on two or three

* *Contributions from the Mount Wilson Observatory, Carnegie Institution of Washington*, No. 672.

[1] HD 149438: 1900 R.A. $16^h29^m.7$; Dec. $-28°1'$; mag. 2.9; spectrum B0.

[2] O. Struve, $\lambda\lambda$ 4026–4713, *Ap. J.*, **74**, 225, 1931; Struve and Dunham, $\lambda\lambda$ 3945–4713, *Ap. J.*, **77**, 321, 1933; R. K. Marshall, $\lambda\lambda$ 3867–4922, *Pub. Obs. Univ. of Mich.*, **5**, 137, 1934; Adams and Dunham, $\lambda\lambda$ 3097–3244, *Mt. W. Contr.*, No. 583; *Ap. J.*, **87**, 102, 1938; O. Struve, $\lambda\lambda$ 3298–3965, *Ap. J.*, **90**, 699, 1939.

[3] *Proc. Nat. Acad. Sci.*, **19**, 879, 1933.

[4] H. Kühlborn, *Zs. f. Ap.*, **8**, 190, 1934; R. F. Sanford, *Pub. A.S.P.*, **50**, 244, 1938.

plates. Lines of *O* III, *C* II, *C* III, *Si* III, and *Si* IV appear slightly wider than those of *O* II, *Ne* II, and *N* II.

Excellent determinations of the profiles of the hydrogen lines and of most of the helium lines could be derived from these high-dispersion spectrograms. The lines of other

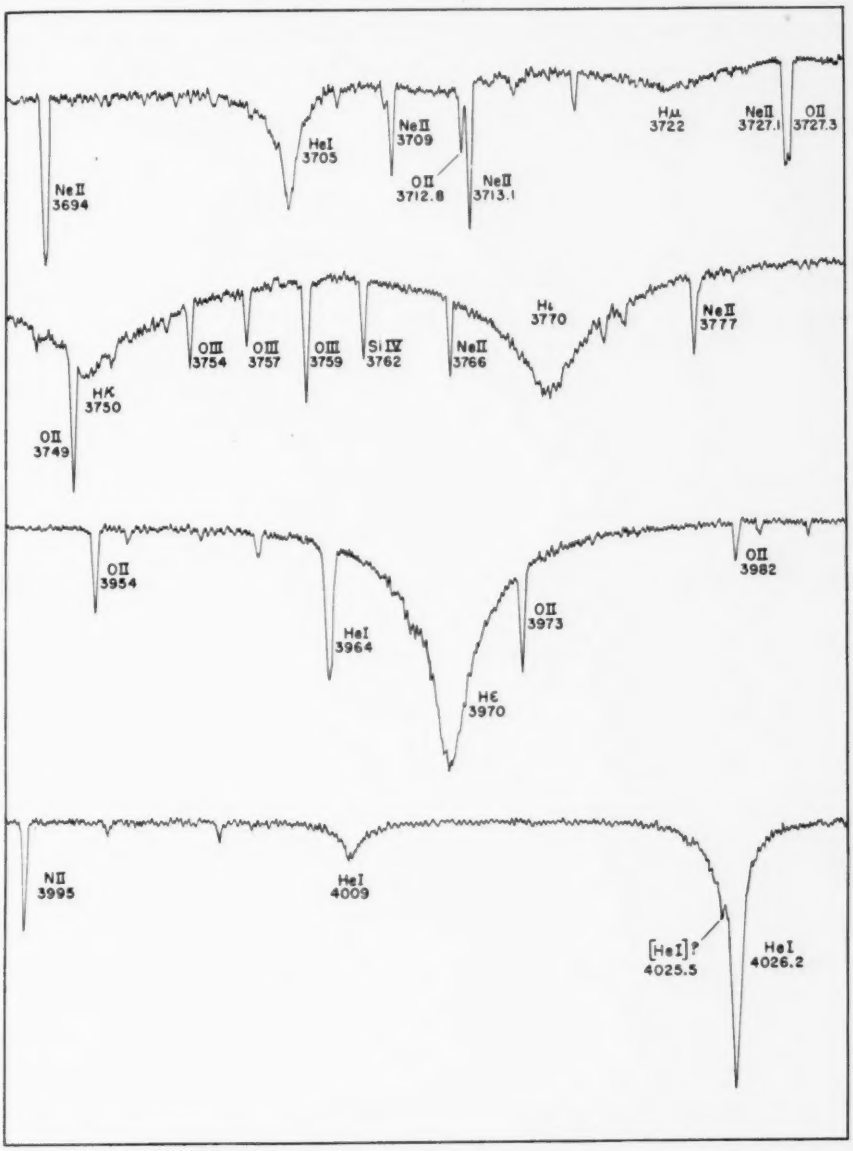

FIG. 1.—Microphotometer tracings of portions of the spectrum of τ Scorpii. Scale, 0.32 A/mm

elements are so narrow that their observed profiles depend largely upon the instrument and the photographic emulsion. The intrinsic profiles are, however, not entirely obscured. Even the narrower lines in τ Scorpii are, for example, appreciably wider than the narrowest interstellar lines shown (in other stars) by the same spectrograph.

In the narrower lines of moderate intensity, nearly all the absorption appears to lie within 0.1 A, or 7 km/sec, of the center of the line. With an allowance for the instrumental profile, this value can be accounted for by the probable kinetic motions of the

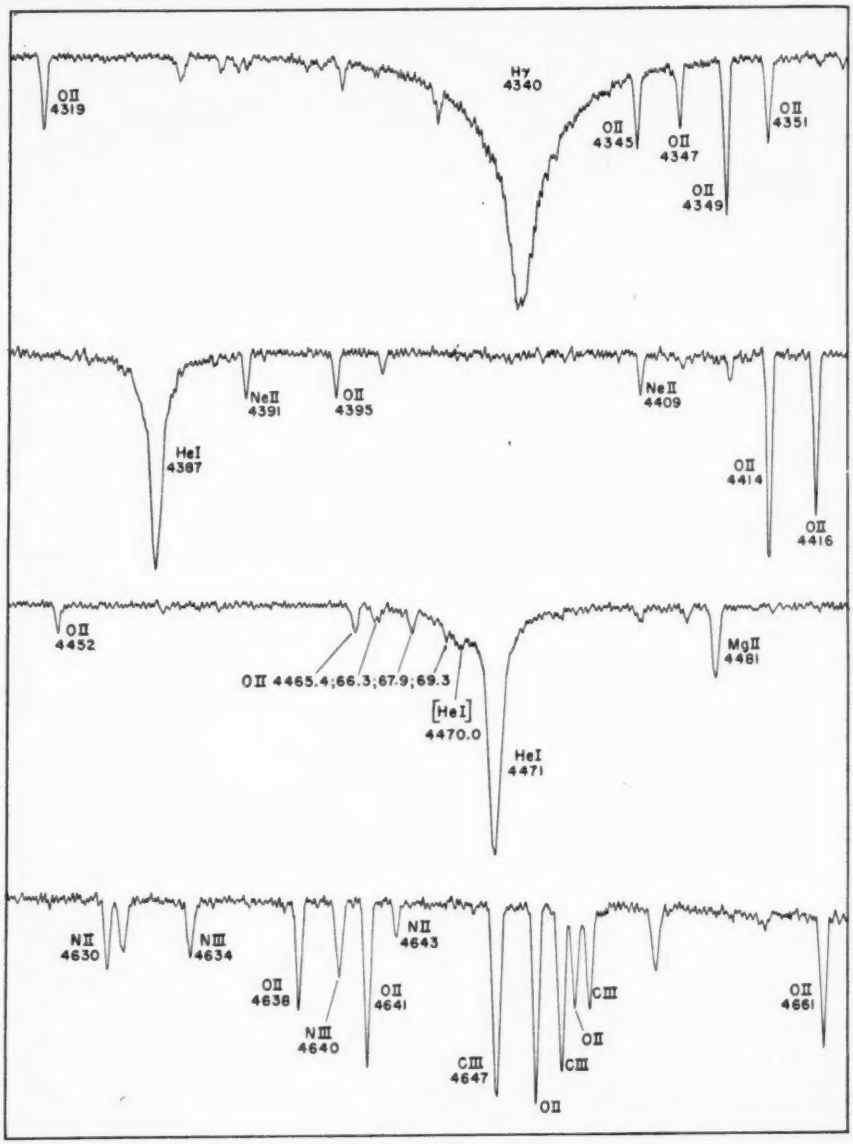

FIG. 2.—Microphotometer tracings of portions of the spectrum of τ Scorpii. Scale, 0.32 A/mm

atoms in the stellar atmosphere. Other types of motion, such as rotation or turbulence, must therefore have very small components in the line of sight. A similar result had previously been obtained by O. Struve[5] for γ Pegasi.

[5] *Proc. Nat. Acad. Sci.*, **18**, 585, 1932.

The temperature of the reversing layer may, in principle, be determined from the structure of the lines if the profiles depend essentially upon the kinetic motions of the atoms. The narrow lines of oxygen (or of elements of higher atomic weight) would not yield accurate values because the intrinsic profiles are too narrow in comparison with the resolving-power of spectrograph and photographic emulsion. Since the widths of the lines, when due to kinetic motions, are inversely proportional to the square roots of the atomic weights of the atoms, the lines of hydrogen should be four times as wide and the helium lines twice as wide as those of oxygen. Because of their sensitivity to Stark effect, the hydrogen lines and most of the helium lines clearly exceed these limits (see Table 1)

TABLE 1

TOTAL WIDTHS OF LINES

HELIUM					HYDROGEN	
Series	Triplets		Singlets		λ	A
	λ	A	λ	A		
Sharp	4713	1.7	4437	1.1	4340 *Hγ*	22
	3867	1.4	.....	.....	4101 *Hδ*	24
	3652	1.6	.....	.....	3970 *Hε*	24
					3889 *Hζ*	23
Principal	.....	.....	3965	1.1	3835 *Hη*	22
	.....	.....	3613	1.1	3797 *Hθ*	22
	.....	.....	3447	1.3	3770 *Hι*	22
Diffuse	3820	7.5	4388	6.3		
	3705	6.5	4143	4.6	VARIOUS ELEMENTS	
	3634	5.2	4009	4.5		
	3587	4.9	3926	3.7		A
	3554	4.9	.....	.....	*O* II λλ 3377–4185	0.48
					λλ 4317–4649	.62
He II	4686	3.3	.....	.....	*Ne* II	.46
					O III	(.6)
					C III	(.7)
					N II	.53
					Si III	.7
					Si IV	(0.7)

and are thus unavailable. The singlets of both the sharp and the principal series of helium are narrower than the other helium lines and on a fine-grained emulsion or with somewhat higher dispersion (say 2 A/mm) might yield an approximate temperature or at least a reliable upper limit. A slight amount of Stark broadening would, however, cause this upper limit to be too high to be of much value.

DISPLACEMENTS OF LINES

With a few exceptions, lines of various elements yield accordant values of the radial velocity (Table 2). Even the hydrogen lines, although diffuse and difficult to measure, give very nearly the same velocity as the narrow lines. Most of the helium lines (Table 3) are displaced toward the red by a few kilometers per second—a fact of interest in the discussion of Stark effect.

Oxygen lines.—The results for the oxygen lines are based on the wave lengths by A. Fowler.[6] The slight divergence of the velocity from *O* III lines (Table 2) may arise from

TABLE 2

DISPLACEMENTS OF LINES OF VARIOUS ELEMENTS

Element	Plate						Mean Velocity
	Cé 2789		Cé 2804		Cé 2814		
	Vel.	No. of Lines	Vel.	No. of Lines	Vel.	No. of Lines	
	km/sec		km/sec		km/sec		km/sec
H	−1.2	2	−1.0	3	−2.8	3	−1.8
N II	−0.8	13	−0.9	13	−2.1	10	−1.2
N III	−1.7	6	−1.3	7	−3.0	4	−1.9
O II	−1.4	53	−1.2	74	−1.7	51	−1.4
O III	+1.3	4	+0.5	3	+1.8	7	+1.4
Ne II	−1.6	10	−2.2	19	−3.3*	16	−2.4
Si III	−0.7	7	+1.0	6	−2.3	5	−0.7
Si IV	−1.3	4	−0.6	5	−1.9	5	−1.3
S III	−1.4	7	−1.9	10	−1.7	10	−1.7
Ca II	−1.8	1	−0.4	1	−4.3	1	−2.2

* −4.4 km/sec from 35 lines. See text.

TABLE 3

DISPLACEMENTS OF HELIUM LINES

Series	Triplets		Singlets	
	λ	Km/Sec	λ	Km/Sec
Sharp	4713	+2	4437	+1.5
	4120	+1.3*	.....	.....
	3867	+4.2	.....	.....
	3732	+8.0	.....	.....
Principal	3888	.....	3965	−1.7
	3188	.....	3613	−3.7
	.....	.....	3447	−7
Diffuse	4471	+0.7	4388	+3.0
	4026	+2.3	4143	+5.3
	3819	+4.5	4009	+4
	3705	+2.7†	3926	+4±
	3634	+4.7	.....	.....

* Several close lines. † Blend with the weak *H*16 line.

some peculiarity of the stellar atmosphere or, more probably, from the instability of the laboratory wave lengths of *O* III mentioned by Fowler.

[6] *O* II, *Proc. Roy. Soc.*, A, **110**, 476, 1926; *O* III, *ibid.*, **117**, 317, 1927.

Neon lines.—The wave lengths of the *Ne* II lines were taken from the investigation by De Bruin and Bakker.[7] Measurements in the spectrum of τ Scorpii appear to show a correlation between intensity and displacement, the stronger lines yielding algebraically greater velocities. The range is about 3 km/sec from the weakest lines measured (intensity 3 on the scale of De Bruin and Bakker) to the strongest (intensity 10). No dependence upon intensity is shown by the numerous lines of *O* II.

On plates Cé 2789 and 2804 all the measurable lines of *Ne* II have longer wave lengths than λ 3470; the mean measured displacements on the two plates are −1.6 km/sec and −2.2, respectively. On plate Cé 2814, numerous lines of shorter wave length also were measured. Mean displacements are in Table 4.

TABLE 4

DISPLACEMENTS OF LINES OF *Ne* II ON PLATE Cé 2814

λ	Km/Sec	No.
3297–3340	−4.0	7
3340–3470	−6.1	12
3470–4409	−3.3	16
All	−4.4	35

The lines λ 4392 and λ 4398 are displaced toward the red with respect to the other lines of *Ne* II by approximately 0.1 A, an amount decidedly above the error of observation; λ 4428 and λ 4430 are systematically displaced in the same direction by a smaller amount. All four lines have been omitted in forming the mean velocity from *Ne* II.

All these relatively small discrepancies are probably to be ascribed to differences in behavior of various multiplets. Possibly some of the lines are slightly unstable under laboratory conditions.

Carbon lines.—The *C* II line λ 3918.98, perhaps somewhat reinforced by *N* II λ 3919.00, is well separated from *O* II λ 3919.28. The *C* II line λ 3920.68 is present in moderate intensity. These *C* II lines, as well as *Si* III λ 3924.44, appear slightly less sharp than *O* II λ 3919.28. The double *C* II line λ 4267.02, λ 4267.27, measured as a blend on two plates, yields the mean wave length, reduced to zero velocity λ 4267.14, which is reasonably accordant with the value λ 4267.16 adopted by the Committee on Radial Velocities of the International Astronomical Union.[8] On plate Cé 2804 the two components, although not well resolved, were measured separately. These components could probably be separated on a fine-grained contrasty emulsion.

The *C* III lines λλ 4647, 4650, and 4651 are very strong (see Fig. 2). The wave lengths of λ 4650 and λ 4651 appear slightly greater in the star than in the laboratory.

HELIUM LINES

Previous observers have concluded that the observed widening of lines of hydrogen and helium in early-type stars is caused largely by Stark effect. A convenient summary of laboratory data for helium has been compiled by Foster and Douglas.[9] We present observational data for τ Scorpii without attempting a general discussion. An adequate theoretical treatment would involve the complex problem of the precise relationship between the behavior of lines in steady electric fields and the broadening which results from the electric fields and kinetic motions of particles in a gas.

Displacement of lines.—The data in Table 3 represent the measured displacements of the helium lines in τ Scorpii. The displacements relative to other lines, obtained by sub-

[7] *Zs. f. Phys.*, **69**, 19, 1931.

[8] *Trans. I.A.U.*, **4**, 187, 1932.

[9] *M.N.*, **99**, 150, 1939.

tracting the stellar velocity, −1.4 km/sec, correspond in many details to displacements which might be given the lines by Stark effect. The principal singlets are displaced to the violet; all other measured series to the red. Moreover, within each series the lines of shorter wave length tend to have the greater displacements. These facts apparently constitute strong evidence in favor of the actual modification of line profiles by electric fields.[10]

Sharp series.—The singlet line λ 4437 is narrow without appreciable asymmetry; λ 4168, blended with a line of *O* II, probably has similar structure. The triplet lines, although slightly wider, are well defined and without wings.

Principal series.—The singlet lines are narrow and sharp. The only triplet line in the observed spectral region, λ 3888, is blended with the strong *Hζ* line.

Diffuse singlets.—The lines in both diffuse series are much wider and more diffuse than those in the other series (Table 1). Those in the singlet series are nearly symmetrical.

Diffuse triplets.—The profile of λ 4471 (Fig. 2) is much like that given by Foster and Douglas[9] for γ Pegasi and ι Herculis. The details on the violet side are somewhat more clearly brought out. These include the *O* II lines, for which Fowler's laboratory wave lengths and intensities[6] are:

λ 4465.40 (4)
66.32 (2n)
67.88 (4)
69.32 (3)

On our plates the second line is wider than the others; it may possibly be double with a separation of about 0.2 A. A trace of a fainter *O* II line, λ 4467.55, may be present. The width of the red wing of the helium line is at least 3 A, possibly 4; that of the violet wing, probably 5 A. The measured wave length of the center of the relatively broad minimum between *O* II λ 4469.32 and the chief helium component λ 4471.48 is λ 4469.96. As previous observers have pointed out, this is near the position of the forbidden line $2^3P - 4^3F$ for an electric field of zero intensity.

In the next line of the series, λ 4026 (Fig. 1), the red wing is about 3.7 A wide, the violet wing 4.5 A. A weak minimum, represented by a notch on two tracings and by a decrease of slope on a third, is at λ 4025.5, the position of the forbidden $2^3P - 5^3F$ and $2^3P - 5^3G$ lines (zero field).

In the three succeeding lines, λ 3819, λ 3705 (Fig. 1), and λ 3634, the violet wing is somewhat stronger than the red. The next line, λ 3587, is weak and diffuse, but appears nearly symmetrical.

In spite of certain important difficulties of interpretation, the general conclusion is that the observed profiles and displacements of the helium lines indicate the influence of Stark effect.

[10] A certain reservation must be made for the triplets, because, according to the usual practice, the wave lengths assumed for these lines were those of the principal components. The weaker components lie to the red and thus, if they appreciably affect the line structure, would cause spurious positive displacements.

THE STRUCTURE OF INTERSTELLAR H AND K LINES IN FIFTY STARS*

WALTER S. ADAMS
Mount Wilson Observatory
Received December 22, 1942

ABSTRACT

The structure of the interstellar H and K lines of *Ca* II appearing in the spectra of 50 stars of early type has been studied in the second order of the grating spectrograph at the coudé focus of the 100-inch telescope. The camera has a focal length of 114 inches and gives a linear scale of 2.9 A/mm.

More than 80 per cent of the stars show complex lines consisting of two to five components. Stars in various regions show differences in complexity, those in Perseus and Scorpius as a rule having single lines or at most lines with a faint component, while those in Orion, Sagittarius, and Cygnus usually show more intricate structure. The intensities of the components have been estimated. Measurements of their radial velocities provide a means of distinguishing individual interstellar clouds in various portions of the sky. Many of the clouds are found to extend over great areas. The narrowness of the components affords strong evidence for the discrete character of the clouds and the absence of any considerable turbulence.

The spectra have been examined for the additional narrow interstellar lines discovered and identified during recent years, and their intensities have been estimated. Lines of *Ca* I and *Fe* I seem to appear only in stars which show very strong H and K lines, while those of the diatomic molecules *CN*, *CH* I, and *CH* II may occur when H and K are relatively weak. The lines of *CH* I and *CH* II showed marked differences of intensity in various stars. The radial velocities from some of these additional lines in a few selected stars have been compared with the velocities from the components of H and K in the same stars. In this way it has been possible to distinguish the interstellar clouds in which the various lines are formed.

Since the original discovery by C. S. Beals[1] of the doubling of the interstellar H and K lines of ionized calcium in the spectra of several stars, a considerable number of additional stars showing similar effects have been found, largely through the work of R. F. Sanford.[2] Most of these spectra have been studied with the moderate dispersion best adapted for the investigation of the broad and hazy stellar lines usually characteristic of early-type stars. The use of very high dispersion, however, is especially favorable for the study of interstellar lines because of their remarkable sharpness and narrowness; and an additional advantage is the fact that stellar H and K, if present, are widened and made so diffuse that the interstellar lines stand out clearly upon them and may be recognized without difficulty.

The 50 stars considered in this investigation range in spectral type from O6 to cApe (υ Sagittarii) and cA2 (α Cygni) and in apparent magnitude from 1.8 to 6.1. The spectra have all been taken in the second order of the grating spectrograph at the coudé focus of the 100-inch telescope. The camera has a focal length of 114 inches with a concave mirror 36 inches in diameter. No Schmidt correcting plate is necessary because of the relatively small ratio of aperture to focal length,[3] and hence there is no glass in the entire optical train. The photographic plates consist of two strips, each 10 inches long, placed end to end upon the slightly curved rails of the plateholder. The region covered on a well-exposed spectrogram usually extends from about λ 3600 to λ 4700. The grating has sometimes been rotated to include the region near $H\beta$. The linear scale of the spectra is closely 1 mm = 2.9 A, becoming slightly larger toward longer wave lengths.

* *Contributions from the Mount Wilson Observatory, Carnegie Institution of Washington*, No. 673.

[1] *M.N.*, **96**, 661, 1936.

[2] *Pub. A.S.P.*, **51**, 238, 1939.

[3] The concave mirror is large in order to provide full illumination over a long plate.

The photographic emulsions used have been chiefly Cramer Hi-Speed Special and Eastman Experimental 103*a*-O. The latter has proved to be the most rapid emulsion so far employed and gives excellent results for fairly wide spectra in spite of the coarseness of its grain. A few spectrograms of exceptionally interesting stars have been made on Cramer Contrast plates, with a marked gain in resolution and visibility of faint lines; but, in general, the necessary exposure times have proved prohibitive. Most of the spectrograms obtained in the course of the search for new interstellar lines have been equally useful for the present study.

Table 1 gives the results for the 50 stars so far investigated. Single spectrograms have been used for about half the stars, and from two to seven for the remainder. The first seven columns give the constellation designations or Henry Draper numbers, right ascensions, declinations, magnitudes, and spectral types, and galactic latitudes and longitudes. The types are taken directly from the list of stars investigated for interstellar lines by P. W. Merrill and others,[4] with the addition of a few from the *Henry Draper Catalogue*, which are given in parenthesis.

The eighth and ninth columns give the intensity of each component observed in the H and K lines, estimated upon an arbitrary scale. Faint components are always better seen in K than in H, partly because of greater intensity and partly because of occasional interference of the wings of $H\epsilon$ with H. The faintest line seen with certainty is given intensity 1; the few lines marked < 1 are not certain but probable. The relative intensities should be reasonably reliable in the lower range but are much more doubtful when the intensity is high. Column 10 contains the radial velocities in km/sec of the individual components reduced to the sun. These values are the combined results for K and H. The wave lengths used for H and K are those in the sun given in the *Revision of Rowland's Preliminary Table*, λ 3933.684 for K and λ 3968.494 for H. Since the limit of resolution of lines of moderate intensity upon the spectrograms is about 0.10 A, differences of velocity of less than 8 km/sec are subject to appreciable uncertainty. The accuracy in the measurement of well-separated components, however, should be high, differences between K and H, or between various spectrograms of the same star, rarely exceeding 2 km/sec.

Although the usual correction for a solar motion of 20 km/sec directed toward R.A. 270°, Dec. +30°, is probably not strictly applicable to stars of spectral types O and B, comparatively little error is introduced by its use. Accordingly, the radial velocities given in the final column of Table 1, the "residual velocities," are those of the preceding column corrected upon this basis.

Finally, some notes are given usually dealing with the character of the lines and the probability of unresolved components.

A simple inspection of the results in Table 1 leads to several conclusions:

1. More than 80 per cent of the stars observed show double or multiple interstellar lines.

2. Areas in the sky show marked differences in complexity of interstellar lines. Stars in the direction of Perseus and Scorpius generally show single lines, while those in Orion, Sagittarius, Cygnus, and Lacerta are usually complex. In general, the lines in the stars nearest the galactic plane show the greatest complexity, although there are some notable exceptions, such as ρ Leonis, galactic latitude +54°, with triple lines, and π Aquarii, latitude −46°, with double lines. In both stars, however, the interstellar lines are of very moderate intensity and indicate relatively thin absorbing clouds.

3. Stars close to one another in the sky usually show much the same structure in the interstellar lines and similar relative intensities in the components. Illustrations are σ and ζ Orionis, ν and ξ Orionis, ω^1 and ν Scorpii, 67 Ophiuchi and HD 165174, μ and 15 Sagittarii, and the stars in Lacerta. A striking exception is formed by 66 and 67 Ophiuchi, in which the intensities of the two components are reversed.

[4] Merrill, Sanford, Wilson, and Burwell, *Mt. W. Contr.*, No. 576; *Ap. J.*, **86**, 274, 1937.

PLATE VIII

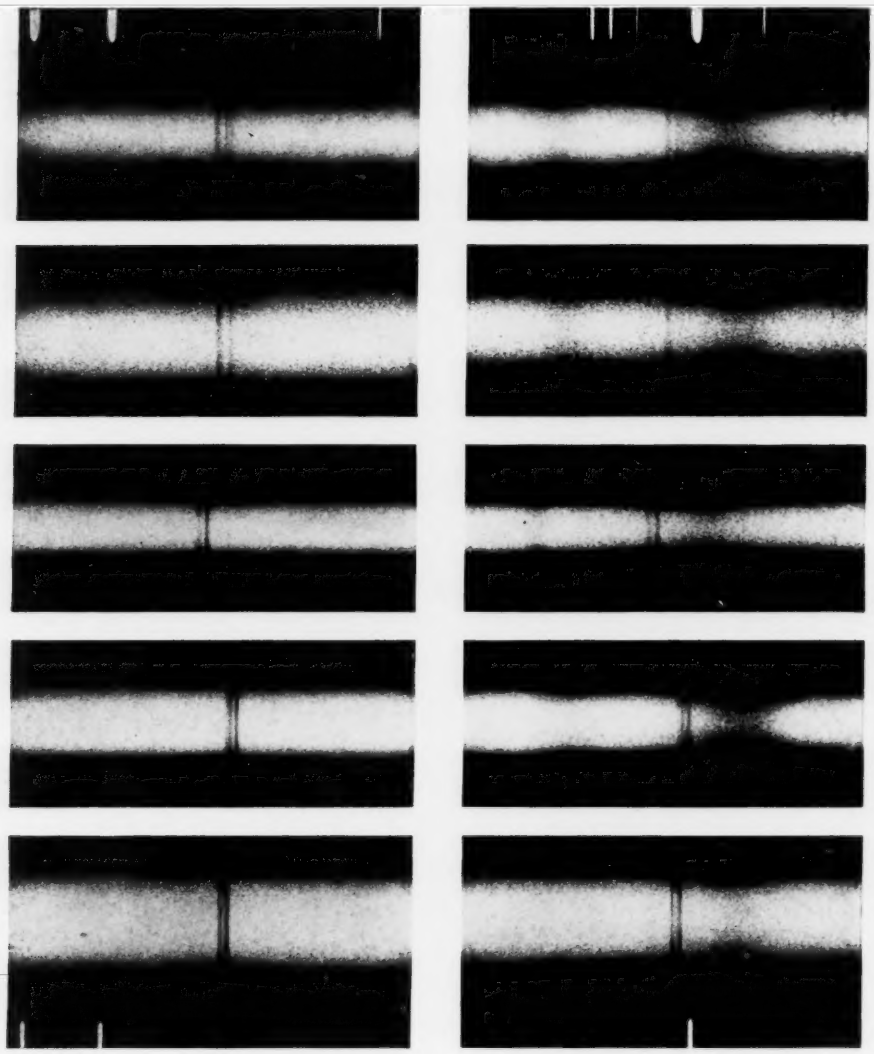

INTERSTELLAR LINES WITH HIGH DISPERSION

Calcium K (*left*) and H (*right*). From top to bottom: κ Orionis, ρ Leonis, 10 Lacertae, ϵ Orionis, λ^1 Orionis. Relative displacements from star to star correspond to the radial velocities at time of observation.

UNIV. OF MICH.

PLATE IX

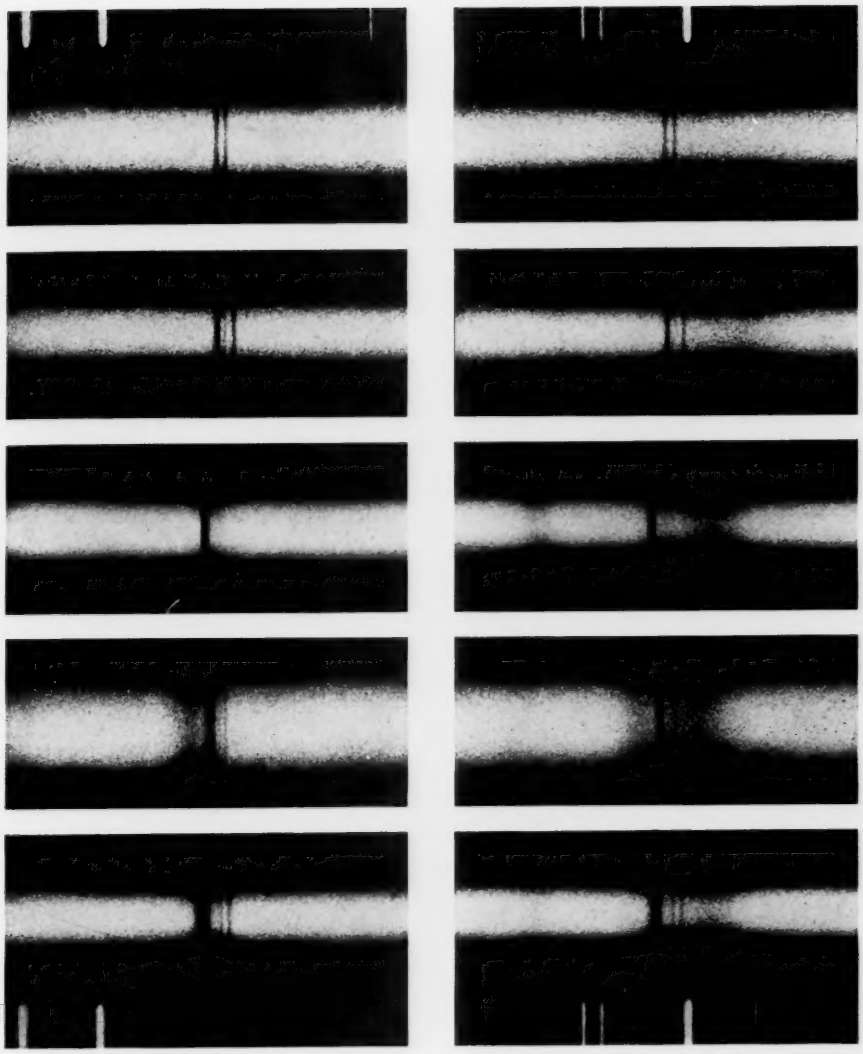

INTERSTELLAR LINES WITH HIGH DISPERSION

Calcium K (*left*) and H (*right*). From top to bottom: κ Aquilae, HD 167264, χ Aurigae, μ Sagittarii, HD 199478.

PLATE X

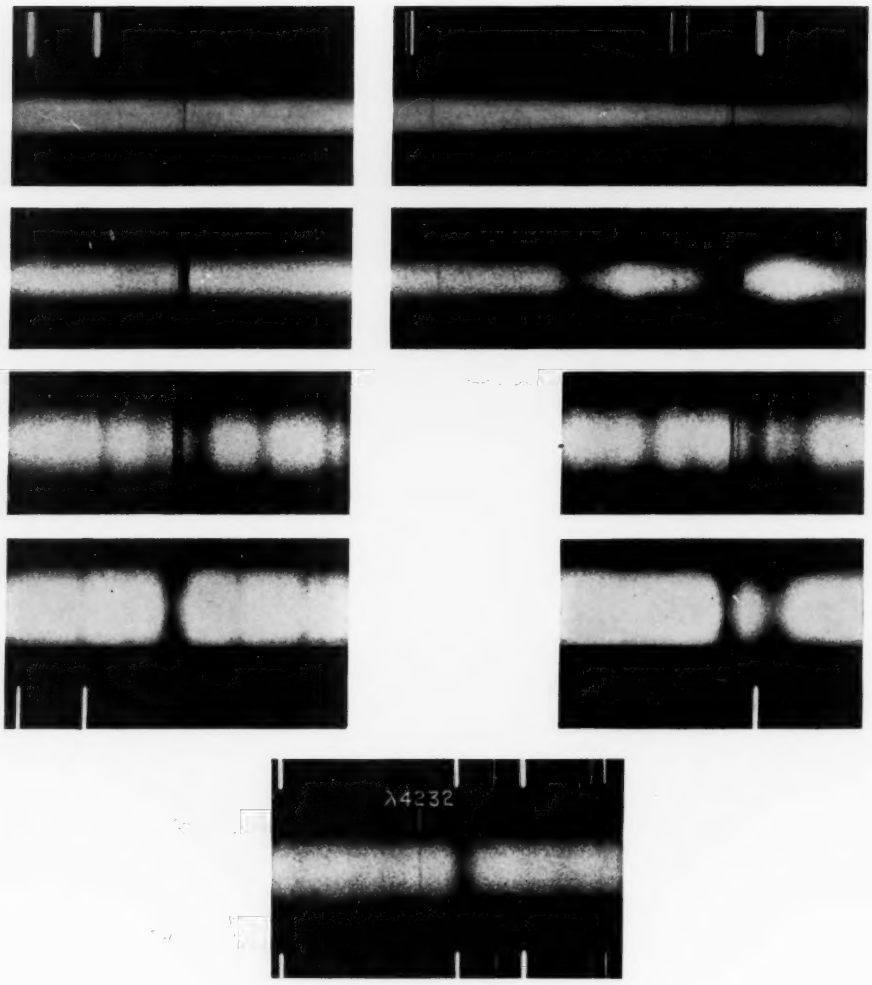

INTERSTELLAR LINES WITH HIGH DISPERSION

From top to bottom:

ζ Ophiuchi:	left, K; right, λ 3957 and H
P Cygni:	left, K; right, λ 3957 and H
υ Sagittarii:	left, K; right, H
α Cygni:	left, K; right, H
υ Sagittarii:	λ 4232

TABLE 1

INTERSTELLAR H AND K LINES

NAME OR HD No.	1900 R.A.	1900 Dec.	m	TYPE	b	l	INTENSITY K	INTENSITY H	VELOCITY	RESIDUAL VELOCITY
									km/sec	km/sec
o Per	3h38m	+31° 58′	3.9	B2	−17°	128°	15	8	+9.5	+2.9
η Tau	3 42	+23 48	3.0	(B5p)	−23	134	2	1	+15.5	+6.5
ζ Per	3 48	+31 35	2.9	cB1	−16	130	15	8	+12.0	+4.8
ξ Per	3 52	+35 30	4.0	O7n	−12	128	18, 2	10, 1	+9.5, +25.4	+3.3, +19.2
η Ori	5 19	− 2 29	3.4	B0	−19	172	5, 1	3, 1	+7.2, +24.2	−10.2, +6.8
χ Aur	5 26	+32 7	4.9	cB3	0	143	9, 12	5, 7	−0.2, +10.6	−9.4, +1.4
δ Ori*	5 27	− 0 22	2.5	B0	−16	171	5	3	+13.2	−4.0
λ^1 Ori	5 30	+ 9 52	3.7	O8	−10	163	6, 2, 9	4, 1, 6	+5.6, +15.0, +23.3	−9.6, −0.2, +8.1
ι Ori	5 31	− 5 59	2.9	O8	−18	177	2, 1, 5	1, <1, 3	+7.4, +22.7, +30.9	−10.7, +4.6, +12.8
ϵ Ori	5 31	− 1 16	1.8	B0	−16	173	2, 4, 8	1, 2, 5	−0.3, +10.2, +25.4	−17.6, −7.1, +8.1
σ Ori	5 34	− 2 39	3.8	B2	−16	175	2, 6	1, 3	+1.0, +22.9	−16.6, +5.3
ζ Ori	5 36	− 2 0	2.0	B0n	−15	175	3, 6	1, 4	−4.7, +21.1	−22.2, +3.6
κ Ori*	5 43	− 9 42	2.2	cB0	−17	182	12, 4, 2	6, 3, 1	−1.7, +18.4, +31.4	−20.5, −0.4, +12.6
χ^2 Ori*	5 58	+20 8	4.7	cB1eα	0	158	40, 2	25, 1	+12.5, +28.6	−0.3, +15.8
ν Ori*	6 2	+14 47	4.4	(B2)	− 2	162	6, 2	3, 1	+15.6, +30.4	+1.5, +16.3
ξ Ori*	6 6	+14 14	4.4	(B3)	− 1	164	6, 1	3, <1	+13.1, +33.5	−1.1, +19.3
ρ Leo	10 28	+ 9 49	3.8	cB0	+54	204	7, 2, 3	4, 1, 2	−13.0, −3.5, +16.4	−17.9, −8.4, +21.3
π Sco	15 53	−25 50	3.0	B0n	+19	315	2	1	−24.8	−15.8
δ Sco	15 54	−22 20	2.5	B1n	+22	318	1, 6	<1, 3	−29.2, −13.6	−19.3, −3.6
β^1 Sco	16 0	−19 32	2.9	B1	+23	321	7	4	−11.0	−0.2
ω^1 Sco	16 1	−20 24	4.1	B2n	+22	321	1, 4	<1, 2	−28.8, −9.5	−18.1, +1.2
ν Sco	16 6	−19 12	4.3	B3n	+22	323	<1, 10	<1, 6	−11.7	−0.7
σ Sco	16 15	−25 21	3.1	B1	+17	319	8	4	−8.5	+1.3
ρ Oph Br	16 20	−23 13	5.2	B3n	+17	321	7	4	−9.7	+0.8
ρ Oph Ft	16 20	−23 13	5.9	B3n	+17	321	6	4	−9.8	+0.7
χ Oph*	16 21	−18 14	4.8	B3e	+20	325	3, 6	2, 4	−27.5, −11.1	−15.7, +0.7
ζ Oph	16 32	−10 22	2.7	B0n	+23	334	2, 8	1, 4	−30.7, −16.3	−16.6, −2.2
66 Oph*	17 55	+ 4 22	4.8	B5ne	+12	359	2, 7	1, 4	−36.6, −19.4	−18.6, −1.4
67 Oph	17 56	+ 2 56	3.9	cB7	+12	358	25, 2	10, 1	−15.4, +2.5	+2.4, +20.3
165174*	18 0	+ 1 55	6.1	B2n	+10	357	30, 2	15, 1	−10.8, +12.6	+6.8, +30.2
102 Her	18 4	+20 48	4.3	B2	+17	15	10, 2	5, 1	−25.7, −7.0	−6.0, +12.7
μ Sgr	18 8	−21 5	4.0	cB8eα	+ 3	338	20, 2, 3	9, 1, 2	−8.2, +11.2, +27.1	+4.3, +23.7, +39.6
15 Sgr	18 9	−20 46	5.4	B0	+ 3	338	10, 2, 5	6, 1, 3	−9.3, +8.4, +28.9	+3.2, +20.9, +41.4
ν Sgr	19 6	−16 9	4.6	(B8p–F2p)	+15	350	10, 4	6, 2	−11.4, +4.2	+1.7, +17.3
8 Cyg*	19 28	+34 14	4.8	B5	+ 6	36	4, 2	2, 1	−44.2, −15.0	−25.4, +3.8
κ Aql	19 32	− 7 15	5.0	B0n	+14	0	9, 5	4, 3	−13.1, +8.2	+0.4, +21.7
187879*	19 47	+40 20	5.6	B2	+ 6	43	3, 6, 2	2, 4, 1	−29.7, −16.6, −7.4	−11.5, +1.6, +10.8
190603	20 1	+31 56	5.7	cB0eβ	0	37	15, 20	8, 10	−20.0, −2.2	−2.0, +15.8
P Cyg*	20 14	+37 43	4.9	B1eq	0	43	6, 15, 2	4, 7, 2	−18.5, −10.8, −0.2	−1.0, +6.7, +17.3
α Cyg*	20 38	+44 55	1.3	cA2eα	+ 1	52	3, 15	2, 10	−24.7, −12.3	−8.2, +4.2
55 Cyg	20 46	+45 45	4.9	cB2eα	+ 1	54	20, 10	10, 4	−15.6, −7.4	+0.6, +8.8
199478*	20 52	+47 2	5.8	cB8eα	0	55	15, 20, 3, 5	8, 10, 2, 3	−19.5, −8.7, +24.9, +43.8	−3.6, +7.2, +40.8, +59.7
199579	20 53	+44 33	6.0	O6	− 1	53	20	10	−14.2	+1.7
σ Cyg*	21 14	+38 59	4.3	cA0	− 8	52	25	15	−12.9	+2.3
A Cyg*	21 15	+43 31	5.1	O8n	− 5	56	35	20	−14.0	+1.1
π Aqr	22 20	+ 0 52	4.6	B1ne	−46	35	8, 2	5, 1	−14.1, −3.9	−6.6, +3.6
8 Lac Br	22 31	+39 7	5.8	B3ne	−17	64	2, 12	1, 7	−31.2, −13.9	−19.8, −2.5
10 Lac	22 35	−38 32	4.9	O9	−17	65	3, 2, 8	2, 1, 5	−36.3, −27.3, −12.5	−25.1, −16.1, −1.3
12 Lac*	22 37	+39 42	5.2	(B2)	−17	65	2, 12	1, 6	−33.4, −11.6	−22.3, −0.5
16 Lac N*	22 52	+41 4	5.5	B3	−17	68	2, 10	1, 4	−38.1, −14.6	−27.7, −4.2

*NOTES ON K AND H LINES IN TABLE 1

δ	Orionis	Broad and probably double or multiple
κ	Orionis	Violet component broad
χ^2	Orionis	Violet component broad
ν	Orionis	Red component broad
ξ	Orionis	Fringe on violet component
χ	Ophiuchi	Violet component broad
66	Ophiuchi	Fringe on red component
HD	165174	Violet component broad
8	Cygni	Not fully separated
HD	187879	Not fully separated
P	Cygni	Components 1 and 2 not fully separated
α	Cygni	Superposed on stellar lines
HD	199478	Third component double; probably 5 components
σ	Cygni	Broad, probably double
A	Cygni	Broad, probably double
12	Lacertae	Both components broad; probably 4 components
16	Lacertae N	Both components broad; probably 4 components

4. A rough comparison of the K line in the two groups of stars of apparent magnitude brighter than 4.0 and fainter than 4.0, respectively, shows about 50 per cent greater intensity for the fainter and more distant stars. A more accurate comparison is not warranted by the estimated intensities.

5. Several stars are of exceptional interest:

η Tauri	This is the first observation of interstellar lines in Alcyone
λ^1 Orionis	An excellent case of triple components
κ Orionis	The width of the violet component indicates probable duplicity. If so, K and H are quadruple
ρ Leonis	K and H found double by Beals. Violet component itself double
υ Sagittarii	K and H well-separated doublets occasionally standing free of the stellar lines according to the phase of velocity-variation of the star
P Cygni	K and H triple, but violet component not fully resolved
HD 199478	Almost certainly 5 components, but components 3 and 4 too close to measure. Separation of components 1 and 5 is 0.82 A
10 Lacertae	K and H interesting triplets. Components 1 and 2 close but resolved

The sharpness and narrowness of the individual components which have been measured make it clear that the interstellar clouds producing them are discrete and subject to little internal motion; and the assumption that when H and K are fairly broad the width is due to unresolved components seems to be justified. Hence, a comparison of the radial velocities of the components affords some basis for conclusions regarding the general distribution of the gaseous clouds.

In the direction of the brighter stars in Perseus there appears to be a general cloud with a residual velocity of about +5 km/sec. In addition, a thinner and probably smaller cloud is shown by the results for ξ Persei. Throughout a large region in Scorpius and Ophiuchus a cloud with a residual velocity of about 0 km/sec seems to persist. A few stars in this region show the presence of a thin cloud (judged by the intensity of the corresponding component) which covers a wide area and has a velocity of approximately −17 km/sec. This seems to be the only cloud in front of π Scorpii.

Two of three stars observed in Sagittarius give accordant results. The principal cloud has a residual velocity of +4 km/sec, a secondary cloud about +22 km/sec, and a third cloud +40 km/sec. It is possible that the first two clouds extend to the third star, υ Sagittarii, although it lies at a considerable distance in both latitude and longitude.

The four stars observed in Lacerta give analogous results. A primary cloud with a residual velocity of about −2 km/sec covers the area, and a second thinner cloud with an average motion of about −24 km/sec also lies in the direction of the stars. The complexity of the lines in the spectra of three of the four stars may modify these conclusions to some extent.

The situation regarding interstellar clouds in Orion and Cygnus is much more complicated. Especially in the direction of Orion, the clouds seem to be more broken and intermingled and perhaps more turbulent than in most other parts of the sky. The six stars in or close to the belt of Orion indicate the presence of two clouds, the more prominent with a velocity of about +7 km/sec, and the other roughly −15 km/sec.[5] In both clouds, however, the dispersion in velocity is abnormally large. At least two other clouds, apparently thin and small in area, are also present. It is of interest to note the abrupt change in the clouds in passing from the belt of Orion to the more northerly stars: χ^2, ν, and ξ Orionis.

Practically all the stars observed in Cygnus show the presence in the line of sight of an extensive cloud, probably of great thickness because of the intensity of the lines, with

[5] These were noted by Sanford (n. 2).

a velocity of about +1 km/sec. Among these stars is α Cygni. The existence of one or two other clouds is indicated by the results.

This brief outline of the distribution of some of the interstellar calcium clouds is, of course, subject to uncertainties imposed by the resolving-power of the spectrograph and to the differences in velocity which may occur within an individual cloud. Several broad lines which are doubtless unresolved doublets or multiplets are indicated by notes in Table 1.

Remarkably high residual radial velocities are shown by a few of the clouds: +40 km/sec for a cloud in front of the two neighboring stars μ and 15 Sagittarii, and +41 km/sec and +60 km/sec for two clouds defined by lines in the spectrum of HD 199478 in Cygnus. In each star the lines involved are of moderate intensity and quite definite. Velocities of this order among interstellar clouds would hardly be expected.

ADDITIONAL INTERSTELLAR LINES

Many of the stars listed in Table 1 show one or more of the recently discovered interstellar lines, identified, for the most part, with *CN* I, *CH* I, or *CH* II. As is to be expected, the greatest number of lines has been found in the spectra of stars which have been studied most extensively, especially of those photographed on fine-grained and contrasty plates. Examples are ζ Ophiuchi, ζ Persei, χ^2 Orionis, and 55 Cygni. Table 2 lists the most important lines and their intensities in the stars observed. The letter "b" following the intensity indicates a broad line; "tr," a trace; a dash, that the line is not seen with certainty.

The only star in which λ 3720 (and the fainter line λ 3860) of *Fe* I has been observed in fair intensity is 55 Cygni. Traces are found in two other stars. Like λ 4227 of *Ca* I, the *Fe* I lines are most likely to occur in stars with very strong H and K. On the other hand, lines due to *CH* I, *CH* II, and *CN* I are often strongest in stars with H and K of moderate intensity. The progression in intensity of the three *CH* II lines λλ 3745, 3957, and 4232 is as it should be on theoretical grounds. One additional fact of interest is the marked reversal in intensity of λ 4300 of *CH* I and λ 4232 of *CH* II in different stars, often near one another. The absence of these lines in practically all the stars in Orion is noteworthy.

Although most of the stars in Table 2 show complex interstellar H and K, in no star has it been possible to measure any of the additional lines as double. This is not surprising, since, if any conclusion can be drawn from the relative intensities of the components of H and K, in most stars the components of the additional lines should be too faint for measurement. It is of interest, however, to examine in a few favorable stars, showing at least two components of H and K of fairly strong intensity, the wave lengths of the additional lines in an attempt to learn in which cloud they originate.

The stars selected for this purpose are χ Aurigae, χ Ophiuchi, υ Sagittarii, P Cygni, 55 Cygni, and HD 199478, all of which show the additional lines and moderately intense components of H and K. The displacements of the principal components of H and K in km/sec, given as residual velocities in Table 1, are compared with the velocities obtained directly from the displacements of the additional lines from their normal wave lengths. These wave lengths have been determined from measurements of about 10 stars which show H and K in moderate strength either with very faint components or with none at all. The displacements of H and K with reversed sign have been applied to the measured wave lengths of the additional lines; and means of all the resulting values have been taken, weighted according to the number of spectrograms of each star. The plates of high contrast of ζ Ophiuchi have been assigned exceptionally high weight. The normal wave lengths derived in this way depend, of course, upon the wave lengths of H and K in the *Revised Rowland Table*, which are slightly longer than most laboratory determinations.

TABLE 2

INTENSITIES OF ADDITIONAL LINES

Name or HD Number	3720 *Fe* I	3745 *CH* II	3874.0 *CN*	3874.6 *CN*	3886 *CH*	3957 *CH* II	4226 *Ca* I	4232 *CH* II	4300 *CH*
o Per	tr	—	—	1	—	tr	—	1	2
η Tau	—	—	—	—	—	—	—	—	—
ζ Per	—	—	1	3	1	—	—	tr	3
ξ Per	—	1	—	tr	tr	2	—	4b	2b
η Ori	—	—	—	—	—	—	—	—	—
χ Aur	—	—	—	1	—	1b	tr	2b	2b
δ Ori	—	—	—	—	—	—	—	—	—
λ^1 Ori	—	—	—	—	—	—	—	—	—
ι Ori	—	—	—	—	—	—	—	—	—
ϵ Ori	—	—	—	—	—	—	—	—	—
σ Ori	—	—	—	—	—	—	—	—	—
ζ Ori	—	—	—	—	—	—	—	—	—
κ Ori	—	—	—	—	—	—	—	—	—
χ^2 Ori	tr	tr	—	—	—	1	2	2	3
ν Ori	—	—	—	—	—	—	—	—	—
ξ Ori	—	—	—	—	—	—	—	—	—
ρ Leo	—	—	—	—	—	—	—	—	—
π Sco	—	—	—	—	—	—	—	—	—
δ Sco	—	—	—	—	—	—	—	—	—
β^1 Sco	—	—	—	—	—	—	—	—	—
ω^1 Sco	—	—	—	—	—	—	—	—	—
ν Sco	—	—	—	—	—	—	—	—	—
σ Sco	—	—	—	—	—	—	—	—	—
ρ Oph Br	—	—	—	tr	—	tr	—	2	3
ρ Oph Ft	—	—	—	tr	—	tr	—	1	2
χ Oph	—	—	—	tr	tr	tr	—	2	4
ζ Oph	—	2	1	3	2	4	—	5	4
66 Oph	—	—	—	—	—	—	—	—	tr
67 Oph	—	—	—	—	—	—	—	—	—
165174	—	—	—	—	—	—	—	tr	—
102 Her	—	—	—	—	—	—	—	—	—
μ Sgr	—	—	—	—	—	1b	—	2b	tr
15 Sgr	—	—	—	—	—	—	—	tr	1b
υ Sgr	—	—	—	—	—	1	—	2	—
8 Cyg	—	—	—	—	—	—	—	—	—
κ Aql	—	—	—	—	—	—	—	tr	—
187879	—	—	—	—	—	—	—	—	—
190603	—	—	—	tr	—	tr	tr	3b	tr
P Cyg	—	tr	—	tr	—	2	—	4	tr
α Cyg	—	—	—	—	—	—	—	—	—
55 Cyg	1	1b	—	tr	1	2	1	4b	2b
199478	—	—	—	—	—	1b	—	2	1
199579	—	—	—	—	—	—	—	tr	1b
σ Cyg	—	—	—	—	—	—	—	—	—
A Cyg	—	—	—	—	—	—	—	—	1b
π Aqr	—	—	—	—	—	—	—	—	—
8 Lac Br	—	—	—	—	—	—	—	tr	—
10 Lac	—	—	—	—	—	—	—	—	—
12 Lac	—	—	—	—	—	—	—	—	—
16 Lac N	—	—	—	—	—	—	—	—	—

Table 3 contains the results of the comparison. The first two rows of figures below the names of the stars give the mean values of the residual radial velocities of the two principal components of H and K together with the intensities estimated for K. These data are from Table 1. The remaining rows of Table 3 give the residual radial velocities for the more prominent additional lines as derived from the normal wave lengths of the first column.

TABLE 3

DISPLACEMENTS OF ADDITIONAL LINES (KM/SEC)

Lines	χ Aur	χ Oph	υ Sgr	P Cyg	55 Cyg	HD 199478
Components of K and H	−9.4(9) +1.4(12)	−15.7(3) + 0.7(6)	+ 1.7(10) +17.3(4)	−1.0(6) +6.7(15)	+0.6(20) +8.8(10)	−3.6(15) +7.2(20)
3745.330 *CH* II	.....	.....	.....	+2.1	.....	.....
3874.634 *CN* I	−0.4	.....	.....	.....	+2.0	.....
3957.712 *CH* II	−4.4	− 0.3	+ 0.6	+3.5	+0.8	−3.7
4226.742 *Ca* I	+0.8	.....	.....	.....	−0.7	.....
4232.573 *CH* II	−3.0	+ 1.8	− 0.2	+2.5	−0.8	−2.2
4300.338 *CH* I	+0.6	− 0.2	.....	.....	−0.1	−4.4

A comparison of the results in Table 3 shows that in χ Aurigae the interstellar cloud giving rise to the second and stronger component of K and H also produces *CN* I λ 3874, *Ca* I λ 4227, and *CH* I λ 4300. The two lines of *CH* II, however, λ 3957 and λ 4232, correspond closely to the mean of the values for K and H, and it is probable that both clouds contribute to the formation of these lines. In both χ Ophiuchi and υ Sagittarii the values from the lines listed correspond to the cloud giving the stronger calcium component, and the same is true for the five lines of 55 Cygni. In P Cygni the components of H and K are very close and only occasionally resolved. It appears that both clouds are involved in the formation of the three *CH* II lines measured in this star. Finally, the results for the lines of HD 199478 indicate that they originate in the cloud which produces the first and slightly fainter of the two major components of complex K and H. These results seem to be quite in harmony with those of Table 2, which show marked differences in the intensities of the various interstellar lines according to the clouds in which they occur.

THE DIRECTION OF ROTATION IN SPIRAL NEBULAE*

EDWIN HUBBLE
Mount Wilson Observatory
Received January 9, 1943

ABSTRACT

Fifteen spirals are now available for which the sense of the spiral pattern and the sense of the spectrographic rotation are known and in which there is conspicuous dissymmetry of obscuration with respect to the major axes of the projected images. On the assumption that dissymmetry of obscuration is a reliable criterion of tilt, all fifteen spirals are rotating in the same direction with respect to the spiral patterns.

In four nebulae—NGC 3190, 4216, 4258, and 4527—the nearer side and, consequently, the actual direction of rotation are unambiguously determined by dark lanes silhouetted against the nuclear bulges. In these nebulae, and by inference in the other eleven as well, the arms are trailing behind the nuclear regions. The results justify the provisional working hypothesis that the arms are trailing in all spirals. As a corollary it appears that the greater general obscuration in the projected image of a spiral identifies the nearer side of the nebula.

The problem of the origin and development of spiral arms in extragalactic nebulae will remain in the realm of speculation until certain fundamental data are established by empirical investigations. One, and perhaps the most essential, of these data is the direction of rotation of the nebulae with respect to the spiral pattern. There are only three possible answers to the question—the arms may be trailing behind the central regions in all spirals, the arms may be leading in all of them, or the direction may vary from nebula to nebula. Theoretical discussions, as is customary under such conditions, have used each of these possible assumptions at one time or another. Actually, the two limiting cases—all arms trailing and all arms leading—now serve to distinguish two competing groups of theories.

The empirical solution of this apparently simple problem is curiously difficult. The nebulae are observed as projected images; and the question of the tilt, which is an essential element in the problem, has been controversial. V. M. Slipher in his great pioneer investigations of the spectra of extragalactic nebulae detected rotation in several spirals and presented evidence suggesting that these systems were all rotating in the same direction. Furthermore, on the plausible assumption that the heavier obscuration should be observed on the nearer half of the projected image, he concluded that the arms were trailing. The direction was opposite to that indicated by current theories of spiral structure and by the only other observational evidence then available, namely, the measures of angular rotations. This particular interpretation of the latter measures has since been abandoned, but meanwhile Lindblad had developed plausible criteria of tilt which directly contradicted those adopted by Slipher. The same phenomena of obscuration were presented as evidence that the arms are not trailing but leading. Thus the direction of rotation continued to be an open question with the criteria of tilt as the controversial element.

The writer has re-examined the problem of tilt in the course of a study of the extensive collection of direct photographs of nebulae assembled with the large reflectors on Mount Wilson. The collection includes all the Shapley-Ames nebulae brighter than the thirteenth magnitude and north of declination $-30°$, those brighter than 12.5 between $-30°$ and $-42°$, and a few thousand of the fainter Dreyer nebulae scattered over the sky. Therefore it seems unlikely that any significant example among the brighter nebulae has been overlooked.

The survey led to a reformulation of the criteria of tilt and to the recognition of four

* *Contributions from the Mount Wilson Observatory, Carnegie Institution of Washington*, No. 674.

spirals in which the direction of rotation could be determined unambiguously. Spectrographic investigations of these test objects, together with a few other border-line cases, led to the following results.

Spectrographic rotation has now been observed in fifteen spirals in which the arms can be traced and in which dissymmetry of obscuration offers a general criterion of tilt.

The consistent application of this general criterion indicates that all these nebulae are rotating in the same direction. The arms are either *all* trailing or *all* leading the nuclear regions.

In four of the spirals special criteria may be applied which indicate tilt without ambiguity. In these spirals the arms are trailing.

Therefore, Slipher's criterion of tilt and direction of rotation is established, and we may assume, as a working hypothesis, that the arms are trailing in all spirals.

FORMULATION OF THE PROBLEM

Spiral nebulae are evidently figures of rotation. This interpretation of the direct photographs is fully confirmed by the distribution of radial velocities observed in many of the systems. The determination of the direction of rotation with respect to the spiral pattern involves three data, namely, the sense of the spectrographic rotation, the sense of the spiral pattern, and the sense of the tilt.

The sense of the spectrographic rotation indicates the end of the major axis of the projected image that is approaching with respect to the nucleus and the end that is receding. This datum is readily determined from the inclination of spectral lines when the slit is placed along the major axis of a nebula whose fundamental plane is tilted to the line of sight by an angle of not more than about 60°.

The sense of the spiral pattern distinguishes "right-handed" spirals, namely, those in which an object traveling inward along one of the arms would move in a clockwise direction, from "left-handed" spirals. This datum is derived by inspection of photographs of spirals in which the tilts are sufficiently large for the arms to be actually traced.

The sense of the tilt distinguishes the end of the minor axis of a projected image that represents the nearer rim of the nebula from the end that represents the farther rim. Consider a photograph (north to the top, west to the right) of a right-handed spiral elongated in an east-west direction. Suppose the west end is approaching and the east end is receding with respect to the nucleus. The direction of rotation in the nebula will evidently be such that the arms are trailing if the north edge of the image represents the farther side of the nebula and such that the arms are leading if the north edge represents the nearer side. Thus the tilt is an essential datum for the problem of rotation. Unlike the two other data, it is not directly observed but is inferred from the interpretation of observations.

The only criteria of tilt now available are furnished by obscuration. Some spirals exhibit heavy peripheral bands of dark material which, when the fundamental planes are nearly in the line of sight, are sharply silhouetted against the bright central regions of the nebulae. In these spirals the dark bands serve as a primary criterion of tilt and identify the nearer side of the nebula without ambiguity. NGC 4594 is an example.

The validity of this primary criterion has never been seriously questioned, but the application, in general, is restricted to nebulae oriented so nearly edge-on that the spiral pattern cannot be traced with confidence. As the tilts increase, the patterns emerge; but the peripheral dark bands move off the nuclear regions, and the criterion loses its primary validity. Thus the search for test objects for the direction of rotation has been a search for critical tilts—large enough to reveal the spiral patterns, yet so small that peripheral bands are still silhouetted against the nuclear bulges. No such cases were known until the recent survey of the entire Mount Wilson collection of photographs brought to light a single nebula that fully meets the specifications (see Pl. XI). This object—NGC 3190 (Sa)—exhibits the unusual phenomenon of a peripheral band that is itself tilted to the

fundamental plane, and the orientation is such that the band crosses the nuclear bulge, although the plane is sufficiently tilted to show the spiral pattern clearly.

Meanwhile, efforts were made to establish valid secondary criteria of tilt by means of general dissymmetry of obscuration. The attempts began shortly after evidence of rotation was first observed, but the results were not established beyond controversy.

The study of spectrographic rotation in extragalactic nebulae falls into two periods—an earlier period from 1913 to 1922 and a later period, from 1934 onward. The first announcements were published in 1914 by V. M. Slipher and Max Wolf. The latter reported inclined lines in the spectrum of M 81, indicating rotation of the order of 100 km/sec near the nucleus in the sense that the eastern side is approaching.[1] Wolf made no further contribution to the subject.

Slipher[2] reported inclined lines in NGC 4594 without other details. He also stated that indications of inclined lines were found in other spirals, including M 31, and that a definite answer to the "interesting question" could be expected after further observations with improved equipment. His later results are summarized in two contributions, the first published in 1917 and the last in 1921.[3]

In the 1917 paper Slipher described the phenomenon of edge-on spirals with peripheral dark bands silhouetted against the nuclei and then continued: "If now we imagine we view such a nebula from a point somewhat outside its plane the dark band would shift to the side and render the nebula unsymmetrical—the deficient edge being, of course, the one nearer us. This appears to be borne out by the nebulae themselves for the inclined ones commonly show this typical dissymmetry. Thus we infer their deficient side to be the one toward us." He presented six spirals which, he considered, met these requirements and in which he had observed inclined lines, namely, NGC 224, 3623, and 4594, together with three others, NGC 2683, 3627, and 5005, which "showed rotation . . . . less well." Applying his criterion of tilt, he concluded that all these objects are rotating in the same direction with respect to the spiral arms (except NGC 4594, which "is not inclined enough to show clearly the arms") and that the arms are trailing. "The central part . . . . turns into the spiral arms as a spring turns in winding up."

The final discussion in 1921 was published in abstract form, but the report is not very clear. The criteria of tilt were described as before, and "details were given and slides shown of the spectra of NGC 221, 224, 1068, 2683, 3623, and 4594, there being evidence of rotation in each case." The report then stated that "the six nebulae discussed all agree in showing rotation in the same direction relative to the spiral arms. The direction is that in which the arbor of a spiral spring turns when the spring is being wound up."

Two spirals previously mentioned—NGC 3627 and 5005—were omitted in the final

[1] *Vierteljahrsschrift der Astr. Gesellschaft*, **49**, 162, 1914. Further details furnished by Dr. Wolf are given by Lundmark, *Arkiv för mat., astr. och. fys.*, **21**, No. 10; *Upsala Medd.*, No. 40, 1928.

[2] *Lowell Obs. Bull.*, No. 62, 1914.

[3] "Nebulae" (published in full), *Proc. Amer. Phil. Soc.*, **56**, 403, 1917; "Spectrographic Observations of the Rotation of Spiral Nebulae" (abstr.), *Pub. A.A.S.*, **4**, 232; *Pop. Astr.*, **29**, 272, 1921. Other contributions in which Slipher mentions the subject are as follows: *Lowell Bull.*, No. 80, 1917, a detailed discussion of NGC 1068, the only instance in which Slipher specifically states the sense of spectrographic rotation (NE end is approaching); three papers published in abstract, *Pub. A.A.S.*, **3**, 98 and 223, and **4**, 284, and reprinted in *Pop. Astr.*, **23**, 21, 1915; **25**, 36, 1917; **30**, 9, 1922. The first of the abstracts confirmed the rotation of NGC 4594 and estimated the velocity at about 100 km/sec at 20″ from the nucleus; the second announced inclined lines in M 31, 65, and 66, and indications of inclined lines in other unspecified spirals; the third mentioned inclined lines in NGC 2841 and 3034, "implying rotation about an axis such as has been established here for a number of other spirals" (however, NGC 3034 is an irregular nebula, not a spiral).

Following Slipher's announcements, F. G. Pease published detailed measures of the rotation in the central regions of NGC 4594 (*Mt. W. Communication*, No. 32; *Proc. Nat. Acad*, **2**, 517, 1916, containing the first published announcement of the sense of the rotation), and of M 31 (*Mt. W. Communication*, No. 51; *Proc. Nat. Acad.*, **4**, 21, 1918). The two papers contained the only reliable quantitative data on rotations published during the early period of the investigations.

PLATE XI

NGC 3190 (*above*); NGC 4216 (*below*)

PLATE XII

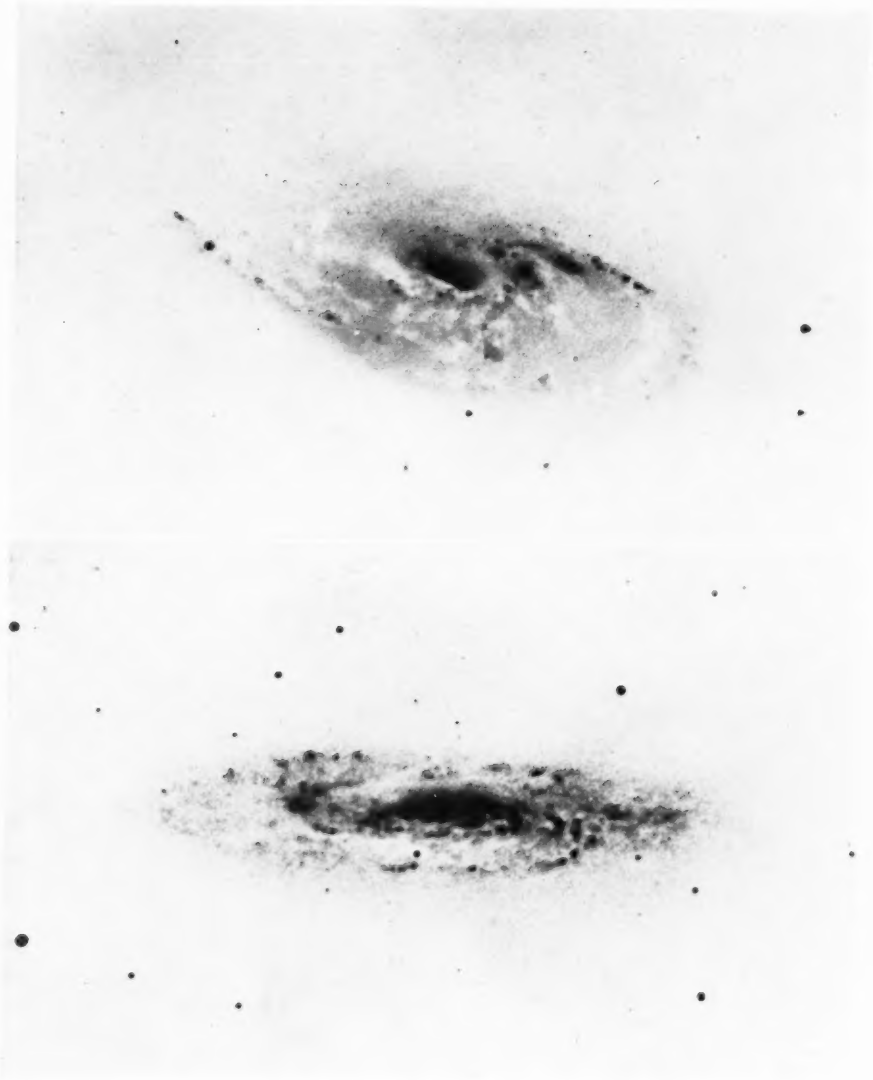

NGC 4258 (*above*); NGC 4527 (*below*)

PLATE XIII

NGC 3623 (*above*); NGC 7331 (*below*)

Two examples of dissymmetry of obscuration which serves as a criterion of tilt

PLATE XIV

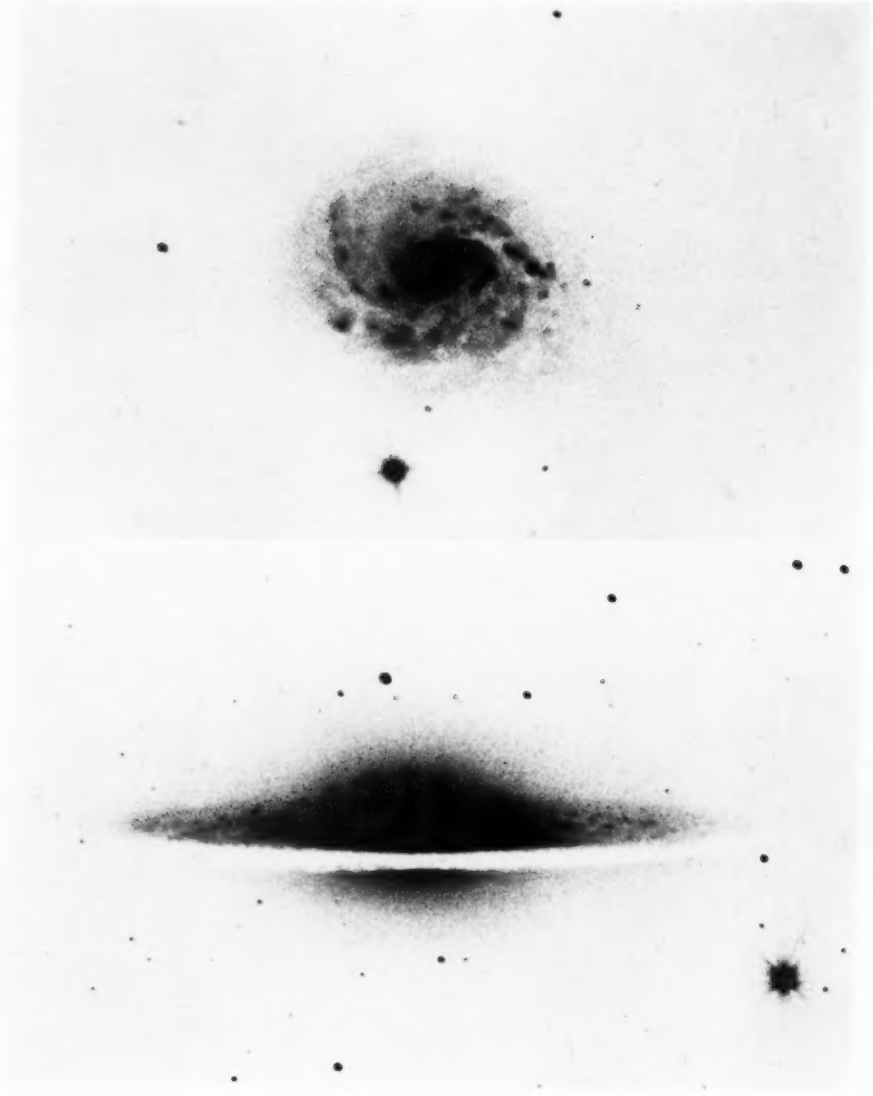

NGC 1068 (*above*); NGC 4594 (*below*)

discussion. The reasons for the omission were not stated, but one of the objects, NGC 3627, has little weight, owing to the almost negligible dissymmetry of obscuration. Moreover, NGC 221 is not a spiral, 1068 shows no appreciable dissymmetry of obscuration (see Pl. XIV), and, in 4594, the direction of the arms cannot be traced on either long or short exposures obtained with the 100-inch telescope under excellent observing conditions (see Pl. XIV).

The two reports, as published, seem to establish a uniform direction of rotation on the basis of the secondary criterion of tilt for the three spirals, NGC 224, 2683, and 3623.[4] NGC 1068 and 4594 are indeterminate, and 3627 and 5005 must be regarded as uncertain, at least until the reports are clarified. The actual direction of rotation depends upon the interpretation of the criterion of tilt, and for this purpose the strongest evidence is furnished by NGC 2683. These results, together with Pease's detailed measures of rotation in the central regions of NGC 4594 and 224, constituted the first phase of the investigations.

The second phase opened with Lindblad's[5] alternative interpretation of the secondary criterion of tilt. He called attention to various full-face spirals (e.g., M 51), in which the bright spiral arms are accompanied by dark lanes on the inner or concave sides, and pointed out that, if these nebulae were seen nearly edge-on, the dark lanes would presumably be more conspicuous on the farther sides of the nuclei than on the nearer sides. Moreover, dark material scattered through the central bulge of a tilted nebula would evidently obscure the farther side and not the nearer side. On these grounds he concluded that the greater general obscuration and the more pronounced "secondary lanes" (interior dark lanes as distinguished from the primary peripheral bands) represented the farther side of a nebula seen nearly edge-on. The two opposite interpretations, by Slipher and by Lindblad, were both plausible, and neither could be established or rejected on the basis of data then available. Slipher's nebulae might all be rotating in the same direction, but that direction was now a controversial question.

The survey of the Mount Wilson photographs has contributed nothing to the interpretation of general obscuration. However, the examination of interior or secondary dark lanes has led to a new criterion of tilt. The lanes are sometimes sharply silhouetted against the central bulges of the nebulae, and under these circumstances evidently lie on the nearer sides of the nuclei. The criterion is, in effect, an extension of the primary criterion of peripheral bands. Consider an edge-on nebula in which a peripheral band is silhouetted against the central bulge. As the tilt is steadily increased, the band normally moves off the bulge before the spiral pattern emerges. Interior lanes, however, if present, will lag behind the peripheral band and may still fall within the critical region even when the spiral pattern is clearly revealed.

The latter situation has been found in the three nebulae,[6] NGC 4216, 4258, and 4527

[4] NGC 2841 might be added to the list because inclined lines were later reported by Slipher (*Pub. A.A.S.*, **4**, 284; *Pop. Astr.*, **30**, 9, 1922), "implying rotation . . . . such as has been established here for a number of other spirals." The sense of the rotation for NGC 2841 was not specifically mentioned, but presumably a discrepancy, if it existed, would have been emphasized.

[5] The criterion seems to have been first discussed by Lindblad in *Arkiv för mat., astr. och fys.*, **24**, No. 21; *Stockholm Medd.*, No. 14, 1934. The subject was further discussed in subsequent contributions, of which the most recent is the paper "On the Interpretation of Spiral Structure in the Nebulae," *Ap. J.*, **92**, 1, 1940.

Lindblad's discussion, together with a growing interest in the dynamics of stellar systems and in particular a rapid development of small-scale spectrographic equipment, introduced the second phase of the investigation, which is still under way with increasing momentum. The observational results, which have all been obtained at the Lick and Mount Wilson observatories, include numerous determinations of the sense of the spectrographic rotation together with the detailed pattern of rotation in various nebulae at different stages in the sequence of classifications.

[6] The prints on Pl. XI are dense in order to show the outer regions which indicate the spiral patterns (left-handed in both nebulae). Lighter prints, showing the silhouettes of the dark lanes to better ad-

(see Pls. XI and XII). In each one, nearly half of the central lens is blotted out by a heavy dark lane with a sharply defined edge, just beyond which the nucleus can be seen.

These three nebulae, together with NGC 3190 (see Pl. XI), to which the primary criterion of tilt is applicable, appear to be the only definitive test objects among the brighter nebulae in the northern sky. A spectrogram of NGC 4258, obtained in April, 1940, indicated that the arms are trailing.[7] A spectrogram of NGC 3190 was also obtained about the same time, but, owing to poor weather, the plate was weak, and the evidence for rotation was inconclusive. An arrangement was then made with Dr. N. U. Mayall of the Lick Observatory, by which this and other nebulae would be observed at either or both observatories at the earliest practicable occasion during the next season. Spectrograms of NGC 3190 were obtained at both observatories in January, 1941, and the arms were again found to be trailing.[8] Later, NGC 4216, observed at both observatories, and NGC 4527, observed at Mount Wilson, gave similar results.

In addition to the four unambiguous cases, the sense of the spectrographic rotation has been recently observed for four other spirals in which the arms can be traced and dissymmetry of obscuration is conspicuous, although definitive criteria of tilt are not present. The nebulae are NGC 3169 and 4826, observed at Mount Wilson, and 2613 and 4088, observed by Dr. Mayall, who communicated the results to the writer with permission to include them in the present discussion. In all four the arms are trailing, provided that the heavier obscuration and sharper dark lanes represent the nearer sides of the nebulae.

These eight spirals, together with seven others previously observed, are listed in Table 1. The data in the second, third, fourth, and fifth columns are taken from Mount Wilson photographs and those in the sixth column from the various spectrographic observers indicated in the last column. The only entry in Table 1 that requires comment is the sense of rotation for NGC 2841. Slipher[9] reported inclined lines "implying rotation about an axis such as has been established for a number of other spirals" but did not otherwise indicate the sense of the rotation.

Inspection of Table 1 indicates that the sense of the spectrographic rotation, combined with that of the spiral pattern, is correlated with the dissymmetry of obscuration. On the assumption that the dissymmetry does indicate the tilt, the fifteen nebulae are all rotating in the same direction with respect to the spiral pattern. Thus Slipher's conclusion based on relatively few objects is fully confirmed. The actual direction (arms trailing) is established by the four newly observed, unambiguous cases included in the list.

The sense of the spectrographic rotation is known for eight other spirals, but, in them, either the patterns cannot be traced with certainty or the dissymmetry is inconspicuous. These nebulae are listed in Table 2 in order to present in this paper all the data now available which bear on the problem of rotation.[10] Four of the nebulae discussed by Slipher—

---

vantage, were published for NGC by Hubble, *Realm of the Nebulae*, Pl. III, 1936; for NGC 4216 by Pease, *Mt. W. Contr.*, No. 132, Pl. XI; *Ap. J.*, **46**, Pl. VI, 1917, and Curtis, *Lick Obs. Pub.*, **13**, Pl. IV, 1918.

The prints on Pl. XII are light in order to show the dark lanes near the nuclei which identify the nearer sides of the nebulae. Denser prints, showing the left-hand patterns in both spirals, were published by Curtis, *Lick Obs. Pub.*, **13**, Pls. IV and V, 1918.

For technical reasons all images are oriented with the major axis horizontal.

[7] *Mt. W. Annual Report*, 1940.

[8] The result was reported in a joint paper by Dr. Mayall and the writer, "The Direction of Rotation in Spiral Nebulae," read at the May, 1941, meeting of the National Academy of Sciences

[9] *Pub. A.A.S.*, **4**, 284; *Pop. Astr.*, **30**, 9, 1922.

[10] The sense of the spectrographic rotation is also known for the following nonspiral extragalactic nebulae: NGC 2685, S0p, SW end approaching (Humason, *Mt. W. Annual Report*, 1939); NGC 2784, S0, E end approaching; and NGC 3034, Irr, SW end approaching (Mayall, letter to the writer; Slipher

NGC 1068, 3627, 4594, and 5005—are placed in the supplementary table for reasons previously mentioned. NGC 4736 shows no dissymmetry with respect to the major

TABLE 1

WELL-OBSERVED NEBULAE

Object	Type	Spiral Pattern*	Major Axis	Side Obscured	End Approaching	Observer†
NGC 224	Sb	Left	NE -SW	NW	SW	S_1, P, B
2613	Sb	Right	NW-SE	SW	NW	M(u)
2683	Sb	Right	NE -SW	NW	NE	S_1
2841	Sb	Left	NW-SE	NE	NW	S_2
3031	Sb	Left	NW-SE	SW	SE	W; B, H(u)
3169	Sa	Left	NE -SW	SE	NE	H(u)
3190	Sa	Left	NW-SE	SW	SE	(H and M)
3623	Sa	Left	N -S	E	N	S_1
4088	Sc	Left	NE -SW	SE	NE	M(u)
4216	Sb	Left	NE -SW	SE	NE	(H and M)(u)
4258	Sb	Left	NW-SE	SW	SE	H
4527	Sb	Left	NE -SW	NW	SW	H(u)
4826	Sb	Right	NW-SE	NE	SE	H(u)
6503	Sc	Left	NW-SE	SW	SE	M
7331	Sb	Right	N -S	W	N	B

* A right-handed spiral is one in which a point following an arm inward toward the nucleus would move in a clockwise direction. In a left-handed spiral such a point would move in a counterclockwise direction.

† Hitherto unpublished reports are indicated by (u). Letters following a semicolon refer to later observations which confirm the first reports. B = Horace Babcock, *Lick Obs. Bull.*, **19**, No. 498, 41, 1939; H = Hubble, *Mt. W. Annual Report*, 1940; (H and M) = Hubble and Mayall, National Academy of Science, May meeting, 1941; M = Mayall, quoted by Lindblad, *Ap. J.*, **92**, 1, 1940; P = Pease, *Proc. Nat. Acad.*, **4**, 21, 1918; S_1 = V. M. Slipher, *Proc. Amer. Phil. Soc.*, **56**, 403, 1917; S_2 = V. M. Slipher, *Pop. Astr.*, **30**, 9, 1922 (the end approaching is not stated but may be inferred from the context); W = Wolf, *Vierteljahrsschrift der Astr. Gesellschaft*, **49**, 162, 1914.

TABLE 2

DOUBTFUL CASES

Object	Type	Spiral Pattern*	Major Axis	Side Obscured	End Approaching	Observer†
NGC 598	Sc	Right	NE -SW	NW(?)	NE	(M and A)
1068	Sc	Left	NE -SW	.....	NE	S_2
3432	Sc	Right(?)	NE -SW	NW	NE	M(u)
3627	Sc	Left	N -S	E(?)	N(?)	S_1
4594	Sa	.....	E -W	S	W	S_1; P
4736	Sb	Right	NW-SE	.....	SE	M(u)
5005	Sb	Left	NE -SW	NW	SW(?)	S_1
5746	Sb	Right(?)	N -S	E	S	(H and M)(u)

* For definitions of right- and left-handed spirals see note to Table 1.

† Hitherto unpublished reports are indicated by (u). (H and M) = Hubble and Mayall; (M and A) = Mayall and Aller, *Ap. J.*, **95**, 5, 1942; P = Pease, *Proc. Nat. Acad.*, **2**, 517, 1916; S_1 = V. M. Slipher, *Proc. Amer. Phil. Soc.*, **56**, 403, 1917; S_2 = V. M. Slipher, *Lowell Obs. Bull.*, No. 80, 1917.

has previously reported inclined lines in NGC 3034 without mentioning the sense of the inclination); NGC 3115, E7, SW end approaching (Humason, *Mt. W. Annual Report*, 1937); NGC 4111, S0, NW end approaching (Humason, *Mt. W. Annual Report*, 1937). Slipher has also reported inclined lines in NGC 221, E2, without giving the sense of the inclination.

axis. The three remaining spirals—NGC 598, 3432, and 5746[11]—seem to be consistent with those in Table 1, but in each case one of the data, indicated by a question mark, is uncertain.

Since the observational data lead to the working hypothesis that the arms are trailing in all spirals, Lindblad's quite plausible interpretation of the criterion of tilt must be re-examined. His arguments depend upon the assumption that the finely divided, obscuring material is distributed through the nebulae in much the same manner as the stars are distributed. However, if the dark material is highly concentrated in the fundamental planes, the effects will be consistent with Slipher's interpretation. This fact can be readily seen in the limiting case of an opaque dark sheet spread throughout the fundamental plane of a tilted spiral. The luminous nuclear bulge above the plane is then projected against the more distant side of the dark sheet, while the nearer side is sharply silhouetted against the lower half of the nuclear bulge. This model would also account for the fact that in M 31 the observed novae and Cepheids are more numerous on the less obscured half of the projected image. Furthermore, even stronger support for this interpretation is furnished in M 31 by the observed asymmetrical distribution of globular clusters, for which the Z-components of the spatial distribution are presumably greater than those for the supergiant stars. Finally, an approximation to a thin sheet of dark material is suggested by Lyman Spitzer's theoretical investigation of the distribution of interstellar matter in elliptical nebulae.[12]

[11] Pease described NGC 5746 as a "fine right-handed spiral," on the basis of a fair plate with the 60-inch reflector (*Mt. W. Contr.*, No. 132; *Ap. J.*, **46**, 24, 1917). The writer has independently concluded that the pattern is right-handed, on the basis of good plates with the 100-inch telescope. Nevertheless, the arms are difficult to trace, and the spiral has been listed in Table 2 in order to keep the data in Table 1 free from controversy. The tilt of the nebula is unambiguously determined by the obscuration, hence the acceptance of the "right-handed" pattern would make the object a fifth definitive case for the direction of rotation.

[12] *Ap. J.*, **95**, 329, 1942.

NOVA OPHIUCHI OF 1604 AS A SUPERNOVA*

W. BAADE
Mount Wilson Observatory
Received January 11, 1943

ABSTRACT

Nova Ophiuchi of 1604 is one of the earliest well-observed novae. Its position has recently been redetermined by Schlier and Boehme from the original measures of Fabricius and Kepler. The light-curve, derived in the present paper, shows that the star was a supernova of type I, which at maximum reached the apparent magnitude −2.2. A check of the Chinese version of the apparition against the light-curve shows that the Chinese reports about new stars were based on careful observations.

A search for the remnant of the supernova led to the discovery of a small patch of emission nebulosity, which is undoubtedly a part of the masses ejected during the outburst. The investigation of this remnant meets with unusual difficulties because the supernova is behind heavy obscuration. The determination of the distance and the luminosity of the supernova must therefore be left to future observations.

The recent investigations of the Crab nebula have supplied data concerning the final state of one particular supernova; but additional examples of former galactic supernovae are highly desirable, since only a comparison of several will enable us to distinguish between those features which are typical and those which are more or less incidental. Thus one would like to know whether the surprisingly low velocity of expansion of the Crab nebula is a general characteristic of the shells of all supernovae. One would like to know, too, whether in every supernova the mass ejected during the outburst is of the order of several solar masses and whether the stellar remnant is always a white dwarf.

To obtain such additional information we have recently investigated the remnant of another galactic supernova, Nova Ophiuchi of 1604. That this star was a supernova of type I is shown beyond doubt by the light-curve derived in the first part of the present paper. The second part deals with the remnant of the supernova found by the writer a year ago. The investigation of this remnant meets with unusual difficulties because the supernova is in a heavily obscured region. It is to be expected, however, that future observations—in particular, measures of the motions of the ejected masses—will provide the answer to questions which have to remain open at present.

I. THE NOVA OF 1604

The nova appeared at the beginning of October, 1604,[1] far down in the southwestern sky, close to Jupiter and Mars. Notwithstanding its unfavorable position, it was discovered promptly, since numerous observers were watching the approaching conjunction of the two planets which took place on October 9. The nova reached its maximum brightness—somewhat brighter than Jupiter—near the middle of October and was still about as bright as Jupiter when it disappeared in the rays of the sun in November. Reappearing in the eastern sky at the beginning of January, 1605, it had become much fainter, equaling Antares in brightness. The decrease in brightness continued throughout the summer, and, when last seen by Kepler in October, 1605, the nova had reached the fifth magnitude. By the spring of the following year it had become invisible to the naked eye.

Since the main interest of the contemporary observers centered on the question of whether the nova, like Tycho's of 1572, was to be classed with the fixed stars, most of

* *Contributions from the Mount Wilson Observatory, Carnegie Institution of Washington*, No. 675.

[1] All dates given in the present paper are Gregorian style. The original observations were partly dated in the old Julian style.

their efforts were directed toward measuring its position relative to neighboring stars. As a result of these measures the position is well determined. Estimates of the brightness played a secondary role but are sufficient to establish the main characteristics of the light-curve. In this respect it was a fortunate circumstance that Jupiter and Mars, both within a few degrees of the nova, provided convenient photometric standards when the nova reached its maximum low in the western sky.

THE POSITION OF THE NOVA

For the determination of the position of the nova two sets of observations are available, one by Kepler and his associates at Prague, the other by David Fabricius. Fabricius measured the distances between the nova and a number of the brighter stars. The Prague series includes distances both from stars and from the near-by planets, Mars, Jupiter, and Saturn. From these observations Kepler[2] derived the position of the nova,

$$\alpha = 17^h 7^m 8^s, \qquad \delta = -21°1'.5 \quad (1605.0).$$

Kepler's value is of only historical interest. That it is poorly determined is obvious from the large discordances, which far exceed the errors of the measures. The reasons for the

TABLE 1

COMPUTED POSITIONS OF NOVA OPHIUCHI OF 1604

α 1605.0		δ 1605.0		Authority
$17^h 7^m 3^s$	$\pm 3^s.0$ m.e.	$-21°\,4'\,42''$	$\pm 57''$ m.e.	Schoenfeld (1865)
17 7 3	± 3.1	$-21\ 5\ 18$	± 42	Schlier (1934)
17 7 3	± 2.0	$-21\ 5\ 17$	± 26	Boehme (1937)

poor agreement seem to be insufficient allowance for the refraction—most of the measures were made in zenith distances greater than 80°—and considerable uncertainties in the reference system, enhanced by the inclusion of the planets as reference objects.

In recent years the observations have been rediscussed by E. Schoenfeld,[3] O. Schlier,[4] and S. Boehme.[5] For obvious reasons only distances between stars and nova were used. Since practically all the reference stars used by Kepler and Fabricius are included in the modern *Fundamental Catalogues*, the star places for the epoch 1605.0 present no further problem. The resulting positions of the nova, together with the computed mean error of each co-ordinate, are given in Table 1. Schoenfeld and Schlier used only the measures of Fabricius,[6] which, judged by their internal agreement, are far superior to the Prague observations. Boehme's solution includes both sets "after some obvious misprints in the Prague observations had been corrected." All three determinations agree within the limits of their respective errors. The mean of the more recent determinations of Schlier and Boehme is adopted in this paper, mainly because their results are based on the accurate proper motions of the modern *Fundamental Catalogues*. That further improvements of the proper motions will not affect these latest solutions is indicated by the insignificant difference between the values of Schoenfeld and those of Schlier, the one

[2] *Gesammelte Werke* (ed. Caspar), **1**, "De nova stella in pede serpentarii," p. 216.

[3] *A.N.*, **65**, 7, 1865.

[4] *A.N.*, **254**, 181, 1934, with a chart of the field of the nova.

[5] *A.N.*, **262**, 479, 1937.

[6] They consist of eleven distances of the nova from five reference stars.

obtained in 1865, the other in 1934. The latest values can therefore be considered as definitive. Reduced to the equinox 1935.0 they give as the position of the nova:

$$\alpha = 17^h26^m44^s.9\,, \qquad \delta = -21°25'55''\ (1935.0)\,,$$

with a computed mean error of $\pm 1'$. The corresponding galactic co-ordinates are:

$$l = 332°.3\,, \qquad b = +5°.4\,.$$

Considering the very unfavorable circumstances under which the observations had to be made and the crude instruments of that time, the accuracy attained by these early observers appears highly satisfactory.

THE LIGHT-CURVE OF THE NOVA

From the reports collected by Kepler in "De stella nova" and the statements of the Italian astronomers we know that on account of the approaching conjunction of Mars and Jupiter the region of the nova had been kept under close observation since the end of September, 1604. The fact that up to October 9 nothing unusual was noticed is of importance, because a conspicuous new object within less than 2° of Jupiter could hardly have failed to attract the attention of some observer. In particular, we have the emphatic statements of Fabricius and several other reliable observers that nothing extraordinary was noticed when they observed Mars and Jupiter on the evening of October 8. During the following days a period of rainy weather interfered with observation, especially for observers north of the Alps, which explains why the independent discoveries of the nova extend over nearly a week.

The nova was first seen on the evening of October 9 by two Italian observers, a physician in Cosenza (Calabria), whose name is unknown and who reported his discovery and observations to the astronomer Chr. Clavius in Rome, and I. Altobelli in Verona. On October 10 it was seen by B. Capra and S. Marius in Padua and by J. Brunowsky in Prague, who caught a glimpse of the nova between clouds and notified Kepler of his discovery. Later discoveries are those of Heck in Rome (October 11), Magini in Bologna, Roeslin in Hagenau (October 12), and David Fabricius in Osteel (October 13). Although a close watch of the sky was kept at Prague after Brunowsky's discovery of the nova on October 10, it was not until October 17 that the sky cleared and Kepler saw the nova for the first time.

These data leave no doubt that the nova was still inconspicuous—probably fainter than magnitude 3—on October 8 but had become a striking object—about as bright as Mars—by the following evening.[7]

The estimates of the brightness of the nova, beginning with October 9, are collected in Table 2. In order to avoid any bias they are reproduced as closely as possible in the original terms of the observers. The list probably contains all important observations except those of David Fabricius, whose reports about the nova were not accessible to the writer. The few estimates occurring under his name in Table 2 are known from his correspondence with Kepler. For three of the estimates in the compilation the approximate date of the observation had to be inferred from the date of the letter in which they were communicated and from some earlier date mentioned therein. They are uncertain by ± 14 days and are therefore marked approximate.

[7] Kepler in "De stella nova" puts the appearance of the nova on October 10 because his former teacher, Maestlin, claimed to have observed Jupiter and Mars on October 9 without noticing anything unusual. It seems, however, that Maestlin's date must be in error. For one thing, there is no reason to doubt the veracity of Altobelli and the anonymous physician. Indeed, the report of the latter contains the best description of the final rise of the nova to its maximum. Moreover, it is hard to believe that the period of bad weather which set in between October 8 and 9 and which eliminated all other observers north of the Alps on October 9 should not have affected Maestlin. It is therefore probable that his observation refers not to October 9 but to October 8. The same conjecture has been made by E. Zinner in his report in *Geschichte und Literatur der veränderlichen Sterne*, **2**, 438.

TABLE 2

ESTIMATES OF BRIGHTNESS AND COLOR OF NOVA OPHIUCHI OF 1604

Date (Gregorian)	Brightness of Nova	Color	Observer
1604 Oct. 8....	Not seen	.....	Several
Oct. 9....	As bright as Mars	Like Mars	Anonymous physician (Cosenza)*
	As bright as Jupiter	Like half of ripe orange	Altobelli (Verona)†
Oct. 10....	Somewhat brighter than on Oct. 9	.....	Anonymous physician*
	Very similar in brightness to Mars	Like Mars	Capra-Marius (Padua)‡
Oct. 11....	Still brighter than on Oct. 10	.....	Anonymous physician*
	Twice as bright as Jupiter	.....	Heck (Rome)§
Oct. 12....	Almost as bright as Jupiter	.....	Roeslin (Hagenau)‖
Oct. 15....	As bright as Jupiter or somewhat more	Like Jupiter	Anonymous physician*
	Much brighter than Jupiter; no further increase after this day	.....	Altobelli†
	As bright as Jupiter or a little more; no further increase afterward	.....	Capra-Marius‡
	A little brighter than Jupiter	Like Jupiter; white, not red	Fabricius (Osteel)¶
	As bright as or brighter than Jupiter	.....	Brenzoni (Verona)**
	Brighter than Jupiter and equal to Venus	.....	Maestlin (Tübingen)††
Oct. 17....	Much brighter than Jupiter (almost twice as bright)	.....	Kepler (Prague)‡‡
1605 Jan. 3....	Brighter than α Sco, much fainter than α Boo	.....	Kepler‡‡
Jan. 13....	Brighter than α Boo and Saturn	.....	Kepler‡‡
Jan. 14....	About as bright as Mars (in Oct., 1604)	.....	Fabricius¶
~Jan. 21....	About as bright as α Sco, a little brighter than Saturn	.....	Maestlin††
End of Jan....	As bright as α Vir	.....	Heydon (London)§§
March 20....	Not much brighter than ζ and η Oph	.....	Kepler‡‡
March 27....	Not much brighter than ζ and η Oph	.....	Brengger (Kaufbeuren)‖‖
~March 28....	Not much brighter than η Oph	.....	Cristini¶¶
April 12....	As bright as η Oph	.....	Fabricius¶
April 21....	As bright as η Oph	.....	Kepler‡‡
Aug. 12–14.	As bright as ξ Oph	.....	Kepler‡‡
Aug. 29....	About as bright as ξ Oph	.....	Kepler‡‡
Sept. 13....	Fainter than ξ Oph	.....	Kepler‡‡
Oct. 8....	Difficult to see; fainter or equal ξ Oph	.....	Kepler‡‡

* The excerpt from the letter of the anonymous physician in Cosenza to Clavius, concerning the nova, is published in A. Favaro, *Carteggio inedito di Ticone Brahe, Giovanni Keplero, etc.*, pp. 283–84, Bologna, 1886.

† Galileo, *Opere* (ed. naz.), **10,** 132–33, 136, 1900.

‡ *Ibid.*, **2,** 293 ff., 1891.

§ *Geschichte und Literatur der veränderlichen Sterne*, **2,** 439.

‖ Kepler, *Gesammelte Werke* (ed. Caspar), **1,** "De stella nova," 483, 1938.

¶ Kepler, *Opera omnia* (ed. Frisch), **2,** 597–98, 1859.

** Galileo, *op. cit.*, **10,** 138.

†† Kepler, *Opera omnia*, **2,** 582–83.

‡‡ Kepler, *Gesammelte Werke*, **1,** 161–64. That the nova at maximum was nearly twice as bright as Jupiter is mentioned on p. 384.

§§ Kepler, *Opera omnia*, **2,** 604.

‖‖ *Ibid.*, p. 588.

¶¶ A. Favaro, *op. cit.*, p. 304.

Since, during the maximum, Mars and Jupiter and, later on, Saturn served as comparison stars, their magnitudes had to be computed. This was done for the dates in Table 3. Positions and distances of the three planets were obtained with the help of the very convenient tables of P. V. Neugebauer.[8] For the computation of the magnitudes Müller's light-elements[9] were used, with the exception of the constant terms, for which the values recently derived by W. Becker[10] were adopted. Allowance for the phase was made only in the case of Mars. In computing the brightness of Saturn the contribution of the ring system was taken into account.

Through the use of Becker's constants in Müller's formulae the magnitudes of Table 3 are on the Harvard system. We adopt, therefore, for the remaining comparison stars the Harvard magnitudes α Boo (0.24), α Sco (1.22), α Vir (1.21), η Oph (2.63), ζ Oph (2.70), and ξ Oph (4.46) to bring the whole light-curve into the Harvard system.

TABLE 3

POSITIONS AND MAGNITUDES OF MARS, JUPITER, AND SATURN, 1604–5

Planet	Date	α 1604.0	δ 1604.0	log r	log Δ	m_v
Mars	1604 Oct. 9	$17^h13^m\ 7^s$	$-24°\ 39'.0$	0.1446	0.1870	+0.90
Jupiter	1604 Oct. 8	17 12 0	−22 51.6	.7180	.7475	−1.87
	Oct. 15	17 17 26	−22 58.2	.7178	.7546	−1.84
	Nov. 12	17 40 40	−23 19.2	0.7171	0.7775	−1.73
		α 1605.0	δ 1605.0			
Saturn	1605 Jan. 13	17 22 9	−21 57.6	1.0044	1.0387	+0.78

We are now able to convert the estimates of Table 2 into magnitudes. It is hardly necessary to remark that in doing so we have to adopt a much larger photometric step than the customary 0.1 mag., which applies to the estimates of the modern variable-star observers. The proper value is probably best indicated by the smallest photometric unit —one-third of a magnitude—used in the star catalogues of that time. Since the nova was mostly intercompared with near-by stars, the accuracy of the estimates may be a little better in the present case. I have therefore adopted the accompanying conversion table:

Much brighter	−0.75 mag.
Brighter	−0.50
Not much brighter	−0.25

For the estimates near the maximum when the nova was brighter than magnitude −1, conversion factors 1.5 times as large have been used to allow roughly for the fact that the width of the photometric step increases rapidly in the range of high intensities.

The magnitudes derived in this manner are given in the second column of Table 4, following one another in the same order as the estimates in Table 2. The adopted magnitudes in the last column are the straight means of the second column, except in the following cases:

1. I have rejected the estimates of Altobelli (October 9, 1604) and of Heck (October 11, 1604), which differ from those of the other observers by more than 2 mag. The dif-

[8] *Tafeln zur astronomischen Chronologie*, **2**, Leipzig, 1914.

[9] G. Müller, *Pub. Ap. Obs. Potsdam*, **8**, 1893.

[10] *Sitzungsberichte Preuss. Akad. d. Wissenschaften*, 1933, p. 839.

ference is much too large to be explained by observational errors. Moreover, the alleged magnitudes imply a final rise of the nova which appears impossible. Probably both writers became victims of a tendency which is all too apparent in certain reports about the new star—the tendency to make the nova of 1604 a worthy rival of Tycho's, at least in print.

2. For similar reasons I have rejected the estimates of Altobelli and Maestlin for October 15. These excessive estimates of the maximum brightness have already been criticized by Fabricius, who insisted in a letter to Kepler that at best the nova became only a little brighter than Jupiter. Kepler himself, who was inclined to stress the similarity

TABLE 4

MAGNITUDES OF NOVA OPHIUCHI OF 1604

Date (Gregorian)	Observed Magnitudes	Adopted Magnitude
1604 Oct. 8.....	Fainter than mag. +3	$>+3^m$
Oct. 9.....	+0.9; (−1.9)	+0.9
Oct. 10.....	+0.1; +0.9	+0.5
Oct. 11.....	−0.7; (−2.9)	−0.7
Oct. 12.....	−1.5	−1.5
Oct. 15.....	−2.1; (−3.0); −2.1; −2.3; −2.2 (brighter than −3.0)	−2.2 } −2.25
Oct. 17.....	−2.6	−2.6 }
1605 Jan. 3.....	+0.7; +1.0	+0.9
Jan. 13.....	−0.3; +0.3	0.0
Jan. 14.....	+0.9	+0.9
~Jan. 21.....	+1.2; (+0.5)	+1.2
End of Jan.....	+1.2	+1.2
March 20.....	+2.4; +2.4	+2.4
March 27.....	+2.4; +2.4	+2.4
~March 28.....	+2.4	+2.4
April 12.....	+2.6	+2.6
April 21.....	+2.6	+2.6
Aug. 12–14...	+4.5	+4.5
Aug. 29.....	+4.5	+4.5
Sept. 13.....	+5.0	+5.0
Oct. 8.....	+4.8	+4.8

to the nova of 1572, admits in "De stella nova" that the star never approached Venus in brightness.

3. Of Maestlin's two estimates of January 21, 1605, I have retained only the comparison with α Boo, since Saturn at that time was still close to the horizon.

The resulting light-curve of the nova is presented in Figure 1. It shows that the nova was discovered about a week before the maximum, which was reached October 17, 1604. This date of the maximum is firmly established, since all observers agree that the nova showed no further increase in brightness after October 15. For the maximum brightness of the nova we obtain the value −2.25 mag., which, in spite of the rejections mentioned above, may still be somewhat too high. But it cannot be far from the truth and is probably correct within 0.25 mag. The gap in the observations after maximum is due to the conjunction of the nova with the sun, and the star was well on its way toward the final decline when it reappeared in January, 1605.

Considering the rather rough estimates on which it had to be based, the light-curve appears most satisfactory. It is a typical light-curve of a supernova of type I. If any proof is needed, it is provided by the curve in Figure 1 representing the decline of the nova from maximum to the end of the observations. This curve is actually the visual light-curve of the recent supernova in IC 4182, properly adjusted. The remarkable agreement in the light-changes of the two stars is characteristic of supernovae of this type, which all follow closely the same pattern. Minor variations in the widths and heights of the maxima occur; but, when supernovae of this type have reached the final decline, which sets in 80–100 days after the maximum, the further decrease in brightness is the same for all, with a linear gradient of $+0.0137 \pm 0.0012$ mag. per day.[11] Since the nova of 1604 conforms to this pattern, we conclude that it was a supernova of type I.

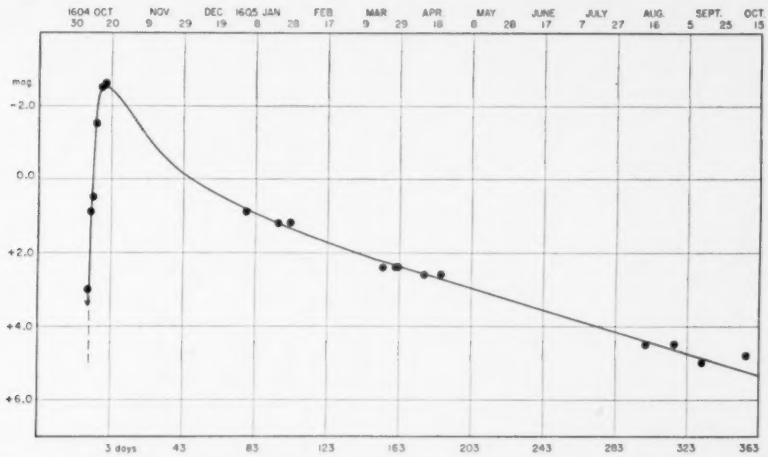

FIG. 1.—Light-curve of Supernova Ophiuchi of 1604. The smooth curve representing the descending branch is the visual light-curve of the recent supernova in IC 4182, properly adjusted.

THE CHINESE OBSERVATIONS OF THE NOVA

In view of the important role which the Chinese records of "guest stars" have recently played in reconstructing the early history of the supernova of 1054,[12] it is most fortunate that for the supernova of 1604 we have a good light-curve with which to check the Chinese version of the apparition. The nova occurs in the She-ke, being one of the last entries in a list of "guest stars" observed in the times of the Ming dynasty. Both Biot[13] and Williams[14] have given translations. We reproduce the text according to Williams, since Biot's version is somewhat abridged. For convenience the Gregorian dates have been added in brackets. The Chinese report concerning the nova of 1604 is as follows:

In the 32nd year of the same epoch, the 9th moon, day Yih Chow [October 10, 1604] a star was seen in the degrees of the stellar division Wei.[15] It resembled a round ball. Its colour was reddish yellow. It was seen in the southwest until the 10th moon [October 27–November 26,

[11] A more detailed discussion of the light-curves of supernovae will be presented in a forthcoming paper by the writer.

[12] J. J. L. Duyvendak, *Pub. A.S.P.*, **54**, 91, 1942, and N. U. Mayall and J. H. Oort, *Pub. A.S.P.*, **54**,95.

[13] *Connaissance des Temps*, 1846.

[14] *Observations of Comets from B.C. 611 to A.D. 1640*, p. 93, London, 1871.

[15] The stellar division Wei (see chart given by Williams, *op. cit.*, n. 14) extends in R.A. from about 16^h40^m to 18^h, in Dec. from $-20°$ south into the constellation Ara. The nova appeared close to the northern boundary of Wei.

1604] when it was no longer visible. In the 12th moon, day Sin Yew [February 3[16], 1605] it again appeared in the southeast, in the stellar division Wei. The next year, in the 2nd moon [March 24–April 23, 1605], it gradually faded away. In the 8th moon, day Ting Maou [October 7, 1605] it disappeared.

This description is in such excellent agreement with the data gathered by the European observers that comment is unnecessary. The test shows that we can place full confidence in the Chinese records and that, whenever specific dates are given, they are obviously based on careful observations.[17]

II. THE REMNANT OF SUPERNOVA OPHIUCHI OF 1604

After Nova Ophiuchi had been established as a supernova, a search was made for the remnant in the expectation that the ejected masses would still be visible, as are those of the supernova of 1054. Since the supernova is in a heavily obscured part of the Milky Way, the search was carried out in red light (λλ 6300–6700). The very first plate of the field, taken at the 100-inch reflector, June 18, 1941, with an exposure time of two hours on an Eastman 103E plate behind a Schott RG2 filter, revealed a small patch of nebulosity close to the expected place (see Pl. XV). Its center has the co-ordinates

$$\alpha = 17^h26^m42^s.8, \delta = -21°25'54'' (1935.0),$$

which differ from those of the nova (p. 121) by only $-2^s.1$ and $+1''$.

The nebulosity appears as a broken mass of bright knots and filaments covering a fan-shaped area, about 40 seconds of arc long. There are indications, however, that this fan-shaped mass, which is quite strong on the red plates, represents only the brightest part of a more extended nebula since faint wisps of nebulosity are scattered over a much larger field, perhaps 80–100 seconds of arc in diameter. This estimate of the extent of the nebula needs further confirmation, since on the plates thus far obtained (which are of only average quality) it is difficult to distinguish small patches of nebulosity from stars.

In the photographic region (λλ 5000–3600) the nebulosity is extremely faint; hence it is easily missed, even in a careful search. Comparisons with extrafocal exposures of S.A. 131 show that the photographic surface brightness of the fan-shaped mass amounts to only 25.2 mag. per square second of arc, which is 4 mag. fainter than the corresponding value for the Crab nebula. The integrated photographic magnitude of the fan-shaped mass is 19.0. This faintness of the nebulosity in the photographic region is without doubt due to selective absorption,[18] and a comparison of the red and the blue images suggests—on the assumption that we are dealing with an emission spectrum—that the color excess may amount to nearly 1 mag. Aside from this weakening by selective absorption, the structure of the nebulosity in the photographic region is quite different from that in the red. It is much more nearly uniform, and the strong knots and filaments which are so prominent on the red exposures barely rise above the level of the faint nebulous background.

The different characteristics of the nebulosity in the blue and in the *Hα* region might lead to the inference that, as in the Crab nebula,[19,20] the main part of the emission be-

[16] Both Biot and Williams give the Gregorian date, January 24, 1605, but according to several independent checks by the writer February 3 seems to be the correct date.

[17] Other records of the nova of 1604, mostly from Korean sources, have been collected by Y. Iba, *Pop. Astr.*, **46**, 142, 1938. One of these reports (from Ressei Jitsuroku) is of special interest because it contains intercomparisons of the nova with Jupiter for October 13 and 15, 1604. According to these estimates the nova at maximum was fainter than Jupiter.

[18] See also the following paper by R. Minkowski, *Mt. W. Contr.*, No. 676; *Ap. J.*, **97**, 128, 1943.

[19] W. Baade, *Mt. W. Contr.*, No. 665; *Ap J.*, **96**, 109, 1942.

[20] R. Minkowski, *Mt. W Contr.*, No. 666; *Ap. J.*, **96**, 121, 1942

PLATE XV

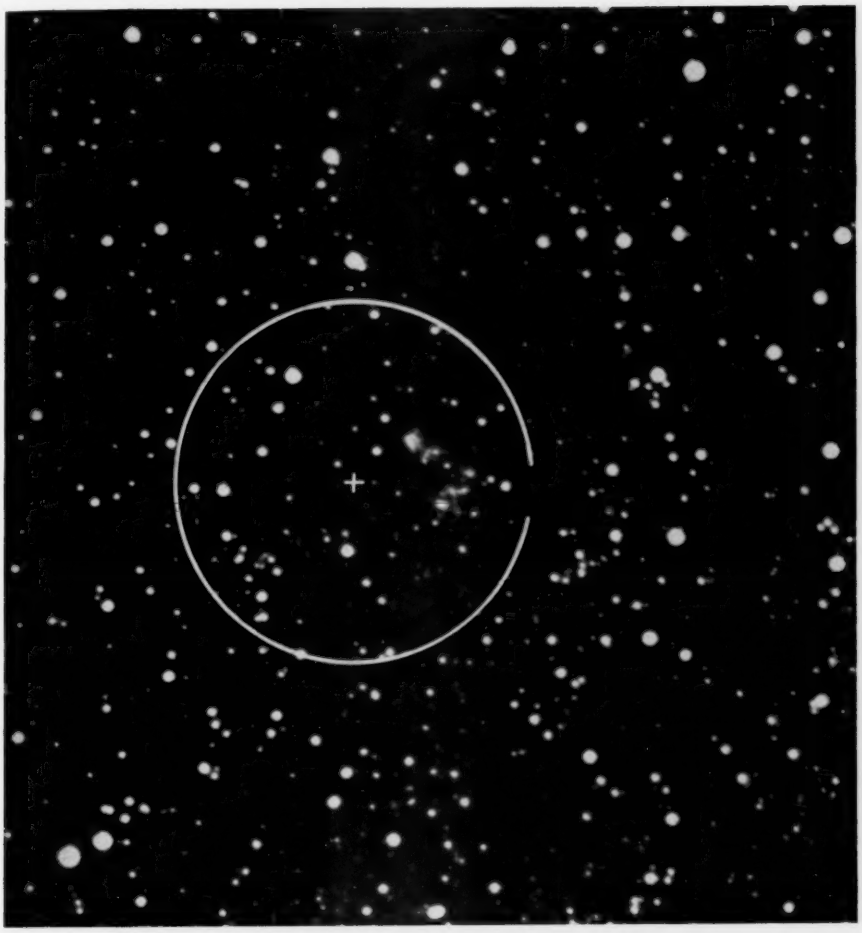

EMISSION NEBULOSITY NEAR NOVA OPHIUCHI OF 1604

Photographed in red light (λλ 6300–6700) with 100-inch reflector, on June 9, 1942, exposure time 3½ hours. Scale of reproduction 1 mm = 2″.51. The computed position of the nova is marked by a cross; the circle indicates the mean error of the computed position.

UNIV. OF MICH.

tween λ 5000 and λ 3500 is due to a continuous spectrum. However, a plate taken in the near infrared between λ 8400 and λ 7200 does not support this conclusion. As pointed out in an earlier paper,[19] this spectral region is free from strong nebular emission lines and is therefore well suited to reveal a continuum. The test should be especially convincing for Nova Ophiuchi, since, on account of the smaller absorption at longer wave lengths, the nebulosity should be an easy object on infrared exposures if a continuum contributes materially to the intensity of the image in blue and violet light. The infrared plate, however, shows only a vague and possibly spurious trace of the nebulosity. There seems to be little doubt, therefore, that the strong continuum characteristic of the Crab nebula is absent in the nebulosity of Nova Ophiuchi and that the high intensity of the knots and filaments in the *Hα* region must be due to unusually strong localized emissions of the pair of [*N* II] lines λ 6548 and λ 6584.

The stellar remnant—the exciting star of the nebulosity—cannot be identified at present. The only object whose association with the nebulosity might suggest a physical connection is a faint star of photographic magnitude 18.6, which is imbedded in the bright patch forming the tip of the fan-shaped mass. It may well be a chance coincidence, but the star deserves further attention because its color index appears to be as small as that of any other star in a field of 50″ radius. Of the other stars within the field the few with magnitudes brighter than 18 can be ruled out because their color indices—allowing for a color excess of 1 mag.—are so large that they must be of advanced spectral types. Altogether it seems quite certain that the stellar remnant of the supernova is fainter than magnitude 18.

The preceding description shows that our present knowledge of the nebulosity is still very meager, but the fact that it is a remnant of the former Supernova Ophiuchi seems to be established beyond doubt. The strongest argument is, of course, the agreement in the positions of nebulosity and supernova, which is perfect, considering the accuracy with which the position of the star is known. But there is another observational fact which supports this view. According to the measures of Humason and Minkowski, the radial velocity of the nebulosity amounts to −200 km/sec.[18] This large velocity is readily explained as due to the motion of the ejected matter if the nebulosity is a part of the expanding shell around the supernova. On the other hand, it presents a very serious difficulty if one tries to dismiss the agreement in the positions of nebulosity and star as a mere chance coincidence. In that case the nebulosity would be a small galactic nebula which happens to be close to the position of the former supernova. The radial velocity has, then, to be explained in terms of galactic rotation alone, since according to all evidence the peculiar motions of interstellar dust and gas are negligible. This would place the galactic nebula at a distance of more than 4000 parsecs, which seems quite impossible in view of the very heavy obscuration extending over the field. We have, therefore, every reason to believe that the patch of nebulosity near the place of the nova is a part of the shell which was ejected during the outburst.

About the structure and the extent of this shell we know at present practically nothing. As mentioned previously, there is good evidence that the recently discovered fan-shaped nebula is only the brightest part of a more extended nebulosity. Perhaps it will be possible to define the extent of the shell with some accuracy in the near future by means of long exposures of excellent definition. Another possible line of attack is the determination of the radial velocities of some of the brighter wisps of nebulosity outside the fan-shaped area, which undoubtedly would help in locating the center of the expansion and the stellar remnant. Finally, some twenty to thirty years hence, we should be able to measure the tangential motions in the fan-shaped mass which, properly combined with the radial velocities, will lead to a reliable determination of the distance of the supernova. Until these data, together with measures of the intervening space absorption, are forthcoming, any conclusions regarding the luminosity and the distance of the supernova will be mere guesses.

THE SPECTRUM OF THE NEBULOSITY NEAR KEPLER'S NOVA OF 1604*

R. MINKOWSKI
Mount Wilson Observatory
Received January 11, 1943

ABSTRACT

The spectrum of the nebulosity near Kepler's nova of 1604 consists of the emission lines [*O* III] λ 5007; [*O* I] λ 6300; [*N* II] λ 6584, λ 6548; *Hα*; and [*S* II] λ 6731. The spectrum is very similar to that of the filaments of the Crab nebula, particularly in the low intensity of *Hα* relative to the [*N* II] lines. The intensity of [*O* III] λ 5007, however, is much less than in the Crab nebula; this suggests heavy space reddening corresponding to a color excess of 2.1 mag. The radial velocity, −200 km/sec at the tip and −260 km/sec at the base of the fan-shaped nebulosity, is too high to admit any other interpretation than that the fan-shaped nebulosity is part of an expanding nebula. The results support the opinion that the nebulosity is actually a remnant of Kepler's nova and that this object was a supernova.

An attempt to observe the blue portion of the spectrum of the nebulosity near Kepler's nova of 1604 found by W. Baade[1] has been made by M. L. Humason. The spectrogram, obtained with the two-prism spectrograph and a 3-inch camera at the Cassegrain focus of the 100-inch telescope, shows only one very faint line which may be interpreted as [*O* III] λ 5007 with a radial velocity of −200 km/sec.

Since the nebulosity is much brighter in the red than in the blue, observations in the red seemed more promising. To obtain sufficient speed together with reasonable linear dispersion (400 A/mm), a plane grating of 400 lines per millimeter was used with a solid Schmidt camera, f/0.65, in an improvised spectrograph at the Cassegrain focus of the 60-inch telescope. The grating, ruled by H. D. Babcock on an evaporated aluminum surface on pyrex, has high energy concentration in the first-order violet; but the efficiency in the first-order red is (necessarily) less, being in fact only about one-third of the attainable maximum.

Two spectrograms of the red region have been taken. The first was obtained with an exposure time of 15^h30^m from May 16 to 19, 1942, with the slit in position angle 90° through the (north following) tip of the fan-shaped part of the nebulosity. It shows the [*N* II] lines λ 6548, λ 6584 and *Hα* with an intensity somewhat higher than that of λ 6548, the fainter of the [*N* II] lines. The second spectrogram (Pl. XVI) was obtained with an exposure time of 16^h45^m from June 8 to 11, 1942, with the slit in position angle 38°.5 through tip and base of the nebulosity. This spectrogram shows, in addition to the [*N* II] lines and *Hα*, the lines [*S* II] λ 6731, [*O* I] λ 6300 (superposed on the same line in the sky spectrum), and [*O* III] λ 5007; *Hα* seems to be somewhat stronger relative to the [*N* II] lines at the base than at the tip.

As a whole the spectrum resembles remarkably closely the spectrum of the Crab nebula[2] (Pl. XVI), particularly in the relative intensities of *Hα* and the [*N* II] lines. The [*S* II] line appears to be fainter than in the Crab nebula, where, however, the intensity of this line relative to the [*N* II] lines varies considerably. The question arises whether the observed intensity ratio of *Hα* and the [*N* II] lines is due to high intensity of the [*N* II] lines or to low intensity of *Hα*. It is well known that in certain objects the [*N* II] lines appear with unusually high intensity relative to the spectrum as a whole. This occurs not only in some planetary nebulae[3] but also in the nebula now surrounding Nova

* *Contributions from the Mount Wilson Observatory, Carnegie Institution of Washington*, No. 676.

[1] *Mt. W. Contr.*, No. 675; *Ap. J.*, **97**, 119, 1943.

[2] R. Minkowski, *Mt. W. Contr.*, No. 666; *Ap. J.*, **96**, 199, 1942.

[3] A. B. Wyse, *Ap. J.*, **95**, 356, 1942.

PLATE XVI

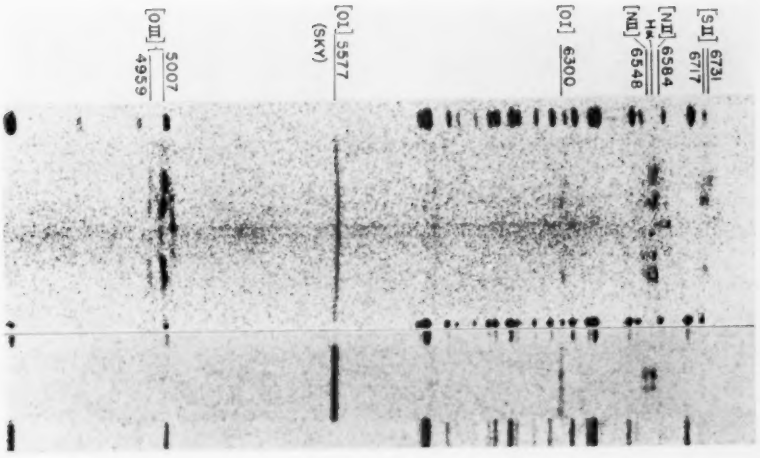

SPECTROGRAMS OF THE CRAB NEBULA (*above*) AND OF THE NEBULOSITY NEAR KEPLER'S NOVA OF 1604 (*below*)

The curvature of the lines in the spectrum of the Crab nebula is due to the use of a curved slit in an improvised grating spectrograph.

Herculis (1934).[4] In the nebulosity near Kepler's nova, however, the intensity of the [*N* II] lines does not appear unusually high compared to the [*S* II] and [*O* I] lines. This suggests that, as in the Crab nebula, the hydrogen line is relatively faint, an effect possibly of low hydrogen abundance.

The line [*O* III] λ 5007 is very definitely fainter relative to the lines in the red than in the Crab nebula. This is undoubtedly mainly an effect of heavy space reddening. The observed ratio of the intensity of the [*N* II] lines to that of the [*O* III] line is about 4.5 times that in the Crab nebula, estimated on the basis of an intensity ratio 3:1 for the [*O* III] lines λ 5007 and λ 4959. Since the mean zenith distance for the exposures on the nebulosity near Kepler's nova was 57°, while that for the exposures on the Crab was 27°, a correction for atmospheric absorption has to be applied which reduces the factor to 4.3. The excess of the color equivalent for the range of 1550 A with the mean wave length 5750 is then 1.6 mag., if differences of the relative line intensities in the two nebulae are negligible. If it is assumed that the selective interstellar absorption varies as λ^{-1}, the excess for the range $\delta\lambda$ varies as $\lambda^{-2}\delta\lambda$. The color excess (for the range of the international color index) then becomes 2.1 mag.

For measurement of the radial velocity at the tip the lines [*N* II] λ 6584, *Hα*, and [*S* II] λ 6731 (on the second spectrogram only) could be used. Only the one line, [*N* II] λ 6584, could be used to determine the difference between base and tip—a difference which is probably real, although not much larger than the error of measurement. The radial velocity is -190 ± 30 km/sec at the tip, -260 km/sec at the base.

The spectroscopic results alone are, of course, not sufficient to establish beyond question the nature of the nebulosity. The most natural interpretation is that the fan-shaped nebulosity is part of an expanding nebula surrounding a nova or supernova. The observed difference between base and tip indicates that the center of expansion is closer to the base. The actual velocity of expansion may be considerably greater than 200 km/sec and, if the center of expansion is at some distance from the fan, may thus be of the order to be expected for a nova or supernova.

The similarity of the spectrum to that of the Crab nebula suggests that the nebulosity is the remnant of a supernova rather than that of an ordinary nova. The results thus give supplementary evidence that the nebulosity is really a remnant of Kepler's nova of 1604 and that this star was a supernova of type I.

[4] Swings and Struve, *Ap. J.*, **92**, 295, 1940.

THE SPECTRUM OF NOVA CYGNI 1942*

ROSCOE F. SANFORD
Mount Wilson Observatory
Received December 24, 1942

ABSTRACT

Changes in the light and spectrum of Nova Cygni 1942 from September 15 to December 17, 1942, are briefly outlined.

Emission lines.—While the nova was bright, emission lines of hydrogen were outstanding; those of *Ca* II and *Na* I were prominent; and many others were present, including lines of *Fe* II, *Ti* II, *O* I, *O* II, and *N* II. After the nova began its rapid decline in magnitude, its continuous spectrum weakened, absorption detail was meager, and emission lines of hydrogen remained prominent. Those of [*Fe* II] appeared and, with those of *Fe* II, gained in strength relative to the hydrogen emission, [*Fe* II] faster than *Fe* II. On November 27 the nova, increasing in brightness, had lost its *Fe* II and [*Fe* II] lines, retained the hydrogen, and showed many of the well-known nebular emissions, some of them in great strength.

Absorption lines.—Several sets of absorption lines accompanied the emission lines on their violet sides. These were especially marked for hydrogen. Data for them are in Table 2 and Figure 1. A sharp set of lines giving a constant radial velocity of −509 km/sec is the most persistent. The other strong absorption set had very wide lines and a displacement of −1185 km/sec when first observed. This increased to −1400 km/sec in five days and remained constant thereafter. Two weaker sets of lines had displacements of −900 to −700 km/sec and about −270 km/sec, respectively.

Interstellar lines.—The mean radial velocity from the interstellar lines is -11.8 ± 0.9 km/sec. The equivalent width of interstellar K is 0.59 A. These two data give an absolute magnitude at maximum of about −4, appreciably less than that of the average nova.

Comparison with Nova Herculis 1934.—The general behavior of Nova Cygni 1942 is quite similar to that of Nova Herculis in respect to variations both in light and in spectrum.

Spectrograms of Nova Cygni 1942 showing the photographic region were obtained at Mount Wilson each night from September 15 to September 25, U.T., inclusive, and on September 29, October 2, November 27, and December 17, 1942. Spectrograms of the visual region were obtained on September 15, 21, 22, and December 17. A preliminary measure of a spectrogram of September 15 has been briefly reported.[1]

From September 15 to September 23 inclusive the visual magnitude of the nova was about 9, with relatively minor fluctuations. During this interval the nova had a continuous spectrum upon which were superposed broad emission lines with several absorption components displaced to the violet; the pattern underwent comparatively minor modifications.

On September 24 the nova had become definitely fainter and thereafter dropped steadily in brightness to an estimated fifteenth magnitude on October 2. Concurrent with the decline in magnitude the continuous spectrum subsided, leaving emission lines of *H* and *Fe* II, in addition to which lines of [*Fe* II] appeared.

Between October 2 and November 27 the nova was very faint, and no spectroscopic observations were obtained. On November 27, after it had brightened, a low-dispersion spectrogram showed that the spectrum had again changed; emission lines of iron had about vanished and several of the conspicuous nebular lines had appeared. A spectrogram on December 17 is very similar to that on November 27.

Several stages in the variation of the spectrum of Nova Cygni 1942 are illustrated by Plate XVII

Emission lines.—During the bright stage of the nova the emission lines of hydrogen extended at least 30 angstroms on either side of their normal positions with hazy in-

* *Contributions from the Mount Wilson Observatory, Carnegie Institution of Washington*, No. 677.

[1] *Pub. A.S.P.*, **54**, 206, 1942.

PLATE XVII

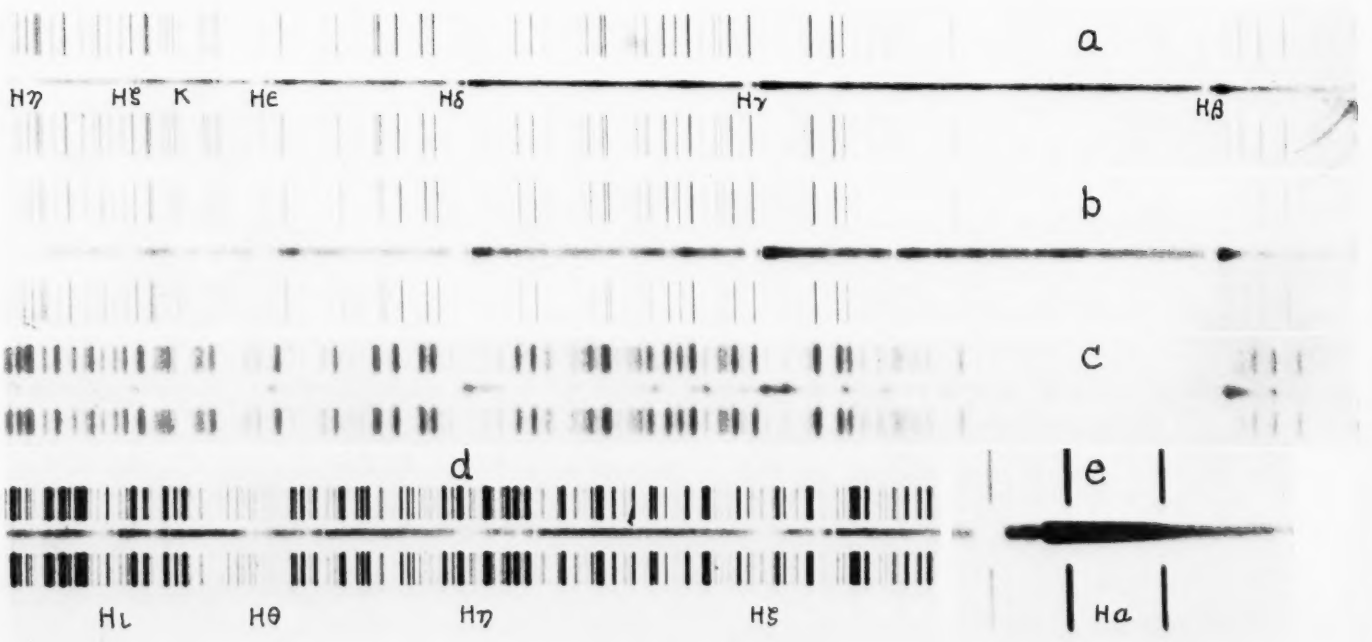

SPECTRUM OF NOVA CYGNI 1942

(*a*) September 15, 1942; (*b*) September 17 (note numerous absorption components not shown in (*a*); (*c*) October 2 (continuous spectrum very much weakened); (*d*) September 22 (second-order coudé); (*e*) September 22.

UNIV. OF MICH.

definite limits and were accompanied by absorption components with large negative displacements. Emissions belonging to *Fe* II, *Ti* II, *O* I, *O* II, and *N* II also are present but are too poorly defined for measurement of either position or extension. After the magnitude began to decline, the hydrogen lines showed little or no emission to the violet of the position occupied by the absorption component of least negative displacement but extended in great strength about 22 angstroms redward from the normal positions. Emissions belonging to *Fe* II and [*Fe* II] were comparatively narrow; their centers were measured on the plates of September 29 and October 2. The dispersion of the first plate is 79 A per mm at $H\gamma$ (sufficient to give measurements of fair accuracy); that of the second, 223 A/mm. Maxima in the hydrogen lines resembling the narrower *Fe* II and [*Fe* II] lines were likewise measured on the spectrogram of September 29. The results are in Table 1.

TABLE 1

EMISSION-LINE VELOCITIES

DATE	*H*		*Fe* II		[*Fe* II]	
	Km/Sec	No. Lines	Km/Sec	No. Lines	Km/Sec	No. Lines
1942, Sept. 29	−322	5	−310	9	−357	5
1942, Oct. 2	.....	.....	−344	7	−343	8

Attention is called to the large negative displacements and to the difference, on the first plate, of values from permitted and from forbidden lines. This is of interest, because, at a similar stage of Nova Herculis, Adams and Joy[2] obtained large negative velocities from measures of emission lines which showed a similar difference for permitted and forbidden lines. For Nova Herculis the large negative displacements seem satisfactorily explained by the great asymmetry of the emission lines from the expanding shell.[3] The difference between the velocities from permitted and forbidden lines has been explained by P. W. Merrill[4] as the effect of the presence of absorption on the violet side of permitted lines and its absence in the forbidden lines. On the spectrograms of November 27 and December 17 the hydrogen emission lines were still prominent but appeared to terminate on their red sides at somewhat shorter wave lengths than on October 2. Lines of *Fe* II and [*Fe* II] had disappeared and the chief nebular lines were prominent. They are λ 3867 [*Ne* III], λ 4069 [*S* II], λ 4267 *C* II, λ 4363 [*O* III], λ 4634, λ 4641 (blend) *N* III, λ 4686 *He* II, λ 4959, and λ 5007 [*O* III]. The line λ 3867 was a little stronger than $H\zeta$; λ 4363 was stronger than $H\gamma$; the blend of λ 4634, λ 4641 greatly exceeded λ 4686 and was comparable with $H\beta$ and λ 4959; λ 5007 considerably exceeded $H\beta$; λ 4069, λ 4267, and λ 4686 just showed with certainty. The spectrogram of December 17, covering the visual as well as the photographic region, showed the lines λ 5754 [*N* II], λ 6300 [*O* I], and $H\alpha$ probably blended with λ 6548 and λ 6583 [*N* II].

The visual region of the spectrum was observed a few times before the magnitude declined. The continuous spectrum was relatively weak; $H\alpha$ was the dominant emission; and interstellar D lines were present. These spectra helped to confirm the presence of emission from certain elements suspected in the photographic region.

Absorption lines.—Until the nova began its rapid decline in magnitude it showed not only a continuous spectrum with emission lines but also several sets of absorption lines.

[2] *Mt. W. Contr.*, No. 545; *Ap. J.*, **84**, 14, 1936.

[3] *Mt. W. Contr.*, No. 530, Pl. X, *l*; *Ap. J.*, **82**, Pl. XVIII, *l*, 1935.

[4] *Mt. W. Contr.*, No. 530, p. 18; *Ap. J.*, **82**, 430, 1935.

These lines were especially prominent in connection with the hydrogen emissions but were also partially represented for other elements, notably *Ca* II and *Na* I.

The detailed measures, depending largely upon the absorption lines of hydrogen (but to some extent upon H and K and D1 and D2), are recorded in Table 2. Four columns contain the radial velocities of four absorption components I–IV. The radial velocities from the interstellar lines also are tabulated. The data on stellar absorption lines in Table 2 are plotted in Figure 1.

TABLE 2

VELOCITIES (KM/SEC) FROM ABSORPTION LINES

MIDEXPOSURE (U.T. 1942)	DISPERSION AT $H\gamma$ (A/MM)	I	II	III	IV*		INTERSTELLAR	OBSERVER†
					Center	Width		
Sept. 15.29....	65	.....	−511	.....	−1185	280	−18.6	M.L.H.
15.36....	65	.....	−505	.....	−1241	312	−10.0	
15.43....	275‡	.....	.....	.....	−1287	.....	.....	
16.27....	65	.....	−508	.....	−1216	359	−14.9	
17.10....	65	−234	−504	.....	−1212	538	−14.0	
18.16....	65	−286	−520	−900	−1304	362	−12.4	
19.26....	79	−272	−512	−853	−1418	395	−10.9	R.F.S.
19.31....	79	.....	−507	−825	−1416	488	−20.6	
20.27....	79	.....	−514	−763	−1395	370	− 6.0	
21.31....	36	−321	−504	−741	−1424	399	− 8.8	G.S.
21.15....	65§	.....	−539	.....	−1388	.....	− 7.0	R.F.S.
21.25....	65§	.....	−511	.....	−1379	.....	−17.8	
22.30....	36	.....	−513	−721	−1398	432	− 9.2	G.S.
22.25....	10§	.....	−503	−717	−1409	386	− 6.3	R.F.S.
22.25....	20§	.....	−497	.....	−1379	.....	.....	R.F.S.
23.29....	36	.....	−479	.....	.....	.....	.....	G.S.
24.28....	79	.....	−518	.....	.....	.....	.....	
25.30....	79	.....	.....	.....	.....	.....	.....	
29.19....	223	.....	.....	.....	.....	.....	.....	A.H.J.
Oct. 2.22....	223	.....	.....	.....	.....	.....	.....	A.H.J.
Nov. 27.19....	223	.....	.....	.....	.....	.....	.....	R.F.S.
Dec. 17.15....	223‖	.....	.....	.....	.....	.....	.....	A.H.J.

* Subcomponents of IV have the following displacements:
Sept. 15.29 −1256, −1114.
19.26 −1545, −1290.
21.31 −1490, −1308.
22.25 −1504, −1372, −1228.

† M. L. Humason, R. F. Sanford, Gustaf Strömberg, A. H. Joy.

‡ Dispersion at $H\alpha$.

§ Plane-grating spectrograms: on Sept. 22.25 the photographic region was photographed in the second order and the red in the first order.

‖ Both photographic and visual regions on this low-dispersion prismatic spectrum.

Component I was very weak and difficult to measure. Hence the tendency for its velocity to increase with time, as shown by the figure, is not to be given any weight. Component II, most persistent of all and best suited for measurement, had a constant radial velocity of −509 km/sec. Component III, which was first measured on September 18, changed from a velocity of about −900 km/sec to one of about −700 km/sec in an interval of 4 days.

Component IV is represented in Figure 1 by a band bounded by dashed lines that correspond to the measured radial velocities of the edges. Within this band, dots represent the measured center of IV and crosses denote subcomponents into which some of the lines seemed to be resolved (see n.* to Table 2). The subcomponents were best shown by the higher members of the hydrogen lines; three were measured on September 22 from

the spectrogram of highest dispersion. The radial velocity for the center of IV appeared to change from about −1200 km/sec on September 15 to −1400 km/sec on September 19, after which it leveled off until this component disappeared. The K line deserves special mention for noteworthy changes in component IV. Its behavior is briefly summarized in Table 3.

The spectrogram of September 17 on which K has the strongest and widest component IV shows numerous absorption lines which on other spectrograms are absent or very

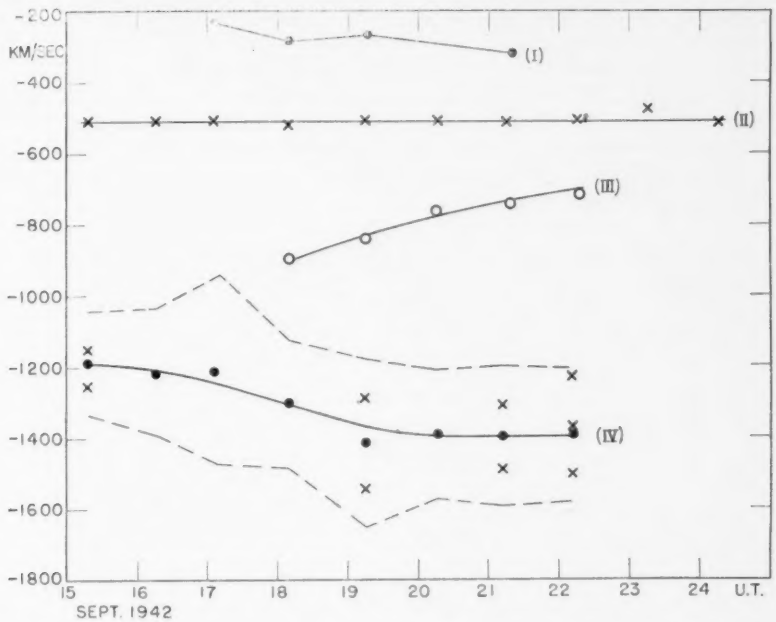

FIG. 1.—Displacements of components I–IV (Table 2). The edges of component IV are indicated by dashed lines; measures of its center, by dots; and measures of subcomponents, by crosses.

TABLE 3

K LINE—ABSORPTION COMPONENT IV

Sept. 15	Exceedingly weak	Sept. 20	As wide but not as strong as on Sept. 17
16	Just apparent	21	Continuing to weaken
17	Maximum strength and width	22	Vanishing
18	Strong but narrower than on Sept. 17	23	Absent
19	Further weakened		

much weaker. When their positions are corrected for the radial velocity of component IV, ten of them can be identified with *Fe* II lines, and one conspicuous line with λ 4481 *Mg* II, a feature absent on all other spectrograms (see Pl. XVII, *a* and *b*). Component IV appeared to attain its greatest intensity on September 17.

The true radial velocity of the nova has not been satisfactorily determined. Several attempts, on rather dubious assumptions, gave values between +50 and +100 km/sec but are not considered to have any weight.

Interstellar lines.—The weighted mean radial velocity from the interstellar lines of Nova Cygni 1942 is −11.8 ± 0.9 km/sec. The equivalent width of interstellar K meas-

ured on the high-dispersion plate of September 22 is 0.59 A. Under certain assumptions, both the interstellar velocity and the equivalent width of K can be used to obtain values of the distance. The interstellar velocity when freed from solar motion must be assumed to represent differential galactic rotation. The distance so obtained is 2280 $\pm$ 500 parsecs. According to data from class B stars,[5] an equivalent width of K of 0.59 A corresponds to a distance of 1500 parsecs. The brightest apparent magnitude so far published for this nova is 7.8. Absolute magnitudes for this apparent magnitude and the two distances derived above are -5.1 ± 0.5 and -3 if 0.5 mag. per kiloparsec absorption in space is assumed. Either value is very appreciably fainter than the generally adopted mean value of $M = -7$ for galactic novae.

Comparison with Nova Herculis 1934.—The variations in light and in spectrum of Nova Cygni 1942 ran parallel to those of Nova Herculis 1934. The most outstanding changes in spectrum occurred when each faded many magnitudes and then recovered a considerable part of its loss. On fading, each suffered a loss in its continuous spectrum, showed *H*, *Fe* II, and [*Fe* II] lines in emission, and on recovery had lost the iron lines and showed instead the nebular radiations.

I am indebted to several of my colleagues who gave generously of their observing time to obtain spectrograms of the nova.

[5] *Mt. W. Contr.*, No. 573; *Ap. J.*, **86**, 141, 1937.

A STUDY OF EMISSION-LINE INTENSITIES IN SOME BRIGHT NORTHERN WOLF-RAYET STARS

LAWRENCE H. ALLER[1]
Harvard College Observatory
Received November 28, 1942

ABSTRACT

From a study of emission-line intensities in a number of bright Wolf-Rayet stars excitation temperatures of their atmospheric envelopes are estimated. These temperatures turn out to be very high and depend upon the ionization potential of the ion employed—in the sense that the higher the ionization potential, the higher the resultant temperature. The emission lines in the Wolf-Rayet stars probably do not arise from the primary mechanism, i.e., photoionization and subsequent recapture of electrons, but rather from the absorption of high-frequency radiation emerging from the lower layers. On the basis of certain plausible assumptions an attempt is made to find the chemical composition of the atmospheric layers. In the carbon stars helium is estimated to be about fifty times as abundant as oxygen and fifteen times as abundant as carbon, while in the nitrogen stars helium appears to be about twenty times as abundant as nitrogen and three hundred times as abundant as carbon. The estimate of the abundance of helium with respect to other gases is very uncertain. The nuclei of BD+30°3639 and NGC 40 seem to be typical carbon stars. The nucleus of NGC 6543, which contains both nitrogen and carbon, seems to show a relatively small range of ionization.

The chemical composition of the Wolf-Rayet stars seems to be more closely related to that of the supernovae than to the envelopes of ordinary novae, which appear to have roughly the same composition, on the average, as the planetary nebulae and normal stars.

The electron densities in the radiating layers of a Wolf-Rayet star appear to be of the order of 10^{11}–10^{12} electrons/cm^3, much greater than the electron densities in the envelope of a nova. The background spectrum of the star is sufficiently intense to blot out any forbidden lines that may appear.

The relatively rare Wolf-Rayet stars have perhaps the most spectacular and least understood of stellar spectra. Broad emission lines of atomic origin, sometimes 50 or 100 A wide and often ten times as intense as the continuous spectrum upon which they are superposed, characterize their spectra. In recent years identifications of the lines and the interpretation of Wolf-Rayet spectra have been discussed by Beals,[2] Menzel,[3] Miss Payne,[4] Edlén,[5] and Swings and Struve.[6] Beals[7] has summarized the spectral features and characteristics of the Wolf-Rayet stars. We have a reasonably good idea of the dimensions and mass of one Wolf-Rayet star, BD+38°4010, from the spectroscopic velocity-curve by Olin Wilson[8] and the light-curve by S. Gaposchkin.[9]

Although considerable attention has been paid to the wave lengths and identifications

[1] Society of Fellows, Harvard University.

[2] *Pop. Astr.*, **37**, 577, 1929; *M.N.*, **90**, 202, 1929; *Pub. Dom. Ap. Obs.*, **4**, 272, 1930.

[3] *Pub. A.S.P.*, **41**, 344, 1929.

[4] *Zs. f. Ap.*, **7**, 1, 1933.

[5] B. Edlén, *Zs. f. Ap.*, **7**, 378, 1933; *Nov. Ac. Reg. Soc. Sci., Upsala*, Ser. IV, **9**, No. 6, 1933. This monograph gives the detailed results for the spectral lines and terms of the atoms of the first row of the periodic table in their various stages of ionization.

[6] See P. Swings, *Ap. J.*, **95**, 112, 1942. See also Swings and Struve, *Ap. J.*, **91**, 546, 1940; **92**, 289, 1940; **92**, 295, 1940; **93**, 349, 1941; **93**, 356, 1941; *Proc. Nat. Acad. Sci.*, **26**, 454, 1940; **26**, 548, 1940; **27**, 225, 1941; *Pub. A.S.P.*, **52**, 394, 1940; **53**, 35, 1941.

[7] *J. R. Astr. Soc. Canada*, **34**, 169, 1940.

[8] *Ap. J.*, **91**, 379, 1940; *Mt. W. Contr.*, No. 623.

[9] *Ap. J.*, **93**, 202, 1941.

of the emission lines, relatively little work has been done on their intensities. Miss Payne[10] and Beals[11] have measured the profiles of a number of emission lines. Such measures are of fundamental importance to any real understanding of the Wolf-Rayet spectra, but they may profitably be made only on relatively unblended lines, and they give the intensity in the emission line only with respect to the intensity of the continuous background.

Measures of an absorption-line profile in an ordinary star with respect to the continuous background are adequate for most theoretical discussions, but the profile or equivalent width of an emission line should be supplemented by measures of the distribution of the continuous energy. Even an approximate knowledge of the latter enables us to convert intensity measures of bright lines into reasonably good estimates of relative radiated energies.

THE OBSERVATIONAL DATA

I undertook a spectrophotometric study of a few of the brightest Wolf-Rayet stars partly to supply data on relative radiated energies. Slitless spectrograms covering the

TABLE 1

WOLF-RAYET STARS OBSERVED

BD	HD	Position		Mag.	Harvard Type	Victoria Type
		α	δ			
35°3953	190918	$20^h\ 2^m2$	+35° 31′	7.01	Op	WN5
35 4001	191765	20 6.5	35 53	7.80	Ob	WN6
35 4013	192103	20 8.1	35 54	7.94	Oa	WC7
37 3821	192163	20 8.4	38 03	7.44	Ob	WN6
36 3956	192641	20 10.8	36 21	7.94	Oa	WC7
36 3987	193077	20 13.3	37 07	7.97	Oc	WN6
38 4010	193576	20 15.8	38 25	8.04	Ob	WN5
43 3571	193793	20 17.1	+43 32	6.83	Oa	WC6

wave-length range from λ 3200 to λ 6400 were taken with the Crossley reflector of the Lick Observatory. The photometric procedure resembled that of a previous investigation of the planetary nebulae[12] except that the spectra were widened by trailing. The Mills spot sensitometer, used in connection with appropriate filters for the red, green, blue, and ultraviolet wave-length regions, provided calibration standards. Each plate exposed in the telescope received two sets of standards: red and green standards on the visual plates, blue and ultraviolet standards on the plates taken especially for the photographic region. In addition, a complete set of photometric standards was impressed upon an otherwise unexposed plate taken from the same box. The entire set of plates was developed together in D11 under constant agitation.

Table 1 lists the Wolf-Rayet stars observed, their positions, magnitudes, Harvard classification, and spectral types according to Beals. Five of the stars belong to the nitrogen sequence, and three to the carbon sequence. Table 2 lists the forty-three spectrograms finally reduced; successive columns give the object, the plate numbers, the date of observation, and the spectral region covered. Generally, exposure times ranging from

[10] *Stars of High Luminosity*, p. 83, 1930.

[11] *M.N.*, **91**, 966, 1931; *Pub. Dom. Ap. Obs.*, **6**, 95, 1934.

[12] *Ap. J.*, **93**, 236, 1941.

TABLE 2

LIST OF OBSERVATIONS

Object	Plate	Date	Spectral Region
BD+35°3953	183	Aug. 24, 1939	ultraviolet
	184		visual
	185		blue
	186		ultraviolet
	187		ultraviolet
	188		visual
	211	Sept. 5, 1939	blue
BD+35°4001	189	Aug. 25, 1939	ultraviolet, blue
	190		ultraviolet
	191		visual
	199		ultraviolet
	212	Sept. 5, 1939	blue
	213		visual
BD+35°4013	202	Aug. 25, 1939	blue, ultraviolet
	203		visual
	214	Sept. 5, 1939	blue
	215		blue
	216		visual
BD+37°3821	253	Oct. 18, 1939	visual
	255		ultraviolet
	256		visual
	257		blue
	276	Oct. 21, 1939	blue
	277		visual
	278		ultraviolet
	279		ultraviolet
	280		blue
BD+36°3956	258	Oct. 18, 1939	visual
	259		visual
	260		blue
BD+36°3987	263	Oct. 19, 1939	visual, blue
	264		visual, blue
	265		ultraviolet
BD+38°4010	266	Oct. 19, 1939	ultraviolet
	267		visual, blue
	268		visual, blue
BD+43°3571	269	Oct. 19, 1939	ultraviolet
	270		visual
	272		blue
	281	Oct. 21, 1939	visual
	282		ultraviolet
	283		ultraviolet
	284		blue

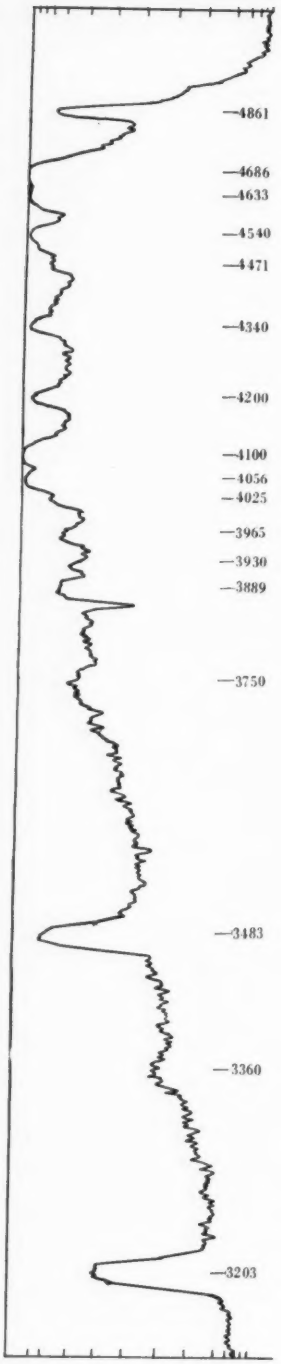

FIG. 1.—Tracing of spectrum of BD+37°3821

two to fifteen minutes sufficed to cover the spectrum from the strongest emission lines to the weak lines in the ultraviolet. A number of plates of each star had to be taken, in order to record both the continuum and the strong lines. Although many of the plates were taken on moonlit nights, the exposures were so short that sky fog introduced no error. Because of vignetting, especially troublesome in a slitless spectrograph of the prismatic type, slight errors in centering the object or the comparison star may give systematic errors depending upon wave length.

The plates were traced with the microdensitometer at the Harvard Observatory by Dr. F. L. Whipple, who planned at the first to collaborate with me on this problem. A tracing of a typical star, BD+37°3821, reproduced in Figure 1, will illustrate some of the difficulties encountered in drawing in the continuous background, estimating the relative contributions of overlapping bands, and so on. Errors in drawing the continuous spectrum—and one usually tends to draw the continuous spectrum too high in an emission-line star—will affect a weak line more than a strong one, in the sense that the weaker line is measured systematically too faintly or too strongly. In addition to such a scale error, the intensities are likely to suffer from a wavelength error. In the visual region, rapidly fluctuating plate sensitivity, high contrast, low dispersion, and frequently strong emission lines conspire to make the location of the continuous spectrum difficult and to decrease the precision of the measured intensities. On the other hand, atmospheric transmission difficulties limit the accuracy obtainable in the ultraviolet.

With the exception of BD+35°3953, the stars I have observed are not suitable for a discussion of their background continua.[13] The continuous spectra should be investigated with care in stars suitable for this purpose.

The tabulated intensities (see Tables 4 and 5) are given separately for the nitrogen and carbon stars. The unit of intensity is so chosen that an emission line at λ 4000 of unit equivalent width will have an inten-

[13] The only data on this problem seem to be those of Gerasimovič (*Harv. Circ.*, No. 339, 1929), who measured the spectrophotometric temperatures of several early-type stars. Color-temperature determinations suffer from galactic absorption as well as from the usual difficulties of photometry in the ultra-violet, but a study of the energy distribution in the Wolf-Rayet stars should be made the subject of a careful investigation. The present data suggest that the color temperatures of a number of the stars increase toward the ultraviolet; i.e., their energy curves rise above that of a black-body curve fitted to the visual region of the spectrum. Further information on this question is very desirable.

sity of 1.0. I estimate the accidental errors in the tabulated intensities to be generally of the order of 10 per cent for the stronger lines.[14]

IDENTIFICATIONS

For the identifications of lines in Wolf-Rayet spectra I have relied chiefly upon the data of Edlén. I have also used Whipple and Mrs. Payne-Gaposchkin's study[15] of the synthetic spectra of supernovae. This paper includes a complete list of multiplets in the astronomically accessible spectra regions with their semitheoretical intensities computed for specified temperatures from modern atomic theory by means of the summation rules and Einstein probability coefficients, supplemented by laboratory intensities. They have proved to be invaluable for the present study. Most of the Wolf-Rayet identifications by Miss Payne are verified. As would be expected, however, the intensity estimates of Whipple and Mrs. Payne-Gaposchkin enable us better to estimate the relative contributions of various members of a blend.

In Table 3 are collected the most important lines of multiplets of the ions of *He* I, *He* II, *O* III, *O* IV, *O* V, *O* VI, *C* II, *C* III, *C* IV, and *N* III, *N* IV, *N* V, and *N* VI observed in

TABLE 3

THE PRINCIPAL LINES AND MULTIPLETS OF THE IONS OBSERVED IN THE SPECTRA OF THE WOLF-RAYET STARS

Ion	Ionization Potential	Principal Lines or Multiplets	Ion	Ionization Potential	Principal Lines or Multiplets
He I	24.46	5876, 4471, 4026, 3889	*N* IV	77.04	3480, 4058
He II	54.14	4686, 3203, 5412, 4859, 4542	*N* V	97.43	4609
C II	24.26	4267, 5140	*O* III	54.62	3962, 3760, 3708, 3265
C III	47.64	4650, 5696, 4069	*O* IV	77.03	3730, 3411
C IV	64.17	5805, 3934	*O* V	113	5590, 5114
N III	47.20	4638, 4525, 4100, 3360	*O* VI	137.48	3812, 3835

Wolf-Rayet spectra. Successive columns give the ion, the ionization potential, and the most outstanding lines. Although the radiations of *C* II and *O* III are divided among a number of strong lines, practically the whole observable energy of *N* V or *O* VI is concentrated in one line. The ionization potentials range from 24 volts to 137 volts.

The successive columns of Tables 4 and 5 give the wave lengths estimated from the slitless plates of BD+37°3821 and BD+35°4013 for the nitrogen and carbon stars, respectively, the atom responsible; the laboratory wave length; the inner quantum number, J, for the two levels of the transition; the multiplet; the strength of the line in terms of the strength of the multiplet as unity (in some cases), as computed on the basis of LS coupling; the theoretical intensity of the multiplet according to Whipple and Mrs. Payne-Gaposchkin; and finally the observed intensities and line widths for the various stars. In the column headed "Identifications," I have listed for each Wolf-Rayet line the various contributors according to the atom and multiplet rather than wave length. The line widths, $\Delta\lambda$, were measured directly with the measuring engine; they are intended only as guides in the identifications. Although these $\Delta\lambda$'s may have some significance in

[14] It is extremely difficult to estimate the actual error in these intensities. The accidental error of a reasonably strong line measured on three or four plates is about 10 per cent, but this does not include systematic errors which may arise from estimating the continuous spectrum, for example. Weak lines, or lines in the far ultraviolet, may easily be in error by a full 100 per cent.

[15] *Proc. Amer. Phil. Soc.*, **84**, 1, 1941.

TABLE 4

EMISSION LINES OBSERVED IN STARS OF THE NITROGEN SEQUENCE

λ	Ion	λ (Lab.)	J'	J	Multiplet	$s/\Sigma s$	I_t	BD +37°3821		BD +35°4001		BD +36°3987		BD +38°4010	
								I	Δλ	I	Δλ	I	Δλ	I	Δλ
3203.....	*He* II	3203.16	.....	.....	$3^2F-5^2F^0$	.....	33†	86	25	96	....	20.3	10	8.5	....
3360.....	*N* III	3353.78	1/2	3/2	$3s'\,^4P-3p'\,^4P$	0.14	58								
		3354.29	3/2	5/2	.....	.15	.....								
		3358.72	1/2	1/2	.....	.03	.....								
		3361.90	3/2	3/2	.....	.043	.....	14.4	....	.....	.....	.....	.....	.....	....
		3365.79	3/2	1/2	.....	.14	.....								
		3367.36	5/2	5/2	.....	.35	.....								
		3374.06	5/2	3/2	.....	.15	.....								
3483.....	*N* IV	3478.69	1	2	$3s^3S-3p^3P$	.55	100†								
		3482.98	1	1	.....	.33	.....	62	19	92	20	12.9	8	11.8	....
		3484.90	1	0	.....	.11	.....								
3705.....	*He* I	3705.00	2, 1	3, 2, 1	$2^3P^0-7^3D$	.....	4								
		3705.14	0	1	.....	.....	.....	5.8	....	.....	.....	.....	.....	.....	....
3733.....	*He* I	3732.85	2, 1	1	$2^3P^0-7^3S$	.....	.....								
		3732.99	0	1	.....	.....	.....	7.2	....	5.7	.....	.....	.....	.....	....
3750.....	*N* IV	3747.66	.....	.....	$3s'\,^1P-3p'\,^1D$	.....	12								
	N III	3745.83	1/2	3/2	$3s^4P^0-3p^4S$	.....	15	15.2	....	13.0	.....	.....	.....	.....	....
		3754.62	3/2	3/2	.....	.....	.....								
		3771.08	5/2	3/2	.....	.....	.....								
3889.....	*He* I	3888.65	.....	.....	$2^3S-3^3P^0$	.....	16	11.5	28						
	He II	3887.47	.....	.....	4^2F-16^2D etc.	.....	.....								
3930.....	*N* III	3934.41	1/2	3/2	$3p'\,^2P-3d'\,^2D$	.07	18			11.4	.....	.....	.....	.....	....
		3938.52	3/2	5/2	.....	.48	.....	3.0	21						
		3942.78	3/2	3/2	.....	.33	.....								
	He II	3923.51	.....	.....	$4^2F^0-15^2G$	.....	.....								
3965.....	*He* I	3964.73	.....	.....	$2'S-4'P^0$	.....	2								
	He II	3968.47	.....	.....	4^2F-14^2G etc.	.....	.....	6.7	24	5.2	.....	.....	.....	.....	....
4025.....	*He* I	4026.19	2, 1	3, 2, 1	$2^3P^0-5^3D$	.....	14								
		4026.36	.....	.....	.....	.....	.....	7.2	20	5.36	30	4.1	.....	.....	....
	He II	4025.64	.....	.....	4^2F-13^2G	.....	.....								
4057.....	*N* IV	4057.80	1	2	$3p^1P^0-3d^1D$	.....	37†	46	24	29.8	30	11	10	8.7	....
4100.....	*He* II	4100.08	.....	.....	$4^2F^0-12^2G$	.....	1								
	N III	4097.31	1/2	3/2	$3s^3S-3p^2P^0$	.67	84	73	32	50.9	35	11.7	24	6.3	....
		4103.37	1/2	1/2	.....	.33	.....								
4200.....	*N* III	4195.70	1/2	3/2	$3s'\,^2P-3p'\,^2D$	.33	21								
		4200.02	3/2	5/2	.....	.60	.....	21.8	24	21.8	29	5.8	7	8.4	....
		4215.69	3/2	3/2	.....	.07	.....								
	He II	4199.87	.....	.....	$4^2F^0-11^2G$	.....	.....								
4340.....	*N* III	4323.93	3/2	5/2	$3p'\,^4D-3d'\,^4D$	.07	10								
		4328.15	3/2	3/2	.....	.08	.....								
		4335.53	5/2	5/2	.....	.18	.....	25.7	24	14.1	35	4.2	7	.....	.....
		4339.52	5/2	3/2	.....	.07	.....								
		4348.36	7/2	7/2	.....	.35	.....								
	He II	4338.71	.....	.....	4^2F-10^2G	.....	1								
4380.....	*N* III	4379.09	.....	.....	$4f^2F-5g^2G$	.....	38								
	He I	4387.93	1	2	$2^1P^0-5^1D$	.....	3	9.0	34	6.7	41	.....	.....	7.0?	....
4471.....	*He* I	4471.48	2, 1	3, 2, 1	$2^3P^0-4^3D$	.....	32								
		4471.69	0	1	.....	.....	.....	9.0	25	9.6	67	.....	.....	7	....
4512.....	*N* III	4510.92	1/2	3/2	$3s'\,^4P-3p'\,^4D$	.08	52								
			3/2	5/2	.....	.21	.....								
		4514.89	5/2	7/2	.....	.40	.....	.....	.....	.....	.....	5.4	8	12	....
		4518.18	1/2	1/2	.....	.08	.....								
		4523.60	3/2	3/2	.....	.11	.....								
4540.....	.....	4530.84	3/2	1/2	.....	.017	.....								
		4534.57	5/2	5/2	.....	.09	.....								
		4547.34	5/2	3/2	.....	0.01	.....								
		.....	.....	.....	.....	.....	.....	43.4	25	28.5	42	7	13	.....	.....
		4527.86	3/2	1/2	$3p'\,^4S-3d'\,^4P^0$	.....	10								
		4535.11	3/2	3/2	.....	.....	.....								
		4546.36	3/2	5/2	.....	.....	.....								
	He II	4541.63	.....	.....	4^2F-9^2G	.....	2								

TABLE 4—*Continued*

λ	Ion	λ (Lab.)	J'	J	Multiplet	$s/\Sigma s$	I_t	BD +37°3821		BD +35°4001		BD +36°3987		BD +38°4010	
								I	Δλ	I	Δλ	I	Δλ	I	Δλ
4609.....	*N* v	4603.2	1/2	3/2	$3s^2S-3p^2P^o$	.....	1240	20	36						
		4619.4	1/2	1/2	$3s^2S-3p^2P^o$	.....	.....	.....	...						
4633.....	*N* III	4634.16	1/2	3/2	$3p^2P^o-3d^2D$.....	0.33	100	67	32	38.5	50	11.8	30	13.5	....
		4640.64	3/2	5/2	.....	.60	.....	.....	...						
		4641.90	3/2	3/2	.....	.07	.....	.....	...						
4686.....	*He* II	4685.81	.....	.....	$3^2D-4^2F^o$	.....	100	270	40	237	58	54.3	28	65	....
4861.....	*He* II	4859.36	.....	.....	$4^2F^o-8^2G$	.....	2								
	N III	4858.74	1/2	3/2	$3p'\ ^4D-3d'\ ^4F$	.10	43								
		4858.88	3/2	5/2	.....	.16	.....	40.8	28	28.0	36	7.4	20	4	....
		4861.33	5/2	7/2	.....	.24	.....								
		4867.18	7/2	9/2	.....	.35	.....								
4932.....	*He* I?	4921.93	1	2	$2^1P^o-4^1D$	.....	4	5.6	30	7.2	....	.....	....	.....	....
5412.....	*He* II	5411.57	.....	.....	4^2F-7^2G	.....	4	38.3	37	36.8	49	9.8	18	9	....
5808.....	*C* IV	5801.51	1/2	3/2	$3s^2S-3p^2P^o$	.67	100†	11.7	35	17.4	56	?	....	8	....
		5812.14	1/2	1/2	.....	0.33	.....								
5876.....	*He* I	5875.62	2, 1	3, 2, 1	$2^3P^o-3^3D$	.....	100	15.5	38	8.4	50	.....	....	6.7?	....
		5875.96	0	1	.....	.....	.....								

the ultraviolet for the stars with the broader bands, it is clear that in the visual region they are widened by seeing, and hence they are partly distorted. My Δλ's are consistently smaller than those tabulated by Beals. Probably we set on the band edges in different ways.

Slitless spectra of the dispersion used, about 100A/mm at $H\delta$, permit the reliable determination neither of profiles nor of line widths. For such an investigation slit spectrograms are required. Therefore, I shall not discuss the question of line profiles in this paper.

Most of the broad lines in the spectra of the Wolf-Rayet stars have been identified. The line at λ 5805 in the nitrogen stars has been attributed by Swings to *C* IV[16] from a careful study of the spectral terms of nitrogen and carbon. From a consideration of theoretical line intensities the author independently reached the same conclusion.[17] I have not noticed any other lines of carbon or oxygen in the spectra of the nitrogen stars I have studied, although λ 5695 of *C* III ought to be observable. The *C* III λ 4658 and λ 4650 lines of *C* IV and *C* III probably would be mostly masked by the λ 4640 line of *N* III, although Swings suggests that the λ 4638 line in HD 192163 seems to extend too far to the red to be attributed to *N* III only. On the other hand, λ 3483 of *N* IV, conspicuous even when other nitrogen lines are not observed, is not found in the carbon stars. We may conclude that, while the nitrogen stars on the list contain carbon, the carbon stars contain no nitrogen.

THEORETICAL LINE INTENSITIES AND EXCITATION TEMPERATURES OF THE WOLF-RAYET STARS

It is probably inaccurate to speak of the temperature of a Wolf-Rayet star. Few spectra suggest greater deviations from conditions of thermal equilibrium. The simultaneous appearance of lines of greatly differing excitation such as those of *He* I and *N* V in the spectrum of the same star apparently requires that the observed radiations originate in a number of different layers. The atmospheres of these stars seem to exhibit considerable stratification.

[16] *Op. cit.* [17] *Pub. A. A. S.*, **10**, 157, 1942.

TABLE 5

EMISSION LINES OBSERVED IN STARS OF THE CARBON SEQUENCE

λ	Atom	λ (Lab.)	J'	J	Multiplet	$s/\Sigma s$	I_t	BD +35°4013		BD +36°3956		BD +43°3571		Notes
								I	$\Delta\lambda$	I	$\Delta\lambda$	I	$\Delta\lambda$	
3203...	*He* II	3203.16	.....	.....	3^2D-5^2F etc.	.....	33†	41	....	.....	.....	11	....	
3262...	*O* III	3260.98	2	3	$3p^3D-3d^3F^0$	0.20	100†	12.8	....	.....	.....	5.3	....	
		3265.46	3	4	.....	.30	.....							
		3267.31	1	2	.....	.43	.....							
	O V	3275.67	2	1	$3s'^3P-3p'^3S$	.....	20							
3381...	*O* III	3382.69	2	3	$3p'^5P-3d'^5D$	.....	9	11.9	....	.....	.....	22	....	
		3382.85	1	2	.....	.....	.....							
		3384.95	3	4	.....	.....	.....							
	O IV	3381.26	3/2	5/2	$3s'^4P-3p'^4D$	.....	19†							
		3385.55	5/2	7/2	.....	.....	.....							
3411...	*O* IV	3403.58	1/2	3/2	$3p^2P-3d^2D$	.....	100†	40	24	.....	.....	.....	.....	
		3411.76	3/2	5/2	.....	.....	.....							
		3413.71	3/2	3/2	.....	.....	.....							
3429...	*O* III	3428.67	1	2	$3p^3P-3d^3P$	.14	13†	9.0	....	.....	.....	.....	.....	
		3430.60	2	1	.....	.14	.....							
3445...	*O* III	3444.10	2	2	$3p^3P-3d^3P$	.42	.....	8.2	....	.....	.....	.....	.....	
		3446.73	1	2	$3p'^5D-3d'^5F$	.08	17							
		3448.06	2	3	.....	.14	.....							
		3450.94	3	4	.....	.21	.....							
		3455.12	4	5	.....	.32	.....							
3560...	*O* III	3556.92	2	2	$3s'^3P_2-3p'^3P_2$	.42	4	7.7	11	.....	.....	2.9	....	
	O IV	3560.42	3/2	5/2	$3p'^3D-3d'^3F$	.....	11							
		3563.36	5/2	7/2	.....	.....	.....							
	He I	3554.44	2, 1	1	$2^3P^0-10^3D$	.....	1	.....	.....	.....	.....	.....	.....	
		3554.57	0	1	.....	.....	.....							
3607...	*C* III	3608.96	1, 0	2, 1	$4p^3P-5d^3D$	.....	5	16.4	....	.....	.....	2.5	....	
		3609.61	2	3	.....	.....	.....							
3708...	*C* III	3703.52	1	1	$3p'^1P-3d'^1P$	.....	.....							
	He I	3705.00	2, 1	3, 2, 1	2^3P-7^3D	.....	4							
		3705.14	0	1	.....	.....	.....							
	O III	3702.75	0	1	$3p^3P-3d^3D$	.11	33†							
		3707.24	1	2	.....	.25	.....							
		3715.08	2	3	.....	.47	.....							
	O III	3695.37	1	2	$3s'^5P-3p'^5D$	.07	18	15.3	....	.....	.....	.....	.....	
		3698.70	2	3	.....	.19	.....							
		3703.37	3	4	.....	.36	.....							
		3704.73	1	1	.....	.09	.....							
		3712.48	2	2	.....	.12	.....							
		3720.86	3	3	.....	.09	.....							
	O V	3700.87	1	1	$3p'^3D-3d'^3D$	.15	.....			22.2	25	8.0	....	
		3717.11	2	2	.....	.23	.....							
	O IV	3736.78	5/2	7/2	$3p^4D-3d^4F$	.25	25	22.7	....	.....	.....	.....	.....	
		3744.73	7/2, 5/2	9/2, 7/2	.....	.35	.....							
	O V	3747.07	3	3	$3p'^3D-3d'^3D$	.42	19							
	He I	3732.85	2, 1	1	2^3P-7^3S	.....	.....							
		3732.99	0	1	.....	.....	.....							
3758...	*O* III	3754.67	1	2	$2s^3P-3p^3D$	.25	86†	13.6	20	7.6	21	6.9	....	
		3757.21	0	1	.....	.11	.....							
		3759.87	2	3	.....	.47	.....							
3815...	*He* I	3819.61	2, 1	3, 2, 1	2^3P-6^3D	.....	7	3.0	10	.....	.....	3	....	
		3819.75	0	1	.....	.....	.....							
	O VI	3811.35	1/2	3/2	$3s^2S-3p^2P$	.67	11,600							
3835...	*O* VI	3834.24	1/2	1/2	$3s^2S-3p^2P$	0.33	.....	2.9	12	.....	.....	.....	.....	
	He II	3833.83	.....	.....	4^2F-18^2G	.....	.....							
3889...	*He* I	3888.65	.....	.....	2^3S-3^3P	.....	16	17.9	21	4.4	28	3	....	
	He II	3887.47	.....	.....	4^2F-16^2G	.....	4							
	C III	3883.80	1	2	$4d^3D-5f^3F$	.....	.....							
		3885.99	2	3	.....	.....	.....							
		3889.18	3	4	.....	.....	.....							
3930...	*C* IV	3936.41	.....	.....	5^2S-6^2P	.....	45	17.1	18	.....	.....	6.3	....	1
	Si III	3924.44	.....	.....	.....	.....	.....							
3965...	*O* III	3961.59	1	0	$3s^1P-3p^1D$	.....	20	7.7	15	.....	.....	.....	.....	
	He I	3964.73	0	1	2^1S-4^1P	.....	2							

TABLE 5—*Continued*

λ	Atom	λ (Lab.)	J'	J	Multiplet	$s/\Sigma s$	I_t	BD +35°4013		BD +36°3956		BD +43°3571		Notes
								I	Δλ	I	Δλ	I	Δλ	
4025...	*He* II	4025.64	.....	.....	4^2F-13^2G	.....	.....							
	He I	4026.19	2, 1	3, 2, 1	$2^3P^0-5^3D$	.....	14	4.9	20	.....	.....	.....	.....	
		4026.36	0	1	.....	.....	.....							
4069...	*C* III	4056.06	2	3	$4d^1D-5f^1F$	.....	1							
		4067.87	2	3	$4f^3F-5g^3G$	.....	62							
		4068.97	3	4	.....	.....	.....	27.4	22	9.0	26	14	....	2
		4070.43	4	5	.....	.....	.....							
	O III	4073.90	1	2	$3s'\,^2P-3p'\,^2D$	.....	6							
		4081.10	2	3	.....	.....	.....							
4100...	*He* II	4100.08	.....	.....	4^2F-12^2G	.....	1	10.3	....	.....	.....	.....	.....	
4123...	*He* I	4120.81	2, 1	1	2^3P-5^3S	.....	.....							
		4120.98	0	1	.....	.....	.....							
	C III	4122.05	1	2	$4p^1P-5d^1D$	.....	1							
	O V	4123.01	0	1	$3s'\,^3P-3p'\,^3D$	0.11	55	11.4	16	5.2	31			
		4123.90	2	3	.....	.47								
		4121.70	1	0	$3p'\,^3S-3d'\,^3P$	.11								
		4135.86	1	1	.....	.33	17							
												11.6	....	
4157...	*O* V	4159.94	1	2	$3p'\,^3S-3d'\,^3P$	.55								
	C III	4156.50	2	3	$3p'\,^3D-5f^3F$	.....								
		4162.80	3	4	.....	.....	.....	8.2	17	.....	.....			
		4152.43	1	2	.....	.....								
	O V	4150.83	1	1	$3s'\,^3P-3p'\,^3D$	.08								
4187...	*O* V	4178.72	2	2	$3s'\,^3P-3p'\,^3D$	.25	.....							
	C III	4187.05	3	4	$4f^1F-5g^1G$	.....	19	9.4	22	.....	.....	.....	.....	
4225	.....	.....	.....	.....	.....	.....	.....	6.4	24	.....	.....	.....	.....	
4269...	*C* II	4267.02	3/2	5/2	$3d^2D-4f^2F$	.....	100							
		4267.27	5/2	5/2, 7/2	.....	.....	.....	9.0	26	.....	.....	5	....	
4330...	*C* III	4325.70	1	1	$3s'\,^1P-3p'\,^1D$	.....	6							
	He II	4338.71	.....	.....	4^2F-10^2G	.....	1	20.8	38	12.9	36	7.5	....	3
	C III	4368.14	.....	.....	$4f'\,^3G-5g'\,^3H$	.....	6							
		4361.85	.....	.....	$4f'\,^1G-5g'\,H$	.....	2	5.1	....	.....	.....			
4375...	*C* III	4379.97	1	0, 1	$4d^3D-5p^3P$	.11	12					6.6	....	
		4383.24	2	1, 2	.....	.25	.....	3.5	....	.....	.....			
		4388.24	3	2	.....	.47	.....							
	He I	4387.93	1	2	$2\,P-5^1D$	.....	3							
4441...	*C* IV	4441.81	1/2, 3/2	3/2, 5/2	$5p^2P-6d^2D$	.....	18	17.0	21	6.8	20			
4471...	*He* I	4471.48	2, 1	3, 2, 1	2^3P-4^3D	.....	32	7.6	28	2.7	...	13.6	....	
		4471.69	0	1	.....	.....	.....							
4515...	*C* III	4516.02	1	1	$4p^3P-5s^3S$	.....	3	5.2	15	.....	.....	.....	.....	
		4516.93	2	1	.....	.....	.....							
4542...	*He* II	4541.63	.....	.....	4^2F-9^2G	.....	2	10.0	23	4.1	....	11.7	....	
4608...	*C* III	4593.47	.....	.....	$4f'\,^3F-5g'\,^3G$	.....	4	5.2	26	.....	.....	.....	.....	
4650...	*C* III	4647.40	1	2	$3s^3S-3p^3P$	.55	100							
		4650.16	1	1	.....	.33	.....							
		4651.35	1	0	.....	.11	.....							
		4663.53	1	0	$3s'\,^3P-3p'\,^3P$	.11	9							
		4665.90	2	2	.....	0.42	.....	238	41	169	37	176	....	4
	C IV	4646.5	3/2, 5/2	5/2, 7/2	$5d^2D-6f^2F$	.....	11							
		4656.5	5/2, 7/2	7/2, 9/2	$5f^2F-6g^2G$	.....	8							
		4658.64	5/2, 9/2	9/2, 11/2	$5g^2G-6h^2H$	.....	5							
		4959.38	7/2, 9/2	5/2, 7/2	$5g^2G-6f^2F$	.....	.....							
		4664.5	5/2, 7/2	3/2, 5/2	$5f^2F-6d^2D$	.....	1							
4686...	*He* II	4685.81	.....	.....	3^2D-4^2F	.....	100	73.6	34	35.5	32	43	....	
4786...	*C* IV	4785.6	3/2, 5/2	1/2, 3/2	$5d^2D-6p^2P$	.....	3							
	O IV	4783.43	3/2	1/2	$3p'\,^4P-3d'\,^4D$	.....	6	7.0	21	8	20	.....	.....	
		4798.25	5/2	3/2	.....	.....	.....							
4861...	*He* II	4859.36	.....	.....	4^2F-8^2G	.....	2	11.2	23	2.6	22	.....	.....	
4938...	*He* I	4921.93	1	2	2^1P-4^1D	.....	7	3.8	....	.....	.....	.....	.....	

TABLE 5—*Continued*

λ	Atom	λ (Lab.)	J'	J	Multiplet	$s/\Sigma s$	I_t	BD +35°4013		BD +36°3956		BD +43°3571		Notes
								I	Δλ	I	Δλ	I	Δλ	
5019...	*He* I	5015.68	0	1	2^1S-3^1P	.....	5	8.0	17	5.5	24	.....	....	
	C IV	5015.9	1/2	1/2	$5p^2P-6s^2S$	.....	7							
		5017.7	3/2	1/2	.....	.....	.....							
5132...	*O* V	5114.45	.....	.....	$3s'^1S-3p^1P$	.....	23	11.8	25	10.0	....	10	....	5
	C II?	5132.96	1/2	3/2	$3s^4P-3p^4P$	0.14	35							
		5133.29	3/2	5/2	.....	.15								
5257...	*C* III	5249.6	2	1	$4d^1D-5p^1P$	.....	2	11.6	24	3.3	53	12.3	....	
		5244.5	0	1	$3s'^3P-3p'^3S$	.....	2							
		5253.55	1	1	.....	.....	.....							
		5272.56	2	1	.....	.....	.....							
	O III	5268.06	1	2	$3p'^1S-3d^1P$	.....	2†							
5302...	*O* IV	5305	.....	.....	predicted	.....	.....	11.6	36	.....	.....	.....	.....	
5412...	*He* II	5411.57	.....	.....	4^2F-7^2G	.....	4	10.1	20	5.4	16	18.5	....	
	O V	5418.3	1	2	$3p^3P-3d^3P$	.14	6	.....	.....	.....	.....	.....	.....	
5470...	*O* V	5474.6	2	2	.....	.42		8.3	26	8.5	24	.....	.....	
5592...	*O* V	5572.1	0	1	$3p^3P-3d^3D$	.11	100	4.8	36	11.5	29	17	....	
		5580.0	1	2	.....	.25	.....							
		5583.1	1	1	.....	.08	.....							
		5597.9	2	3	.....	0.47	.....							
		5603.9	2	2	.....	.....	.....							
	O III	5592.37	1	2	$3s^1P-3p^1D$	.....	6†							
5695...	*C* III	5696.0	1	2	$3p^1P-3d^1D$	.....	25†	96	40	65	40	62	....	
5805...	*C* IV	5801.51	1/2	3/2	$3s^2S-3p^2P$	.....	100†	82.5	52	140	40	200	....	
		5812.14	1/2	1/2	.....	.....	.....							
5876...	*He* I	5875.62	2, 1	3, 2, 1	2^3P-3^3D	.....	100	30.6	36	14	30	33	....	
		5875.96	0	1	.....	.....	.....							
6147...	*C* III	6154.4	.....	.....	.....	.....	.....	3.9	40	.....	.....	.....	.....	
		6155.4	.....	.....	.....	.....	.....							
		6156.7	.....	.....	.....	.....	.....							
6235...	.....	.....	.....	.....	.....	.....	.....	1.4	50	.....	.....	.....	.....	

NOTES FOR TABLE 5

1. The *C* II doublet, $3p^2P^0-4s^2S$, λ 3921, for which Whipple and Mrs. Gaposchkin find an intensity of 74, may contribute to this blend.

2. The *C* II $3d'\ ^4D-4f'\ ^4F$ multiplet at λ 4075 for which Whipple and Mrs. Gaposchkin give an intensity of 24 probably does not contribute to this line.

3. The *C* II $3s^4P-3p^4P^0$ multiplet for which Whipple and Mrs. Gaposchkin predict an intensity of 68 may contribute to the λ 4330 and λ 4375 lines:

λ	$s/\Sigma s$	λ	$s/\Sigma s$
4317.16	0.14	4349.44	0.35
4319.65	.15	4366.91	0.15
4345.57	0.14	.....	.....

4. Swings concludes from the relative laboratory intensities in the 5–4 transitions that λ 4658.64 must be the strongest of the 6–5 transitions and that λ 4656.5 and λ 4646.5 are weaker. According to the J-file sum rules, the relative strengths of λλ 4658.6, 4656.5, and 4646.5 should be 990, 504, and 210.

5. The identification of this line is unsatisfactory. The stronger lines of the *C* II quartet at λ 5145.16 and λ 5151.08, or relative strengths 0.35 and 0.15, have not been measured.

Color temperatures require careful spectrophotometric measures of the continuous background over a considerable wave-length range; we cannot discuss them here for lack of suitable data. Gerasimovič's measures,[18] made some fifteen years ago, are not precise enough for our purposes. The calculation of effective temperatures requires a knowledge of both the sizes and total brightnesses of the stars in question, but these quantities are

[18] *Harv. Circ.*, No. 339, 1929.

known for only one Wolf-Rayet star, a component of the eclipsing binary BD+38°4010, for which S. Gaposchkin finds an effective absolute temperature of 13,000°. Ionization temperatures depend upon assumptions concerning the electron density, a quantity we cannot estimate well enough for these stars. In this paper we shall use estimates of the populations of certain upper levels to define an excitation temperature according to the Boltzmann formula. The measured line intensities tell us the relative populations of the excited levels which we try to represent by using this formula as sort of an interpolation device. The nearer the levels are to the ionization limit, the more accurately should such an excitation temperature represent the electron temperature of the region where these lines are produced.

Let the measured intensities of two lines (or multiplets) of a given ion be I_1 and I_2, their wave lengths be λ_1 and λ_2, and their upper levels be a and b and their lower levels c and d, respectively (Fig. 2). Let χ_a and χ_b be the excitation potentials of a and b, and

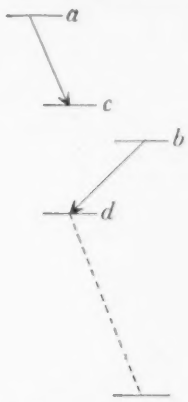

FIG. 2.—Schematic energy diagram

A_1 and A_2 be the Einstein probability coefficients for the lines of wave lengths λ_1 and λ_2. In thermodynamic equilibrium, I_1 and I_2 are given by

$$\left.\begin{aligned} I_1 &= \frac{N_0}{\varpi_0}\, e^{-\chi_a/kT} \Sigma\varpi_a A_1 h\nu_1 , \\ I_2 &= \frac{N_0}{\varpi_0}\, e^{-\chi_b/kT} \Sigma\varpi_b A_2 h\nu_2 , \end{aligned}\right\} \tag{1}$$

where N_0 is the number in the ground level of statistical weight and where the summation is carried out over the lines of a multiplet. The intensity ratio I_1/I_2 is related to the temperature T by

$$\frac{I_1}{I_2} = e^{-(\chi_a-\chi_b)/kT}\, \frac{\Sigma\varpi_a A_1\nu_1}{\Sigma\varpi_b A_2\nu_2} . \tag{2}$$

Let I_1° and I_2° be the predicted intensities at a temperature T_0 of the two emission multiplets whose upper terms are a and b. We may use the intensity estimates by Whipple and Mrs. Payne-Gaposchkin. Then

$$I_1^\circ = C_1 e^{-\chi_a/kT} ; \qquad I_2^\circ = C_2 e^{-\chi_b/kT} . \tag{3}$$

where C_1 and C_2 are constants related to N_0, A_1, A_2, λ_1, and λ_2 and the unit of intensity chosen (the I° of the strongest line usually is called 100 on the Whipple-Gaposchkin scale). For a temperature T_0, the predicted multiplet ratio will be

$$\frac{I_1^\circ}{I_2} = \frac{C_1}{C_2}\, e^{-(\chi_a - \chi_b)/kT_0}. \tag{4}$$

If I_1 and I_2 are the observed intensities, then

$$\frac{I_1}{I_2} = \frac{C_1}{C_2}\, e^{-(\chi_a - \chi_b)/kT}$$

and

$$\log \frac{I_1}{I_2} = \log \frac{I_1^\circ}{I_2^\circ} + 5040\,(\chi_a - \chi_b)\left(\frac{1}{T_0} - \frac{1}{T}\right). \tag{5}$$

The first term on the right is computed from the tables of Whipple and Mrs. Payne-Gaposchkin; χ_a and χ_b are taken from Edlén's term tables; and $\log (I_1/I_2)$ is an observed quantity. Since T_0 is given, the estimate of T follows at once.

Since the intensity estimates of Whipple and Mrs. Payne-Gaposchkin are of a semi-empirical character, I considered it worth while to compute the intensities of the lines used in the temperature determinations by purely theoretical methods. In thermodynamic equilibrium the intensity of a line is given by

$$\left.\begin{aligned} E = N A\, h\nu = \frac{\varpi_i}{b(T)}\, N_0 e^{-\chi/kT} A\, h\nu = \frac{2J+1}{b(T)}\, N_0 e^{-\chi/kT} \frac{1}{2J+1} \frac{64\pi^4\nu^4}{3c^3} \frac{\epsilon^2 a^2}{4l^2-1} \\ \times S\rho^2 \frac{s}{\Sigma s}, \end{aligned}\right\} \tag{6}$$

since

$$A(J, J') = \frac{1}{2J+1} \frac{64\pi^4\nu^4}{3hc^3} \frac{\epsilon^2 a^2}{4l^2-1} \rho^2 S \frac{s}{\Sigma s}, \tag{7}$$

where J' and J refer to the inner quantum numbers of the lower and upper levels of the transition, $a = 0.528 \times 10^{-8}$ cm is the radius of the first Bohr orbit, l is the larger of initial or final values of this quantum number, S is the strength of the multiplet, s is the strength of a single line of the multiplet (hence $s/\Sigma s$ is the fraction contributed by the given line to the total strength of the multiplet), N_0 is the total number of atoms of the given kind, and $b(T)$ is the partition function. Finally, ϵ, c, h, m, and ν have their usual meanings. The radial quantum integral,

$$\rho = \int_0^\infty R_{nl} R_{n'l'} r^3 dr, \tag{8}$$

where

$$\int_0^\infty R_{nl}^2 r^2 dr = 1,$$

differs for each configuration; and, since we shall be interested in comparing lines of different configurations, we shall have to estimate the radial wave functions.

An accurate evaluation of the radial functions for complex atoms is difficult and laborious. With lighter atoms the variation treatment has been used effectively.[19] The method of the self-consistent field has been used to calculate wave functions for the

[19] See, e.g., Zener, *Phys. Rev.*, **36**, 51, 1930.

ground levels of a number of atoms and ions; it could be employed also to calculate the radial wave functions for excited levels. Unfortunately, these methods involve considerable numerical calculation for each transition array. Hence a simpler approach was employed for the problem at hand.

Slater[20] proposed a hydrogen-like radial wave function which contains certain parameters whose values may be adjusted according to specified rules. Menzel and the author[21] have computed the radial quantum integral for a number of transitions in O III with the aid of these wave functions. This same procedure has been employed in the present paper to compute theoretical ρ's for the transitions of importance in temperature estimates.

The strengths, S, depend upon the angular factors in the wave functions. Goldberg[22] has tabulated S for a number of multiplets of interest. In other cases the application of Shortley's "J-file sum rule" has yielded values of S.[23] Exclusive of the radial quantum integral, the total strength of the lines of the transition array originating in (or ending on) any term is given by

$$(2S+1)\,(2L+1)\,l(2l-1), \qquad \text{if} \qquad l'=l-1\,,$$

or

$$(2S+1)\,(2L+1)\,(l+1)\,(2l+3), \qquad \text{if} \qquad l'=l+1\,.$$

As an example, let us consider the 3360 multiplet of N III:

$$2s2p3s'\ {}^4P - 2s2p3p'\ {}^4P\,.$$

Now the $3p\,{}^4P$ term can combine only with the ^4P term in the 2s2p3s configuration. Therefore, the sum of the strengths of all transitions of the 2p3s − 2p3p configuration originating in the $3p\,{}^4P$ term is simply the strength of the 3360 multiplet. For the upper level, $S = 3/2$, $L = 1$, and $l = 1$; hence, $S = 12$.

Table 6 summarizes the results of the theoretical calculations for the lines in which we are interested. Successive columns give the mean wave length of the multiplet,[15] the designation of the multiplet, the strength calculated from Goldberg's tables, or, by the J-file sum rule, ρ, and finally $\Sigma(2S+1)A(J,J')$ for the multiplet in question. Inserting numerical values, we get

$$A = 2.01\times10^{-6}\,\frac{1}{2J+1}\,\frac{\rho^2 S}{(4l^2-1)}\,\frac{s}{\Sigma s}\times\frac{1}{\lambda^3}\,, \tag{9}$$

and, accordingly,

$$\Sigma\,(2J+1)\,A\,(J,J') = 2.01\times10^{-6}\,\frac{\rho^2 S}{(4l^2-1)\,\lambda^3}\,, \tag{10}$$

while

$$\frac{I_1}{I_2} = \frac{\dfrac{\rho_1^2 S_1}{(4l_1^2-1)}\,\lambda_2^4}{\dfrac{\rho_2^2 S_2}{(4l_2^2-1)}\,\lambda_1^4}\,e^{-(\chi_a-\chi_b)/kT}\,. \tag{11}$$

[20] *Phys. Rev.*, **36**, 57, 1930.

[21] *Ap. J.*, **94**, 436, 1941. These radial quantum integrals are but rough approximations of the true values. The Slater functions neglect the nodes and loops in the wave functions and are only approximately accurate for large distances from the nucleus.

[22] *Ap. J.*, **82**, 1, 1935; **84**, 11, 1936.

[23] See Condon and Shortley, *Theory of Atomic Spectra*, p. 247.

Table 8 lists the excitation temperatures of the various Wolf-Rayet stars, as determined from the different line ratios. Successive columns list the ion, the lines used, and their adopted intensities, frequently corrected for blending, the temperatures determined from the semi-empirical multiplet intensities, and the temperatures determined from the purely theoretical intensities. In some cases the agreement between the temperature found by the two methods is excellent; in other cases it is poor. Table 7 gives

TABLE 6

THEORETICAL MULTIPLET STRENGTHS AND INTENSITY DATA

Atom	λ	Multiplet	S	ρ	$\Sigma(2J+1)A(J,J')$
C III	3609	$2s4p\,^3P-2s5d\,^3D$	90	5.45	7.65×10^9
	4069	$2s4f\,^3F-2s5g\,^3G$	756	5.45	1.06×10^{10}
	4187	$2s4f\,^1F-2s5g\,^1G$	252	5.45	3.28×10^9
	4368	$2p4f'\,^3G-2p5g'\,^3H?$	924	5.45	1.07×10^{10}
	4383	$2s4d\,^3D-2s5p\,^3P$	90	5.45	4.26×10^8
	4650	$2s3s\,^3S-2s3p\,^3P$	9	3.34	6.68×10^8
	5696	$2s3p\,^1P-2s3d\,^1D$	30	3.40	2.52×10^8
C IV	3930	$5s\,^2S-6p\,^2P$	6	4.50	1.45×10^9
	4441	$5p\,^2P-6d\,^2D$	60	4.67	1.99×10^9
	5805	$3s\,^2S-3p\,^2D$	6	2.62	1.41×10^9
N III	3360	$2s2p3s'\,^4P-2s2p3p'\,^4P$	12	3.18	2.13×10^9
	3750	$2s2p3s'\,^4P-2s2p3p'\,^4S$	4	3.18	1.54×10^9
	4100	$2s^23s\,^2S-2s^23p\,^2P$	6	3.18	5.87×10^8
	4200	$2s2p3s'\,^2P-2s2p3p'\,^2D$	10	3.18	9.10×10^8
	4379	$2s4f\,^2F-2s5g\,^2G$	504	5.45	5.69×10^9
	4525	$2s2p3s'\,^4P-2s2p3p'\,^4D$	20	3.18	1.46×10^9
	4536	$2s2p3p'\,^4S-2s2p3d'\,^4P$	40	3.30	6.27×10^8
	4638	$2s^23p\,^2P-2s^23d\,^2D$	60	3.30	8.78×10^8
N IV	3483	$2s3s\,^3S-2s3p\,^3P$	9	2.53	9.19×10^8
	3748	$2p3s'\,^1P-2p3p'\,^1D$	5	2.53	4.09×10^8
	4057	$2s3p\,^1P-2s3d\,^1D$	30	2.57	3.99×10^8
O III	3265	$2s^22p3p\,^3D-2s^22p3d\,^3F$	126	3.20	5.0×10^9
	3708	$2s^22p3p\,^3P-2s^22p3d\,^3D$	135/2	3.20	1.84×10^9
	3760	$2s^22p3s\,^3P-2s^22p3p\,^3D$	15	3.04	1.75×10^9
O IV	3386	$2s2p3s'\,^4P-2s2p3p'\,^4D$	20	2.45	2.08×10^9
	3411	$2s^23p\,^2P-2s^23d\,^2D$	60	2.52	1.28×10^9
	3562	$2s2p3p'\,^2D-2s2p3d'\,^2F$	84	2.52	1.58×10^9
	3730	$2s2p3p'\,^4D-2s2p3d'\,^4F$	168	2.52	2.75×10^9
O V	4124	$2p3s'\,^3P-2p3p'\,^3D$	15	2.04	6.00×10^8
	4147	$2p3p'\,^3S-2p3d'\,^3P$	30	2.07	2.42×10^8
	5590	$2p3p\,^3P-2p3d\,^3D$	135/2	2.07	2.21×10^8

the excitation potentials of the lines used in the temperature determinations. Table 9 lists the excitation temperature adopted for each ion in each star. As one would expect, there is a very marked tendency for the excitation temperature to depend upon the degree of ionization. Generally, the greater the ionization potential the higher the excitation temperature, but frequently there are large discordances between the temperatures calculated from different lines of the same ion. These discrepancies may arise from a number of causes. First, there are the inevitable errors of observation, especially serious for the weaker lines and for the comparison of lines falling in widely separated portions of the spectrum. Second, the theoretical intensities suffer largely from our ignorance of the

true radial-quantum wave functions and from possible deviations from *LS* coupling. Russell-Saunders coupling is a good approximation only when electrostatic interaction is much more important in separating the levels than is spin-orbit interaction. Deviations from *LS* coupling become important for the higher terms of an atom.[24]

There are a number of serious theoretical objections to this method of temperature determination. We have assumed that the Wolf-Rayet atmosphere is transparent to its own radiations, i.e., that there is no self-reversal. If there is self-reversal, the intensity of a line is no longer simply proportional to the number of atoms acting to produce it, and a "curve of growth effect" obtains. The stronger lines tend to become weakened with respect to the fainter ones, and this is precisely the effect observed in a number of stars.

TABLE 7

THE EXCITATION POTENTIALS OF THE UPPER LEVELS OF CERTAIN EMISSION LINES OR MULTIPLETS OBSERVED IN WOLF-RAYET STARS

Ion	λ	x	Ion	λ	x	Ion	λ	x
C III...	3609	42.64	*N* III...	3360	39.08	*O* III..	3265	40.10
	4069	42.78		3750	38.70		3708	40.41
	4187	42.78		3938	41.26		3760	36.30
	4368	50.81		4100	30.28			
	4383	42.49		4200	39.59	*O* IV..	3386	57.80
	4650	32.06		4379	41.31		3411	51.79
				4517	38.26		3562	63.08
C IV....	3934	58.12		4543	41.42		3730	61.12
	4441	58.19		4638	32.95			
	5805	39.51				*O* V...	4124	83.60
			N IV...	3483	49.99		4147	87.40
				3748	61.60		5590	74.15
				4057	52.90			

At a temperature of 36,000° the *He* II 4686 line should be roughly thirty-five times as strong as the *He* II 5411 line of the Pickering series. Actually, it is only six or seven times stronger in the four stars of the nitrogen sequence (where λ 4686 is the strongest line in the spectrum) and in BD+35°4013 and BD+36°3956, while it is only about twice as strong in BD+43°3571.

The strongest lines are generally those arising from the lower levels, and, if they are weakened systematically by self-reversal, our computed temperatures will come out too high. Furthermore, if the excited levels of the atoms are populated principally by the capture and subsequent cascading of electrons, the partition of atoms among the excited levels will differ from that in thermodynamic equilibrium, in the sense that the lower levels will have too small a population. Such an effect, even without self-reversal, would tend to make the computed temperatures come out too high. Swings[25] has shown, however, that the dilution of radiation in the envelopes of Wolf-Rayet stars cannot be great, and we may reasonably suppose that line excitation plays an important role in populating the excited levels. Theoretical studies of gaseous nebulae[26] suggest that in this case deviations from a Boltzmann distribution may even take place in the opposite sense; i.e., the lower excited levels may have too large a population.

[24] *Ibid.*, chap. vii. See also H. E. White, *Introduction to Atomic Spectra*, p. 200, noting Figs. 12, 13. Configuration interaction may also be of importance for certain levels in complex atoms.

[25] Swings found that the dilution of radiation in the helium lines is small. As he and Struve remark, however, this result does not necessarily require that the extent of the envelope be small but merely that the helium line radiation remains intense throughout the gaseous shell. See n. 32, below.

[26] *Ap. J.*, **88**, 422, 1938.

TABLE 8*

EXCITATION TEMPERATURES OF THE WOLF-RAYET STARS

Ion	Line Ratio	I_1	I_2	T_W	T_A	Notes
	BD+43°3571					
He II.....	3203/4686	.....	.....	18,000	.....	
C III.....	4069/4650	14	176	24,000	23,000	
	(4383+4368)/5696	6.6	62	22,500	.....	
C IV.....	3934/5805	<6.3	200	⩽ 45,000	35,000	
O III.....	3760/3265	6.9	5.3	26,500	30,000	
O IV.....	(3386+3411)/3562	22.0	2.9	140,000	70,000	
O V.....	(4124+4147)/5590	9.0	17	79,000	52,000	
	BD+35°4013					
He II.....	3203/4686	.....	.....	200,000	.....	1
O III.....	3760/3265	13.6	12.8	26,600	35,000	
	3708/3760	10.0	13.6	73,000	133,000	2
O IV.....	3411/3734	40.0	18.7	230,000	75,000	
	3411/3562	40.0	6.0 7.7	130,000–160,000	70,000	4
O V.....	4124/5590	.....	.....	.....	250,000	
C III.....	(4187+4069)/4650	9.4+27.4	220	26,200	25,000	
	4368/4650	5.1	220	24,200	33,000	
	3609/4650	16.4	220	46,000	23,200	
C IV.....	(4441+3934)/5805	17.0+10.0	82.5	77,000	47,000	5
	BD+36°3956					
O III.....	3708/3760	8	7.6	150,000	.....	2
O V.....	4124/5590	3.7	11.5	70,000	45,000	6
C III.....	4069/4650	9.0	160	22,000	21,600	
C IV.....	(3934+4441)/5805	⩽5.5+6.8	140	52,000	36,400	
	BD+36°3987					
He II.....	3203/4686	20.3	54.3	36,000	.....	
N III.....	4518/4638	6.15	11.8	40,000	51,000	8
	4518/4100	6.15	10	.....	70,000	9
	BD+35°4001					
He II.....	3203/4686	95.7	237	44,000	.....	
N III.....	4380/4638	6.7	38.3	31,000	34,000	
	4200/4100	14	45.4	43,000	68,000	9
N IV.....	4057/3483	30	92	72,000	260,000	
	BD+38°4010					
He II.....	3203/4686	8.5	6.5	10,000	.....	
N III.....	4379/4638	7.0	13.5	45,000	42,000	
	(4517+4543)/4638	⩽12.0	13.5	63,000	57,000	

* A comparison of the intensities in Table 8 with those in Tables 4 and 5 will show many cases where the relative contributions of the different components of a blend have been estimated for the purpose of the temperature calculations.

TABLE 8—*Continued*

Ion	Line Ratio	I_1	I_2	T_W	T_A	Notes
	BD+37°3821					
He II.....	3203/4686	86	270	23,000	27,600	
N III.....	4379/4638	9.0	67	29,000	.....	
	3938/4638	3.0	67	25,400	18,500	
	3750/4638	(4.0)	67	25,800	.....	7
	3360/4638	14.4	67	28,000	.....	
	4379/4100	9.0	70	29,400	33,000	9
	3938/4100	3.0	70	26,700	.....	9
	3750/4100	.....	.....	27,200	25,000	9
	3360/4100	14.4	70	27,200	33,000	9
N IV.....	3748/3480	(11.2)	62	130,000	160,000	

NOTES FOR TABLE 8

1. The intensity of λ 3203 is based on one plate and may be subject to large accidental error.
2. Two *O* III multiplets contribute to λ 3708. Their excitation potentials are different, so that it is hard to allow for them.
3. The line 3730 has been corrected for blending with *O* V.
4. The uncertainty arises from the necessity of correcting the *O* IV line for blending by *O* III. The line λ 5590 of *O* V seems abnormally weak.
5. The line 3934 has been corrected for blending with a *C* II multiplet.
6. The intensity of λ 4124 has been corrected for blending of *C* III.
7. The λ 3750 band is a blend of *N* III and *N* IV radiations. On the basis of an excitation temperature of 25,000°, the predicted intensity of 3750 of *N* III is 4.0. Hence, I have computed the relative contributions of *N* III and *N* IV and have estimated the excitation temperature of *N* IV.
8. The 4518 band includes 88 per cent of the intensity of the $3s'\ ^4P-3p'\ ^4D$ multiplet. The observed intensity was therefore increased.
9. The line 4100 has been corrected for the *He* II contribution to this predominantly *N* III band.

The temperature derived from the bright lines of an atom in the nth stage of ionization should be closely related to the Maxwellian temperature of the electrons captured by the atom in the $(n + 1)$th stage of ionization. Thus, the temperature derived from the bright lines of *O* III corresponds to the temperature characterizing the velocity distribution of the electrons captured by the *O* IV ions. The higher the levels from which we determine the temperature, the more closely should this approximation hold. The electron temperatures of the radiating layers of a Wolf-Rayet star must be very much higher than those existing in the gaseous nebulae. The radiation density is very much greater in the former case, and the cooling effect of inelastic collisions plays a negligible role.

As previous writers have pointed out, the large range in ionization represented in some of the individual stars cannot be interpreted on the basis of a single temperature and pressure. We are looking through a stratified atmosphere, whose transparency in the ordinary wave-length regions is rather high. We cannot see the photospheres of these stars; indeed, we are not even sure that they possess photospheres, in the ordinary sense of the word. Such evidence as the simultaneous appearance of lines of *He* I and *Ne* V suggests that the transparency of the atmosphere is great in the ordinary spectral regions, although it may be small in the ultraviolet, where the bulk of the radiation flows. The planetary nebulae provide a rather extreme analogy. In the observable spectral regions these bodies are quite transparent, and we normally see the central star; but, if they could be observed below the Lyman limit, it has generally been believed that the planetaries would appear quite opaque and that the central star would be totally obscured. The evidence for the small dilution effects in Wolf-Rayet atmospheres must be remembered, however, before one draws too close an analogy with the planetary nebulae.

Beals[11] suggested that the bright-line emission originates entirely through the operation of the Zanstra and Menzel mechanism for the hydrogen and helium radiations in the gaseous nebulae. Atoms in the ground level become photoelectrically ionized; the electrons are recaptured in the higher levels and cascade downward to give rise to the observed radiations. In this way, Beals accounted for the great intensities of the emission

TABLE 9

COMPARISON OF THE EXCITATION AND ZANSTRA TEMPERATURES FOR THE WOLF-RAYET STARS

Star	Atom	Excitation Temperature	Zanstra Temperature (Beals)	Notes
BD+43°3571	*He* II	18,000		
	C III	23,000		
	C IV	40,000	60,500	1
	O III	28,000		
	O IV	70,000	(Adopted $T=110{,}000$)	3
	O V	80,000		
35°4013	*He* II	.....		
	C III	28,000	66,500	1
	C IV	60,000	74,000	2
	O III	30,000	87,000	2
	O IV	75,000		
	O V	200,000?	(Adopted $T=90{,}000$)	3
36°3956	*C* III	22,000	(Adopted $T=90{,}000$)	3
	C IV	45,000		
	O V	70,000		
36°3987	*He* II	36,000	(Adopted $T=95{,}000$)	3
	N III	40,000		
35°4001	*He* II	44,000	72,500	1
	N III	40,000	(Adopted $T=85{,}000$)	3
	N IV	75,000		
38°4010	*He* II	10,000?		
	N III	55,000		
37°3821	*He* II	23,000	71,000	2
	N III	27,000	(Adopted $T=95{,}000$)	3
	N IV	130,000		
	N V	.....	90,500	2

NOTES TO TABLE 9

1. *Pub. Dom. Ap. Obs.*, **6**, 139, 1934, Table 8.
2. *J. R. Astr. Soc. Canada*, **34**, 179, 1940, Table 3.
3. *Ibid.*, Table 4.

lines with respect to the background continuum and derived temperatures of the Wolf-Rayet stars by the Zanstra method. He obtained a lower limit to the temperature when he applied the method to an ion like *N* III, *C* III, or *C* IV by supposing that all the recaptured electrons, in cascading, acted to produce one or another of the observed lines. For example, the number of quanta radiated in the 4650 *C* III line would be equated to the number of quanta absorbed by *C* III ions to become photoelectrically ionized, since it was assumed that every recaptured electron is regained on an excited level and that, as it cascades downward, the atom radiates the 4650 line. Beals pointed out that this assumption would give a lower limit to the temperature because most of the electrons are likely

PLATE XVIII

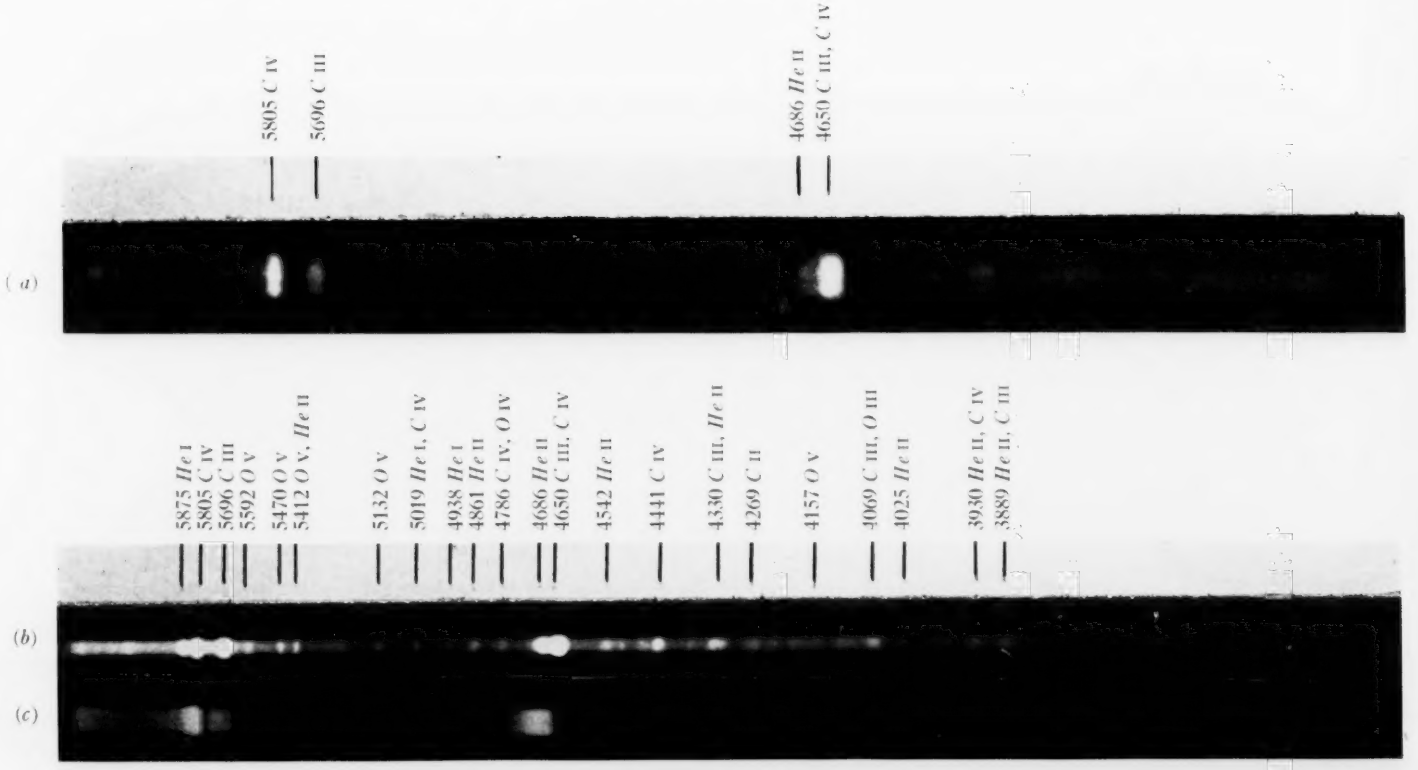

STARS OF THE CARBON SEQUENCE

(*a*) BD+36°3956; (*b*) BD+35°4013; (*c*) BD+43°3571

PLATE XIX

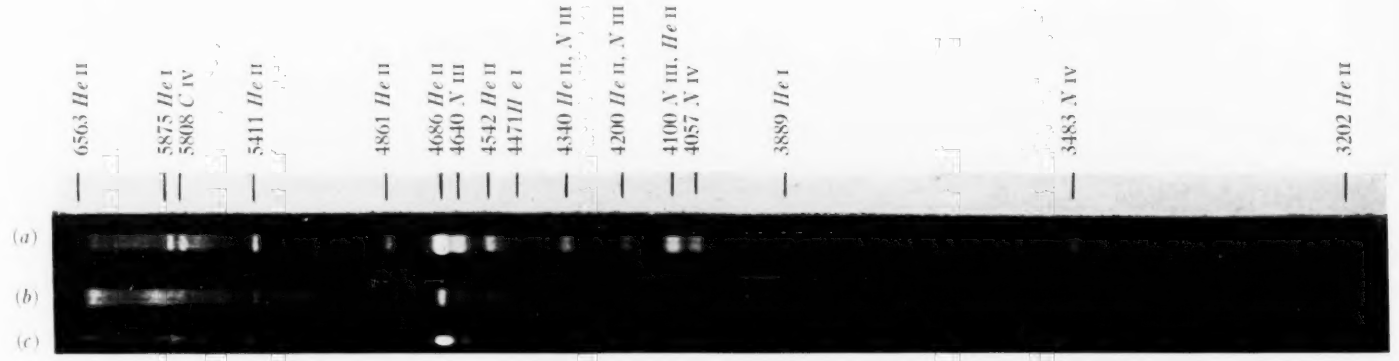

STARS OF THE NITROGEN SEQUENCE

(*a*) BD+37°3821; (*b*) BD+30°3987; (*c*) +35°4001

to be recaptured on the lower levels, not to produce observable lines at all. In his discussion of the origin of the permitted lines of *C* III and *N* III in NGC 6543, Swings[27] suggested that strong nuclear ultraviolet radiations of *O* IV, *C* IV, *N* IV, and *N* V may play an important role in photo-ionization processes. In the Wolf-Rayet atmospheres such line radiation may play an important role in exciting the higher levels of the observed ions; and, if the dilution of radiation is small, the primary mechanism is probably not so effective in the production of emission lines and the straight absorption and re-emission of line radiation. In that case the assumptions underlying the method of Beals are open to serious question. In any event, the Wolf-Rayet stars probably do not radiate as black bodies in the ultraviolet but have spectra characterized by a number of strong emission lines.[16] Hence, the temperatures of planetary nuclei and classical Wolf-Rayet stars derived by the Zanstra method can at best be regarded as only orders of magnitude. The last column of Table 9 lists the temperatures obtained by Beals by the application of the Zanstra method; they are generally higher than the excitation temperatures.

In Figure 3, I have plotted the mean excitation temperature as a function of ionization potential. The points give the mean temperature for all stars for a given ion; ions of the same ionization potential have been grouped together. The individual points on which this curve is based show much scatter, but there is a marked indication that the temperature rises as the ionization potential increases. The interpretation is simple; a high temperature is required to multiply ionized atoms of carbon, nitrogen, and oxygen. As far as emission-line excitation is concerned, the temperature of the Wolf-Rayet star depends upon the type of atomic thermometer used.

THE CHEMICAL COMPOSITION OF THE WOLF-RAYET STARS

Our plot of excitation temperature against ionization potential amounts to a plot of temperature against some function of depth in the star. The lower layers, wherein the radiations of ions such as *C* IV and *O* V originate, have temperatures of the order of eighty or a hundred thousand degrees, while the lines of *O* II and *He* I appear in the outer layers, where the temperature may be of the order of ten or twenty thousand degrees. This stratification of the Wolf-Rayet atmospheres makes a semiquantitative determination of their chemical composition difficult. We may know the temperature as a function of ionization potential, but we have no information concerning the increase of electron density with depth in the star. Nevertheless, I have attempted a preliminary analysis on the basis of my temperature calculation and line-intensity measurements.

The amount of energy radiated per unit volume by N_n atoms in the level n in the line ν is $N_n A h\nu$, where A is the Einstein coefficient. The number of atoms in the level n is given by the combined Boltzmann and Saha equations[28]

$$N_n = b_n \frac{N_i N_e}{T_e^{3/2}} \frac{h^3}{(2\pi mk)^{3/2}} \frac{\varpi_n}{\varpi_j} e^{I_n/kT_e}, \tag{12}$$

where b_n is a measure of the deviation of the level from thermodynamic equilibrium, ϖ_n is the statistical weight of the level in question, and ϖ_j is the weight of the ground level of the ion,

$$I_n = \chi_n - \chi_1, \tag{13}$$

where χ_1 is the ionization potential of the atom, and χ_n is the excitation potential of the level in question. From (12) we obtain

$$\left.\begin{aligned} N_i N_e = \frac{(2\pi mk)^{3/2}}{h^3} \frac{E\varpi_j}{\varpi_n A h\nu} T_e^{3/2} e^{-I_n/kT_e} = 2.39 \times 10^{15} \frac{\varpi_j}{\varpi_n A h\nu} T_e^{3/2} e^{-I_n/kT_e} E \\ = C_\lambda T_e^{3/2} e^{-I_n/kT_e} E . \end{aligned}\right\} \tag{14}$$

[27] *Ap. J.*, **92**, 289, 1940.

[28] *Ap. J.*, **85**, 336, 1937.

Because of its simple hydrogenic structure, we may write for *He* II

$$E_{nn'} = b_n \frac{N_i N_e}{T_e^{3/2}} \frac{hKg2RZ^6}{n'^3 n^3} e^{X_n},$$

where $X_n = \frac{hRZ^2}{n^2 kT_e}$ and $hK = 2.097 \times 10^{-32}$. For any *He* II line our formula becomes

$$E_{nn'} = C_{nn'} b_n \frac{N_i N_e}{T_e^{3/2}} e^{a_n/T}, \tag{15}$$

whence we obtain for λ 4686 and two lines of the Pickering series, 5411 and 4542, the following values of $C_{nn'}$ and a_n:

λ	n	n'	$C_{nn'}$	a_n
4686	4	3	3.92×10^{-18}	3.93×10^{4}
4542	9	4	1.70×10^{-19}	0.77
5411	7	4	3.51×10^{-19}	1.28

In the calculations I have neglected self-reversals and have assumed that the intensity of a line is simply proportional to E. I have adopted the temperature from the curve of

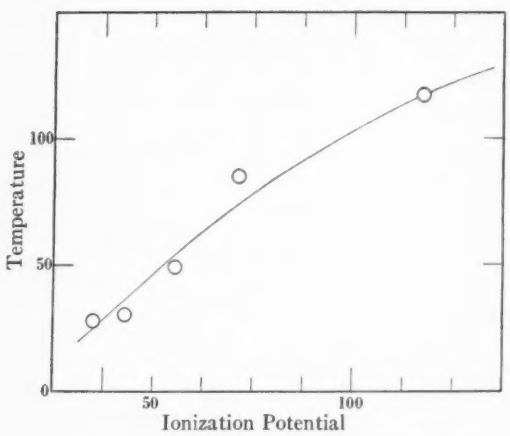

FIG. 3.—Relation between excitation temperature and ionization potential

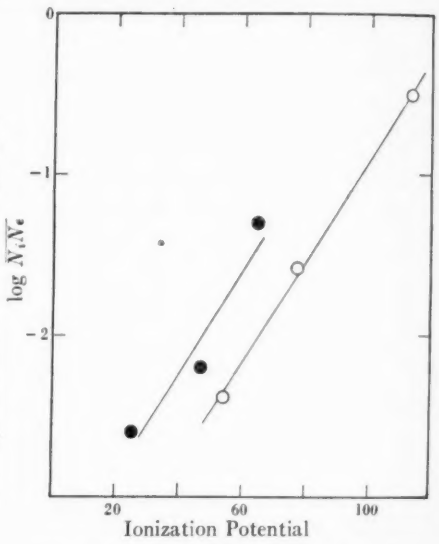

FIG. 4.—Relation between $\overline{N_iN_e}$ and ionization potential

Figure 4 except for a few ions in some stars, where I have used the temperatures directly from Table 9. The ϖA's have been taken from Table 6. Table 10 lists the lines used in the stars of the two sequences C_λ and I_n. Table 11 shows the values of log $\overline{N_iN_e}$ for the various ions, expressed in terms of the value of $\overline{N_iN_e}$ for *He* II. Notice that, as the degree of ionization increases, so does the value of $\overline{N_iN_e}$. I interpret this as meaning not that there is an overwhelming preponderance of the most highly ionized atoms of each sort, e.g., *C* IV, *O* VI, etc., in the radiating layers of the star's atmosphere but rather that in the

lower layers N_e increases rapidly, so that the product $\overline{N_i N_e}$ rises. In Figure 4, I have plotted log $\overline{N_i N_e}$ against χ for carbon and oxygen for BD+35°4013.

Let us try to compare the relative amounts of helium, oxygen, and carbon in the atmospheres of the stars of the carbon-oxygen sequence. The fact that oxygen and carbon

TABLE 10

FACTORS FOR CALCULATING ABUNDANCES OF VARIOUS IONS

Ion	λ	log C_λ	I_n	Ion	λ	log C_λ	I_n
C II	4267	17.37	3.36	*He* II	4542	18.77	0.90
C III	3609	17.36	5.00		4686	17.41	4.57
	4069	17.27	4.86		5411	18.45	1.49
	4187	17.79	4.86				
				N III	3360	17.58	8.12
C IV	3934	17.82	6.05		3750	17.77	8.50
	4441	17.73	5.98		4100	18.23	16.92
	5805	18.00	24.66		4200	18.05	7.61
					4380	17.27	5.89
O III	3708	18.17	14.21		4525	17.88	9.06
	3760	18.19	18.32		4638	18.11	14.25
O IV	3411	17.81	25.24	*N* IV	3483	18.26	27.05
	3562	17.74	13.95		3748	18.65	15.43
	3734	17.52	15.91		4057	18.69	24.13
O V	4124	18.53	29.70				
	5590	19.09	39.2				

TABLE 11*

VALUES OF $N_i N_e$ WITH RESPECT TO *He* II

Ion	BD +35°4013	BD +43°3571	BD +36°3956	Ionization Potential
C II	−2.6	.....	.....	24.26
C III	2.20	−2.66	−2.14	47.64
C IV	1.30	2.05	0.97	64.17
O III	2.38	3.55	2.00	54.62
O IV	1.47	2.00	1.20	77.03
O V	−0.5	−0.5	−0.30	113.3

Ion	BD +37°3821	BD +35°4001	BD +36°3987	BD +38°4010	Ionization Potential
N III	−2.03	−2.20	−2.00	−1.10	47.20
N IV	0.95	1.08	−1.27	1.44	77.04
C IV	−2.91	−2.79	.....	−2.45	64.17

* This table gives the value of $\overline{N_i N_e}$ relative to $\overline{N_i N_e}$ for *He* II. For example, the entry for *C* II gives the relative number of *C* III ions multiplied by N_e.

can exist in several stages of ionization, while helium can exist in but two, complicates the problem. For example, although *O* III and *He* II have about the same ionization potential, the lines of *He* II may yet be radiated in the deeper layers, where *O* IV has all been ionized, so that recombination lines of *O* III may not appear. For the three carbon-oxy-

gen stars, the average $\overline{N_e N(He\ \text{III})}/\overline{N_e N(O\ \text{IV})}$ ratio turns out to be about 450. Evidently, this is a lower limit to the oxygen abundance. It would be the correct value if the *He* II radiation were confined to the same layers as the *O* III radiation. The distribution of the oxygen atoms among the various stages of ionization within the radiating layers is unknown. Probably the number of oxygen atoms is not greater than ten times the number of *O* IV ions, and it seems likely that most of the helium in these layers is doubly ionized. Therefore, we may conclude that within the limitations of our present knowledge a helium/oxygen ratio of about 50 is capable of explaining the observed features of the Wolf-Rayet stars.

The problem of estimating the carbon/oxygen ratio is somewhat easier, as both may exist in several stages of ionization. We recall, however, that the *C* V ion is stripped to the K shell. Hence, in so far as the radiating layers are concerned, it acts like doubly ionized helium because the permitted levels lie several hundred volts above the ground level. Hence, to compare the abundance of carbon and oxygen, it is better to compare the $N_i N_e$ curves for these atoms in the lower stages of ionization. In this way we find from the observed data for the three carbon-oxygen stars that carbon is about three times as abundant as oxygen in the carbon Wolf-Rayet stars. The carbon-oxygen ratio seems more constant from star to star than the helium-carbon ratio, although this may be an excitation or ionization effect.

Turning, now, to the stars of the nitrogen sequence, we find the $\overline{N_e N(He\ \text{III})}/\overline{N_e N(N\ \text{IV})}$ ratio to be about 100. If about a fifth of the nitrogen exists as *N* IV, helium is about twenty times as abundant as nitrogen. We emphasize that these estimates are exceedingly rough, since we have no knowledge of the partition of the atoms among the various stages of ionization; it may well be that, in the nitrogen stars, nitrogen is more abundant with respect to helium than oxygen is in the carbon-oxygen stars. I have also estimated the abundances of carbon from *C* IV in the three nitrogen stars BD+37°3821, BD+35°4001, and BD+38°4010 by assuming that $N_i N_e$ varies with depth in the radiating layers in the same way as in the carbon-oxygen stars. The results suggest that carbon is about one-twentieth as abundant as nitrogen and roughly ten or twenty times less abundant than in the carbon-oxygen stars.

ELECTRON DENSITIES

We may obtain an estimate of the electron density in the atmosphere of a Wolf-Rayet star from the brightness of the λ 4686 line. Let us consider the Wolf-Rayet component of BD+38°4010, whose dimensions are known from the work of Gaposchkin and Wilson. The photographic magnitude of the binary is 8.39; and the magnitude of the λ 4686 line, if it could be observed alone, would be about 11.0. We may apply to the Wolf-Rayet stars the theory which Menzel and I have developed[29] for the calculation of the electron densities in planetary nebulae. For an order of magnitude estimate I shall suppose that the radius of the radiating layers of a Wolf-Rayet star is about 40 per cent larger than that of the star itself. The work of Swings suggests that this is about the correct order of magnitude. If the radius of the star is about twenty times that of the sun, the volume contributing to the Wolf-Rayet lines is roughly equivalent to that of a sphere of about 20 ⊙, taking into account the occultation effects. If the emission per unit volume is $E_{nn'}$, the total amount of energy radiated by a sphere of radius a is $\frac{4\pi}{3} E_{nn'} a^3$. The surface through which this energy must flow has an area $4\pi a^3$, so that the average surface brightness S_n will be $\frac{1}{3} E_{nn'} a$. Now, Menzel and I have shown that the surface brightness in terms of magnitudes per square minute of arc is given by

$$S_n = 8.40 \times 10^2 (2.512)^{-m_\lambda} . \qquad (16)$$

[29] *Ap. J.*, **93**, 195, 1941.

From our expression for $E_{nn'}$ we get

$$N_i N_e = 6.44 \times 10^{20} (2.512)^{-H_\lambda} T_e^{3/2} 10^{-1.70 \frac{(10{,}000)}{T}} a^{-1}. \qquad (17)$$

Since the distance of the star is about 2600 parsecs, the angular radius of a sphere of radius of 20 $\odot$ will be

$$0.093 \times \tfrac{1}{2}\tfrac{1}{6}\tfrac{1}{0}\tfrac{1}{0} \times \tfrac{1}{6}\tfrac{1}{0} = 6 \times 10^{-7} \text{ minutes of arc}.$$

Accordingly, to reduce to surface brightness in terms of square minutes of arc, we must apply a correction factor, $\Delta m = 2.5 \log (110 \times 10^{-14}) \sim -30$, whence $H_\lambda \sim -19$. If $T_e \sim T \sim 36{,}000°$ and most of the helium atoms are in the doubly ionized condition, so that we can set $N_i = N_e$, we find[30] that $N_e \sim 10^{11} - 10^{12}$ electrons/cm^3. This means that the total mass of the Wolf-Rayet atmosphere is of the order of 6×10^{24} grams; and, if the ejection velocity of the atoms is 2000 km/sec, the total dissipation of mass by such a process would amount to $\sim 10^{29}$ grams/year and a star ten times as massive as the sun; i.e., 2×10^{34} grams could last but 200,000 years. This result is in disagreement with that of Beals.

It is of interest to investigate the possibility of the appearance of the forbidden lines at the densities obtaining in the Wolf-Rayet stars. Let us compare, for example, the emissivity per cubic centimeter of the *He* II 4542 line and the [*O* III] 4363 auroral line. For the temperatures and densities prevailing in the Wolf-Rayet stars we would expect the auroral transitions to yield stronger lines than the nebular transitions. Since the density is sufficiently high for a Boltzmann distribution to be maintained among the metastable levels, we have

$$\log \frac{N_s}{N_p} = -0.95 - \frac{5040 \times 5.3}{T},$$

where N_s is the number of atoms in the ^{1}S level and N_p is the number in the ^{3}P level. For the auroral transition in *O* III, I have found that $A = 1.97$. Hence,

$$E = 9 \times 10^{-12} N_s = 10^{-12} N_p 10^{-2.67/T} = 1.8 \times 10^{-13} N_p \qquad (T = 36{,}000°),$$

$$E = 2.14 \times 10^{-15} N_p \qquad (T = 10{,}000° \text{K}),$$

while

$$E_{4542} = 3 \times 10^{-26} N_i N_e \qquad (T = 36{,}000° \text{K}),$$

$$E = 3.7 \times 10^{-25} N_i N_e \qquad (T = 10{,}000° \text{K}).$$

If the number of *O* III atoms is 1/1000 the number of *He* III ions, we find the intensity ratio of 4542 to 4363 as given by the accompanying table. The intensity of the auroral

N_e	$T = 36{,}000°$ K	$T = 10{,}000°$ K	N_e	$T = 36{,}000°$ K	$T = 10{,}000°$ K
10^{12}	170	1.6×10^5	10^{10}	1.7	1.6×10^3
10^{11}	17	1.6×10^4	10^9	0.17	1.6×10^2

line depends very markedly upon the temperature. These calculations show, however, that for a density of 10^{11}–10^{12} atoms/cm^3, the forbidden lines should be at least twenty times fainter than the λ 4542 *He* II line, i.e., about 0.05 on our scale. We may conclude that the nonappearance of forbidden lines in the spectra of the Wolf-Rayet stars is consistent with a density of 10^{11}–10^{12} atoms/cm^3 in the radiating layers of their atmospheres.

[30] If we adopt a volume equivalent to a sphere of twice the solar radius, the density comes out about thirty times larger. I am inclined to favor the larger volume, about 10^4 that of the sun.

Menzel and also Beals attributed the great breadths of the lines in the Wolf-Rayet stars to the continuous ejection of atoms from their atmospheres. This hypothesis explains the great widths of the emission lines, the absorption components, sometimes observed on their violet edges, and the fact that the radiations of the most highly ionized atoms, which originate in the deepest layers, are widest, indicating that the gases are accelerated as they move outward.

Olin Wilson[31] has criticized the expansion hypothesis in his recent paper on BD+38°4010. If the radiating shell is small, a pronounced occultation effect should take place and the lines should show a violet shift and asymmetry. Since such a shift is not observed, we should have to postulate processes working to absorb energy on the violet side of the line and emitting energy on the redward side. On the other hand, if the shell is large, Wilson shows that, since the ejected layers whose velocity we measure spectrographically are left behind, so to speak, as the star moves in its orbit, there should be a phase difference between the eclipses predicted from the spectrographic orbit and those actually observed. Such a phase difference, amounting to as much as 1 per cent of the period, is not observed; and large occultation effects causing a violet shift of hundreds of kilometers per second should come into play. Since such a shift is not observed, Wilson concludes that the expanding-shell hypothesis needs serious modification. He mentions the possibility of large-scale turbulence as a possible contributing cause to the widths of the lines. The chief difficulty here seems to be that the required turbulent velocities would have to be greater than the velocity of escape.

In any case, physical conditions differing so wildly from those obtaining in the atmospheres of ordinary stars, suggest deep-seated disturbances in the Wolf-Rayet stars. The expansion hypothesis has so many attractive features that it does not seem desirable to discard it at the present time. One might expect an expansion to be accomplished by large-scale and violent turbulence. The mechanics of a Wolf-Rayet envelope and the transfer of radiation through it provide a difficult theoretical problem.

The sizes of the envelopes surrounding Wolf-Rayet stars have been estimated by Swings from the dilution factor and from the breadths of the absorption components of the emission lines. The former method compares the intensities of lines arising from high metastable levels with those arising from normal levels. The latter method assumes that the width of the violet absorption line is mostly due to the range in the ejection velocity component along the line of sight, within the cylinder defined by the limb of the star. The method of the dilution factor seems the more reliable, as it does not depend upon the questionable assumption that turbulence in Wolf-Rayet atmospheres is negligible.[32] The work of Swings suggests that probably the radii of the shells are not more than 50 per cent larger than those of the stars. The sizes that he and Beals have derived for a number of Wolf-Rayet stars, of the order of twice that of the sun, are in marked disagreement with the conclusions of Gaposchkin and Wilson regarding the diameter of the Wolf-Rayet component of BD+38°4010. These stars do not radiate as black bodies, and in the calculation of their diameters from their absolute brightnesses it does not seem legitimate to assume a temperature and to apply a formula valid only for a star radiating as a black body. Until energy-distribution studies have been made of these objects, we can place little confidence in diameters calculated from assumed temperatures.

[31] *Ap. J.*, **95**, 1, 1942.

[32] More recently (*Ap. J.*, **96**, 262, 1942) Swings and Struve have suggested that in the shell of a Wolf-Rayet star the line excitations are produced mostly by the emission lines of the shell, which attain large radiation densities and are, therefore, subject to little or no dilution. Consequently, one cannot conclude from the relative intensities of helium lines arising from normal and metastable levels very much about the geometrical dilution factor. They suggest that we continue to use the ejection mechanism as a working hypothesis and that we might explain the absence of the occultation effect in the emission profiles by supposing that the radius of the shell is about four times that of the star, or by some reabsorption phenomenon.

In some Wolf-Rayet stars absorption lines are quite conspicuous. Some of these absorption lines, notably those on the violet edges of emission lines, doubtless originate in the atmospheres of Wolf-Rayet stars; but others may come from normal O- or B-type companions. Most O stars are binaries, and it seems quite possible that Wolf-Rayet stars are associated quite generally with ordinary O or B stars. BD+38°4010 is one example, and Olin Wilson[33] has announced three others as spectroscopic binaries.

Unfortunately, the present slitless data permit only eye estimates of the intensity on an arbitrary scale and are not adequate for a definitive study of dilution effects. Slit spectra should be used for this purpose.

THE SPECTRA OF THE NUCLEI OF THREE PLANETARY NEBULAE

In 1938 at the Lick Observatory I observed the spectra of three planetary nebulae: NGC 40, NGC 6543, and BD+30°3639. Provisional intensities of lines in the photographic regions of these stars are now available. For the identifications I have relied mainly on the recent papers by Struve and Swings.

The nuclei of NGC 40 and BD+30°3639 are carbon stars, but the emission lines are considerably narrower than in the ordinary Wolf-Rayet spectra. The nucleus of NGC 6543 contains lines of carbon, oxygen, and nitrogen, with comparable intensity. Wright[34] and, more recently, Swings[27] have described its spectrum in detail.

The interesting character of the spectrum of BD+30°3639 was first noticed by Mrs. Fleming in 1890.[35] Later, W. W. Campbell,[36] during the course of his studies of the Wolf-Rayet stars, found the star to be surrounded by an envelope of hydrogen; it is, therefore, often referred to as "Campbell's hydrogen-envelope star." Wright[37] found that the envelope is not a disk but a minute ring. The object is a small planetary nebula. Wright studied the spectrum of the central star in detail from λ 3342 to λ 6676 and described it as "continuous with many superposed bright lines and a few dark ones." Stoy[38] measured a number of lines in the ultraviolet, and, more recently, Swings and Struve have made detailed measures of the lines in the photographic region.[39] Table 12 gives the wave lengths, identifications, and intensities of the lines observed in this star. Helium, carbon, and oxygen in various stages of ionization contribute nearly all the lines. The intensities of the weaker lines are subject to considerable uncertainty. *C* II and *C* III are both strong, and the star is classified as WC8.

The nucleus of NGC 40 displays a somewhat similar spectrum. Paddock first observed this star, but the most detailed study was that of Wright.[40] The 4650 band is extremely strong and stands out conspicuously when viewed with the slitless spectrograph. The provisional intensities of Table 13, based on only one plate, are uncertain, especially in the neighborhood of the hydrogen lines, where it was necessary to correct for the superposition of the nebular images. The identifications have been taken from the table for BD+30°3639. The 3360 band may be due to *N* III; but this assignment seems unlikely, as the strong 3483 line of *N* IV seems to be missing. This star appears to be a more or less typical carbon star.

The nucleus of NGC 6543 shows a few, relatively faint, emission lines superposed upon a continuous spectrum. A remarkable feature of this star is that it shows the lines of *C* IV, *N* IV, and *O* IV with comparable intensity (see Table 14), while *N* III is missing and the presence of *O* III has not been confirmed. The strong line of *C* III near λ 4650 is missing, and the rather weak line found in this vicinity is to be attributed to *C* IV, according to Swings. The range of ionization is limited, as compared with the other Wolf-Rayet stars.

[33] *Pub. A.S.P.*, **53**, 295, 1941.

[34] *Pub. Lick Obs.*, **13**, 211, 1913.

[35] *A.N.*, **125**, 155, 1890.

[36] *Astr. and Ap.*, **13**, 461, 1894.

[37] *Op. cit.*, p. 221.

[38] *Pub. A.S.P.*, **47**, 162, 1935.

[39] *Proc. Nat. Acad. Sci.*, **26**, 548, 1940.

[40] *Op. cit.*, p. 196.

TABLE 12

THE SPECTRUM OF BD+30°3639

Stellar Wave Length	Laboratory Wave Length	Iden.	Int.*
3132	3132.87	O III	0.46
3165	3150 3166	Si IV	0.70
3188	3188	He I	0.41
3202		He II	0.67
3264	3260.95 3265.41 3267.29	O III	0.67
3285			0.16
3294	3299.39	O III	0.07
3311	3312.35	O III	0.29
3332–40	3330.40 3333.00 3340.74	O III	0.38
3404	3403.58	O IV	0.16
3412.9	3411.76	O IV	0.16
3445	3440.39 3444.10 3446.73 3450.94	O III	0.32
3503			0.26
3564	3560.42 3563.36	O IV	0.19
3609.4	3609.61 3608.96	C III	0.64
3640.0	3638.70	O III	0.33
3665			0.20
3703	3702.75 3703.37 3704.73 3707.24	O III	0.40
3712–14	3712.48 3715.08	O III	0.49
3760	3759.87	O III	0.54
3774	3774.00	O III	0.32
3791	3791.26	O III	0.21
3804			0.21
3813	3813.53 3810.96	He II O III	0.2?
3820	3816.75 3819.61	O III He I	0.1?
3889	3888.65 3889.18	He I C III	1.52
3916–20	3918.98 3920.68	C II	0.68
3934	3934.1	C IV	0.21
3951	3951.82	O III	0.1?
4026	4026	He I, He II	0.21
4057	4056.06	C III	0.47
4069	4067.87 4070.30	C III C III	1.97
4115 4120 4128	4116.10 4120.81 4128.05	Si IV He I Si II	0.75
4155	4152.43 4156.50	C III C III	0.41
4163	4162.80	C III	0.40
4186	4187.15	C III	0.40
4201	4199.87	He II	0.2?
4213	4212.44	Si IV	0.2?
4267	4267.27 4267.02	C II C II	1.00
4325	4325.70	C III	0.77
4368	4368.14	C III	0.53
4385	4387.93 4388.24	He I C III	0.43
4414	4411.52 4411.20 4414.89	C II C II O II	0.55
4441	4441.81	C IV	0.62
4472	4471.48	He I	0.28
4516	4516.02 4516.93	C III C III	0.44
4542	4541.63	He II	0.16
4553	4552.61	Si III	0.26
4593	4593.47 4590.98 4596.19	C III O II O II	0.46
4619	4618.85	C II	0.38
4650 4655	4647.40 4650.16 4651.35 4654.14 4656.5 4658.64	C III C III C III Si IV C IV C IV	4.75
4666	4665.90 4663.53 4664.5	C III C III C IV	0.86
4686	4685.81	He II	1.00
4702			0.31
4786	4785.6 4783.4	C IV O IV	0.32
4924		He I	1?

* The intensity of λ 4686 is chosen as 1.00 in Tables 12, 13, and 14.

I have tried to estimate the relative abundances of oxygen, carbon, nitrogen, and helium in these stars. It is difficult to make a guess for helium, but the relative proportions of the other constituents may be inferred from the data with less trouble. In BD+30°3639 carbon appears to be eight or ten times as abundant as oxygen, while helium is presumably about ten times as abundant as carbon. We find a similar composition

TABLE 13

LINE INTENSITIES IN THE NUCLEUS OF NGC 40

Wave Length	Iden.	Int.	Wave Length	Iden.	Int.
3203	*He* II	0.59	4069	*C* III	0.84
3266	*O* III	.38	4122	*He* I, *C* III	0.21
3345	*O* IV	.30	4156	*C* III, *O* V	0.28
3360	*N* III??	.21	4187	*C* III	0.27
3381	*O* III	.35	4230	.....	0.20
3411	*O* IV	.74	4266	*C* II	0.30
3429, 3445	*O* III	.20	4323	*C* III	0.91
3560	*O* IV	.28	4412	*C* II	0.17
3609	*C* III	.32	4443	*C* IV	0.23
3889	*He* I, *C* III	.27	4471	*He* I	0.13
3925	*C* II, *C* IV	.27	4514	*C* III	0.18
3963	*He* I	.18	4545	*He* II	0.19
4028	*He* I	0.09	4650	*C* III, *C* IV	4.36
			4686	*He* II	1.00

TABLE 14

RELATIVE LINE INTENSITIES IN THE NUCLEUS OF NGC 6543

Line	Ion	Int.	Line	Ion	Int.
3202	*He* II	0.61	4650	*C* IV	0.45
3411	*O* IV	.92	4686	*He* II	1.00
3483	*N* IV	0.34			

for the nucleus of NGC 40. The observations may be explained by supposing that carbon is six times as abundant as oxygen and that helium is roughly ten times as abundant as carbon.

The composition of the nucleus of NGC 6543 is of particular interest. For this star I have assumed the relative abundances of carbon, nitrogen, and oxygen to be the same as the relative proportions of *C* IV, *N* IV, and *O* IV. Oxygen and nitrogen then appear to be about equally abundant, and carbon is four times as abundant as either. The proportion

of helium is more difficult to estimate. We may suppose that the helium radiations originate at a much higher level than those of carbon, nitrogen, or oxygen. If this is true, we would expect the *C* III radiations to be present in the intermediate layers; but the evidence is strong that the *C* III is scarce, if present at all, and we are forced to the conclusion that in this star most of the radiations originate in a layer which is remarkably homogeneous in density and temperature. In that case the abundance of helium is probably not much different from that of carbon, nitrogen, and oxygen!

The planetary nuclei present a number of interesting problems. Perhaps the most perplexing is that exhibited by NGC 40 and BD+30°3639, where nebulae showing strong nitrogen lines surround stars which show no trace of nitrogen in their spectra. While the ordinary Wolf-Rayet stars seem to fall into either the nitrogen sequence or the carbon-oxygen sequence, the planetary nuclei often show the lines of carbon and nitrogen with comparable strength. The planetary nuclei seem to be about 3 mag. fainter than the classical Wolf-Rayet stars, and their spectra sometimes display sharper lines.[41]

The ultraviolet temperatures of the nuclei of the planetaries may be derived from a comparison of the intensities of the Balmer lines and the forbidden lines by a method very similar to that suggested ten years ago by Stoy.[42] The present method takes into account the finite electron temperature of the nebula, and the resultant temperatures of the central stars are a bit higher than those found by an application of the Stoy theory. The ultraviolet temperatures of the nuclei of BD+30°3639, NGC 40, and NGC 6543 turn out to be 15,000°, 17,000°, and 47,000°, respectively. The significance of these temperatures is not too clear. Probably they are little more than rough indicators of the amount of energy radiated beyond the Lyman limit in these stars. The great range of ionization exhibited in certain planetary nebulae is difficult to reconcile with a central star radiating as a black body.

The Wolf-Rayet stars, although few in number, appear to have considerable cosmogonic importance. Their lack of hydrogen sets them apart from all other stars, save the supernovae. One suggestion which may prove fruitful is that these objects are supergiant stars that have reached the end of their energy resources. According to the Bethe mechanism, the stars of the main sequence shine by the conversion of hydrogen into helium. The rate of energy generation is so high for the B stars that we may expect them to burn up their hydrogen in a few million years. Since other nuclear sources are not known, we might expect the star to start contracting under its own gravitational attraction. Under such conditions it is conceivable that the star might reach no equilibrium and might eject its atmosphere continuously into space. Chandrasekhar[43] has pointed out that a star with a mass greater than $M_3 = 5.7M_0/\mu$ (where M_0 is the mass of the sun and μ is the molecular weight) must eject the excess mass before it can reach the final completely degenerate state. He has also suggested that the supernova phenomenon may result from the inability of a star of mass greater than M^3 to settle down to the final white-dwarf stage without getting rid of its excess mass. It is tempting to suppose that the Wolf-Rayet process represents an alternative evolutionary path, whereby a massive star may eject its outer layers and ultimately attain a degenerate white-dwarf state.[44]

How close is the relationship between the classical Wolf-Rayet stars and the planetary nuclei? Conceivably a Wolf-Rayet star on the downgrade might become a planetary

[41] Dr. R. Minkowski has kindly informed me that several planetary nuclei, i.e., those of NGC 6751, IC 351, and NGC 6905, have bands of a width quite comparable to those of the classical Wolf-Rayet stars. NGC 1501 also belongs to this group, and there are indications that some of the fainter central stars are to be added when satisfactory spectrograms have been obtained. Dr. Minkowski further remarks that "if the ejection hypothesis is adopted to explain the great width of the nuclear lines, the presence of a surrounding nebula with the usual small range of velocities appears not quite satisfactory." This additional difficulty in relating the nebulae and their central stars is not to be overlooked.

[42] *M.N.*, **93**, 593, 1933. [43] *Ap. J.*, **96**, 172, 1942.

[44] Goldberg and Aller, *Atoms, Stars, and Nebulae*, p. 277 (in press).

nucleus, but it seems difficult to credit these stars with the origin of the planetary nebulae.[45] The velocities of ejection would have to diminish considerably. Furthermore, the studies of Wyse and Bowen[46] and of others have shown that the planetaries consist mostly of hydrogen. On the other hand, we have seen that the Wolf-Rayet atmospheres seem to be composed essentially of helium but with varying admixtures of other elements. Nevertheless, on any hypothesis, the disparity in chemical composition between the nuclei and the nebulae surrounding them presents a fundamental difficulty for which no satisfactory explanation has yet been presented.[47] For the time being, we may find it convenient to regard the planetary nuclei and the classical Wolf-Rayet stars as somewhat different types of objects—in size, luminosity, and sometimes chemical composition.

NOTES ON INDIVIDUAL STARS

1. *The nitrogen sequence.*—BD+37°3821 shows strong emission lines, 20–30 A wide; those of ionized helium are particularly intense. Absorption lines on the violet edges of emission lines are conspicuous. Table 15 lists the intensities of the absorption lines as estimated on an arbitrary scale; "s" and "d" signify sharp and diffuse lines, respectively. The simultaneous appearance, with comparable intensity, of *He* I lines arising from both normal and metastable levels indicates that dilution effects of the type described by Struve and Wurm are not important.

TABLE 15

ABSORPTION LINES IN THE SPECTRUM OF BD+37°3821

λ	Int.	Ion	λ	Int.	Ion
5876	8	*He* I	4025	1	*He* I
4686	4	*He* II	3930	2	*N* III
4605	3	*N* V	3889	10	*He* I
4471	1s	*He* I	3483	8d	*N* IV
5056	3?	*N* IV			

BD+35°4001 shows a spectrum very similar to that of the preceding object except that the emission lines tend to be broader and the absorption lines are less conspicuous.

BD+36°3987 has much weaker and narrower emission lines than the other two stars. The λ 4543 and λ 4517 lines are well separated and distinct; λ 4640 and λ 4100 are fairly diffuse. The only line observed in the visual region is λ 5414.

[45] A more attractive hypothesis is that the planetary nebulae originate from the "slow novae," whose ejection velocities are low. The methods developed by Menzel and his colleagues for the study of physical processes in gaseous nebulae may be applied to an analysis of the envelopes of novae. If we suppose that, on the average, the composition of the envelopes of novae is the same as that of the envelopes of normal stars, it is possible to explain the observed emission-line intensities with the aid of a few plausible assumptions. From nova to nova there are indications of appreciable variations of the relative amounts of elements such as neon and sulphur, however. To what extent these variations are real and to what extent they are the effects of physical conditions cannot be settled until a detailed investigation of the problem has been made. For the present, however, it seems safe to assume that the envelopes of novae are more nearly akin to those of normal stars and to the planetary nebulae than to the Wolf-Rayet stars and the supernovae.

[46] *Lick Obs. Bull.*, **19**, 1, 1939; see also *Ap. J.*, **95**, 356, 1942.

[47] It might be possible to save the situation if we could show that the conditions of line excitation in the atmosphere of the nuclei of objects like BD+30°3639 or NGC 40 were such as to suppress all the nitrogen radiations and that the surrounding envelope consisted of selectively ejected gases. Hydrogen supposedly would have been ejected, but helium would have been retained by the star. Menzel (*Harvard Reprint 161*) has suggested the possibility of the separation of hydrogen and helium by selective radiation pressure. Such an *ad hoc* explanation seems highly unlikely. It is very difficult to assign reasons for the nonappearance of any nitrogen lines in these stars if appreciable nitrogen is present in their atmospheres.

BD+38°4010 shows only λ 4686 with high intensity, although I have measured a number of weak bands upon the tracing. The measures of the continuous spectrum are in accord with the low temperature found by Gaposchkin. Additional observations of this star are desirable.

BD+35°3953 shows weak lines of λλ 4686, 3483, and 3203 upon an otherwise continuous spectrum.

2. *The carbon-oxygen stars.*—BD+35°4013 contains the greatest number of lines of the stars of the program and has been used as the basis of Table 5. The lines, as measured on slitless plates, are relatively narrow, and most of them have been identified. Beyond λ 3800 the intensities are based upon a single plate and are to be regarded as distinctly provisional.

BD+36°3956 is a carbon star for which the data are restricted to the wave-length interval from λ 3700 to λ 6400 because of the overlapping image of a much brighter star

TABLE 16

ABSORPTION LINES IN BD+36°3956

Wave Length	Associated Emission Line	Int.	Wave Length	Associated Emission Line	Int.
3748	3760	5			
3780		1	4098	4121	1d
3800		2	4194		2s
3871	3889	0s	4293	4330	5

TABLE 17

THE STRONGEST EMISSION LINES IN BD+43°3571

Approximate Wave Length	Int.	Principal Contributor	Approximate Wave Length	Int.	Principal Contributor
5876	33	*He* I	4686	43	*He* II
5805	200	*C* IV	4650	176	*C* III
5696	62	*C* III	3400	22	*O* III, *O* IV
5590	21	*O* V			

beyond λ 3700. The *C* III and *C* IV lines λλ 5805, 5696, and 4650 are the dominating features of the spectrum. The *He* II λλ 4686, 5412, 4861, and 4343 lines are easily visible, but higher members are weak; λ 4471 of *He* I is very weak. Lines of *O* III, *O* IV, and *O* V are in evidence. From the assumed wave lengths of the emission lines λλ 3708, 4069, and 4861 I have derived rough wave lengths for a number of the absorption lines. Table 16 gives the absorption-line intensities on an arbitrary scale, wave lengths, and associated emission lines for this star.

BD+43°3571 exhibits broad bands which are difficult to measure and to identify. The spectrum is composite,[9] showing absorption O7 and emission WC6 characteristics. Such an association of emission and absorption spectra is consistent with the suggestion that many Wolf-Rayet stars are components of binaries. Beals remarks that there appears nothing unusual in the absorption spectrum to differentiate it from other absorption O stars. The intensity tables of Whipple and Mrs. Payne-Gaposchkin greatly aided the analysis of the spectrum and the disentanglement of overlapping emission lines (see Table 17).

He I exhibits a strong 5876 line; λ 4472 seems to be mixed with a broad blend, λ 4026 is missing, and λ 3889 may be a part of a blend. *He* II is represented by the strong 4686 and 3202 lines and also by 5414; the other lines are weak and blended. *C* II may be the principal contributor to the broad diffuse band near the 4266 line. *C* III contributes the strongest line, 4650, in the photographic region, and also the strong 5696 line. The *C* IV 5805 line, the excitation of whose upper level is 20 volts lower than the other relevant levels of this ion, is particularly strong. All the other lines appear in blends. Although the presence of *O* II cannot be established, the 3762 and 3205 lines, principally due to *O* III, are observed. A comparison of the 3386–3411 band of *O* IV with the 3562 band of the same ion leads to an excitation temperature of 70,000°. The 5590 *O* V band is strong; *O* VI is probably the principal contributor to the blend at 3820.

Despite the difficulty of disentangling the overlapping lines that contribute to the broad bands of the spectrum of BD+43°3571, most of the observed bands seem to have been satisfactorally identified. In a number of cases I have attempted to estimate the relative contributions of the different members of a blend. Slitless plates of relatively low dispersion seem to be the most suitable for the study of the broad lines in such a star as BD+43°3571.

Accurate measures of the continuous spectra of the Wolf-Rayet stars, especially in the ultraviolet, are urgently needed. Also, additional work on the profiles and intensities of the emission lines should be done.

I am grateful to Director Wright of the Lick Observatory, who made it possible for me to secure the plates used in this investigation. I am indebted to Dr. Whipple and to Mrs. Payne-Gaposchkin for helpful discussions of the problems of the Wolf-Rayet stars. Thanks are also due to Dr. O. C. Wilson, and Dr. R. Minkowski, and Dr. P. W. Merrill, of the Mount Wilson Observatory; Dr. C. S. Beals, of Victoria; the late Dr. A. B. Wyse, of Lick Observatory; Dr. O. Struve and Dr. P. Swings, of Yerkes; and Dr. D. H. Menzel, of Harvard, who have read one or the other of the successive versions of this paper and have made numerous valuable suggestions. I am grateful to Director Bobrovnikoff and Dr. J. A. Hynek of the Perkins Observatory for the opportunity of securing some slit spectrograms of a number of Wolf-Rayet stars. Additional plates will have to be secured before a complete study of the intensities and profiles of the emission and absorption lines can be made.

THE VARIABLE STAR S DORADUS AS AN ECLIPSING BINARY

SERGEI GAPOSCHKIN
Harvard College Observatory
Received November 28, 1942

ABSTRACT

On the basis of 1120 photographic plates in the Harvard collection a light-curve of S Doradus has been derived. The light-curve can be interpreted as that of an eclipsing star with a period of 40.2 years. Four minima are observed: in 1890, 1900, 1930, and 1940; the system has the large eccentricity of 0.4. In addition to the four minima, secondary fluctuations appear in the light-curve. The eclipse lasts over 3 years. The maximum brightness of the star was $8^m.8$, and the range for both minima was $0^m.64$.

Calculations based on the light-curve, an adopted bolometric correction, and the known modulus of the Large Magellanic Cloud lead to masses of 60 and 55 ⊙ and radii of 1400 and 1260 ⊙. By the use of a method that has been found to be valid for normal eclipsing stars, radii of 2100 and 1900 ⊙ are deduced, masses of 160 and 145 ⊙, and absolute bolometric magnitudes of −12.7 and −12.5; but the stars are probably underluminous and may lie about 3 mag. below the extrapolated mass-luminosity relation.

The spectrum shows the bright lines of hydrogen, which did not disappear during the minimum of 1930.

1. *General.*—It has been shown in a recent note[1] that the variation of S Doradus can be interpreted as that of an eclipsing binary with a period of 40 years—the longest known—and an eccentricity of 0.4. The present paper contains a detailed presentation of the material and a discussion of some details of the system.

2. *Observations and comparison stars.*—The photographic estimates are given in Table 1. The first column gives the Julian day; the second and third columns contain two independent estimates by the writer, made with reference to different comparison stars; the fourth column, an estimate by Miss Virginia Brenton relative to one of the two sets of comparison stars. Three independent estimates are given in the table in order to indicate the size of the systematic and accidental errors. The original estimates were made not in magnitudes but in arbitrary units (which, on this occasion, happen to be $0^m.11$); the second decimals given in Table 1 are to be regarded as computational.

The magnitudes of the comparison stars were determined by the author from 6 plates in relation to Selected Area 190.[2] This Selected Area is 9° from S Doradus; the zero point may be slightly uncertain, but the scale is probably reliable. Table 2 and Figure 1 summarize information concerning the comparison stars. Comparison star *a* is a red star and may be slightly variable; star *b* is essentially equal in brightness to the eclipsing system and constitutes a good check on the magnitude, although it is in the center of a small cluster.

3. *The spectrum.*—In addition to the plates on which the brightness of S Doradus could be estimated, there are 52 plates on which the spectrum of the variable is seen. Most of these spectra are of poor quality, and many show no features. They can, nevertheless, be successfully used for estimation of brightness, since the images are comparable to extrafocal images. Table 3 gives the results of such estimates and some remarks on the spectra.

The spectrum shows no absorption lines, and only on about a dozen plates are the bright lines conspicuously present. As may be seen from the light-curve (Fig. 2), the estimates made from spectrum plates are consistent with the other estimates. It should be noted that during the minimum of 1930 the bright lines did not disappear.

[1] S. Gaposchkin, *Pub. A.S.P.*, **54**, 264, 1942.

[2] S. Gaposchkin, *Harvard Ann.*, **89**, No. 9, 1938.

TABLE 1

PHOTOGRAPHIC OBSERVATIONS OF S DORADUS

JD 24+	IPg			JD 24+	IPg			JD 24+	IPg		
11313....	8m84	....	....	15590....	9m29	....	....	16825....	8m84	....	8m89
313....	8.95	....	....	630....	9.29	....	....	855....	8.89	9m00	9.00
621....	9.29	9m23	....	636....	9.29	....	....	855....	8.89	....	....
623....	9.29	9.23	....	660....	9.34	9m12	9m12	859....	8.89	....	8.78
627....	9.29	9.34	....	722....	9.12	....	....	869....	8.78	....	....
12014....	9.34	9.45	....	747....	9.34	9.23	9.23	908....	8.78	....	....
014....	9.40	9.34	....	956....	9.07	8.95	....	17020....	8.89	8.89	....
023....	9.51	....	....	16013....	8.89	8.89	8.78	028....	8.78	8.78	....
027....	9.34	....	....	017....	8.89	....	....	039....	8.78	....	....
028....	9.45	....	....	037....	8.89	8.78	9.00	040....	8.89	....	....
034....	9.34	9.45	....	043....	8.89	....	....	066....	8.89	....	....
036....	9.45	9.34	....	043....	9.00	....	....	075....	8.78	....	....
066....	9.40	9.40	....	061....	8.78	....	....	076....	8.67	....	8.67
066....	9.56	9.40	....	072....	9.23	8.89	8.89	080....	8.67	....	....
066....	9.40	9.45	....	073....	9.00	....	....	081....	8.78	....	8.78
066....	9.56	....	....	073....	9.12	....	....	095....	8.67	....	....
697....	8.95	8.78	....	079....	8.78	9.00	8.89	097....	8.56	....	8.89
728....	9.07	....	....	080....	8.95	....	....	097....	8.78	....	....
13119....	8.89	....	....	086....	8.89	....	....	105....	8.89	8.45	8.67
145....	8.78	8.78	....	093....	8.73	....	8.78	108....	8.67	....	....
176....	8.78	....	....	126....	8.78	8.78	8.67	110....	8.67	8.67	8.78
479....	8.89	....	....	130....	9.07	....	....	117....	8.45	....	8.67
496....	8.78	8.78	....	166....	8.89	....	8.89	125....	8.84	....	....
875....	8.89	....	....	179....	9.12	9.12	....	128....	9.12:	8.56	8.67
948....	8.89	....	....	337....	9.23	....	....	129....	8.67	....	....
14169....	8.78	....	....	339....	9.18	....	....	166....	8.78	....	....
300....	8.89	....	....	340....	9.00	....	8.89	174....	8.45	....	8.78
596....	9.00	....	....	361....	9.12	....	....	177....	8.78	....	....
613....	9.07	....	....	377....	9.00	9.12	9.12	213....	8.67	9.00	8.78
639....	9.18	....	....	396....	9.00	....	8.89	237....	8.56	....	....
891....	9.51	....	....	397....	9.07	....	....	416....	8.45:	....	....
892....	9.29	....	....	407....	9.00	....	9.00	433....	8.78	....	....
899....	9.45	....	....	407....	8.95	....	....	445....	8.78	....	....
904....	9.34	....	....	432....	9.12	9.12	8.89	465....	8.67	9.12	8.67
905....	9.45	....	....	437....	9.00	8.89	9.12	473....	8.67	....	....
907....	9.51	....	....	438....	9.07	....	....	480....	8.67	....	8.45
910....	9.45	....	....	459....	9.12	....	9.12	494....	8.67	....	8.45
924....	9.56	9.56	....	465....	9.29	....	....	497....	8.78	....	....
925....	9.56	9.56	....	476....	....	....	9.12	499....	8.78	8.78	8.78
928....	9.45	....	....	477....	9.34	....	....	502....	8.73	....	....
937....	9.23	9.45	9m34	492....	9.12	9.12	9.23	507....	8.67	....	8.67
939....	9.56	9.56	9.56	557....	9.40	9.34	9.12	532....	8.78	....	8.78
940....	9.56	....	....	579....	9.00	....	9.29	824....	8.67	....	....
941....	9.45	....	....	594....	9.29	9.34	9.12	828....	8.67	....	....
955....	9.56	9.67	9.67	603....	9.23	9.34	9.56	832....	8.78	8.67	8.67
955....	9.51	....	....	647....	9.12	....	8.89	834....	8.89	....	....
956....	9.40	9.56	....	724....	9.00	....	....	858....	8.73	....	....
990....	9.45	9.56	9.45	724....	8.95	....	....	866....	8.73	....	....
995....	9.34	....	....	736....	9.29	....	9.23	886....	8.45	....	....
15089....	9.45	....	....	745....	9.07	....	9.00	18126....	8.67	....	....
224....	9.45	....	....	754....	9.07	....	....	184....	8.67	....	....
263....	9.51	....	....	760....	9.00	....	9.12	202....	9.12	8.73	8.89
266....	9.56	9.45	....	781....	9.07	....	....	249....	8.67	....	....
267....	9.45	9.23	....	785....	9.00	9.00	9.00	266....	8.67	8.67	8.34:
274....	9.67	9.56	9.45	787....	9.12	8.89	9.12	271....	8.78	....	....
280....	9.45	....	....	789....	9.00	....	....	332....	8.78	8.56	8.67
283....	9.56	9.45	9.56	802....	9.18	....	....	366....	8.78	....	....
283....	9.56	....	....	819....	9.07	....	....	369....	8.78	8.56	8.45
372....	9.40	....	....	821....	8.89	....	....	371....	9.00	8.78	8.78
465....	9.29	....	....	822....	8.89	8.89	8.89	374....	8.73	8.78	....

TABLE 1—*Continued*

JD 24+	IPg			JD 24+	IPg			JD 24+	IPg		
18377....	8m78	8m78	8m56	20145....	8m89	....	....	21362....	8m89	....	....
393....	8.67	....	8.67	146....	8.67	8m45	8m56	366....	9.00	8m78	8m78
426....	8.78	8.78	8.78	177....	8.67	8.67	8.67	388....	8.89	....	8.45
523....	8.89	....	....	257....	8.78	....	....	488....	8.78	....	....
552....	8.89	....	....	393....	8.45	8.67	....	489....	9.07	....	....
552....	9.00	....	....	400....	8.67	....	....	493....	9.07	....	....
562....	8.67	....	....	421....	8.56	8.62	8.67	495....	8.84	....	....
572....	8.78	....	....	430....	8.56	....	....	512....	8.78	8.67	....
574....	8.78	....	....	433....	8.56	....	....	513....	8.62	....	....
574....	8.95	....	....	446....	8.62	....	....	538....	8.67	....	....
589....	8.67	....	8.89	448....	8.56	8.45	8.78	568....	8.67	....	....
592....	8.67	....	....	460....	8.67	....	....	687....	8.89	....	....
595....	8.78	8.56	8.67	482....	8.45	....	....	696....	9.00	9.00	....
595....	8.73	....	....	483....	8.45:	....	....	697....	9.00	8.78	....
598....	8.84	....	....	571....	8.89	8.56	8.67	756....	9.07	....	....
599....	8.67	....	....	606....	8.56	....	....	757....	9.18	....	....
602....	8.89	....	8.78	611....	8.45	8.67	....	864....	9.00	....	....
602....	8.95	....	....	612....	8.67	....	....	864....	8.89	....	....
603....	8.67	8.56	8.67	650....	8.67	....	....	872....	9.12	8.89	....
611....	8.89	....	....	750....	8.45	....	....	22000....	8.78	8.89	....
613....	8.84	....	....	750....	8.56	....	....	027....	8.56	....	....
614....	8.78	8.78	8.78	753....	8.89	8.62	8.67	072....	8.95	....	....
615....	8.84	....	....	767....	8.67	....	....	224....	8.73	....	....
622....	8.73	....	....	769....	8.89	8.67	8.89	424....	9.07	....	....
626....	8.89	8.89	8.67	769....	8.78	....	....	433....	8.56	....	....
631....	8.78	8.78	8.67	774....	8.56	....	....	436....	8.67	....	....
632....	8.84	....	....	775....	8.56	....	....	437....	9.00	8.67	....
644....	8.67	8.84	8.78	776....	8.56	....	....	585....	8.84	....	....
651....	9.00	....	8.78	783....	8.56	....	....	591....	8.84	....	....
652....	8.78	....	....	787....	8.89	....	....	609....	8.67	8.67	....
698....	8.73	....	....	805....	8.67	....	....	670....	8.78	8.56	....
698....	8.89	....	....	811....	8.78	....	....	23271....	8.56	....	....
701....	8.89	8.78	8.89	812....	8.67	....	....	325....	8.73	....	....
701....	9.00	8.78	8.78	817....	8.67	....	....	346....	8.67	....	....
750....	8.78	8.89	8.78	838....	8.56	8.67	....	386....	8.56	8.67	8.67
814....	8.84	....	8.78	864....	8.56	....	....	388....	8.78	....	....
898....	8.84	....	....	962....	8.67	8.45	....	503....	8.67	8.78	8.67
917....	8.84	....	....	985....	8.67	8.56	8.56	523....	8.56	8.78	8.67
925....	8.78	....	....	21007....	8.67	8.56	8.67	649....	8.62	....	....
946....	8.67	....	....	046....	8.62	....	....	668....	8.78	....	....
946....	8.89	....	....	056....	8.62	....	....	768....	8.67	....	....
984....	9.00	....	....	123....	8.67	....	....	768....	8.56	8.78	8.56
985....	8.78	....	8.56	129....	8.73	....	....	768....	8.56	....	....
19029....	8.78	....	8.78	135....	8.67	....	....	785....	8.78	8.62	8.67
300....	8.67	....	....	146....	8.78	....	....	791....	8.67	8.56	8.67
302....	8.67	8.95	8.56	155....	8.67	8.67	....	791....	8.56	8.89	8.34
303....	8.56	8.45	8.56	157....	8.78	8.56	....	799....	8.56	....	....
323....	8.56	....	....	169....	8.89	8.56	8.67	800....	8.67	....	....
392....	8.67	8.34	8.34	181....	8.78	....	....	815....	8.67	8.56	8.45
531....	8.67	....	....	194....	8.45	....	8.56	815....	8.56	....	....
660....	8.67	....	....	194....	8.67	....	....	816....	8.67	....	....
749....	8.67	....	....	202....	8.78	....	....	822....	8.56	8.56	8.34
755....	8.67	....	8.45:	217....	8.56	....	....	822....	8.56	....	....
775....	8.67	8.67	8.67	222....	8.78	....	....	823....	8.67	....	8.34
992....	8.56	....	8.45	226....	8.56	8.78	....	823....	8.67	....	....
20008....	8.62	....	....	227....	8.45	....	....	24055....	8.67	....	....
015....	8.56	....	....	271....	8.56	8.78	....	056....	8.78	8.89	....
036....	8.56	8.45	8.34	331....	8.78	8.67	....	056....	8.89	....	....
090....	8.56	....	....	333....	8.56	....	....	083....	8.78	....	....
098....	8.34	....	....	335....	8.78	8.84	....	088....	9.00	....	....

TABLE 1—*Continued*

JD 24+	IPg			JD 24+	IPg			JD 24+	IPg		
24135....	8m67	....	....	24523....	8m95	8m56	8m67	25287....	8m78	....	....
136....	9.00	8m78	8m89	526....	8.89	8.67	8.67	299....	9.12	....	9m12
136....	9.00	8.78	8.67	527....	9.07	8.56	8.89	319....	8.78	8m67	8.67
136....	8.56	....	8.45	530....	8.56	....	....	325....	9.00	9.00	....
138....	8.67	....	....	530....	8.89	....	....	328....	8.67	....	....
141....	8.67	....	....	531....	8.78	....	....	387....	8.78	8.56	8.78
144....	8.67	8.56	....	533....	9.00	8.67	8.89	420....	8.78	8.67	8.89
155....	8.78	8.78	....	534....	8.95	8.67	8.67	426....	9.00	....	....
203....	8.78	8.56	8.78	536....	8.95	8.67	8.78	452....	8.89	8.56	8.78
254....	8.78	....	....	538....	8.89	8.67	8.89	483....	8.89	....	....
298....	9.00	....	....	538....	8.67	8.78	8.78	484....	8.89	....	....
302....	8.89	9.00	....	538....	8.78	....	....	496....	8.89	8.56	8.89
313....	8.45	....	....	547....	8.78	8.67	8.89	528....	8.78	....	....
324....	8.67	8.67	8.89	548....	8.78	8.67	8.56	531....	9.00	....	....
325....	8.78	....	8.78	550....	8.78	8.78	8.89	564....	8.67	....	9.12
346....	8.67	....	8.89	553....	8.89	....	8.89	594....	8.89	....	8.89
364....	8.62	....	....	558....	8.78	....	8.78	613....	8.89	8.67	8.78
369....	8.78	8.78	8.78	563....	8.89	8.89	8.78	621....	9.00	....	8.89
370....	8.95	8.78	8.78	563....	8.95	....	....	650....	9.00	....	9.12
371....	8.89	8.78	8.89	565....	8.89	8.78	8.78	655....	8.67	8.67	8.78
373....	8.78	8.89	8.56	616....	8.89	8.84	8.78	658....	9.00	8.78	9.23
374....	8.89	8.67	8.78	626....	9.00	8.89	8.89	669....	8.67:	9.12	9.34
376....	9.00	8.78	9.00	634....	8.89	8.78	8.78	710....	8.67	8.67	9.00
380....	8.89	8.67	8.89	637....	8.89	8.73	8.89	711....	8.78	....	8.78
383....	8.89	8.67	8.89	648....	8.89	8.78	8.56	867....	9.12	....	9.12
387....	8.95	8.78	8.89	650....	8.89	8.67	8.67	917....	9.23	9.34	9.34
390....	8.89	8.67	8.78	680....	8.78	8.56	8.78	943....	9.00	....	9.00
397....	8.89	8.78	8.89	716....	9.12	....	....	943....	8.89	....	9.12
399....	8.89	8.78	8.89	717....	8.84	8.56	8.67	966....	9.23	....	....
402....	8.89	8.67	8.78	757....	8.95	....	....	967....	9.45	....	9.12
405....	9.00	8.67	8.89	758....	8.67	....	....	986....	9.23	....	9.23
408....	8.89	8.78	8.78	760....	8.89	8.67	8.78	997....	9.00	9.12	9.12
409....	8.89	8.67	8.78	763....	9.00	....	....	26007....	9.45	....	9.23
412....	8.78	8.67	8.78	766....	8.67	8.56	8.67	011....	9.00	....	9.12
415....	8.84	8.73	8.89	774....	8.78	....	....	011....	9.12	....	9.00
418....	9.00	8.67	8.89	776....	8.89	8.67	8.67	028....	9.34	....	9.12
422....	9.00	8.89	8.78	787....	8.89	8.67	8.67	036....	9.12	....	9.34
424....	8.89	8.73	8.89	797....	8.89	8.67	8.67	057....	9.45	....	9.45
429....	9.00	8.84	9.00	798....	9.00	9.23	9.12	060....	9.23	9.34	9.23
431....	8.78	8.78	8.67	798....	8.89	....	....	085....	9.45	9.45	0.56
433....	9.00	....	....	814....	8.89	8.78	8.89	086....	9.45	....	....
437....	8.89	8.73	8.78	821....	8.56	8.56	8.67	244....	9.34	9.23	9.12
487....	9.00	8.73	8.89	825....	8.73	8.78	8.67	250....	9.40	....	9.34
488....	9.00	8.73	8.89	826....	9.12	....	9.18	270....	9.34	....	9.45
489....	9.00	8.78	9.00	830....	8.89	8.73	8.89	272....	9.45	....	9.56
491....	8.89	8.78	8.78	830....	8.89	....	....	328....	9.56	9.45	9.56
492....	9.00	8.84	8.89	863....	8.78	8.67	8.89	334....	9.34	....	....
494....	9.07	8.89	8.67	864....	8.67	8.56	....	335....	9.29	....	....
495....	9.12	9.00	9.12	25154....	8.78	8.56	8.67	355....	9.45	....	....
495....	9.00	9.00	8.89	181....	9.12	....	....	359....	9.56	....	9.34
496....	8.67	....	....	188....	8.78	8.56	8.78	366....	9.34	....	9.34
497....	8.89	8.67	8.67	188....	8.84	....	....	394....	9.56	9.34	9.23
499....	9.00	8.67	8.89	199....	9.00	....	....	412....	9.56	....	....
506....	9.07:	8.56	8.89	201....	9.12	....	....	456....	9.34	....	9.34
507....	9.00	8.89	9.00	201....	8.67	8.56	8.56	460....	9.34	....	9.34
507....	8.89	....	....	210....	8.73	....	....	593....	9.34	....	....
516....	8.89	8.67	8.67	236....	8.78	....	....	629....	9.18	....	9.23
517....	8.95	8.67	8.95	245....	9.00	8.89	9.12	629....	9.23	....	9.12
521....	9.00	8.67	8.89	267....	8.89	8.89	9.00	662....	9.18	....	....
522....	8.89	....	8.89	286....	8.78	8.67	8.67	664....	9.12	....	....

TABLE 1—*Continued*

JD 24+	IPg		
26690....	8m89	....	9m12
714....	9.00	....	....
715....	8.89	....	....
724....	9.12	....	....
769....	8.89	....	8.89
970....	9.00	....	....
970....	9.00	....	....
971....	8.87	....	....
978....	8.89	....	....
980....	8.78	....	....
989....	8.89	....	9.00
997....	9.00	8m67	9.00
998....	9.00	....	9.00
27011....	8.78	....	8.89
033....	8.84	....	....
046....	8.89	8.78	8.78
046....	8.89	....	8.89
076....	8.89	....	....
120....	9.00	8.73	9.00
129....	9.00	....	8.89
190....	9.00	....	8.78
193....	9.00	8.56	8.78
339....	8.89	....	....
456....	8.67	....	....
457....	8.67	....	8.67
457....	8.67	....	....
457....	8.67	....	....
483....	8.67	....	....
516....	8.89	....	....
523....	9.00	....	9.00
547....	8.67	....	8.78
579....	8.67	....	8.67
592....	8.67	....	....
694....	8.56	....	....
695....	8.56	....	9.00
750....	8.78	....	....
801....	8.78	....	8.78
809....	8.78	....	....
945....	8.67	....	....
947....	8.78	....	....
28034....	8.73	....	....
064....	8.78	8.56	8.67
071....	9.00	8.56	8.67
075....	8.78	8.56	....
079....	8.67	....	....
099....	8.89	....	....
135....	8.56	....	....
145....	8.89	8.78	8.89
154....	8.67	....	9.00
167....	8.78	....	....
181....	8.67	....	....
189....	8.78	8.84	....
212....	9.00	....	....
214....	8.56	....	....
219....	9.00	8.45:	8.89
224....	8.89	8.78	....
227....	9.12	....	8.78
248....	8.78	....	....
250....	8.56	....	....
276....	8.89	8.56	8.89

JD 24+	IPg		
28288....	8m67	....	8m89
302....	8.45	....	....
306....	8.67	....	....
315....	8.78	....	....
322....	8.89	....	....
364....	8.78	....	....
380....	9.12	....	....
393....	9.00	....	....
393....	9.12	....	....
397....	8.89	8m67	8.78
405....	9.12	....	....
408....	8.56	8.67	8.56
433....	8.56	....	....
455....	8.67	8.67	8.67
455....	8.78	8.78	9.00
456....	8.89	9.00	....
457....	8.67	....	....
482....	9.00	....	....
486....	8.67	....	....
497....	8.67	....	....
504....	8.95	....	....
512....	8.67	....	8.67
516....	8.78	....	8.89
516....	8.67	8.56	8.67
551....	8.56	....	....
553....	9.00	....	....
566....	8.67	....	....
568....	8.56	....	....
578....	8.78	....	9.00
579....	8.45	....	8.78
595....	8.34	8.56	8.67
600....	8.67	....	....
602....	8.45	....	....
603....	8.67	....	....
612....	8.34	8.67	....
615....	8.67	....	....
623....	8.67	....	....
625....	8.78	8.67	9.00
625....	8.78	....	....
631....	8.45	....	8.78
631....	8.67	....	....
633....	8.89	8.67	9.07
637....	8.78	....	....
638....	8.89	....	....
638....	8.45	....	8.89
639....	8.89	8.89	8.89
639....	8.67	8.95	8.89
640....	8.56	....	....
640....	8.45	....	....
652....	8.56	....	8.67
654....	8.62	....	....
654....	8.78	....	8.78
657....	8.56	....	....
668....	8.67	8.78	8.67
668....	8.62	....	....
670....	8.34	....	....
672....	8.34	....	....
682....	8.45	....	....
685....	8.78	....	....
688....	8.45	....	8.45

JD 24+	IPg		
28688....	8m67	....	....
691....	8.67	8m67	8m67
694....	8.45	....	....
695....	8.78	8.67	8.89
702....	8.78	....	....
713....	8.78	....	....
717....	8.45	....	8.56
719....	8.34	....	....
720....	8.34	....	....
722....	8.34	....	8.67
722....	8.45	....	....
724....	8.67	8.78	8.95
728....	8.89	8.78	8.89
730....	8.56	....	....
731....	8.67	....	8.78
733....	8.67	....	....
748....	8.67	....	8.67
752....	8.56	....	....
754....	8.56	....	....
755....	8.45	....	....
756....	8.67	....	....
758....	8.56	....	8.45
758....	8.67	....	....
759....	8.67	8.56	8.78
761....	8.67	....	....
764....	8.56	....	....
776....	8.56	....	....
777....	8.78	8.67	8.78
780....	8.67	....	8.89
780....	8.56	....	....
782....	8.89	8.78	8.67
783....	8.45	8.56	....
789....	8.34	....	....
790....	8.62	....	....
791....	8.67	....	....
804....	8.78	8.89	9.12
804....	8.67	....	....
815....	8.67	....	8.78
817....	8.73	....	....
819....	8.56	....	....
833....	8.67	....	....
838....	8.56	....	....
842....	8.78	8.34	8.89
843....	8.78	....	8.89
845....	8.67	....	....
845....	8.78	....	8.89
845....	8.78	....	....
846....	8.67	....	....
847....	8.34	....	....
849....	8.67	....	....
850....	8.78	....	8.89
850....	8.73	....	....
851....	8.45	....	....
853....	8.67	8.45	8.67
861....	8.67	....	....
863....	9.00	....	9.12
863....	8.73	....	....
864....	8.73	8.56	8.89
872....	8.78	....	....
875....	8.67	8.89	....

TABLE 1—*Continued*

JD 24+	IPg		
28877....	8m89	8m67	9m00
878....	8.89	8.67	8.89
878....	8.89	8.78	8.89
878....	8.78	8.56	8.78
878....	8.67	....	....
892....	8.56	....	....
896....	8.56	....	....
896....	8.73	....	....
898....	8.89	8.78	9.00
904....	8.78	....	8.89
904....	8.73	....	....
905....	8.78	8.78	8.89
906....	8.78	8.56	8.78
911....	8.78	....	....
919....	8.45	....	....
923....	8.67	....	8.78
925....	8.78	....	....
931....	8.56	8.67	8.67
932....	8.67	....	....
933....	8.67	....	....
937....	8.89	....	....
951....	8.78	8.84	8.89
951....	8.78	....	....
952....	8.56	....	8.78
959....	8.78	....	....
960....	8.78	....	8.78
960....	8.84	....	....
962....	8.56	....	....
978....	8.78	....	....
988....	8.67	....	9.12
994....	8.78	8.67	....
994....	8.78	....	....
995....	8.67	....	....
29014....	8.89	....	8.95
015....	8.45	....	8.78
016....	8.67	....	....
017....	8.56	8.78	9.12:
018....	8.84	....	....
019....	8.67	....	....
019....	8.78	....	....
020....	8.34	....	....
022....	8.89	....	8.78
023....	8.56	....	....
028....	8.84	....	....
039....	8.45	8.45	....
042....	8.67	....	....
042....	8.73	....	8.78
044....	8.56	....	....
051....	8.78	8.78	9.12
051....	8.73	....	....
053....	8.67	....	9.00
053....	8.73	....	....
072....	8.89	....	....
073....	8.78	8.78	8.89
073....	8.78	....	....
077....	8.56	....	....
100....	9.12	8.56	9.12
102....	8.84	....	....
106....	9.00	....	8.89
107....	8.78	8.78	8.89

JD 24+	IPg		
29108....	8m67	....	....
113....	8.67	....	....
113....	8.78	8m67	9m00
115....	8.78	....	....
115....	9.00	....	9.00
118....	8.89	....	9.00
129....	8.67	....	....
129....	8.78	8.67	8.78
129....	8.67	....	....
134....	8.89	8.78	8.89
141....	8.56	....	8.78
141....	8.73	....	....
142....	8.78	8.89	8.78
144....	8.45	....	....
155....	8.67	9.12	8.89
155....	8.67	8.89	8.67
158....	8.67	....	....
158....	8.78	....	....
160....	8.45	....	....
161....	8.89	....	9.00
161....	8.89	....	9.00
162....	8.78	8.56	....
184....	8.78	....	....
184....	8.67	....	....
185....	8.78	....	....
188....	9.00	8.78	8.78
188....	8.78	8.78	8.89
190....	8.78	....	....
190....	8.67	9.12	9.00
199....	8.78	....	....
202....	9.00	....	....
203....	9.00	....	9.00
204....	8.67	....	....
205....	8.67	....	....
214....	8.56	8.56	8.78
217....	8.78	....	....
217....	8.45	8.56	8.89
220....	8.67	....	....
222....	8.67	....	....
223....	8.56	8.78	8.89
224....	8.56	....	....
227....	8.67	....	....
229....	8.56	8.56	....
246....	9.00	....	8.89
246....	9.12	....	8.78
247....	9.23	8.89	9.12
254....	8.78	9.12	9.00
266....	8.67	9.12	8.89
272....	8.78	9.00	....
287....	8.89	8.78	....
288....	8.89	....	....
291....	8.78	....	....
300....	8.89	....	....
300....	9.00	9.12	9.00
300....	9.00	....	9.23
304....	8.89	....	....
311....	9.23	....	9.00
311....	8.89	....	....
313....	9.00	9.12	9.12
314....	8.89	....	....

JD 24+	IPg		
29315....	9m12	....	....
322....	9.12	....	....
335....	8.67	....	....
339....	8.84	....	....
339....	9.23	....	9m00
340....	8.89	9m00	9.12:
341....	9.34	....	9.23
342....	8.89	....	....
343....	8.95	....	....
344....	9.12	9.00	....
347....	9.00	9.00	....
349....	9.45	....	9.23
350....	9.07	9.07	....
360....	9.00	....	8.89
364....	9.12	....	....
365....	8.95	....	....
368....	9.23	....	9.00
370....	9.12	....	....
373....	9.07	....	....
374....	9.12	....	9.00
374....	9.00	....	....
375....	9.18	8.89	9.12
381....	9.34	....	....
382....	9.00	9.18	9.12
382....	8.95	....	....
389....	9.00	....	....
389....	8.78	....	....
391....	9.00	....	....
393....	9.23	....	9.18
394....	9.18	9.23	9.18
399....	9.23	9.23	....
407....	9.00	....	....
408....	9.12	9.45	9.23
408....	9.07	....	....
409....	9.12	9.18	....
410....	9.12	....	....
414....	9.07	....	....
420....	9.12	....	....
421....	9.12	....	9.12
422....	9.12	9.34	9.34
424....	9.34	....	....
431....	9.23	....	....
431....	9.45	9.23	9.23
433....	9.07	....	....
436....	9.34	9.23	9.12
442....	9.18	....	....
454....	9.12	....	....
454....	9.12	....	....
458....	9.34	9.12	....
463....	9.18	....	....
464....	9.00	....	....
464....	9.23	....	....
465....	9.23	9.00	....
466....	9.18	....	....
466....	9.23	....	9.12
468....	9.34	9.12	....
472....	9.45	9.34	....
482....	9.29	....	....
485....	9.29	....	....
485....	9.23	9.34	9.23

TABLE 1—*Continued*

JD 24+	IPg			JD 24+	IPg			JD 24+	IPg		
29486....	9m12	....	....	29701....	9m45	9m56	....	29871....	9m45	9m34	9m34
489....	9.12	9m34	9m12	703....	9.45	9.45	....	872....	9.34	....	9.45
489....	9.12	....	....	717....	9.29	....	....	874....	9.34	9.23	....
493....	9.23	....	....	727....	9.34	....	9m34	875....	9.45	....	....
514....	9.34	....	....	728....	9.45	....	9.12	875....	9.23	....	9.56
514....	9.29	....	....	729....	9.56	9.56	9.56	877....	9.56	....	9.23
517....	9.34	....	9.23	730....	9.51	....	....	881....	9.45	9.45	....
517....	9.23	....	....	730....	9.56	....	9.23	884....	9.51	....	....
518....	9.34	9.23	....	731....	9.40	....	....	897....	9.23	....	....
519....	9.23	9.45	9.23	739....	9.56	9.56	9.34	903....	9.23	....	....
520....	9.56	....	9.45	743....	9.34	....	9.34	911....	9.45	....	9.23
521....	9.34	9.23	....	743....	9.45	....	....	912....	9.45	9.34	9.45
522....	9.34	9.23	....	745....	9.45	....	9.45	912....	9.29	....	....
925....	9.29	....	....	745....	9.45	....	....	914....	9.45	....	9.56
926....	9.23	9.34	....	746....	9.56	....	9.34	923....	9.34	....	9.12
527....	9.56	....	....	749....	9.45	....	....	923....	9.34	....	9.23
528....	9.34	....	....	751....	9.45	9.56	....	925....	9.34	....	9.34
545....	9.45	....	....	756....	9.45	....	9.45	928....	9.45	....	....
546....	9.23	....	....	756....	9.56	....	9.23	952....	9.45	9.45	9.23
546....	9.23	9.45	9.45	756....	9.45	....	....	955....	9.34	....	....
547....	9.23	....	....	759....	9.34	....	....	955....	9.40	....	....
550....	9.45	....	....	760....	9.45	....	....	959....	9.34	9.45	9.34
554....	9.34	....	....	762....	9.56	9.45	9.23	961....	9.45	....	....
562....	9.12	....	8.89	764....	9.56	9.56	....	962....	9.34	9.45	....
563....	9.23	....	9.12	776....	9.45	9.56	9.23	962....	9.45	....	....
574....	9.34	9.45	....	777....	9.56	9.45	....	969....	9.45	9.12	9.23
576....	9.45	....	9.34	778....	9.56	....	....	970....	9.45	9.56	....
578....	9.45	9.34	....	787....	9.56	9.34	9.45	973....	9.12	....	9.12
583....	9.45	....	....	788....	9.56	....	....	973....	9.34	....	9.00
584....	9.34	9.34	....	805....	9.45	....	9.23	986....	9.23	....	9.23
586....	9.34	9.45	9.34	805....	9.45	....	....	988....	9.29	....	....
587....	9.34	....	9.34	806....	9.45	....	9.34	994....	9.40	....	....
591....	9.12	....	....	806....	9.34	....	....	30004....	9.56	9.34	....
598....	9.23	9.45	....	807....	9.40	....	....	005....	9.34	9.34	....
598....	9.23	....	....	808....	9.45	....	....	010....	9.29	....	....
601....	9.12	....	8.89:	808....	9.56	9.34	9.45	017....	9.12	....	....
601....	9.29	....	....	811....	9.34	....	9.45	018....	9.34	9.23	....
602....	9.56	....	....	811....	9.45	....	....	043....	9.40	....	....
605....	9.34	....	....	813....	9.29	....	....	043....	9.56	....	9.56
605....	9.34	....	9.12	815....	9.56	....	....	043....	9.23	9.34	9.23
619....	9.23	....	9.34	820....	9.40	....	....	044....	9.23	....	9.23
619....	9.45	....	....	821....	9.34	9.45	9.34	045....	9.34	....	....
627....	9.12	....	9.00	822....	9.45	....	....	049....	9.23	....	....
629....	9.45	....	....	825....	9.23	....	....	054....	9.45	....	....
637....	9.45	9.34	....	825....	9.40	....	....	057....	9.45	....	....
638....	9.45	9.23	....	836....	9.62	....	....	058....	9.34	9.23	....
639....	9.29	....	....	839....	9.45	9.45	....	063....	9.23	9.23	9.12
639....	9.45	....	9.45	842....	9.56	9.45	9.34	063....	9.23	....	....
640....	9.45	9.45	9.45	843....	9.45	....	....	073....	9.29	....	....
651....	9.45	....	9.45	847....	9.34	9.45	9.23	079....	9.34	....	....
651....	9.23	....	9.23	847....	9.45	....	....	080....	9.18	....	....
666....	9.45	9.45	9.45	847....	9.23	9.34	9.34	085....	9.00	....	....
671....	9.45	....	....	853....	9.51	....	....	093....	9.23	9.12	9.12
671....	9.34	....	....	854....	9.45	9.45	9.23	101....	9.12	9.23	9.00
672....	9.34	....	9.23	855....	9.34	9.34	9.34	102....	9.18	....	....
674....	9.45	....	....	865....	9.34	....	9.23	102....	9.00	....	....
690....	9.51	9.34	....	867....	9.51	....	....	104....	9.07	....	9.12
696....	9.56	....	....	867....	9.45	9.56	9.56	110....	9.00	....	....
697....	9.34	....	9.45	868....	9.45	....	....	112....	9.12	9.12	9.12
698....	9.40	....	....	870....	9.12	....	9.23	116....	9.12	9.00	9.00

TABLE 1—*Continued*

JD 24+	IPg			JD 24+	IPg			JD 24+	IPg		
30117....	9m00	9m12	....	30158....	9m12	....	....	30177....	9m00	....	....
119....	9.12	9.12	....	158....	9.07	....	....	178....	9.18	....	....
129....	9.00	....	....	159....	9.12	8m89	9m00				
130....	9.07	8.89	9m12	159....	9.00	9.12	9.12	182....	9.23	....	....
133....	9.12	....	....	160....	9.07	9.00	9.00	190....	9.07	....	....
135....	9.18	....	....	162....	9.07	....	....	193....	9.12	....	9m12
136....	9.00	9.00	....					196....	9.07	....	....
138....	8.95	....	....	164....	9.12	....	....	200....	9.00	9m00	....
143....	9.00	....	....	164....	9.12	....	....	201....	9.00	8.89	9.12
148....	8.95	9.12	9.00	168....	8.89	9.12	9.12	201....	9.00	....	....
				169....	9.00	9.23	9.12	203....	8.89	8.89	....
148....	9.18	....	....	169....	9.12	....	....	206....	8.95	....	....
149....	8.89	9.07	8.89	171....	9.00	8.78	9.00	221....	8.78	....	8.89
150....	9.00	9.23	9.00	175....	9.07	....	....				
150....	9.18	....	....	176....	9.12	....	....				

TABLE 2

COMPARISON STARS

Designation	IPg	Designation	IPg
a.....	8m31	*c*.....	9m02
b.....	8.80	*d*.....	9.98

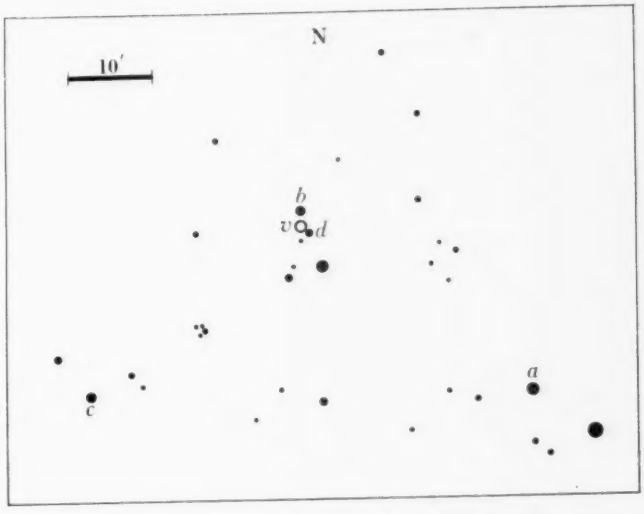

FIG. 1.—Comparison stars for S Doradus

4. *Light-curve and dimensions of the system.*—Table 4 summarizes the mean light-curve. The grouping of the plates in means was influenced by the distribution of the observations in time. Table 5 summarizes the means from the spectral estimates.

TABLE 3

ESTIMATIONS OF SPECTRUM OF S DORADUS

B PLATES		A PLATES		MF PLATE	
JD 24+	IPg	JD 24+	IPg	JD 24+	IPg
12245	9^m23	13965	8^m84†	26304	9^m40
456	8.89	965	8.89		
13076	8.62	996	8.89		
082	8.67	997	8.89		
513	8.67*	14244	8.78‡		
514	8.67	247	8.78‡		
784	8.67	248	8.67‡		
959	8.78	252	8.84‡		
14197	8.67	252	8.73‡		
924	9.34	253	8.67		
		253	8.78		
938	9.23	959	9.34		
953	9.23	960	9.23		
968	9.34	961	9.45		
980	9.45	962	9.56		
981	9.45	962	9.45		
17882	8.78	965	9.45		
18630	8.73	17240	8.67		
19364	8.67	241	8.67		
		23403	8.78§		
		403	8.73		
		403	8.78		
		403	8.67		
		464	8.67‖		
		464	8.67		
		26294	9.34¶		
		298	9.23		
		299	9.34¶		
		302	9.45		
		302	9.34		
		302	9.45		
		28181	8.89**		
		182	8.67		

* Two bright lines seen ($H\beta$, $H\gamma$).

† $H\beta$ is about 0^m5 brighter than $H\gamma$, which about equals the brightest part of the continuum.

‡ $H\beta$ is about equal to $H\gamma$, $H\delta$ is seen, about 0^m3 fainter than $H\gamma$.

§ Only $H\beta$ is seen; very bright (about 0^m7 brighter than continuum).

‖ As for (§), $H\gamma$ is very faint; violet part of continuum seems to be brighter than the red part of it.

¶ More or less as for (§), only the red part of the continuum seems to be brighter than the violet part of it.

** Similar to (§).

The light-curve shows four well-pronounced minima of approximately the same depth. In addition, there are several small fluctuations. From a detailed plot were deduced the values given in Table 6.

The mean magnitude of the maximum has been computed from 1287 estimations (see Table 1) outside of the four minima; it is $8^m.78$. The mean minimal brightness from 196

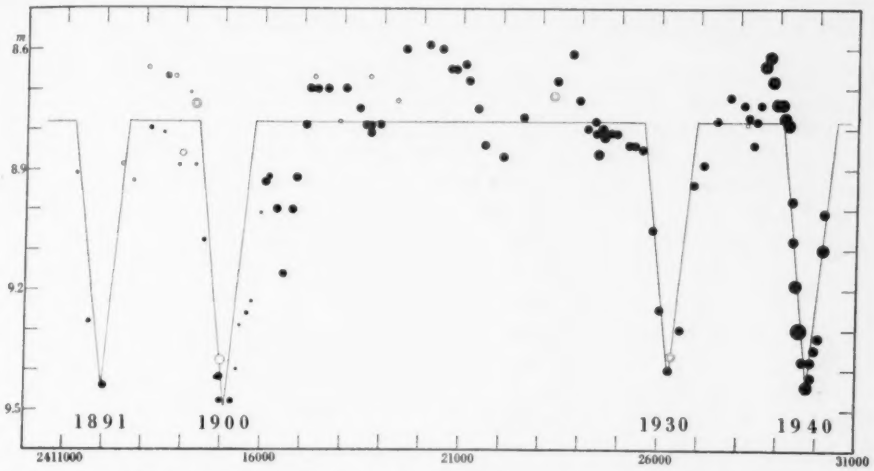

FIG. 2.—Mean light-curve of S Doradus. Ordinates and abscissas are photographic magnitudes and time (Julian days and years). Dots are estimates from photographic plates; circles are estimates from spectra; double circles denote bright-line spectra. The size of the symbols is proportional to the weight of the point.

TABLE 4

MEAN LIGHT-CURVE OF S DORADUS

JD 2400000+	IPg	No. of Plates	JD 2400000+	IPg	No. of Plates	JD 2400000+	IPg	No. of Plates	JD 2400000+	IPg	No. of Plates
11313....	$8^m.91$	2	16744....	$9^m.00$	10	23790....	$8^m.61$	10	28453....	$8^m.78$	10
11624....	9.28	3	16832....	8.92	10	23944....	8.73	10	28544....	8.74	10
12044....	9.44	10	17050....	8.79	10	24171....	8.80	10	28641....	8.64	30
12713....	8.93	2	17111....	8.70	10	24338....	8.78	10	28738....	8.62	30
13147....	8.80	3	17320....	8.70	10	24386....	8.81	10	28834....	8.68	30
13487....	8.81	2	17600....	8.70	10	24448....	8.86	20	28923....	8.74	30
13911....	8.89	2	18074....	8.70	10	24520....	8.80	20	29043....	8.74	30
14161....	8.71	1	18408....	8.75	10	24610....	8.82	20	29153....	8.77	30
14300....	8.89	1	18580....	8.79	10	24778....	8.81	10	29232....	8.79	30
14516....	9.08	3	18610....	8.79	10	24900....	8.81	10	29320....	8.98	20
14894....	9.42	3	18675....	8.81	10	25222....	8.84	10	29373....	9.08	20
14922....	9.42	10	18975....	8.79	10	25372....	8.84	10	29443....	9.19	30
14965....	9.48	6	19578....	8.60	10	25573....	8.85	10	29540....	9.30	40
15089....	9.45	1	20136....	8.59	10	25835....	9.05	10	29655....	9.38	20
15270....	9.48	8	20457....	8.60	10	26028....	9.25	10	29750....	9.44	30
15372....	9.40	1	20700....	8.65	10	26283....	9.40	10	29821....	9.42	20
15465....	9.29	1	20798....	8.65	10	26526....	9.30	10	29870....	9.38	20
15626....	9.26	4	21045....	8.64	10	26848....	8.94	10	29946....	9.35	20
15735....	9.23	2	21192....	8.68	10	27104....	8.89	10	30037....	9.32	20
15956....	9.01	1	21359....	8.75	10	27407....	8.78	10	30144....	9.10	30
16051....	8.93	10	21596....	8.84	10	27735....	8.72	10	30185....	9.04	20
16122....	8.92	7	22056....	8.87	10	28102....	8.74	10			
16378....	9.00	10	22532....	8.77	10	28224....	8.77	10			
16514....	9.21	10	23373....	8.68	10	28346....	8.84	10			

estimations during the lowest portion of the minima is $9^m.42$. The minima show slight differences; those of 1900 and 1940 seem to be about $0^m.03$ deeper. The difference is

probably accidental, and its effect on our previously published results[1] would not be significant.

The relative dimensions of the system were first computed, under an assumption of a central eclipse, by the formulae

$$0.64 = 2.5 \log (1 + k^2\gamma), \tag{1}$$

$$r_1(1+k) = \sin \tfrac{1}{2} D . \tag{2}$$

By inserting the value of 1.0 for γ (the ratio of surface brightness) and of 13.9° for $\frac{1}{2}D$, we find that $k = 0.9$ and $r = 0.126$. Another approach, assuming a total eclipse, leads to practically the same value, 0.127, for r.

TABLE 5

MEAN MAGNITUDES FROM SPECTRA OF S DORADUS

JD 2400000+	IPg	No. of Plates	JD 2400000+	IPg	No. of Plates	JD 2400000+	IPg	No. of Plates
12245.....	9^m23	1	13984.....	8^m86	5	18630.....	8^m73	1
12456.....	8.89	1	14243.....	8.74	8	19364.....	8.67	1
13079.....	8.65	2	14960.....	9.38	12	23423.....	8.72	6
13513.....	8.67	2	17240.....	8.67	2	26300.....	9.37	7
13784.....	8.67	1	17882.....	8.78	1	28182.....	8.78	2

TABLE 6

MINIMA OF S DORADUS

Minimum	Duration (Days)	Middle of Eclipse	Range	Minimum	Duration (Days)	Middle of Eclipse	Range
1890.....	?	JD 2411900:	8^m78–9^m42	1930.....	$\geqslant 1130$	JD 2426300	8^m78–9^m38
1900.....	>1130	2415100	8.78–9.45	1940.....	1130	2429760	8.78–9.42

The eccentricity of the orbit is determined[3] from the formula

$$\tfrac{1}{2}\,(0^P.26\pi) = e \cos \omega \tag{3}$$

[3] Dr. Z. Kopal suggests the following more rigorous derivation of the eccentricity: "Assuming the orbital plane to be perpendicular to the line of sight ($i = 90°$),

$$\frac{2\pi}{P}\,(t_2 - t_1) = \psi - \sin \psi ,$$

where

$$\psi = \pi + 2 \tan^{-1} \frac{e \cos \omega}{\sqrt{1 - e^2}} .$$

A solution of the above equation yields

$$\frac{e \cos \omega}{\sqrt{1 - e^2}} = 0.471 ."$$

and by adopting $\omega = 0$. The value of the eccentricity thus obtained is, of course, a minimum. It should be pointed out that the two secondary minima (1890 and 1930) are not exactly at the same distance from the corresponding primary minima, but the minimum of 1890 was not well observed. Perhaps the middle of this eclipse fell about a year earlier than is given in Table 6.

In addition to the four minima that we have interpreted in terms of the eclipsing system, there are several noteworthy fluctuations. The long-term fluctuations are shown in Figure 2; the differences which are seen in Table 1 to represent fluctuations within one or two days may be attributed to the uncertainty of the material at our disposal. The principal long-term fluctuations are summarized in Table 7. In giving the table we do

TABLE 7

SECONDARY FLUCTUATIONS OF S DORADUS

SECONDARY MAXIMA		SECONDARY MINIMA	
JD	Deviation from Mean Curve	JD	Deviation from Mean Curve
2417750	-0^m15	2416500	$+0^m35$
2420400	−0.20	2418750	+0.05
2423600	−0.20	2422000	+0.15
2428700	−0.25	2425000	+0.10
		2427000	+0.10

not commit ourselves as to the reality or the exact amount of variation, either in brightness or in time.

The depression around 2416500 is a very conspicuous one. Excepting this one, the minima are not outside the errors of observations. The maxima, however, seem to be of more persistent character.

5. *Absolute dimensions and constitution of the system.*—It goes without saying that the system of S Doradus can only be thoroughly investigated physically when radial velocities are obtained and the orbital velocities and velocities of the bright lines are determined. There are no observations of radial velocity in existence for S Doradus. Such observations would probably be decisive in confirming our suggested interpretation of the observed variations of light. If, however, our interpretation is correct, we can make a rough estimate of the fundamental physical characteristics of the system, without knowing the radial velocities, by applying a method that has been shown to be applicable for many "normal" eclipsing stars.[4] The quantity first computed is the mass of each component from the formula

$$\log \mu = 0.26\,(2.17 + 2 \log P + 3 \log r + 6 \log T)\,. \qquad (4)$$

The quantities P (period in days) and r (relative radius in terms of the distances between the centers) are approximately known. The quantity T (effective temperature, in terms of solar effective temperature) was taken from the compilation of Dufay[5] for P Cygni, which S Doradus resembles spectroscopically; he gives a color temperature of 7130° for this star. For want of a better value, I have adopted this value for the effective temperature of S Doradus. If we adopt 5730° as the effective temperature of the sun, we find for

[4] S. Gaposchkin, *Harvard Reprints*, No. 201, 1940.

[5] *Pub. de l'Obs. Lyon*, **1**, No. 1, 1930.

the larger component a mass of 160⊙. Its absolute bolometric magnitude, from the formula $L \propto \mu^{3.2}$, is then −12.75. The radius, computed from the formula

$$\log R = \tfrac{1}{3}(4.37 + 3 \log r + 2 \log P), \tag{5}$$

is 2100⊙. We proceed similarly for the second component. Our results are summarized in Table 8. It is obvious that any moderate bolometric correction (less than a magnitude) places S Doradus far beyond the Magellanic Cloud, which is absurd.

The computed central temperature in Table 8 refers to the point-source model. Both it and the central condensation (ξ^*) refer to both stars and are computed by the well-known formulae given by Chandrasekhar.[6]

TABLE 8

THE SYSTEM OF S DORADUS

PHOTOMETRIC ELEMENTS

Min.	=	JD 2429760+14670^d·E
P	=	40^{y}2
e	=	0.4
D	=	1130^d
M_{max}	=	8^{m}78
A_1	=	0^{m}64
A_2	=	0^{m}64

RELATIVE DIMENSIONS

i	=	90° (adopted)
γ	=	1.0
k	=	0.9
L_1	=	0.55
L_2	=	0.45
r_1	=	0.13
r_2	=	0.11
m_1	=	9^{m}43
m_2	=	9^{m}65

ABSOLUTE DIMENSIONS

First component (larger):

Spectrum: P Cygni

T_e	=	7130°
μ	=	160⊙*
R	=	2100⊙*
ρ	=	$2 \cdot 10^{-8}$⊙
M_{bol}	=	−12^{m}7*
$T_{central}$	=	$1.5 \cdot 10^6$

Second component:

Spectrum: P Cygni

T_e	=	7130°
μ	=	145⊙*
R	=	1900⊙*
ρ	=	$2 \cdot 10^{-8}$⊙
M_{bol}	=	−12^{m}5*
ξ^*	=	$\ll 0.3$

* See text, sec. 6.

It may be noted that the system of VV Cephei has a period of 20 years and a (spectroscopic) eccentricity of 0.2; ϵ Aurigae, with a period of 27 years, has a (spectroscopic) eccentricity of 0.3; while S Doradus, with a 40-year period, has an eccentricity of 0.4. But the correlation of the periods and eccentricities of visual binaries is somewhat problematical, and the progression just mentioned may not be significant, except to show that three long-period eclipsing stars have appreciable eccentricities, comparable to those of visual binaries of similar period.

6. *Discussion.*—The absolute dimensions given in Table 8 are based on the adopted values of r, P, and T_e and on the assumed mass-luminosity relation $L \propto \mu^{3.2}$. We may now use the known modulus of the Large Magellanic Cloud, which is given by Shapley[7] as 17^{m}1, to estimate the magnitude of the uncertain factors, the temperature, and the adopted mass-luminosity relation. The latter is the subject of the greatest uncertainty, for it is based on observational material that contains no masses greater than 40 ⊙.

If the modulus is taken to be 17^{m}1, the photographic magnitude at maximum 8^{m}8, the color index +0^{m}8 (appropriate to a P Cygni star[8]), a bolometric correction −0^{m}8 (ap-

[6] *M.N.*, **96**, 647, 1936.

[7] *Star Clusters*, p. 189, 1930.

[8] Cf. F. Sherman and W. W. Morgan, *Ap. J.*, **89**, 513, 1939.

propriate[9] to a star with an expanding photosphere and a temperature of 7000°), and a relative brightness for the two components of 0.55 and 0.45, we obtain for the brighter component an absolute bolometric magnitude −9.3. Similar reasoning may be applied to the second component. If the resulting absolute bolometric magnitudes are used with equation (4), we obtain for the first component a mass of 60⊙ and a radius of 1400⊙. Thus, while the stars are obviously large and massive, they are probably underluminous. It is noteworthy that the Trumpler stars, the only known group of stars with such high masses,[10] and also of early type, are recognized to be considerably underluminous.

The star S Doradus is situated in a nebula, and the apparent magnitude may be affected slightly thereby.

I should like to use this opportunity to thank Dr. Shapley for his continued interest in the work on this star and for putting some unpublished observations at my disposal. Dr. Shapley and Dr. Kopal have kindly read the manuscript and made valuable suggestions. I am also indebted to Mrs. Margaret Mayall and Mrs. Payne-Gaposchkin for their examination of the spectrum plates and to Miss Virginia Brenton for making many estimates of brightness.

[9] F. L. Whipple and C. Payne-Gaposchkin, *Harvard Circ.*, No. 413, 1936.

[10] R. Trumpler, *Pub. A.S.P.*, **37**, 249, 1935.

PROFILES IN THE ALPHA BAND OF ATMOSPHERIC OXYGEN

H. A. A. PANOFSKY
New York University
Received December 7, 1942

ABSTRACT

Seven lines in the alpha band of atmospheric oxygen in the sun's spectrum have been photographed with the Berkeley solar spectrograph and interferometer, and their profiles have been measured. The general consistency of the observational results with one another and with theory indicates that there are no serious errors in the measurement of profiles by the interferometric method, after the important instrumental effects have been eliminated.

The total absorption coefficient of the alpha band was computed by two independent methods, yielding 8.7×10^{4} and 9.4×10^{4} sec $^{-1}$ per cm. of normal atmosphere, respectively. The mean molecular diameter for collisions between O_2 molecules, on the one hand, and air molecules, on the other, was estimated to be 5.15×10^{-8} cm.

I. INTRODUCTION

The profiles of telluric lines have been discussed by Woolley, by Childs, and by Allen.[1,2] Both Childs and Allen were able to show from the curve of growth of these lines that the profiles must vary in the wings as $1/(\nu - \nu_0)^2$.

Allen has also derived a theory for the central parts of the profile, based on a combination of the effects of Doppler broadening and pressure broadening. This theory has never been checked experimentally, since high dispersion is required and instrumental errors greatly influence the measured profile, owing to the sharpness of the line.

In this paper Shane's[3] method of deriving profiles of solar lines is applied to a number of telluric O_2 lines, in order both to check Allen's theoretical profile and to test the reliability of this method of eliminating instrumental errors.

II. THE OBSERVATIONS

Lines near the origin of the alpha band of O_2 were photographed in the first order of the Berkeley 9-meter grating spectrograph (dispersion 1.85 A/mm) by means of an etalon interferometer in front of the spectrograph slit. Seven of the first eight lines in the P branch[4] were measured. The fifth line ($\lambda = 6304$, $J = 8$, for the lower state) was omitted, since it is affected by two strong adjacent solar lines.

The profiles of the lines in the alpha band of O_2 are based on sixteen plates, six of which were obtained with the 5-mm separators and ten with the 10-mm separators. The method of measurement of the plates and the conversion of galvanometer readings into intensities, as well as the application of instrumental corrections, have been discussed by Shane[3] and will not be repeated here. The instrumental corrections for this spectral region had to be determined before the investigation was started.

[1] Childs (*Ap. J.*, **77**, 212, 1933) computes the wings of the profiles and checks the square-root part of the curve of growth. Woolley's earlier results in this respect (*Ap. J.*, **73**, 185, 1931) were shown to be based on faulty observations.

[2] Profiles were computed by Allen (*Ap. J.*, **85**, 156, 1937) and checked with the experimental curve of growth. Total absorptions of the various bands were also found from it.

[3] *Lick Obs. Bull.*, **16**, 76, 1933.

[4] There is some confusion concerning the notation of the branches of these bands. The notation used here is that of Mulliken (*Phys. Rev.*, **37**, 1711, 1931), who first interpreted the band structure correctly. For other notations see the summary in Jevons, *Report on Band Spectra*, London, 1932. References to earlier papers concerning structure of the atmospheric O_2 bands are also found there.

The results for the mean values of the profiles, as determined from photographs with the two different separators, are given in Table 1. They are reduced to a common zenith distance ($\cos z = 0.700$).

In general, the intensities at $|\nu - \nu_0| < 0.01$ and $|\nu - \nu_0| > 0.13$ are not so reliable as the remainder of the profile. Otherwise the internal agreement among the 5-mm spectrograms is excellent but among the 10-mm exposures only fair. As is seen from Table 1, the mean intensities are somewhat smaller in the case of the 5-mm exposures

TABLE 1

OBSERVED PROFILES $I(\nu)$

($\cos z = 0.700$)

$\nu - \nu_0$ (In Cm^{-1})	λ 6287		λ 6290		λ 6293		λ 6296		λ 6299		λ 6307		λ 6313	
	10 Mm	5 Mm	10 Mm	5 Mm	10 Mm	5 Mm	10 Mm	5 Mm	10 Mm	5 Mm	10 Mm	5 Mm	10 Mm	5 Mm
0.00	0.558	0.592	0.435	0.388	0.357	0.311	0.337	0.285	0.352	0.267	0.440	0.425	0.525	0.535
.01	.608	.619	.456	.405	.372	.343	.357	.316	.377	.285	.465	.460	.546	0.565
.02	.698	.697	.528	.510	.437	.426	.429	.405	.466	.370	.544	.544	.651	0.628
.03	.758	.770	.606	.614	.521	.517	.518	.497	.570	.462	.644	.631	.732	0.700
.04	.803	.828	.686	.694	.607	.606	.615	.597	.657	.545	.716	.707	.782	0.760
.05	.842	.869	.749	.746	.684	.681	.692	.656	.716	.630	.771	.770	.823	0.809
.06	.875	.895	.797	.807	.745	.742	.754	.716	.761	.716	.815	.810	.858	0.850
.075	.915	.923	.853	.853	.813	.812	.816	.789	.812	.806	.859	.860	.808	0.898
.10	.953	.955	.908	.915	.884	.886	.885	.869	.873	.870	.909	.914	.939	0.948
0.15	0.983	0.985	0.963	0.973	0.968	0.953	0.949	0.943	0.949	0.930	0.966	0.972	0.979	1.000

than for the 10 mm exposures. If this discrepancy is real, it indicates an underestimate of the scattered light rather than of the instrumental profile.

III. INTERPRETATION OF THE OBSERVATIONS

In this section, the following notation is used:

i = Weight × transition probability;

E = Excitation potential of lower level;

$I(\nu)$ = True intensity distribution in the line, $\cos z = 0.700$;

$C(\nu)$ = Line absorption coefficient, $z = 0$;

$c(\nu)$ = Line-absorption coefficient of a line of $i = 1$, $E = 0$;

$A(\nu)$ = Line absorption coefficient of a line broadened by collisions only, integrated through the atmosphere;

$D(\nu)$ = Line-absorption coefficient of a line broadened by Doppler effect only.

The reduction of the observations, summarized in Table 1, was as follows: Means were taken of the means from 5-mm and 10-mm exposures, in order to derive the final intensity profiles of $I(\nu)$. These were then reduced to absorption coefficients at zero zenith distance by application of the absorption-tube formula:

$$I(\nu) = e^{-C(\nu)\sec z}. \tag{1}$$

The results for the $C(\nu)$ thus obtained are given in Table 2.

Assuming that all $C(\nu)$ profiles are similar, only transition probabilities, weights, and Boltzmann factors differ from line to line. In that case we may write

$$C(\nu) = c(\nu)\, i e^{-E/kt}, \tag{2}$$

where $c(\nu)$ denotes an absorption coefficient, constant from line to line but varying within a line. It may also be defined as the absorption coefficient of a line of unit weight and zero excitation potential.

The wave lengths of the lines and the excitation potentials were determined by Dieke and Babcock[5] and others.[6] The i-factors were found experimentally by Childs and Mecke,[7] and theoretically by Schlapp.[8] The observed and theoretical i-factors agree in the case of the lines measured but differ in the case of the other branches of the band.

We may determine a kind of mean temperature for the earth's atmosphere by using equation (2). If we plot log $C(\nu)/i$ against E, the slope will be $-1/kT$. In this case a least-squares solution, made from points at different distances from the center of the

TABLE 2

PROFILE OF ABSORPTION COEFFICIENT C(ν)

($z=0$)

$\nu-\nu_0$ (In Cm^{-1}	λ 6287	λ 6290	λ 6293	λ 6296	λ 6299	λ 6307	λ 6311
0.00	0.380	0.635	0.786	0.818	0.856	0.586	0.445
.01	.341	.604	.734	.765	.809	.541	.413
.02	.253	.464	.590	.613	.643	.426	.314
.03	.187	.345	.459	.475	.489	.316	.234
.04	.139	.259	.351	.354	.379	.238	.182
.05	.106	.205	.268	.276	.294	.183	.142
.06	.083	.153	.208	.216	.218	.146	.101
.075	.058	.111	.146	.153	.149	.106	.076
.10	.033	.066	.089	.092	.097	.065	.041
0.15	0.013	0.021	0.029	0.039	0.046	0.022	0.007

line, gives $T = 265°$ K. This is the temperature that an isothermal atmosphere should have in order to produce the observed intensity distribution of the lines within the alpha band. This may be compared with the value of the mean temperature with respect to mass of 255° K.

If the absorption-coefficient profiles $C(\nu)$ are divided by $ie^{-E/kT}$, using $T = 265°$ K, the $c(\nu)$ profiles are obtained (Table 3). These should be the same for all lines. The last column in Table 3 gives the mean of the first seven columns. The values given here represent the best possible determination of the absorption coefficient for a line of $i=1$, $E = 0$, from the present observations.

In the theory of the profiles of the telluric O_2 lines natural damping may be neglected, since these bands represent forbidden transitions, as shown both from an analysis of the spectra and from the observed lines of the states concerned. Also the lower states are sharp, because they belong to the ground state of O_2 and interrotational transitions are forbidden.

Probably the profiles of lines in telluric bands are the result of the combined action of Doppler effect and collision damping. Then we may write

$$c(\nu) = \int_{-\infty}^{+\infty} A(n)\, D(n-\nu)\, dn\,, \qquad (3)$$

[5] *Proc. Nat. Acad.*, **13**, 670, 1927.

[6] See Jevons, *loc. cit.*

[7] *Zs. f. Phys.*, **68**, 344, 1931.

[8] *Phys. Rev.*, **51**, 342, 1937.

where n is an integration variable of frequency units. This expression may be solved for $A(\nu)$ by successive approximations. $T = 265°$ K was used in the Doppler profile. The resultant $A(\nu)$ may be compared with the theoretical profile of the mass-absorption coefficient for collision broadening. This is given by

$$a(\nu) = \frac{1.35 a \sigma^2}{\pi^{3/2}\sqrt{\frac{m}{kT}}} \frac{n}{\frac{7.60}{2\pi}\frac{n^2\sigma^4 kT}{m} + (\nu - \nu_0)^2}, \tag{4}$$

according to Dennison.[9]

In this equation, σ represents a mean diameter for the collisions, n denotes the number of molecules per cubic centimeter (air, in the present case), and a is $\int_0^{+\infty} a(\nu)\, d\nu$. In order to obtain coefficients per centimeter, $a(\nu)$ has to be multiplied by the number of O_2 atoms per cubic centimeter. This number is proportional to n. Finally, for comparison

TABLE 3

PROFILE OF ABSORPTION COEFFICIENT C(ν) DIVIDED BY $ie^{-E/kT} = c(\nu)$

$\nu - \nu_0$ (In Cm^{-1})	λ 6287	λ 6290	λ 6293	λ 6296	λ 6299	λ 6307	λ 6311	Mean
0.00	0.386	0.349	0.330	0.316	0.344	0.342	0.347	0.345
.01	.346	.332	.308	.296	.325	.317	.332	.322
.02	.257	.255	.248	.236	.258	.249	.252	.251
.03	.190	.190	.193	.183	.197	.185	.188	.189
.04	.141	.142	.147	.137	.156	.139	.146	.144
.05	.107	.113	.112	.107	.118	.107	.114	.111
.06	.084	.084	.087	.083	.088	.086	.089	.086
.075	.059	.061	.061	.059	.060	.062	.061	.060
.10	.033	.036	.037	.035	.039	.038	.033	.036
0.15	0.013	0.012	0.012	0.015	0.018	0.013	0.005	0.013

with the observed collision profile, the formula has to be integrated through the atmosphere. We may thus write

$$A(\nu) = A\int_0^{\infty} \frac{n^2\sqrt{\frac{kT}{m}}\, dh}{1.21 n^2 \frac{kT}{m} + \frac{(\nu - \nu_0)^2}{\sigma^4}}, \tag{5}$$

where A contains only quantities invariant with height. T varies less than n, and its variation is sometimes entirely neglected.

Apparently, equation (5) goes to infinity at $\nu = \nu_0$, independently of the law of density chosen. The singularity disappears only after integration over the Doppler profile.

Allen used an exponential density law that fits directly observed densities rather well up to a height of 10 km. Beyond 10 km the observed densities[10] decrease more rapidly

[9] *Phys. Rev.*, **31**, 503, 1928.

[10] Humphreys, *Physics of the Air*, New York, 1929. The observed density distribution referred to in the text is Table 74 in this book. The "observed" temperatures are those of p. 56, Fig. 18.

with elevation than would be indicated by the exponential law describing the decrease in lower layers. Integrating equation (5), Allen obtained

$$A(\nu) = B \log \left[1 + \frac{a\sigma^4}{(\nu - \nu_0)^2} \right], \tag{6}$$

where B and a are quantities depending on ground values of density, temperature, etc. The quantity B is also a function of σ. Allen determined his σ by fitting observed and computed curves of growth. He found $\sigma = 4.2 \times 10^{-8}$ cm, substituted it into equation (6), and integrated it over a Doppler profile with $T = 270°$ K. The profile thus obtained is analogous to our $c(\nu - \nu_0)$ profile. The corresponding intensities, $I(\nu) = e^{-c(\nu-\nu_0)}$, are entered in our figure as open circles. The quantity B in equation (6) was chosen so as to yield the best fit with the observed profile (continuous curve in Fig. 1). Some disagreement is apparent.

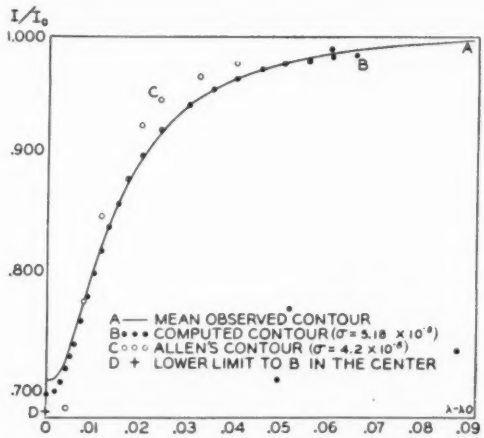

FIG. 1.—Profile of average line of α-band of atmospheric oxygen

It was clear from the comparison of results from spectrograms made with the 5-mm and the 10-mm separators that the width of the instrumental profile was probably not underestimated. Therefore, the discrepancy is not likely to be due to instrumental influences.

It is possible to obtain a fair agreement between equation (6) and the observations by using $\sigma = 5.2 \times 10^{-8}$ cm. Even so, the absorption coefficient in the center of the line comes out too high (too low intensities in Fig. 1).

Therefore, it was decided to integrate equation (5) numerically through the known portion of the atmosphere and to make use of the observed densities and temperatures,[10] instead of employing an exponential approximation. This numerical integration was carried out for several values of $\nu - \nu_0/\sigma^2$, and σ was determined in such a way as to yield the best agreement between observed and computed $A(\nu)$.

Again, the computed $A(\nu)$ goes to infinity at $\nu = \nu_0$. But now the computed $A(\nu)$ is no longer an analytic function but is given in tabular form. Hence numerical integration over the Doppler profile seems difficult.

As an approximation, the central value of $A(\nu)$ was assumed fairly high but finite. The $c(\nu)$ profile obtained from the approximate $A(\nu)$, by integration over the Doppler profile, was transformed into an intensity distribution by $I(\nu) = e^{-c(\nu)}$. The $I(\nu)$ are given as full dots in Figure 1. The center of the dotted curve, of course, does not cor-

respond to the true central intensity, since a finite value was used here in the $A(\nu)$ profile. The singularity in the actual $A(\nu)$ profile is extremely sharp—sharper, in fact, than that in Allen's formula (6). Hence, if we used the numerically integrated value of $A(\nu)$ outside of $(\nu - \nu_0) = 0.0025$ and Allen's formula within that region, the resultant $c(\nu)$ profile would inclose slightly too large an area.

The central intensity computed in this manner would therefore be a lower limit to the true central intensity. The plus sign (+) in Figure 1 was computed in this fashion. The true computed value of the central intensity should lie between the plus mark and the dotted curve. The singularity will, of course, affect the other part of the profile also, but to a smaller degree. Hence the fit may be regarded as satisfactory.

On comparing equations (4) and (5) it is seen that the total absorption coefficient a for a line of unit i and zero E may be found from the observed $A(\nu)$. The result is

TABLE 4

$\nu - \nu_0$ (In Cm^{-1})	Mean of First Five Lines of Table 3	Mean of Last Two Lines of Table 3	$\nu - \nu_0$ (In Cm^{-1})	Mean of First Five Lines of Table 3	Mean of Last Two Lines of Table 3
0.01	0.321	0.324	0.075	0.060	0.061
.02	.251	.251	0.100	0.036	0.035
0.04	0.145	0.143			

1.44×10^3 cm^{-1} sec^{-1}. Also, a may be found directly by integration of the $c(\nu)$ profile over all ν, assuming that the absorption coefficient varies as $1/(\nu - \nu_0)^2$ for $|\nu - \nu_0| > 0.15$ cm^{-1}. The result is 1.34×10^3 cm^{-1} sec^{-1}.

The total absorption coefficient for the whole band may be found by multiplying the above by $\Sigma i e^{-E/kT}$, summed over all branches of the band. The results are $a = 9.4$ and 8.7×10^4 cm^{-1} sec^{-1}, respectively, as compared to Allen's value 7.8×10^4 cm^{-1} sec^{-1}.

It has been taken for granted that all lines have similar profiles, both when the mean of the observed $c(\nu)$ was found and when equation (5) was computed. Actually, this is not quite correct. Because of the Boltzmann factor, lines of low excitation potential are less sensitive to temperature than lines of high excitation potential. The wings of lines originate in lower parts of the atmosphere than the centers. One would expect, therefore, that lines of low excitation potential would have steeper profiles than those of high E. In other words, the Boltzmann factors should cut down the central absorption coefficient of lines, the initial states of which have high energy.

Table 4 serves to show that, if such an effect should exist, it must be smaller than the errors of observation. The first column gives the means of the observed $c(\nu)$ of the first five lines (E = 3, 17, 43, 80, 129 cm^{-1}). In the second column means of the last two lines are tabulated (E = 261, 345 cm^{-1}). The difference between the columns is inappreciable.

I am glad to express here my sincere gratitude to Dr. C. D. Shane for instruction and advice during most of this investigation and to Dr. F. A. Jenkins for invaluable assistance in certain spectroscopic matters. Thanks are due also to Messrs. Nagtegaal and Salanave, students of the Astronomy Department at Berkeley, for help in some details.

THE VARIABLE PROPER MOTION OF THE STAR CINCINNATI 1244

DIRK REUYL
Leander McCormick Observatory
University of Virginia
Received December 23, 1942

ABSTRACT

Photographic observations of Cincinnati 1244 at the Leander McCormick Observatory indicate the presence of a second body. The material consists of 109 plates taken in the years 1915–1917, 1923–1925, 1930, 1935–1936, and 1939–1942. An analysis of the perturbations in right ascension and declination, with a period of 26.5 years, gives a value of 0.54 astronomical units for the semimajor axis of the orbit of Cin 1244 about the center of mass. The mass of the "dark" companion amounts to about 0.03 ⊙.

Cincinnati 1244 ($\alpha = 10^h14^m2$, $\delta = +20°22'$, 1900.0) is one of the relatively small number of dwarf M stars featuring emission lines. It is of apparent photovisual magnitude 9.5, of proper motion 0".49, and has a parallax of 0".20. The spectrum has been variously classified as M4e[1], M3+,[2] M4,[3] and M5.[4] Because of its proximity, the star has been included in a systematic study at the McCormick Observatory of the motions of all observable stars within a range of 10 parsecs. However, it was given special attention, along with the other dMe stars, upon Vyssotsky's noting the large proportion of close binaries among the Me dwarfs,[5] coincident with his finding emission lines in the spectrum of Ross 614. The latter constitutes the first star for which a companion was found through a photographic study of the proper motion.[6] It is noted that such investigations on near-by dwarf stars are likely to yield, if at all, companions of small mass, as is shown by the mass of less than 0.1 ⊙ for Ross 614B.[7] Hence they prove to be of considerable interest, even if the spectra do not exhibit emission features.

The preliminary investigation of Cin 1244 was completed early in 1941 and resulted in the finding of the variability of its motion.[8] Strongly supporting evidence for the star's duplicity was furnished by Swings and Struve,[9] who noted striking similarity in line emission in the otherwise different spectra of Cin 1244 and Castor C, the latter a well-known eclipsing binary.

The present discussion, including all the material up to date, shows that the additional observations have greatly increased the weight of the original material and have left the preliminary results essentially the same. The material consists of 109 plates, with a total of 204 exposures, taken with the 26-inch refractor between the years 1915 and 1942, as listed in Table 1. The plates were measured on a Gaertner machine in the usual direct and reversed positions and were reduced by the familiar method of dependences, a reference system of three stars having been used. The resulting solutions were then freed of the effects of parallax and proper motion through the subtraction of the quantities

$$P_{x,\,y}\pi + t\mu_{x,\,y} + c_{x,\,y}\,,$$

[1] Adams, Joy, Humason, and Brayton, *Ap. J.*, **81**, 187, 1935.
[2] Morgan, *Ap. J.*, **87**, 589, 1938.
[3] Kuiper, *Ap. J.*, **87**, 592, 1938.
[4] Kuiper, *Ap. J.*, **95**, 201, 1942.
[5] *Harvard Announcement Card*, No. 550, 1940.
[6] Reuyl, *A.J.*, **45**, 133, 1936.
[7] Reuyl, *Pub. A.A.S.*, **10**, 143, 1941.
[8] *Pub. A.A.S.*, **10**, 186, 1942.
[9] *Pub. A.S.P.*, **53**, 244, 1941.

in which c_x and c_y are arbitrary constants and $\pi = +0''.201$, $\mu_x = -0''.4863$, and $\mu_y = -0''.0242$, the value of the parallax having been obtained from three McCormick series of plates and the values of the motion derived from a comparison of the early and recent plates in the material. The resulting plate values were then combined into the yearly means X and Y, given in Table 1. The probable errors given are the quantities $\epsilon_{x,y}/\sqrt{p}$, where ϵ_x and ϵ_y are the probable errors for a plate of unit weight in X and Y, respectively,

TABLE 1

RESIDUAL DISPLACEMENTS IN RIGHT ASCENSION (X) AND DECLINATION (Y)

Epoch	Plates	X	X_c	ΔX	Y	Y_c	ΔY
1915.23	9	−0″.017±0″.013	+0″.008	−0″.025	−0″.015±0″.012	−0″.006	−0″.009
1916.14	11	+ .050 .012	+ .040	+ .010	− .017 .011	− .029	+ .012
1917.14	10	+ .056 .013	+ .056	.000	− .039 .012	− .040	+ .001
1923.22	6	+ .027 .016	+ .032	− .005	− .017 .015	− .019	+ .002
1924.11	8	+ .025 .013	+ .024	+ .001	− .012 .012	− .013	+ .001
1925.13	6	+ .019 .017	+ .013	+ .006	− .002 .016	− .004	+ .002
1930.07	1	− .064 .038	− .040	− .024	+ .021 .035	+ .034	− .013
1935.18	7	− .068 .014	− .078	+ .010	+ .081 .013	+ .061	+ .020
1936.13	4	− .066 .019	− .081	+ .015	+ .044 .018	+ .063	− .019
1939.26	5	− .068 .018	− .069	+ .001	+ .079 .017	+ .052	+ .027
1940.08	4	− .033 .019	− .050	+ .017	+ .087 .018	+ .037	+ .050
1941.20	13	+ .002 .011	− .012	+ .014	− .023 .010	+ .009	− .032
1942.11	25	−0.006±0.008	+0.026	−0.032	+0.015±0.007	−0.018	+0.033

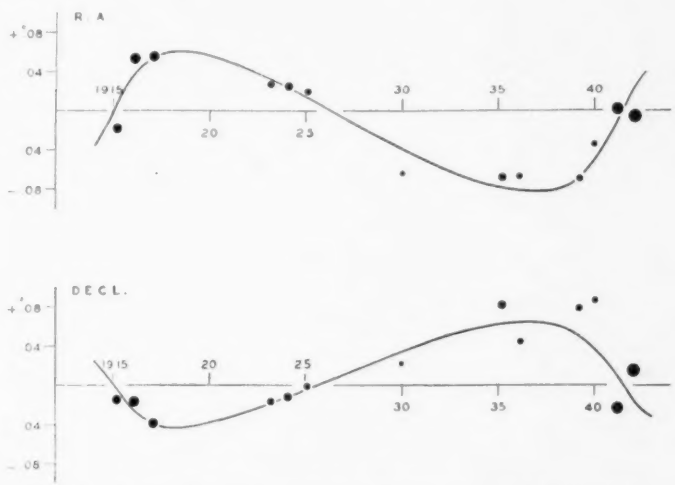

FIG. 1.—Residual displacements in right ascension and declination

and p is the weight of a normal point. The errors ϵ_x and ϵ_y were derived from all the differences between the plate values and their respective yearly means and were found to be $\pm 0''.038$ and $\pm 0''.035$ in X and Y, respectively. It is seen at once from the table, as also from Figure 1, that the residual quantities X and Y are not distributed at random with respect to time. The length of the period of the perturbation is obviously dependent upon the manner of derivation of the proper motion. It is easily ascertained, through different assumptions regarding the motion of the center of mass, that the true period may possi-

bly be longer than the present value—a value which, however, is the best approximation obtainable from the available material.

For the derivation of the elements of the orbit of Cin 1244 about the center of mass, the method used by Peters[10] in his classical discussion of the motion in right ascension of Sirius was followed. This method, applied also to the measures in declination in the present case, includes a partly graphical analysis by trial and error of the curves in X and Y. It is ideally suited to cases where the length of the period has not been definitely established, thus making a rigorous treatment unnecessary. The observed points are represented by the expressions

$$x,\ y = c_{x,\ y} + a_{x,\ y} \cos E + b_{x,\ y} \sin E\ ,$$

where E is the eccentric anomaly and a and b are functions of the orbital elements, with the exception of the period and the time of periastron passage, and are related closely to the familiar Thiele-Innes constants. In each co-ordinate a curve is drawn empirically to fit the observed points. From the curve are then read the values of the maximum and the minimum and their corresponding times, and also the times at which the curve crosses the zero line. From these readings the values for e and T and the quantities c, a, and b are easily derived. Small adjustments may be necessary, so that after successive approximations identical values of P, e, and T will be obtained for both X and Y, while simultaneously the fit between curve and observed points should remain as close as possible. In the present case the final curves, resulting from the third trial and considered entirely satisfactory for the purpose, are defined as follows:

$$P = 26\overset{y}{.}5,$$

$$e = 0.60,$$

$$T = 1915.0,$$

$$c_x = -0''.010, \qquad c_y = +0''.010,$$

$$a_x = +0''.010, \qquad a_y = -0''.010,$$

$$b_x = +0''.071, \qquad b_y = -0''.052,$$

For each epoch the computed points on the curves, X_c and Y_c, are given in Table 1, as also the differences ΔX and ΔY between the observed and computed values.

From the quantities a_x, b_x, a_y, and b_y, the remaining orbital elements may now be calculated. Of these, only the semimajor axis, a', is of interest, and it is found to be

$$a' = 0''.110 = 0.54 \text{ astronomical unit},$$

the value of the absolute parallax being $0''.204$.

In order to evaluate the mass of the companion, it is necessary to assume a value for the mass of Cin 1244. In view of the divergence of the spectral classifications, it appears advisable to use the empirical relation between the masses and photovisual absolute magnitudes of late M dwarfs. For a value of M_{pv}, equal to 11.0, we arrive at a mass of $0.35\ \odot$ for Cin 1244. With a period of 26.5 years, by Kepler's third law through successive approximations, we find for the semimajor axis of the orbit of the binary system:

$$a = 6.44 \text{ astronomical units},$$

[10] *A.N.*, **32**, 1, 1851.

and a mass ratio of

$$\frac{M_2}{M_1+M_2}=0.084\,,$$

and hence

$$M_2=0.032\odot\,.$$

The present discussion and the resulting value of the mass ratio have been based upon the assumptions that (1) the length of the period is about 26 years and (2) the companion does not contribute any appreciable light to the formation of the image.

Regarding the first assumption, it has been stated before that the length of the period may possibly have to be increased because of a change in the motion necessitated by further observations. With this larger period, however, the amplitude will be seen to increase also. Consequently, the relations between the masses, and hence the conclusion that the companion is of very small mass, will remain essentially unchanged. As to the possibility of a very much shorter period, this is not excluded but cannot be ascertained from the present material.

Concerning the possible blending of the images of the two stars, resulting in the measurement of the center of light, it would seem that, with a semimajor axis of 1".3, this would have shown as an elongation in some of the exposures. Under good conditions and for nearly equal components, a distance of 0".6 is easily observable on the McCormick photographs as an elongated image. A distance of 0".3 can still be detected, as was shown in the case of Wolf 424.[11] It is possible to assume different values for the magnitude difference and derive the corresponding distances between the position of the center of light and the brighter star. However, it is readily seen that the assumption of a difference of, say, $\Delta m = 0.5$ involves an increase in the total mass and therefore also in the value of a, thus making the detection of an elongation correspondingly easier.

Summarizing, it appears to be unlikely that the companion contributes to the formation of the photographic image of Cin 1244. From the material available at the present time, and assuming a value of 0.35 $\odot$ for the mass of Cin 1244, it is concluded that the "dark" companion has a mass of 0.03 $\odot$.

I wish to express my sincere appreciation to Professor Henry Norris Russell for his interest shown in the preliminary discussion.

[11] Reuyl, *Pub. A.S.P.*, **53**, 336, 1941; **54**, 52, 1942.

RESOLUTION OF THE TELLURIC BANDS ω_1 AND ω_2

ARTHUR ADEL[1]
Lowell Observatory
Received December 24, 1942

ABSTRACT

The carbon dioxide bands ω_1 and ω_2, which appear in the solar spectrum at 20,061 A and 20,568 A, respectively, have been resolved into their rotational structures.

When the solar spectrum is examined with low dispersion, as, for example, with a small glass prism, there appear at 2.01 μ and 2.05 μ the two small absorptions ω_1 and ω_2. These belong to the carbon dioxide system of bands, and they are, in fact, two members of the group of three bands which arise in transition from the ground state to the levels[2]

$$\nu_3 + \begin{bmatrix} 4\nu_2 \\ 2\nu_2 + \nu_1 \\ 2\nu_1 \end{bmatrix}.$$

The third member of this set of bands, which we may call ω_0, has, like the two others, been observed in the laboratory.[3] Unlike the other two, however, ω_0 does not appear in the usual solar spectrum, since it falls into the broad region of absorption occupied by the strong water-vapor band Ω (1.9 μ). Prismatic solar spectra recorded on the driest days at the observatory clearly indicate the presence of ω_0.

Although ω_1 and ω_2 appear as single notches in the low-dispersion solar spectrum, each is, in reality, composed of numerous lines due to transitions between the rotational levels of the molecule. Alternate lines are completely forbidden by the selection rules, and the resolution of the bands is thereby greatly facilitated.[4] The actual spacing of the band lines is thus about 1.5 cm^{-1}, or about 6 A at 20,000 A.

A grating ruled with 600 lines per millimeter was generously loaned by the Mount Wilson Observatory, and the resolution of the bands ω_1 and ω_2 was achieved early in January, 1942. An original recorded observation of ω_1 is reproduced in Figure 1, while simpler envelope tracings of such originals of both ω_1 and ω_2 appear in Figures 2 and 3. Intensity of the solar spectrum is plotted downward. The well-known doublet structures of the bands are apparent.

The grating, particularly suitable for the experiment because of its strong fourth-order green spectrum, was calibrated by observation of the A band of oxygen, and the spectrometer constant was found to be 32,346.4 A. The wave lengths of the band lines and band centers were accordingly given by the formula

$$\lambda = 32{,}346.4 \sin \vartheta ,$$

where ϑ is the angle between the normal to the grating and the bisector of the angle formed by the incident and diffracted beams. The angle ϑ is indicated by the abscissa in Figures 1, 2, and 3.

[1] At present on leave in the department of physics, University of Michigan.

[2] A. Adel and C. O. Lampland, *Ap. J.*, **87**, 198, 1938.

[3] E. F. Barker and Ta-You Wu, *Phys. Rev.*, **45**, 1, 1934.

[4] D. M. Dennison, *Rev. Mod. Phys.*, **12**, 175, 1940.

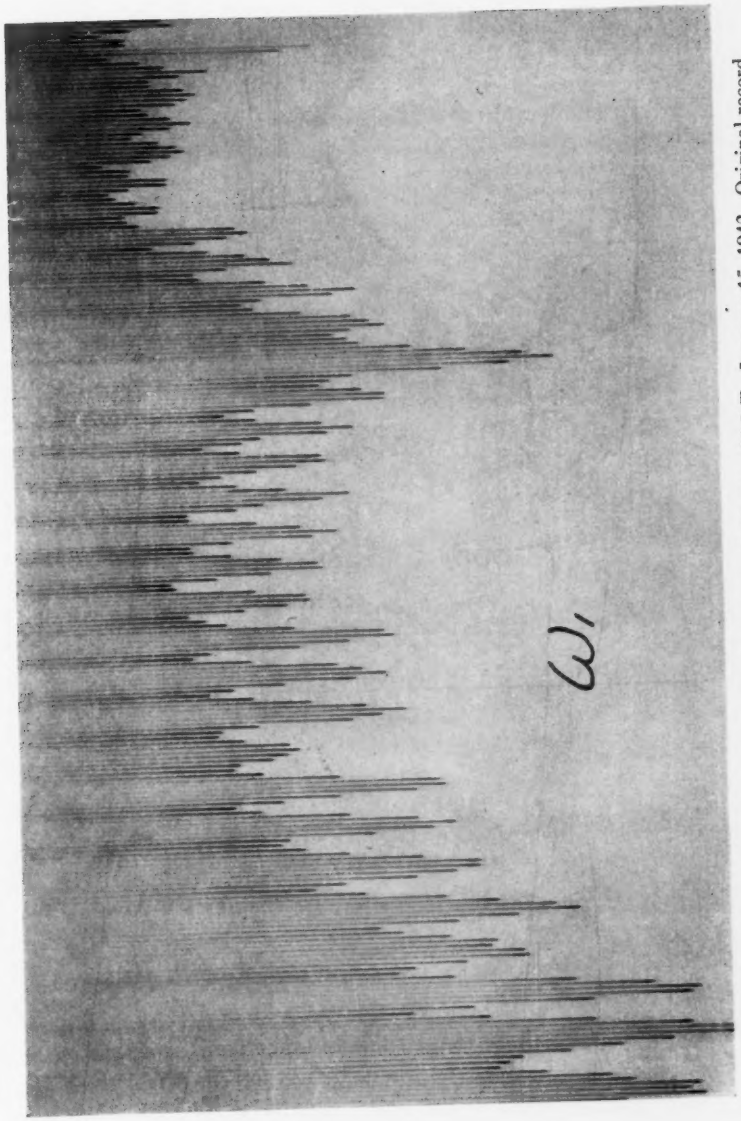

FIG. 1.—ω_1 in the solar spectrum, Flagstaff, Arizona, 1:20 P.M., M.S.T., January 15, 1942. Original record

The observed wave lengths of the lines and band centers in ω_1 and ω_2 are given in Tables 1 and 2, respectively. It may readily be shown that the line positions are well correlated by the formulae

$$\omega_1 : \tilde{\nu} = (4984.9 \pm 0.745\, N - 0.0045\, N^2)\ \text{cm}^{-1},$$

$$\omega_2 : \tilde{\nu} = (4861.8 \pm 0.782\, N - 0.0021\, N^2)\ \text{cm}^{-1},$$

where N, the ordinal number of the line, takes the values 2, 4, 6, 8, 10, ... , for the negative branch and the values 1, 3, 5, 7, 9, 11, ... , for the positive branch.[5]

The adequacy of these formulae to represent the bands may best be judged from the comparison, provided in Tables 1 and 2, of the observed wave lengths with those com-

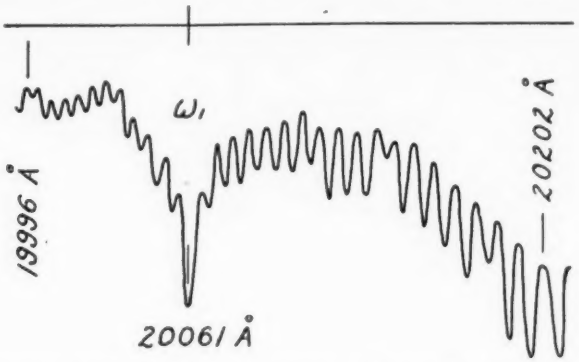

FIG. 2.—ω_1 in the solar spectrum, Flagstaff, Arizona, 1:20 P.M., M.S.T., January 15, 1942. Trace made from original.

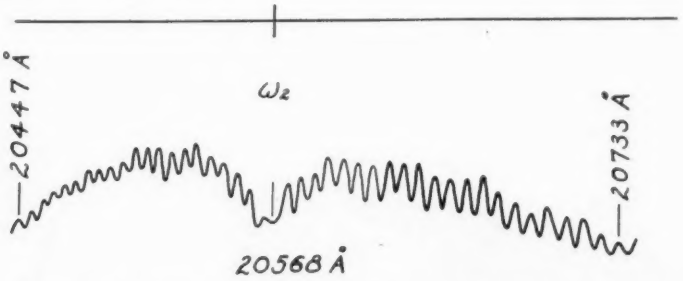

FIG. 3.—ω_2 in the solar spectrum, Flagstaff, Arizona, 10:17 A.M., M.S.T., January 15, 1942. Trace made from original.

puted from the formulae. The lines in the positive branch of ω_1 are seriously affected by additional atmospheric absorptions. In consequence, neither their observed nor their computed positions are given at this time.[6]

From the data presented in this paper one may deduce the average temperature of the

[5] A given value of N for the negative branch is also the value of the corresponding rotational quantum number of the ground level involved in the transition, while N for the positive branch is synonymous with the rotational quantum number of the upper or excited level.

[6] There has also been omitted a listing and discussion of a number of lines of ω_0 mapped during the course of the experiment, because the principal features of ω_0 in the solar spectrum are largely obscured by the overlying heavy absorption by water vapor. The mapping of the lines in ω_0 and those in the positive branch of ω_1 will eventually be completed in the laboratory. A discussion of the formulae of line positions may be postponed with profit until such time.

carbon dioxide mass above Flagstaff on the day of the observations.[7] The measurements for Figures 2 and 3 were taken near noon on January 15, 1942. It appears that the average temperature of the carbon dioxide was at that time in the neighborhood of −18° C.

TABLE 1

THE BAND AT 20,060.6 A, ω_1

Negative Branch							
N	λ(A) Obs.	$\bar{\nu}$(cm^{-1}) Obs.	$\bar{\nu}$(cm^{-1}) Comp.	N	λ(A) Obs.	$\bar{\nu}$(cm^{-1}) Obs.	$\bar{\nu}$(cm^{-1}) Comp.
2	20066.7	4983.4	4983.4	22	20136.6	4966.1	4966.3
4	20071.9	4982.1	4981.8	24	20142.8	4964.6	4964.4
6	20078.7	4980.4	4980.2	26	20150.8	4962.6	4962.5
8	20084.9	4978.9	4978.6	28	20158.3	4960.7	4960.5
10	20092.0	4977.1	4977.0	30	20167.0	4958.6	4958.5
12	20099.1	4975.4	4975.4	32	20175.4	4956.5	4956.5
14	20106.5	4973.5	4973.6	34	20183.8	4954.5	4954.4
16	20112.7	4972.0	4971.8	36	20192.2	4952.4	4952.3
18	20120.8	4970.0	4970.0	38	20201.9	4950.0	4950.1
20	20128.2	4968.2	4968.2	40	20211.7	4947.6	4947.9

TABLE 2

THE BAND AT 20,568.4 A, ω_2

Positive Branch				Negative Branch			
N	λ(A) Obs.	$\bar{\nu}$(cm^{-1}) Obs.	$\bar{\nu}$(cm^{-1}) Comp.	N	λ(A) Obs.	$\bar{\nu}$(cm^{-1}) Obs.	$\bar{\nu}$(cm^{-1}) Comp.
1	20564.9	4862.7	4862.6	2	20575.2	4860.2	4860.2
3	20557.8	4864.3	4864.1	4	20581.7	4858.7	4858.7
5	20552.3	4865.6	4865.6	6	20588.8	4857.0	4857.0
7	20545.8	4867.2	4867.2	8	20594.3	4855.7	4855.4
9	20539.0	4868.8	4868.6	10	20602.7	4853.7	4853.8
11	20532.5	4870.3	4870.1	12	20609.2	4852.2	4852.1
13	20527.7	4871.5	4871.6	14	20616.3	4850.5	4850.5
15	20520.9	4873.1	4873.0	16	20624.4	4848.6	4848.8
17	20514.7	4874.6	4874.5	18	20631.5	4847.0	4847.0
19	20509.6	4875.8	4875.9	20	20638.3	4845.2	4845.3
21	20503.7	4877.2	4877.3	22	20646.1	4843.5	4843.6
23	20497.6	4878.6	4878.7	24	20653.2	4841.9	4841.8
25	20491.1	4880.2	4880.1	26	20660.9	4840.1	4840.1
27	20485.9	4881.4	4881.4	28	20668.7	4838.2	4838.3
29	20481.1	4882.6	4882.7	30	20675.2	4836.7	4836.5
31	20474.9	4884.0	4884.0	32	20683.9	4834.7	4834.6
33	20469.8	4885.2	4885.3	34	20691.3	4832.9	4832.8
35	20464.3	4886.6	4886.6	36	20699.1	4831.1	4830.9
37	20459.7	4887.7	4887.8	38	20708.8	4828.9	4829.1
39	20453.0	4889.3	4889.1	40	20715.9	4827.2	4827.2
41	20446.8	4890.7	4890.4	42	20724.3	4825.3	4825.3
				44	20733.0	4823.2	4823.3

The courtesy of the Mount Wilson Observatory in providing the Lowell Observatory with a grating for this work is gratefully acknowledged.

[7] See, e.g., the author's note on the temperature of Venus, *Ap. J.*, **86**, 337, 1937.

SPECTROGRAPHIC OBSERVATIONS OF PECULIAR STARS. V*

P. SWINGS AND O. STRUVE
McDonald and Yerkes Observatories
Received December 28, 1942

ABSTRACT

I. Z Andromedae displayed strong [*Fe* VII] lines in July and November, 1942. A table is given, describing the spectrum of this star in three successive years. Attention is called to several bright lines recently found in CI Cygni. A description is given of the line emission in RS Ophiuchi; this became quite conspicuous in 1942. On July 19, 1942, the red coronal line was found in RS Oph; the green coronal line was absent at that time. New data on the emission lines of *Fe* I, *Fe* II, [*Fe* II], [*Fe* III], and [*Fe* V] in peculiar stars are provided.

II. Four stars with absorption shells are described in detail: HD 195407 = MWC 346 has strong shell lines of *H*, *He* I 3965, and *He* I triplets (2^3P^0—n^3D). HD 172694 = MWC 303 shows only a strong and sharp shell line of *He* I 3889, while the other observable *He* I lines are broad. HD 155851 = MWC 253 shows a somewhat weaker shell line of *He* I 3889. HD 187399 = MWC 321 shows a set of strong sharp Balmer lines displaced to the violet of the centers of the broad *H* wings. All four stars belong to the main sequence.

III. This section contains descriptions of the spectra of 83 Be stars from the catalogue of Merrill and Burwell. The bright lines of several stars have changed since Merrill's last published descriptions. Attention is called especially to MWC 23, which has a strong shell spectrum of *H*, and to MWC 342, which has strong emission lines of *H*, *Fe* II, [*Fe* II], and shows structure in the lines of *H*.

IV. The fluorescence and recombination mechanisms of line emission in shells are related to the general characteristics of the shell spectra. Emphasis is placed on the effects of ejection, axial rotation, and turbulence. The spectacular "nitrogen flaring stages" of novae are discussed, and the associated spectroscopic phenomena are interpreted.

I. NEW OBSERVATIONAL DATA ON PECULIAR BRIGHT-LINE STARS

Z ANDROMEDAE

Our observations of Z And in July and November, 1942, show strong forbidden lines of [*Fe* VII] in the nebular part of the spectrum. This is the first time in the history of Z And that such an observation of [*Fe* VII] is recorded; it renders the analogy of Z And and AX Persei still more striking, since both stars combine a late-type spectrum and a nebulosity of variable excitation, reaching sometimes the [*Fe* VII] state. Forbidden [*Fe* V] is also present in Z And, although it is less conspicuous than [*Fe* VII]. On our recent spectrograms there are hardly any absorption lines, except for the late-type features in the visual region. Compared with the previously observed stages, the high-excitation lines have gained in intensity relative to the neutral or singly ionized metals. But Z And has not quite reached the stage of high [*Fe* VII] intensity displayed by CI Cygni and sometimes by AX Persei. Plate XX shows the ultraviolet spectrum of Z And on August 6, 1941, and on July 15, 1942.

In our last report on Z And[1] we mentioned that from August, 1941, to January, 1942, the [*Ne* V] lines had increased considerably in intensity, so that the January, 1942, appearance—six months after the minor outburst of 1941—was similar to the appearance in August, 1940, approximately nine months after the major outburst of 1939. The evolution toward high excitation has thus continued from January to July, 1942. Our spectrogram of November 23 reveals a slightly lower excitation than in July, 1942; it is probable that a peak in excitation was reached during the summer of 1942.

Since Z And is a remarkable representative of a variable peculiar spectrum, combining bright lines of low and high excitation, it is useful to compile the lines observed at several

* *Contributions from the McDonald Observatory, University of Texas*, No. 64.

[1] *Ap. J.*, **96**, 257, 1942.

typical stages (Table 1). Such a compilation will be of value in future discussions of peculiar stars. The spectrum of the summer of 1939 was excluded because of its character of a slow nova in the early stages.

It is our plan to prepare compilations similar to Table 1 for a few typical representatives of peculiar stars, covering excitations higher (AX Per, CI Cyg, etc.) or lower (T C Br, RS Oph, etc.) than Z And or revealing certain forbidden lines more conspicuously (e.g., [*Fe* II] and [*Fe* III] have always been rather weak in Z And).

Among a number of more or less striking changes, Table 1 shows strong variations in the relative intensities of the triplets and singlets of *He* I (e.g., 4471/4388, 4026/4009, 4026/4144). This means that the relative contributions of the recombination and fluorescence mechanisms have varied in the course of the evolution of Z And.

CI CYGNI

The spectrograms obtained in July, 1942, cover the region from λ 3100 to *Hα* (Pl. XXI). On the short wave-length end (λ < 3500 A), the spectrum is similar to that of the high-excitation nebula IC 2165,[2] but a few additional faint lines appear in CI Cygni. Because of the importance of the few, still unidentified emissions in such stars as AX Per or CI Cyg (especially in relation to additional identifications of the still incompletely known spectra of [*Fe* IV, V, VI, VII] and other metals and also in relation to the novae), attention is called here to the following lines of CI Cygni: λλ 3382.0 (int. 1–2), 3428.5 (int. 3), 3386.5 (int. 0–1), 3411.9 (int. 1–2), 3736.7 (int. 3), 3754.8 (int. 4), and 3910.0 (int. 1). Other features concerning *Fe* I and *Fe* II will be discussed in another section.

a) λλ *3382.0 (int. 1–2) and* λ *3428.5 (int. 3).*—These lines coincide with two predicted [*Fe* II] transitions of the a^4F-b^2F multiplet: $3\frac{1}{2}-3\frac{1}{2}$, λ_{pred} 3381.9, and $2\frac{1}{2}-3\frac{1}{2}$, λ_{pred} 3429.2 (exc. pot. $a^4F_{3\frac{1}{2}}$: 0.30 v.; $a^4F_{2\frac{1}{2}}$: 0.35 v.; $b^2F_{3\frac{1}{2}}$: 3.95 v.). In the line λ 3382.0, *Cr* II can be only a very minor contributor. In λ 3428.5 the predicted $^5D_1-{}^7S_3$ transition of [*Fe* III] (λ_{pred} 3428.8) cannot contribute appreciably, since it is absent in the star BF Cygni, in which [*Fe* III] is very strong. The forbidden transition $^5D_4-{}^3G_5$ of [*Fe* V] is predicted at λ 3430.3; but the observed line cannot be due to [*Fe* V], since it is stronger in CI Cyg than in AX Per, contrary to the well-identified [*Fe* V] lines at λλ 3895.4, 3891.4, and 3839.3. The usual [*Fe* II] lines are fairly strong in the blue-violet region; hence, the identification of the new a^4F-b^2F multiplet appears plausible. In high-excitation objects λ 3428.5 requires a fairly high resolving-power in order to be clearly separated from the usually strong [*Ne* V] line 3425.8. The fact that the two new hypothetical [*Fe* II] lines were not observed in the course of our previous work on the ultraviolet spectrum of the two [*Fe* II] stars, WY Geminorum and B 1985,[3] may be due to instrumental conditions. It is our plan to reinvestigate the spectra of these two stars in the region λλ 3382–3428. Pending their confirmation, these [*Fe* II] identifications should be considered as provisional.

b) λ *3386.5 (int. 1) and* λ *3376 (int. 0–1).*—The forbidden [*Fe* II] line $a^4F_{4\frac{1}{2}}-b^4D_{2\frac{1}{2}}$ is predicted at λ 3387.1; but, according to our observations in WY Gem and B 1985, we should then expect the $4\frac{1}{2}-3\frac{1}{2}$ transition at λ 3376.2 to be stronger,[3] whereas the present stellar line, λ 3376, is weaker than λ 3387. The higher intensity of λ 3387 may be due to a blend with two permitted *Fe* II lines: λ 3386.45 (lab. int. 1) and λ 3386.72 (lab. int. 2). The first *Fe* II line is classified and corresponds to fairly high levels (3.93–7.57 v.), hence, its influence should be minor; the second *Fe* II line is not classified. The attribution of λ 3386.5 and λ 3376 to [*Fe* II] should also remain provisional for the time being.

c) λ *3411.9 (int. 1–2).*—This line is also observed in AX Per, where it reaches about the same intensity as λ 3428.5, whereas it is much weaker than λ 3428.5 in CI Cygni. The contribution of *O* IV 3411.76 (lab. int. 4) is certainly unimportant. The line should be considered as entirely unidentified.

[2] Reproduced in *ibid.*, p. 310 (Pl. XXI).

[3] *Ibid.*, **91**, 546, 1940; **93**, 455, 1941.

TABLE 1

SPECTRUM OF Z ANDROMEDAE

AUGUST 1940	JULY–AUGUST 1941	JULY 1942	IDENTIFICATION		
			Elem.	λ	Int.
3121.5(1E)		21.7(2E)	*O* III	3121.71	5
3132.7(6E)		32.9(7E)	*O* III	3132.86	6
3202.9(6E)		03.1(6E)	*He* II	3203.16	100
3277.0(1E)		77.3(1E)	*Fe* II	3277.35	9
3281.1(1E)		81.3(1E)	*Fe* II	3281.29	7
3312.3(4E)		12.3(2E)	*O* III	3312.30	5
3323.6(1E)		23.1(1E)	*Fe* II	3323.07	8
3340.5(5E)		40.7(5E)	*O* III	3340.74	6
3345.8(4E)		45.8(5E)	[*Ne* V]	3345.8	.....
	3420.83(0E)		*Cr* II	3421.20	75
	3422.71(1E)		*Cr* II	3422.74	125
3425.85(6E)	26.05(1–0E)	25.74(10E)	[*Ne* V]	3425.8	.....
3443.60(6E)	43.45(4E)	43.72(8E)	*O* III	3444.10	5
3455.27(0E)			*O* III	3455.12	5
	3554(0A)		*He* I	3554.39	7
		3586.30(3E)	[*Fe* VII]	3586.3	.....
	3587(1A)		*He* I	3587.25	10
			He I	3587.40	2
	3633.45(3A)		*He* I	3634.24	15
			He I	3634.37	2
3662.08(1A)			H_{30}	3662.26	.....
3663.03(1A)			H_{29}	3663.40	.....
3664.25(1A) 3664.92(0E)	64.37(0–1E)		H_{28}	3664.68	.....
3665.70(1A) 3666.53(0E)	65.86(1E)	66.01(0E)	H_{27}	3666.10	.....
3667.47(1A) 3668.26(0E)	67.59(2E)	67.65(1–0E)	H_{26}	3667.68	.....
3669.12(1A) 3669.94(1E)	69.40(2E)	69.68(1E)	H_{25}	3669.47	.....
3671.21(1+A) 3672.00(1E)	71.39(3E)	71.44(1E)	H_{24}	3671.48	.....
3673.24(1+A) 3674.42(1E)	73.90(3–4E)	73.55(1E)	H_{23}	73.76	.....
3676.07(2A) 3676.94(1E)	76.38(3–4E)	76.59(1E)	H_{22}	76.36	.....
			Cr II	3677.69	40
	3677.34(2E)		*Cr* II	3677.86	50
			Cr II	3677.93	30
3679.10(2A) 3679.75(1E)	79.42(4E)	79.54(2E)	H_{21}	3679.35	.....
	3681.02(1E)		.....	.....	.....
3682.37(2A) 3683.27(1E)	82.66(4E)	82.65(2–3E)	H_{20}	3682.81	.....
	3684.71(1E)	85.06(0–1E)	*Cr* II	3684.25	25
			Ti II	3685.19	700
3686.19(1+A) 3687.35(1E)	86.93(4E)	86.86(3E)	H_{19}	3686.86	.....
3689.24(1+A) 3690.37(0E)			.....	.....	.....
3691.30(1+A) 3692.21(1+E)	91.57(4E)	91.52(4E)	H_{18}	3691.56	2

TABLE 1—*Continued*

August 1940	July–August 1941	July 1942	Identification		
			Elem.	λ	Int.
3696.88(1+A)					
3697.79(1E)	97.18(5E)	96.98(4E)	H_{17}	3697.15	3
	3700.01(0E)		*V* II	3700.34	200
	3703.42(5E)	.....	H_{16}	3703.85	(4)
3704.18(1+A)					
3705.62(1+Enn)		3704.57(5En)	H_{16}		
	3705.55(4En)		*He* I	3705.00	30
			He I	3705.14	3
			(*Fe* I	3705.57	700)
			(*Ti* II	3706.23	125)
			(*Ca* II	3706.03	40)
3711.56(1+A)					
3712.72(2E)		12.21(5E)	H_{15}	3711.98	5
	3712.21(5En)	.....	H_{15}+		
			Cr II	3712.97	35
			Cr II	3713.04	15
	3714.73(1E)	15.46(1–0E)	*Cr* II	3715.19	20
			Cr II	3715.45	20
			V II	3715.48	1200
			O III	3715.08	6
3718.76(0A)					
3719.91(0E)	19.83(0E)	20.24(1E)	*Fe* I	3719.93	1000R
3721.40(1+A)					
3722.53(2E)	22.05(5E)	21.78(6E)	H_{14}	3721.95	6
	3724.04(0E)		*Cr* II	3723.40	15
	3726.88(1E)	26.88(0EN)	[*O* II]	26.12	.....
			Cr II	27.37	40
			Fe II	27.04	4
			V II	27.35	1000
	3728.55(0–1E)		[*O* II]	28.91	.....
3733.43(1A)					
3734.94(2E)	34.51(6E)	34.42(6E)	H_{13}	3734.37	8
3737.10(1E)	37.03(2E)	36.60(2E)	*Cr* II	3737.55	10
			Fe I	3737.13	1000
			Ca II	3736.90	50
	3739.19(0–1E)		(*Cr* II	38.38	25)
3741.39(0E)	41.58(2E)		*Ti* II	3741.65	200
	3745.71(2–3E)	45.45(1E)	*V* II	3745.81	800
			Fe I	3745.56	500
3748.34(1E)	48.00(2E)	47.99(1E)	*Fe* II	48.49	8
			Fe I	48.26	500
			(*Cr* II	48.68	7)
3749.57(1+A)					
3750.86(2E)	50.30(6E)	50.18(6E)	H_{12}	3750.15	10
3755.00(2E)	54.60(2E)	54.46(3E)	*Cr* II	3754.57	20
			(*O* III	3754.67	7)
			(*Fe* II	3755.56	4)
			(*N* III	3754.62	6)
			[*Fe* V]	3754.8	.....
3757.81(1E)	57.48(1E)		*Ti* II	3757.69	100
			Fe I	3758.23	700
			O III	3757.21	5
3760.08(2En)	3759.23(2E)		*Fe* II	3759.46	6
			O III	3759.87	9
			Ti II	3759.30	400

TABLE 1—*Continued*

August 1940	July–August 1941	July 1942	Identification		
			Elem.	λ	Int.
		3759.29(10E)	[*Fe* VII]	3759.9	.....
			O III	3759.87	9
	3760.83(1E)		*Ti* II	3761.32	300
3762.35(0E)			*Fe* II	3762.89	5
			Ti II	3761.32	300
			O II	3762.51	120
	3764.22(1–0E)		*Fe* I	3763.79	500
			Fe II	3764.09	m
	3766.74(0E)		*Fe* I	3767.19	500
			(*Cr* II	3766.65	4)
{3770.52(1A)		}			
{3771.25(2E)	70.73(7E)	70.63(7E) }	H_{11}	3770.63	15
		3773.40(1E)*	.....	.....	.....
	3783.14(2E)	83.19(1E)	*Fe* II	3783.35	4
			([*Fe* V]	3784.2	.....)
3795.27(1E)	95.47(1E)		*Fe* I	3795.00	500
{3797.30(1A)		}			
{3798.69(3E)	97.96(7E)	98.01(8E) }	H_{10}	3797.90	20
	3806.26(0–1En)	05.66(0E)	*Fe* I	3805.34	400
			He I	3805.76	3
			(*Si* III	3806.56	5)
	3813.73(2En)	13.97(1En)	*Fe* II	3814.12	4
			Cr II	3814.00	12
			Fe I	3812.96	400
			Ti II	3813.39	20
			Ti II	3814.58	35
		}	*He* I	3819.61	50
{3819.35(1A)	18.66(3A)	19.89(2E) }	*Fe* I	3820.43	800
{3819.93(2E)	20.12(3E)	}	([*Fe* V]	3820.	....)
3824.47(0E)	24.88(1E)	24.72(1E)	*Fe* II	3824.91	4
	3827.11(0E)		*Fe* II	3827.08	4
	3829.60(1–0E)		*Mg* I	3829.35	100
	3832.90(1E)†	33.12(1E)‡	*Mg* I	3832.31	250
			Fe II	3832.96	2
{3834.48(1A)					
{3835.63(3E)	35.55(6E)	35.43(8E)	H_9	3835.39	40
	3838.24(1–2E)		*Mg* I	3838.26	300
	3845.23(1E)		.....	.....	.....
3847.06(1E)			.....	.....	.....
	3848.39(1E)	48.03(2–1E)	*Mg* II	3848.24	10
	3849.80(1–2E)	50.61(1E)	*Mg* II	3850.40	5
			Fe I	3849.97	500
3853.94(1E)			*Si* II	3853.67	3
{	3854.84(1A)	}			
{3855.92(3E)	56.12(4E)	56.12(3E) }	*Si* II	3856.03	8
	3859.73(1E)		*Fe* I	3859.91	1000
{	3861.23(1A)	}			
{3862.60(2E)	62.40(4E)	62.30(2E) }	*Si* II	3862.59	6
	3865.45(1E)		*Cr* II	3865.59	75
3868.75(7E)	68.64(4E)	68.71(10E)	[*Ne* III]	3868.7	.....
	3872.35(1E)		*He* I	3871.82	5
			Fe II	3872.76	pred.
	3878.71(2E)		*V* II	3878.71	300
			Fe I	3878.57	300
{3880.69(0A)		}			
{3882.22(0E)		}	*O* II	3882.19	35

* Also present in BF Cygni. † Mainly *Mg* I. ‡ Mainly *Fe* II.

TABLE 1—*Continued*

August 1940	July–August 1941	July 1942	Identification		
			Elem.	λ	Int.
{3887.84(5A)	87.76(2A)	}	H_8	3889.05	60
{3889.28(5E)	89.03(9E)	89.05(10E) }	*He* I	3888.65	1000
		3891.52(1–2E)	[*Fe* V]	3891.4	.....
		3895.20(1E)	[*Fe* V]	3895.4	.....
	3895.83(1E)		*Fe* I	3895.66	400
3899.58(1E)			*Fe* I	3899.71	500
	3900.12(2E)		*Ti* II	3900.54	50
			Al II	3900.68	200
3902.91(1E)	03.19(1E)		*Fe* I	3902.95	500
			V II	3903.26	250
3905.62(1E)	05.57(2E)		*Si* I	3905.53	15
			Cr II	3905.64	25
			Fe II	3906.04	5
3914.19(1En)	13.84(2–3E)	14.04(2E)	*Fe* II	3914.48	2
			Ti II	3913.46	70
3919.22(1En)			*C* II	3918.98	80
			C II	3920.68	200
			N II	3919.00	35
			O II	3919.28	35
3923.24(1E)			*Fe* I	3922.91	600
			He II	3923.51	.....
3926.55(1E)	26.57(1–2E)		*He* I	3926.53	7
3930.47(1E)	30.31(2–3E)	30.65(0E)	*Fe* I	3930.31	600
	3933.78(3E)		*Ca* II	3933.67	600
3934.95(1E)		34.69(1–2E)	*Ca* II	3933.67	600
			He I	3935.91	4
			Fe II	3935.94	6
			(*N* III	3934.41	3)
3938.39(1+E)	38.31(3–4E)	38.42(3E)	*Fe* II	3938.29	2
	3943.38(1–0E)		(*Al* I	3944.03	2000)
3945.35(1E)	45.15(2E)	44.79(1E)	*O* II	3945.04	20
			Fe II	3945.21	pred.
			(*Cr* II	3945.11	1)
	3951.50(0En)		*V* II	3951.97	500
			(*Fe* I	3951.17	150)
3961.77(1+E)	61.00(1En)	61.56(2E)	*Fe* II	3960.89	3
			Al I	3961.53	3000
			O III	3961.59	8
3964.84(2E)	65.01(4E)	64.83(4E)	*He* I	3964.73	50
3967.33(2E)	67.89(2E)	67.28(3E)	[*Ne* III]	3967.5	.....
			Ca II	3968.47	500
3970.34(4E)	70.32(8E)	70.12(10E)	$H\epsilon$	3970.08	80
3973.83(1E)	73.78(1–2E)	73.84(4E)	*Fe* II	3974.16	3
			V II	3973.64	300
			O II	3973.27	125
	3978.32(1–0E)		(*Fe* I	3977.75	300)
	3981.89(1–0E)	82.43(1E)	(*Fe* I	3981.77	150)
			Fe II	3981.61	pred.
			[*Fe* II]	3981.5	.....
	3987.20(1–0E)		.....	.....	.....
	3991.56(0–1E)		(*Si* II	3991.77	2n)
		3995.50(0E)	*N* II	3994.99	300
	3997.87(0–1E)		(*Si* II	3998.00	1n)
			Fe I	3998.05	150
	4002.35(1E)		*Fe* II	4002.55	3
		4003.37(1E)	*Cr* II	4003.33	25
	4005.36(0–1E)		*V* II	4005.71	800

TABLE 1—*Continued*

August 1940	July–August 1941	July 1942	Identification		
			Elem.	λ	Int.
4009.24(1E)	09.58(2E)	09.37(4E)	*He* I	4009.27	10
	4012.60(1–2E)		*Cr* II	4012.50	30
			(*Fe* II	4012.47	1)
{4013.95(2A)					
{4014.85(1E)			.....	.....	.....
	4015.51(1E)		*Ni* II	4015.48	1
{4016.62(1+A)					
{4017.56(0E)			.....	.....	.....
{4025.56(2A)	25.61(2A)				
{4026.43(2E)	26.65(5E)	26.86(4E)	*He* I	4026.19	70
	4054.02(1E)	53.61(1Enn)§	*Cr* II	4049.16	18
			Cr II	4051.97	12
			Cr II	4054.18	8
			Fe II	4057.46	2
	4063.80(0E)		*Cr* II	4064.14	1
			Fe I	4063.60	400
	4066.97(1E)		*Ni* II	4067.05	30
		4067.71(2E)	[*S* II]	4068.62	.....
			(*Fe* I	4067.98	150)
			(*Ni* II	4067.05	30)
4070.30(2En)	69.28(0E)		(*S* II]	4068.62	.....
			C III	4068.94	10
			C III	4070.30	8
			O II	4069.90	125
	4071.56(1E)		*O* II	4072.16	300
			Fe I	4071.74	300
			(*Cr* II	4070.90	10)
		4072.00(2E)	[*Fe* V]	4071.4	.....
			O II	4072.16	300
			Fe I	4071.74	300
{4073.89(2A)	.....	.....	*O* II	4075.87	800
			[*S* II]	4076.22	.....
{4075.82(2E)	75.87(2E)	76.07(2E)	(*Si* II	4075.45	2)
			(*Cr* II	4075.97	4)
		4089.30(1En)	*Cr* II	4089.49	2
			Cr II	4088.90	1
4097.35(4E)	97.40(4E)	97.29(4E)	*N* III	4097.31	10
4101.97(6E)	02.20(10E)	01.93(12E)	*Hδ*	4101.75	100
4103.54(2E)		03.40(4E)	*N* III	4103.37	9
		4112.92(0E)	*Cr* II	4113.24	5
4121.31(1E)	21.16(1–2E)	20.94(1E)	*He* I	4120.81	25
4123.65(0E)	22.46(1–2E)		*Fe* II	4122.64	4
	4124.88(0E)		*Fe* II	4124.79	1
	4128.15(1–2E)		*Si* II	4128.05	20
			Fe II	4128.73	3
	4131.19(1E)		*Si* II	4130.88	25
4144.25(1En)	43.71(3E)	43.75(4–5E)	*He* I	4143.76	15
	4161.27(0–1E)		*Ti* II	4161.54	30
4162.35(1E)			*C* III	4162.80	4
	4163.71(2E)		*Ti* II	4163.65	150
	4166.11(1–0E)				
	4169.00(1–0E)		*He* I	4168.97	7
	4171.51(1–0E)		*Ti* II	4171.90	70
4173.12(2En)	73.68(2–3E)	73.40(2–3E)	*Fe* II	4173.45	8

§ From λ 4049.6 to λ 4057.3.

TABLE 1—*Continued*

August 1940	July–August 1941	July 1942	Identification		
			Elem.	λ	Int.
{4175.78(2A)					
{4178.17(2En)	78.63(3E)	78.43(3E)	*Fe* v	4178.85	8
		4200.32(1Enn)	*He* II	4199.87	2
{4225.15(0A)			*Ca* I	4226.73	500
{4226.21(0E)	4227.35(0E)		*Al* II	4226.81	35
			Al II	4227.50	30
			Al II	4227.98	20
			Fe I	4227.43	300
{4230.95(1A)					
{4233.13(3E)	32.89(5E)	33.38(6E)	*Fe* II	4233.17	11
4244.83(0En)	.....	43.86(2E)	[*Fe* II]	4243.97	.....
		4251.69(0E)	(*Mn* II	4251.77	2)
		4258.01(1–2E)	*Fe* II	4258.15	3
{4264.55(1A)			*C* II	4267.02	350
{4267.17(1E)	67.37(1E)	67.23(1En)	*C* II	4267.27	500
4277.23(0E)		77.51(1E)	[*Fe* II]	4276.87	.....
4288.70(0E)	86.85(1E)	87.18(1E)	[*Fe* II]	4287.40	.....
	4289.81(1E)		*Ti* II	4290.23	60
	4293.53(1E)		*Ti* II	4294.12	80
			Fe I	4294.13	700
	4296.56(1E)	96.64(0E)	*Fe* II	4296.58	6
	4307.42(1E)		*Ti* II	4307.90	100
			Fe I	4307.91	1000
	4313.12(1E)		*Ti* II	4312.87	100
	4315.07(1E)		*Ti* II	4314.98	20
			Fe I	4315.09	500
	4320.97(1E)		*Ti* II	4320.96	40
			Sc II	4320.74	40
	4331.36(1E)		*Fe* II	4331.53	3
4340.67(8E)	40.79(10E)	40.67(15E)	*H*γ	4340.46	200
4351.83(3E)	51.60(4E)	51.36(1E)	*Fe* II	4351.76	9
			(*Mg* I	4351.91	15)
	4358.66(1E)		[*Fe* II]	4359.34	.....
4363.46(6E)	63.21(5E)	63.08(8E)	[*O* III]	4363.21	.....
4366.92(0E)			*O* II	4366.91	100
	4368.22(0E)		*O* I	4368.30	1000
			Fe II	4368.26	1
			Ti II	4367.66	25
4369.24(1+E)			(*O* II	4369.28	50)
			Fe II	4369.40	2
4379.66(0E)			*N* III	4379.09	10
4384.16(1E)	84.30(2–3E)	85.4(2E)	*Fe* II	4385.38	7
			Fe I	4383.55	1000
			(*Mg* II	4384.64	8)
4387.63(2E)	87.47(3E)	87.96(5E)	*He* I	4387.93	30
	4390.48(1–0E)		*Mg* II	4390.58	10
4395.19(1E)	94.91(2En)		*Ti* II	4395.04	150
4399.92(1E)	99.60(2E)		*Ti* II	4399.77	100
4404.65(1E)	04.88(1E)		*Fe* I	4404.75	1000
		4407.97(1E)	(*Ti* II	4407.68	10)
			(*Fe* I	4407.72	100)
4413.86(0E)	14.70(1E)	14.64(2E)	[*Fe* II]	4413.78	.....
			Fe I	4415.12	600
			O II	4414.89	300
4416.78(2En)	17.08(3En)	17.38(4E)	*Fe* II	4416.82	7

TABLE 1—*Continued*

August 1940	July–August 1941	July 1942	Identification		
			Elem.	λ	Int.
			[*Fe* II]	4416.28	.....
			Ti II	4417.72	80
			O II	4416.97	150
4437.67(0E)			*He* I	4437.55	10
4444.97(0E)	43.20(1E)		*Ti* II	4433.80	125
4447.41(0E)			*N* II	4447.03	300
			O II	4448.20	70
4451.23(0E)			*Fe* II	4451.54	4
4457.37(1E)			[*Fe* II]	4457.97	.....
	4468.40(1E)		*Ti* II	4468.50	150
{4470.08(1A)					
{4472.08(3E)	72.12(5E)	71.53(5E)	*He* I	4471.48	100
4480.96(2E)	80.93(3E)	80.45(2E)	*Mg* II	4481.33	100
4488.98(1E)	88.75(1–2E)	89.05(2E)	*Fe* II	4489.18	4
			Ti II	4488.32	125
4491.32(1E)	91.62(1–2E)		*Fe* II	4491.40	5
4501.07(1E)	01.21(1E)		*Ti* II	4501.27	100
{4506.84(1A)					
{4508.26(1+E)	08.73(2E)	08.20(2E)	*Fe* II	4508.28	8
{4514.10(1A)					
{4515.29(2E)	15.43(2E)	15.69(1E)	*Fe* II	4515.34	7
4521.06(1E)	20.54(2E)		*Fe* II	4520.22	7
4522.89(1+E)	22.86(2E)	22.53(1E)	*Fe* II	4522.63	9
4528.75(1E)	29.11(1E)		*Ti* II	4529.46	40
			V II	4528.51	300
			Fe I	4528.62	600
4534.64(1E)	34.17(2E)	34.34(1E)	*Fe* II	4534.17	2
			Ti II	4533.97	150
			Mg II	4534.26	4
			(*N* III	4534.57	3)
4540.92(1+E)	41.46(2En)	41.90(2En)	*Fe* II	4541.52	4
			He II	4541.63	5
4549.04(1E)	49.74(3–4E)	49.70(1E)	*Fe* II	4549.47	10
			Ti II	4549.63	200
4556.30(1E)	55.95(3E)	55.99(1E)	*Fe* II	4555.89	8
	4558.19(1E)		*Cr* II	4558.66	100
	4564.04(0E)		*Ti* II	4563.77	200
	4571.57(0E)	72.26(0E)	*Ti* II	4571.98	300
			Mg I	4571.15	20
4576.51(0E)	76.89(0E)	76.80(1E)	*Fe* II	4576.33	4
4583.11(2E)	83.93(4E)	83.54(2E)	*Fe* II	4583.84	11
	4589.29(1–0En)		*Cr* II	4588.22	75
			Ti II	4589.95	100
			(*Cr* II	4589.89	3)
	4619.87(2Enn)	20.45(1E)	*Fe* II	4620.51	3
			Cr II	4618.83	35
4629.86(3E)	29.53(4E)	29.56(3E)	*Fe* II	4629.34	7
			(*N* II	4630.55	300)
{4631.69(1A)			*N* III	4634.16	8
{4634.70(3En)	35.06(3–4E)	34.24(4E)	*Fe* II	4635.33	5
{4637.66(3A)			*N* III	4640.64	10
{4640.30(4En)	41.23(4–5E)	40.48(6E)	(*N* III	4641.90	3)
{4645.74(3A)					
{4648.10(3En)	49.19(3Enn)‖	48.82(4Enn)¶	*C* III	4647.40	10
{4651.05(2En)			*C* III	4650.16	9

‖ Extending from λ 4646.3 to λ 4651.9. ¶ Extending from λ 4645.5 to λ 4651.9 with maxima at λ 4647.0 and λ 4649.9.

TABLE 1—*Continued*

August 1940	July–August 1941	July 1942	Identification		
			Elem.	λ	Int.
			C III	4651.35	8
{4653.87(1A?)			*C* IV	4658.64	5
{4657.92(1+E)	57.53(1E)	58.66(1E)	*C* IV	4656.5	4
			[*Fe* III]	4658.05	.....
4685.46(10E)	85.58(12E)	85.80(15E)	*He* II	4685.81	300
	4709.65(1–0E)		(*Fe* II	4708.97	3)
4713.82(1+E)	13.99(3E)	13.57(2E)	*He* I	4713.14	40
			He I	4713.37	7
	4732.17(1E)		*Fe* II	4731.44	3
4861.59(10E)	61.95(15E)	61.34(20E)	*Hβ*	4861.34	500
{4920.08(2A)	19.64(1A)		*He* I	4921.93	50
{4922.59(2+En)	22.80(6E)	23.89(2E)	*Fe* II	4923.92	12
	4936.55(1E)		.....	.....	.....
4958.86(3E)	59.36(4E)		[*O* III]	4958.91	.....
	4993.96(1E)		*Fe* II	4993.35	1
5007.23(5E)	07.05(6E)		[*O* III]	5006.84	.....
5012.21(2A)			*He* I	5015.67	100
5015.74(3E)	5017.33(5E)				
5018.93(2E)			*Fe* II	5018.43	12
	5040.16(1–0E)		(*Si* II	5041.13	8)
	5048.01(1E)		*He* I	5047.74	15
5169(1E)	68.82(3E)		*Fe* II	5169.03	12
	5183.66(1–0En)		*Mg* I	5183.62	500
	5197.60(2E)		*Fe* II	5197.57	6
	5226.66(0E)		*Ti* II	5226.55	50
			Fe I	5227.19	400
5235(1E)	34.64(1–2E)		*Fe* II	5234.62	7
	5275.16(3E)		*Fe* II	5275.99	7
	5283.95(1E)		*Fe* II	5284.09	3
5317(2E)	5316.92(4E)		*Fe* II	5316.61	8
			Fe II	5316.78	4
	5362.82(2E)		*Fe* II	5362.86	5
5412(2E)			*He* II	5411.55	50
	5534.79(2E)		*Fe* II	5534.86	4
5876(5Es)	5876(10E)		*He* I	5875.62	1000
6563(20E)	6563(20E)		*Hα*	6562.82	2000

d) λ *3736.7 (int. 3) and* λ *3754.8 (int. 4).*—These two lines, also observed in AX Per, coincide with two predicted [*Fe* v] transitions: $^5D_0-{}^3F_2$ (λ_{pred} 3736) and $^5D_1-{}^3F_2$ (λ_{pred} 3755). When these lines are appreciably weaker than the leading [*Fe* v] lines, λ 3891.4 and λ 3895.4, as in AX Per (January–February, 1942), their attribution to [*Fe* v] may be considered as satisfactory. But in CI Cyg they are stronger than λ 3891; hence, contributions by elements other than [*Fe* v] must play an important part. The $a^6D_{1½}-a^2F_{2½}$ transition of [*Fe* II] is predicted at λ 3736.2; but since no other transition of the a^6D-a^2F multiplet can be identified with any degree of certainty, the attribution of λ 3736 to [*Fe* II] remains very doubtful. The line λ 3736.7 is also strong in BF Cygni[4] and in Z Andromedae, where it should be mainly attributed to *Ca* II 3736.90 (50), *Cr* II 3737.50 (10), and *Fe* I 3737.13 (1000). It seems that in CI Cyg these three contributions should be added to [*Fe* v] and possibly to [*Fe* II]. As for λ 3755, it is absent in BF Cyg, but it is

[4] Unpublished material.

present as a fairly strong line in Z And, where it is attributed to *Cr* II 3754.57 (lab. int. 20), with minor contributions of *Fe* II, *O* III, *N* III, and [*Fe* V]. An unidentified line was found by A. B. Wyse,[5] at λ 3755.6 in the high-excitation nebula NGC 7662. The line λ 3755 in CI Cyg should be related to the nebular feature of NGC 7662, plus [*Fe* V], rather than to the line in Z And.

e) λ *3910.0* (*int. 1*).—This line has not been observed in nebulae or in BF Cyg, AX Per, or Z And. It is completely unidentified.

f) *Fe II lines at* λλ*3914.4* (*int. 2*), *3938.3* (*int. 4*),[6] *and 3944.8* (*int. 1*).—These lines belong to the *Fe* II multiplet $a^4P-z^6D^0$; the laboratory intensity of λ 3914 and λ 3938 is only 2; λ 3945 is predicted. The enhancement of this multiplet must be related to the low energy of z^6D^0 (4.8 v.), as compared with the other *Fe* II lines of the violet-blue-green region. This point is discussed in another section.

g) *Fe I lines.*—Several faint lines observed in CI Cygni must be attributed to *Fe* I, for example, $a^5D_3-z^5D^0_4$, λ 3930.31 (lab. int. 600; exc. pot. 0.09–3.23 v.), which can be only slightly blended by a predicted *Fe* II line. The same *Fe* I lines are found in BF Cygni. CI Cygni presents, thus, the remarkable characteristics of combining emission lines of *Fe* I, II, and [*Fe* VI, VII]. Evidently the emitting atoms are not necessarily located in the same region of the star. *Fe* I may possibly be excited in the atmosphere of the late-type companion by the early-type star. No selectivity of the type observed in the Me long-period variables is found for the *Fe* I lines in CI Cygni. This means that the mechanism of emission of *Fe* I is quite different from that in long-period variables.

RS OPHIUCHI

Compared with 1941,[7] the bright-line spectrum of RS Oph became much more pronounced in July, 1942. Our spectrogram of July 19, 1942, reveals a conspicuous emission line coinciding in wave length with the red coronal line λ 6374. No other identification can be found for the observed feature. For example, a neighboring *Si* II line (λ 6371) is excluded because the other stronger line (λ 6347) of the doublet is absent. There is no trace of the green line λ 5303. It may be recalled that, shortly after the outburst of 1933, Adams and Joy[8] discovered five coronal lines in the spectrum of RS Oph, the intensity of the green line λ 5303 being comparable to *Hβ*.[9] According to Edlén's interpretation of the line spectrum of the corona, λ 6374 is due to [*Fe* X], whereas λ 5303 belongs to [*Fe* XIV]. Hence it is not excluded that the excitation on July 19, 1942, could have been high enough to reach the ninth stage of ionization of iron but not the thirteenth. On our spectrogram the bright lines of *H*, *He* I, and *He* II are strong. In 1939 we also observed in AX Per and CI Cygni a weak emission line near λ 6371, which we tentatively attributed to [*Fe* X];[10] there was no trace of a line near λ 5303 in these two stars.

Our spectrograms of July 29 and August 1, 1942, show a considerable number of emis-

[5] *Lick Obs. Contr.*, ser. II, No. 4; *Ap. J.*, **95**, 356, 1942.

[6] In our first report on CI Cyg (*Ap. J.*, **91**, 546 [Table 29], 1940) the line λ 3938.0 should be attributed to *Fe* II.

[7] See our previous report on RS Oph (*Ap. J.*, **94**, 291, 1941).

[8] *Pub. A.S.P.*, **45**, 249, 1933.

[9] A minor outburst may have been present around April 25, 1942, according to the following data kindly communicated by Mr. Leon Campbell:

"Regarding any variation in RS Ophiuchi, during the past summer, our curve shows that the star appears to have been perhaps abnormally bright, magnitude 10.7, late in April to early in May, with the peak at JD 2430475.

"Usually, RS Ophiuchi is around magnitude 11.5 to 12.0, although recent observations make it nearer 11.0 to 11.5. To be sure, the scatter among observers is rather larger than for most of our stars."

[10] *Ap. J.*, **91**, 613, 1940.

PLATE XX

THE ULTRAVIOLET SPECTRUM OF Z ANDROMEDAE: (1) ON AUGUST 6, 1941, (2) ON JULY 15, 1942

PLATE XXI

THE SPECTRUM OF CI CYGNI ON JULY 4, 1942

The lines λλ 3914, 3938, and 3945 belong to the $a^3P-z^5D^0$ multiplet of *Fe* II

The lines λλ 3914, 3938, and 3945 belong to the $a^3P - z^3D^0$ multiplet of *Fe* II

PLATE XXII

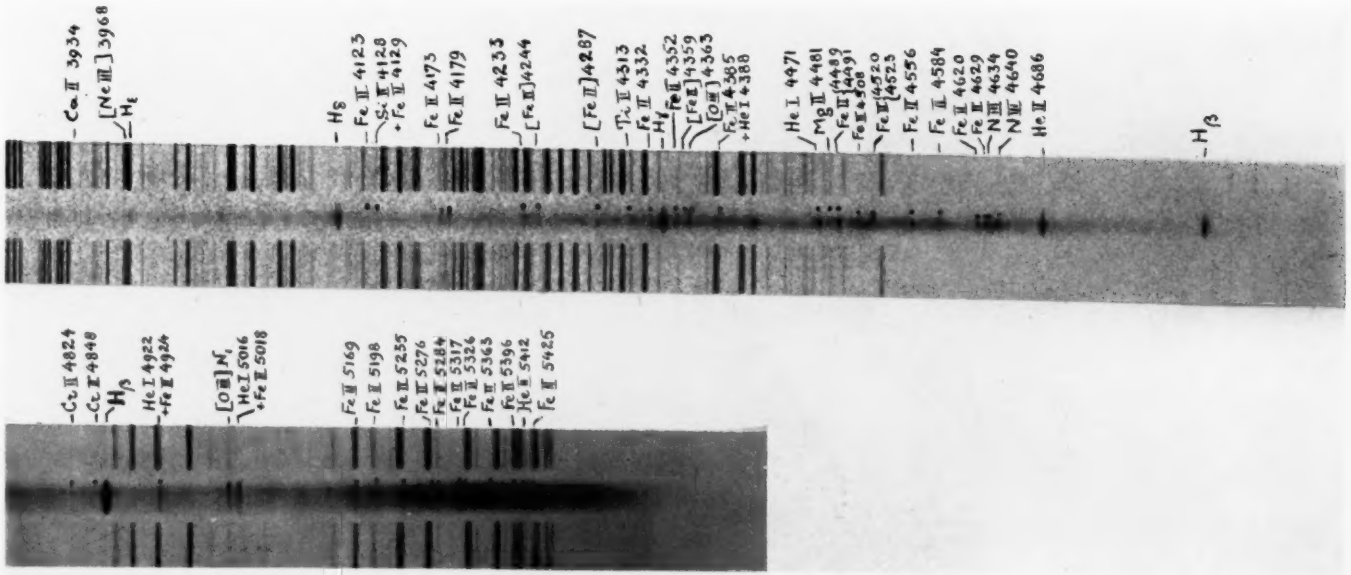

THE SPECTRUM OF RS OPHIUCHI ON JULY 29–AUGUST 1, 1942

PLATE XXIII

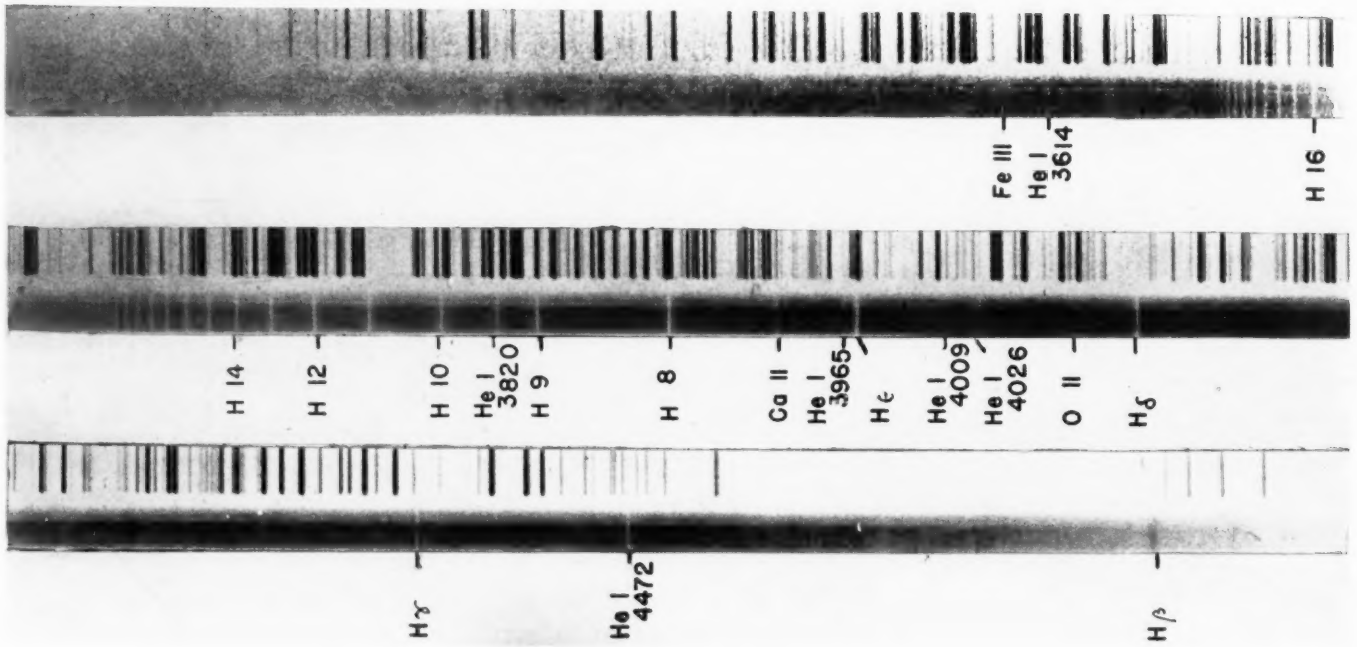

THE SPECTRUM OF MWC 346 = HD 195407

PLATE XXIV

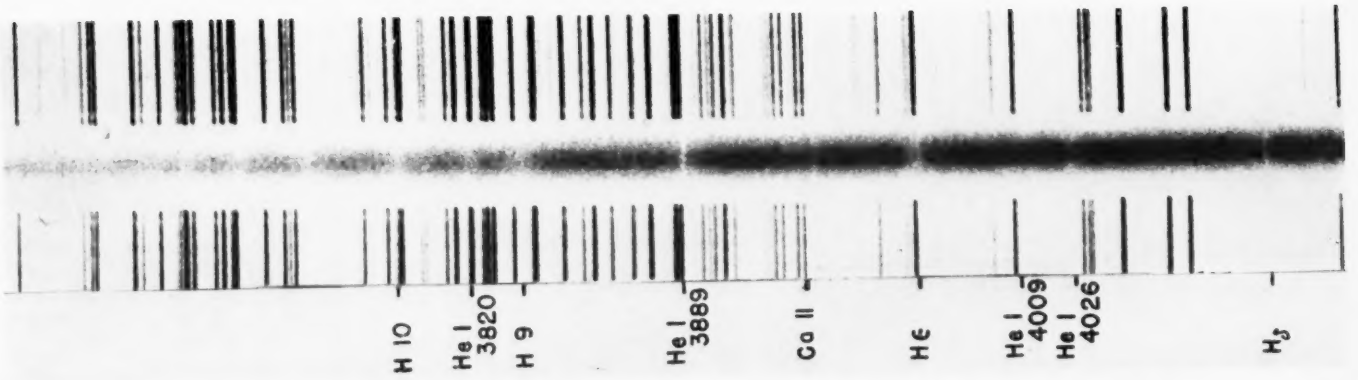

THE SPECTRUM OF MWC 303 = HD 172694

PLATE XXV

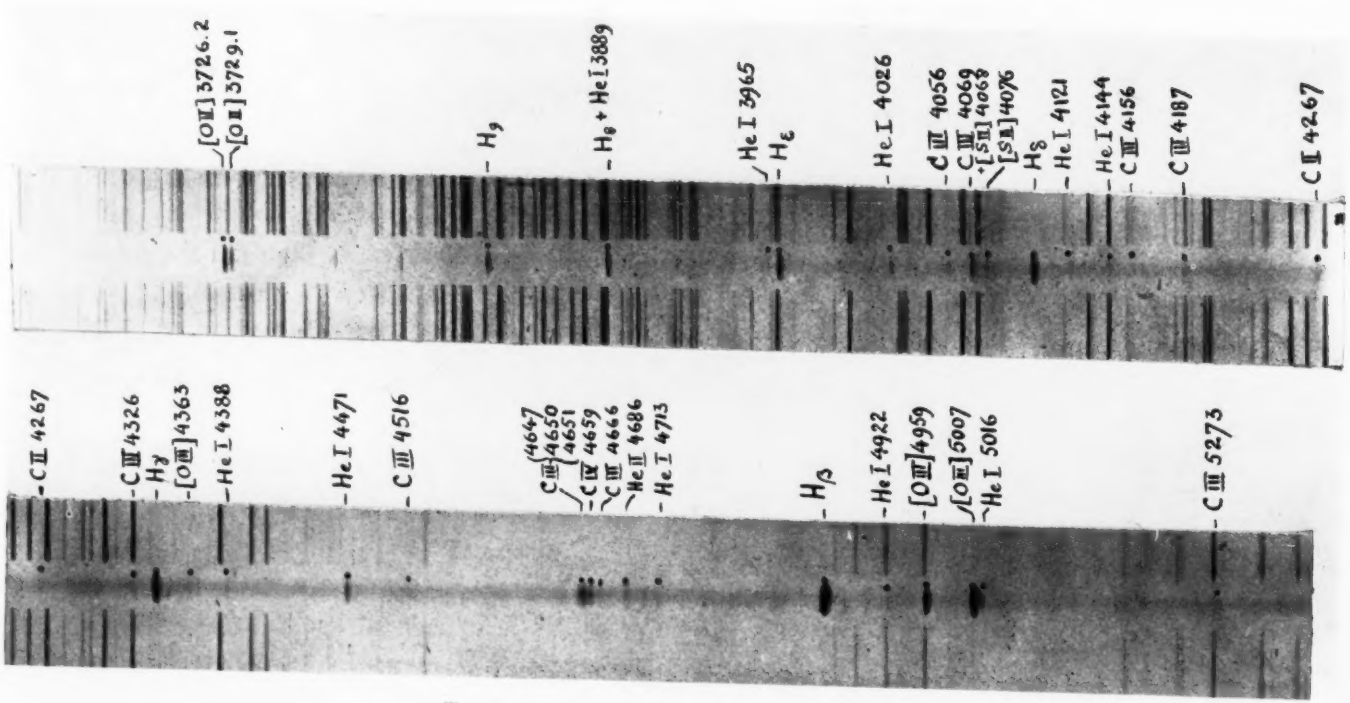

THE SPECTRUM OF HD 167362 ON JULY 31, 1942

sion lines (Pl. XXII). The Balmer series is observed in emission to H_{11}. Other observed bright lines are as follows:

He I: 4026 (1); 4144 (1); 4388 (3 bl.); 4471 (6); 4713 (1); 4922 (6 bl.); 5016 (8 bl.); 5048 (1); 5876 (8)
He II: 4200 (1?); 4542 (2bl.); 4686 (10); 5412 (2)
C II: 4267 (1)
C III: 4650 (1)
N II: 3995 (1–0); 4447 (1–2)
N III: 4097 (2); 4634 (5, slightly blended by *Fe* II); 4640 (6)
[*O* III]: 4363 (6); N_2 (1); N_1 (4)
[*Ne* III]: 3869 (3); 3968 (2)
Mg II: 4481 (4)
Si II: 3856 (1); 3862 (1); 4128 (2 bl.)
[*S* II]: 4069 (2)
Ca II: 3934 (1)
Ti II: 4300 (1–2 bl.); 4313 (2); 4395 + 4400 (1–2n); 4444 (1); 4501 (2); 4550 (2 bl.); 5189 (1); 5227 (1)
Cr II: 4052 + 4054 (1n); 4253 (1–0); 4619 (2 bl.); 4824 (1); 4848 (1–2); 5335 (2).
Fe II: 3974 + 3975 (1); 4002 (1); 4123 (1–2); 4129 (2 bl.); 4173 (2); 4179 (3); 4233 (6); 4258 (2); 4297 (2); 4303 (2 bl.); 4332 (2); 4352 (6); 4385 (3 bl.); 4417 (2 bl.); 4451 (2); 4489 + 4491 (5); 4508 (3); 4515 (2); 4520 + 4523 (3); 4542 (2 bl.); 4549 (2 bl.); 4556 (2); 4576 (1); 4584 (4); 4621 (2 bl.); 4629 (4); 4924 (6 bl.); 4993 (1); 5018 (8 bl.); 5169 (5); 5198 (4); 5217 (2); 5235 (5); 5260 + 5265 (2); 5276 (5); 5284 (4); 5317 (5); 5326 (3); 5363 (5); 5387 (2); 5396 (1); 5425 (2)
[*Fe* II]: 4244 (1–2); 4277 (1); 4287 (2); 4359 (3); 4414 + 4416 (2 bl.); 5159 (1)

The *Fe* II lines will be discussed in another section. The observed [*Fe* II] lines are the strongest transitions of the a^6D-a^6S, b^4F, and a^4F-a^4G, a^4H multiplets. *Cr* II has only faint lines: the main features belong to the $a^4F-z^4D^0$ (λ 4253), $a^4F-z^4F^0$ (λ 4824, λ 4848), $b^4F-z^4D^0$ (λ 4619), and $b^4F-z^4F^0$ (λ 5335) multiplets. *Ti* II is also rather faint; only the strongest members of the leading multiplets are found.

The only outstanding unidentified line has the approximate wave length λ 3738 (int. 2s). It seems too strong to be due to *Ca* II 3736.92 and *Fe* I 3737.13. The line is probably identical to the feature discussed in CI Cygni.

AX PERSEI AND AG PEGASI

These two objects with "combination spectra" have continued to display variations of their emission lines. Between February and November, 1942, AX Per has, on the whole, shown a decrease in ionization; this is especially apparent in the considerable decrease of the intensity ratios [*Ne* V]/*O* III, and [*Fe* VII]/[*Ne* III]. [*Fe* V] was still present in November, 1942.

As for AG Peg, a comparison between spectrograms of July 13–15 and of November 23, 1942, reveals a decrease in the intensity of the *Fe* II lines relative to the other emissions (*H*, *He* I, etc.). In fact, this star displays appreciable fluctuations of the intensity of the metallic emission. In July, 1942, the ratio *Si* IV/*He* I was greater than in 1939, and the *N* II lines were weaker.

New data on the emission lines of Fe I, Fe II, [*Fe II*], [*Fe III*], *and* [*Fe V*] *in peculiar stars.*—On the basis of our material on Z And, RS Oph, and other stars, new information may be gathered concerning the permitted and forbidden emission lines of iron in its successive stages of ionization. Such data are useful, especially for the discussion of the spectra of novae. For the permitted lines it is known, in a general way, that the geometrical and physical dilution factors, as well as the excitation potentials, play an important role. But what their actual effect is can be decided only by observations. The properties of the forbidden spectra of *Fe* III and *Fe* V are similar; hence, an increased knowledge of [*Fe* III] will improve the situation with respect to [*Fe* V], and vice versa.

Besides the results obtained from Z And, RS Oph, and B 1985, important data are provided by a discussion of our numerous spectrograms of BF Cygni. Merrill discovered[11] that this star exhibits numerous bright lines of *H*, *He* I, oxygen, iron, and other elements; he noticed the great strength of [*Fe* III] and the variability of [*O* III] 4363. Merrill has announced that he is preparing an investigation of the object. Hence our material will be used only in so far as it provides data on the iron spectra, and no general description of the spectrum[12] or of its variations will be attempted.

Fe I.—When present in emission in long-period variables, *Fe* I exhibits peculiar selectivities (incomplete multiplets) which have been tentatively attributed to fluorescence effects.[13] A careful check is required to ascertain whether selectivities of some sort or another are also present among the bright *Fe* I lines found in early-type objects, since these lines are usually very weak and some may easily escape detection.

A detailed discussion of the spectra of Z And, BF Cyg, CI Cyg, AG Peg, and several other objects reveals no peculiar selectivity among the emission lines of *Fe* I. The observed lines belong to the multiplets $a^5D-z^5F^0$, z^5D^0, z^7P^0, z^7F^0; $a^5F-y^5F^0$ (and possibly also $a^5F-z^3P^0$, y^5D^0), and (slightly blended) $a^3F-y^3D^0$, y^3F^0, z^5G^0. Most of these lines are in the ultraviolet region. The terms a^5D, a^5F, and a^3F are the three lowest terms: a^5D from 0.00 to 0.12 v.; a^5F from 0.85 to 1.01 v.; a^3F from 1.48 to 1.60 v.

In the presence of emission lines of *H*, *He* I, *Fe* II, *Ti* II, and *Si* II, relatively few *Fe* I lines can appear unblended. The best are listed in Table 2.

Fe II.—The behavior of *Fe* II has been considered previously in various examples of peculiar stars. In Z Canis Majoris and in other similar stars (17 Leporis, CD−27°11944, BD+47°3487, HD 160529, etc.) the sextets ($a^6S-z^6P^0$, z^6F^0) exhibit strong violet absorption-components, whereas the quartets ($b^4P-z^4D^0$, z^4F^0; $b^4F-z^4D^0$, z^4F^0, and $a^4G-z^4F^0$) appear in pure emission.[14] Such behavior may be similar to the selectivities observed in shells of high excitation among the lines of *Si* III, *N* II, *N* III, *N* IV, *C* III, etc.; we have attributed these selectivities to fluorescence phenomena.

In the case of B 1985 and WY Gem[15] the *Fe* II emission lines of low excitation were found to be considerably enhanced, relative to the lines of high excitation, when using for comparison the laboratory intensities obtained by Dobbie near the pole of the iron arc. In order to facilitate future discussions of the behavior of the *Fe* II lines in bright-line stars, we have compiled in Table 3 all the bright *Fe* II lines found on our McDonald spectrograms of B 1985 (for $\lambda<3420$), BF Cyg, RS Oph (for $\lambda>3970$), and Z And, which are four excellent representatives of "iron stars." The table contains, besides the usual spectroscopic data, the estimated intensities in absorption in α Cygni.[16]

Examination of Table 3 reveals immediately that the decrease in intensity with increasing excitation potential is much more pronounced for the stellar emission lines than for the absorption lines in α Cygni or for the laboratory lines. In terms of excitation temperature, this behavior of the bright *Fe* II lines may be considered as corresponding in a

[11] *Pub. A.A.S.*, **10**, 168, 1942.

[12] The following elements are present in emission on our spectrograms of July, 1942, of BF Cygni: *H*, *He* I, *He* II, [*N* II], [*O* III], *Mg* I and II, *Al* II (?), *Si* I and II, [*S* II], *Ca* I and II, *Ti* II, *V* II, *Cr* II, *Mn* II (?), *Fe* I and II, [*Fe* II and III] (no permitted *Fe* III), *Ni* II (?), and the strongest lines of *C* II and III, *N* II and III, *O* III.

[13] Thackeray and Merrill, *Pub. A.S.P.*, **48**, 331, 1936; **49**, 120, 1937; Thackeray, *Ap. J.*, **86**, 499, 1937; Swings and Struve, *Ap. J.*, **96**, 269, 1942. Besides the incomplete multiplets, certain long-period variables reveal also as faint emission the stronger lines of the ultimate multiplets of the violet region $a^5D-z^7P^0$ and $a^5D-z^7F^0$.

[14] *Ap. J.*, **96**, 254, 1942.

[15] *Ap. J.*, **93**, 455, 1941.

[16] From J. H. Rush, *Ap. J.*, **95**, 213, 1942 (for $\lambda<3298$); O. Struve, *Ap. J.*, **90**, 699, 1939 (λ 3298 to λ 3900); Struve and Swings, *Ap. J.*, **94**, 344, 1941 (for $\lambda>3900$).

general way to a fairly low excitation-temperature, say, of the order of 5000° or 6000°. But it is far from certain that a true Boltzmann distribution is present.

At any rate, this behavior of *Fe* II is important for identification work. It enables us, for example, to understand why the *Fe* II line, λ 3938.29 (lab. int. 2), may be present as a fairly strong emission while the line λ 3938.97 (lab. int. 4) is absent. Such a behavior has been observed in all bright line stars, as is indicated in Table 4.

TABLE 2

CHARACTERISTIC *Fe* I LINES, NOT BLENDED BY *H*, *He* I, *Fe* II, *Ti* II, OR *Si* II

TRANSITION		LABORATORY			INT. IN EMISSION IN				NOTES
		λ	Int.	Exc. Pot.	Z And			BF Cyg	
$a^5D-z^5F^0$	4–5	3719.93	1000	0.00–3.32	0	0	1	1	
	2–3	3745.56	500	0.09–3.38	....	2+	1	1	1
$a^5D-z^5D^0$	4–4	3859.91	1000	0.00–3.20	....	1	....	.....	
	2–1	3878.57	300	0.09–3.27	....	2	....	.....	1
	1–0	3895.66	400	0.11–3.28	....	1	....	.....	
	2–2	3899.71	500	0.09–3.25	1	.....	....	.....	
	3–4	3922.91	600	0.05–3.20	1	.....	....	.....	2
	2–3	3930.31	600	0.09–3.23	1	2	0	.....	
$a^5D-z^7P^0$	3–3	4206.70	125	0.05–2.98	....	.....	....	1–0?	
	4–4	4216.19	200	0.00–2.93	....	.....	....	1–0?	
	3–4	4291.47	125	0.05–2.93	....	.....	....	0	
$a^5D-z^7F^0$	4–3	4325.76	1000	0.00–2.85	....	.....	....	1	
	4–5	4375.93	500	0.00–2.82	....	.....	....	1?	
	2–3	4461.65	300	0.09–2.85	....	.....	....	1–0?	
$a^5F-y^5F^0$	2–2	3763.79	500	0.99–4.26	....	1–0	....	1	
	1–1	3767.21	500	1.01–4.28	....	0	....	.....	
	2–3	3795.00	500	0.99–4.24	1	1	....	2	
$a^5F-z^5G^0$	3–4	4404.75	1000	1.55–4.35	1	1	....	.....	

NOTES TO TABLE 2

1. In Z And, the *Fe* I line is blended with *V* II. 2. May be very weakly blended by *He* II.

As already mentioned in the section on CI Cygni, it so happens that λ 3938.29 belongs to the $a^4P-z^6D^0$ multiplet which, among all observable *Fe* II lines, possesses the lowest excited level ($z^6D^0 = 4.80$ v.). On the other hand, λ 3938.97 is one of the high-level lines ($d^2D-x^4F^0$; exc. pot. of $x^4F^0 = 9.02$ v.).[17] Despite its low laboratory intensity, the other line of the $a^4P-z^6D^0$ multiplet, λ 3914.5, is also found in the bright-line stars. In addition, three predicted lines of the multiplet are appreciable contributors in blends.

[17] The effect of the energies of the lower levels a^4P (1.66 v.) and d^2D (5.88 v.) appears strikingly when we compare the intensities of λ 3938.29 and λ 3938.97 in absorption in the sun, Canopus, α Cygni, and α^2 Canum Venaticorum. In Canopus, λ 3938.29 is slightly affected by a *Mg* I line; the comparison in

	Sun	α Car	α Cyg	α^2 CVn
3938.29 (lab. int. 2)	2	8	6	5
3938.97 (lab. int. 4)	−1	2	4	5

types later than the sun or earlier than A0 is impossible because of blends.

TABLE 3

BEHAVIOR OF *Fe* II LINES IN PECULIAR BRIGHT-LINE STARS

TRANSITION		LABORATORY				INT. IN α CYG (ABS.)	INT. IN EMISSION IN			
		λ	Int.	Ex. Pot.			B 1985*	BF Cyg	RS Oph†	Z And
$a^4D-z^6D^0$	$3\frac{1}{2}-4\frac{1}{2}$	3277.35	9	0.98	4.75	4	4	6	.....	1
	$2\frac{1}{2}-3\frac{1}{2}$	3302.86	4	1.04	4.77	bl.	2 bl.	1	.....	.....
	$3\frac{1}{2}-3\frac{1}{2}$	3255.88	8	0.98	4.77	4	3	4	.....	.....
	$2\frac{1}{2}-2\frac{1}{2}$	3281.29	7	1.04	4.80	2	3	1–2	.....	1
	$1\frac{1}{2}-1\frac{1}{2}$	3295.81	6	1.07	4.82	bl.	1	1	.....	.....
	$\frac{1}{2}-\frac{1}{2}$	3303.47	4	1.09	4.83	bl.	2 bl.	1–0	.....	.....
	$1\frac{1}{2}-\frac{1}{2}$	3285.42	(3)	1.07	4.83	1	0	1–0	.....	.....
$a^4P-z^6D^0$	$2\frac{1}{2}-2\frac{1}{2}$	3938.29	2	1.66	4.80	6	.....	5	.....	3
	$2\frac{1}{2}-1\frac{1}{2}$	3914.48	2	1.66	4.82	5	.....	4	.....	2
	$\frac{1}{2}-1\frac{1}{2}$	3981.61	pred.	1.72	4.82	0 bl.	.....	2 bl.	.....	1–0
	$1\frac{1}{2}-1\frac{1}{2}$	3945.21	pred.	1.69	4.82	(4) (1)	.....	3 bl.	.....	1 bl.
	$1\frac{1}{2}-\frac{1}{2}$	3930.31	pred.	1.69	4.83	(4) (3)	.....	2 bl.	.....	1 bl.
$a^4P-z^4D^0$	$2\frac{1}{2}-3\frac{1}{2}$	3227.73	13	1.66	5.49	5	6	5	.....	.....
	$1\frac{1}{2}-2\frac{1}{2}$	3213.31	13	1.69	5.53	8	5	4	.....	.....
	$\frac{1}{2}-1\frac{1}{2}$	3210.45	10	1.72	5.56	7	4	2–3	.....	.....
	$2\frac{1}{2}-2\frac{1}{2}$	3192.92	9	1.66	5.53	3	5 bl.	3 bl.	.....	.....
	$1\frac{1}{2}-1\frac{1}{2}$	3186.74	11	1.69	5.56	6 bl.	3–4	1 bl.	.....	.....
	$\frac{1}{2}-\frac{1}{2}$	3193.81	11	1.72	5.58	3	5 bl.	3 bl.	.....	.....
	$2\frac{1}{2}-1\frac{1}{2}$	3166.67	4	1.66	5.56	2	1–0	.....	.....	.....
	$1\frac{1}{2}-\frac{1}{2}$	3170.34	6	1.69	5.58	4	1–0	.....	.....	.....
$a^4P-z^4F^0$	$2\frac{1}{2}-3\frac{1}{2}$	3196.07	10	1.66	5.52	3	5	3	.....	.....
	$1\frac{1}{2}-2\frac{1}{2}$	3183.11	8	1.69	5.56	5 bl.	4	2	.....	.....
	$\frac{1}{2}-1\frac{1}{2}$	3185.31	5	1.72	5.59	3	.....	1–0	.....	.....
	$2\frac{1}{2}-2\frac{1}{2}$	3163.09	5	1.66	5.56	5 bl.	3	1	.....	.....
$a^2P-z^4D^0$	$1\frac{1}{2}-2\frac{1}{2}$	3783.35	4	2.27	5.53	5	.....	3	.....	1
	$\frac{1}{2}-1\frac{1}{2}$	3821.92	pred.	2.33	5.56	3	.....	1–0	.....	.....
$a^2P-z^4P^0$	$1\frac{1}{2}-\frac{1}{2}$	3416.02	5	2.27	5.88	4	0–1	.....	.....	.....
$a^2D-z^4F^0$	$2\frac{1}{2}-3\frac{1}{2}$	4124.79	1	2.53	5.52	3	.....	.....	.....	0
$b^4P-z^4D^0$	$2\frac{1}{2}-3\frac{1}{2}$	4233.17	11	2.57	5.49	12	.....	10	6	6
	$1\frac{1}{2}-2\frac{1}{2}$	4351.76	9	2.69	5.53	10	.....	7	6	4
	$\frac{1}{2}-1\frac{1}{2}$	4416.82	7	2.77	5.56	6	.....	6 bl.	2 bl.	3–4 bl.
	$2\frac{1}{2}-2\frac{1}{2}$	4173.45	8	2.57	5.53	8	.....	8	2	2–3
	$1\frac{1}{2}-1\frac{1}{2}$	4303.17	8	2.69	5.56	9	.....	4	2 bl.	.....
	$\frac{1}{2}-\frac{1}{2}$	4385.38	7	2.77	5.58	8	.....	3	3 bl.	2 bl.
	$2\frac{1}{2}-1\frac{1}{2}$	4128.73	3	2.57	5.56	3	.....	3 bl.	2 bl.	1–2 bl.
	$1\frac{1}{2}-\frac{1}{2}$	4273.32	3	2.69	5.58	5	.....	1	.....	.....
$b^4P-z^4F^0$	$2\frac{1}{2}-3\frac{1}{2}$	4178.85	8	2.57	5.52	8	.....	9	3	3
	$1\frac{1}{2}-2\frac{1}{2}$	4296.57	6	2.69	5.56	7	.....	3	2	1–0
	$\frac{1}{2}-1\frac{1}{2}$	4369.40	2	2.77	5.59	3	.....	2 bl.	.....	.....
	$2\frac{1}{2}-2\frac{1}{2}$	4122.64	4	2.57	5.56	5	.....	3	1–2	1
	$1\frac{1}{2}-1\frac{1}{2}$	4258.15	3	2.69	5.59	4	.....	3	2	1–2
$b^4P-z^4P^0$	$2\frac{1}{2}-2\frac{1}{2}$	3824.91	4	2.57	5.80	4	.....	3	.....	1
	$2\frac{1}{2}-1\frac{1}{2}$	3764.09	m	2.57	5.85	4 bl.	.....	1 bl.	.....	1–0 bl.
	$1\frac{1}{2}-\frac{1}{2}$	3872.76	pred.	2.69	5.88	7 bl.	.....	3 bl.	.....	1 bl.

* Only the region $\lambda < 3420$. † Only the region $\lambda > 3970$.

TABLE 3—*Continued*

Transition		Laboratory				Int. in α Cyg (Abs.)	Int. in Emission in			
		λ	Int.	Ex. Pot.			B 1985*	BF Cyg	RS Oph†	Z And
	$1\frac{1}{2}$–$2\frac{1}{2}$	3974.16	3	2.69	5.80	4	.....	3	1 bl.	2 bl.
	$\frac{1}{2}$–$1\frac{1}{2}$	4002.07	2	2.77	5.85	3	.....	1–0	1 bl.	1
$b^4F-z^6P^0$	$4\frac{1}{2}$–$3\frac{1}{2}$	4993.35	1	2.80	5.27	1	.....	1	1	1–0
$b^4F-z^4F^0$	$4\frac{1}{2}$–$4\frac{1}{2}$	4629.34	7	2.80	5.46	9	.....	6	4	3–4
	$3\frac{1}{2}$–$3\frac{1}{2}$	4555.89	8	2.82	5.52	6	.....	6	2	2
	$2\frac{1}{2}$–$2\frac{1}{2}$	4515.34	7	2.83	5.56	7	.....	6	2	1–2
	$1\frac{1}{2}$–$1\frac{1}{2}$	4491.40	5	2.84	5.59	6	.....	6	5 bl.	1
	$4\frac{1}{2}$–$3\frac{1}{2}$	4520.22	7	2.80	5.52	6	.....	6	3 bl.	1–2
	$3\frac{1}{2}$–$2\frac{1}{2}$	4489.18	4	2.82	5.56	5	.....	6	5 bl.	2 bl.
	$2\frac{1}{2}$–$1\frac{1}{2}$	4472.92	2	2.83	5.59	3	.....	bl.	.....	.....
	$3\frac{1}{2}$–$4\frac{1}{2}$	4666.75	2	2.82	5.46	3	.....	2 bl.	.....	.....
	$2\frac{1}{2}$–$3\frac{1}{2}$	4582.83	3	2.83	5.52	4	.....	bl.	.....	bl.
	$1\frac{1}{2}$–$2\frac{1}{2}$	4534.17	2	2.84	5.56	7 bl.	.....	2 bl.	.....	1 bl.
$b^4F-z^4D^0$	$4\frac{1}{2}$–$3\frac{1}{2}$	4583.83	11	2.80	5.49	9	.....	8	4	3
	$3\frac{1}{2}$–$2\frac{1}{2}$	4549.47	10	2.82	5.53	15 bl.	.....	7 bl.	2 bl.	3
	$2\frac{1}{2}$–$2\frac{1}{2}$	4522.63	9	2.83	5.56	7	.....	6	3 bl.	2
	$1\frac{1}{2}$–$\frac{1}{2}$	4508.28	8	2.84	5.58	7	.....	5	3	2
	$3\frac{1}{2}$–$3\frac{1}{2}$	4620.51	3	2.82	5.49	4	.....	1	2 bl.	1–2 bl.
	$2\frac{1}{2}$–$2\frac{1}{2}$	4576.33	4	2.83	5.53	4	.....	1	1	1–0
	$1\frac{1}{2}$–$1\frac{1}{2}$	4541.52	4	2.84	5.56	4	.....	1 bl.	2 bl.	2 bl.
$a^6S-z^6F^0$	$2\frac{1}{2}$–$3\frac{1}{2}$	5284.09	3	2.88	5.21	4	.....	3	4	1
$a^6S-z^6P^0$	$2\frac{1}{2}$–$3\frac{1}{2}$	5169.03	12	2.88	5.27	8	.....	8	5	3
	$2\frac{1}{2}$–$2\frac{1}{2}$	5018.43	12	2.88	5.34	10	.....	8	8 bl.	5 bl.
	$2\frac{1}{2}$–$1\frac{1}{2}$	4923.92	12	2.88	5.38	10	.....	8	6 bl.	4 bl.
$a^6S-z^4D^0$	$2\frac{1}{2}$–$3\frac{1}{2}$	4731.44	3	2.88	5.49	6	.....	.....	.....	3
$a^4G-z^4D^0$	$4\frac{1}{2}$–$3\frac{1}{2}$	5362.86	5	3.19	5.49	6	.....	5	.....	2
	$3\frac{1}{2}$–$2\frac{1}{2}$	5316.78	4	3.21	5.53	8 bl.	.....	10 bl.	.....	3 bl.
	$2\frac{1}{2}$–$1\frac{1}{2}$	5264.80	2	3.22	5.56	3	.....	.....	2	.....
$a^4G-z^4F^0$	$5\frac{1}{2}$–$4\frac{1}{2}$	5316.61	8	3.14	5.46	8 bl.	.....	10 bl.	5	3 bl.
	$4\frac{1}{2}$–$3\frac{1}{2}$	5275.99	7	3.19	5.52	6	.....	6	5	3
	$3\frac{1}{2}$–$2\frac{1}{2}$	5234.62	7	3.21	5.56	7	.....	5	5	1–2
	$2\frac{1}{2}$–$1\frac{1}{2}$	5197.57	6	3.22	5.59	7	.....	5	4	2
	$4\frac{1}{2}$–$4\frac{1}{2}$	5425.27	2	3.19	5.46	2	.....	1–2	.....	.....
	$3\frac{1}{2}$–$3\frac{1}{2}$	5325.56	2	3.21	5.52	3	.....	2	3	.....
$b^2H-z^4F^0$	$5\frac{1}{2}$–$4\frac{1}{2}$	5534.86	4	3.23	5.46	5	.....	4	.....	2
$b^2G-z^4H^0$	$3\frac{1}{2}$–$3\frac{1}{2}$	3289.35	7	3.80	7.55	3	1–0 bl.	.....	.....	.....
$b^2G-z^2G^0$	$3\frac{1}{2}$–$3\frac{1}{2}$	3167.85	11	3.80	7.69	3	1	.....	.....	.....
$b^4D-y^4F^0$	$3\frac{1}{2}$–$4\frac{1}{2}$	3259.05	10	3.89	7.67	7 bl.	0–1	1	.....	.....
	$2\frac{1}{2}$–$3\frac{1}{2}$	3258.77	10	3.88	7.66					
$b^4D-x^4D^0$	$3\frac{1}{2}$–$3\frac{1}{2}$	3177.53	10	3.89	7.77	5	1	.....	.....	.....
	$2\frac{1}{2}$–$2\frac{1}{2}$	3135.36	9	3.88	7.81	4	0–1	.....	.....	.....
$b^2F-z^2D^0$	$2\frac{1}{2}$–$1\frac{1}{2}$	3297.89	5	3.93	7.67	1	0	.....	.....	.....

TABLE 3—*Continued*

Transition	Laboratory				Int. in α Cyg (Abs.)	Int. in Emission in			
	λ	Int.	Ex. Pot.			B 1985*	BF Cyg	RS Oph†	Z And
$b^2F-z^2G^0$ $3\frac{1}{2}-4\frac{1}{2}$	3323.07	8	3.95	7.66	6 bl.	.....	.....	.....	1
$c^2G-z^2F^0$ $3\frac{1}{2}-2\frac{1}{2}$	3232.79	7	4.14	7.95	4 bl.	.....	1?	.....	.....
$c^2G-y^2G^0$ $4\frac{1}{2}-4\frac{1}{2}$	3187.29	8	4.13	8.00	6 bl.	3–4 bl.	.....	.....	.....
$3\frac{1}{2}-3\frac{1}{2}$	3162.80	8	4.14	8.04	5 bl.	3 bl.	.....	.....	.....
$b^2D-z^4G^0$ $1\frac{1}{2}-2\frac{1}{2}$	4012.47	1	4.46	7.54	6 bl.	.....	1 bl.	.....	1 bl.
$2\frac{1}{2}-2\frac{1}{2}$	4032.95	3	4.48	7.54	3	.....	abs.	abs.	abs.
$b^2D-y^4D^0$ $1\frac{1}{2}-1\frac{1}{2}$	3725.30	3	4.46	7.77	2	.....	1?	.....	abs.
$c^2D-z^2F^0$ $2\frac{1}{2}-3\frac{1}{2}$	3827.08	4	4.71	7.94	3	.....	1	.....	0
$1\frac{1}{2}-2\frac{1}{2}$	3814.12	4	4.72	7.95	4	.....	0?	.....	1 bl.
$c^2D-z^2P^0$ $2\frac{1}{2}-1\frac{1}{2}$	3748.49	8	4.71	8.00	6 bl.	.....	2 bl.	.....	1–2 bl.
$1\frac{1}{2}-\frac{1}{2}$	3759.46	6	4.72	8.00	6 bl.	.....	1 bl.	.....	1–2 bl.
$1\frac{1}{2}-1\frac{1}{2}$	3755.56	4	4.72	8.00	1	.....	abs.	.....	abs.
$c^2D-y^2F^0$ $2\frac{1}{2}-3\frac{1}{2}$	3179.50	8	4.71	8.59	4 bl.	1–2 bl.	1–0	.....	.....
$1\frac{1}{2}-2\frac{1}{2}$	3180.16	7	4.72	8.60					
$2\frac{1}{2}-2\frac{1}{2}$	3175.08	4	4.71	8.60	0	0–1 bl.	abs.	.....	.....
$c^2F-x^2G^0$ $3\frac{1}{2}-4\frac{1}{2}$	3935.94	6	5.54	8.68	3	.....	1	.....	bl.
$2\frac{1}{2}-3\frac{1}{2}$	3906.04	5	5.55	8.71	4	.....	bl.	.....	bl.
$d^2D-y^2F^0$ $2\frac{1}{2}-3\frac{1}{2}$	4635.33	5	5.93	8.59	4	.....	abs.	abs.	bl.
$d^2D-x^4F^0$ $2\frac{1}{2}-3\frac{1}{2}$	4002.55	3	5.93	9.01	2	.....	abs.	1 bl.	1–0
$1\frac{1}{2}-2\frac{1}{2}$	3938.97	4	5.88	9.02	4	.....	abs.	abs.	abs.
$d^2D-y^2P^0$ $2\frac{1}{2}-1\frac{1}{2}$	3975.03	2	5.93	9.04	2	.....	abs.	1 bl.	abs.
$d^2G-v^2G^0$ $4\frac{1}{2}-4\frac{1}{2}$	3960.89	3	7.24	10.35	1	.....	abs.	abs.	1 bl.
$3\frac{1}{2}-3\frac{1}{2}$	4057.46	2	7.24	10.28	3	.....	abs.	abs.	abs.

From Table 3 one would gather that the multiplet $a^4P-z^6D^0$ is enhanced relative to the multiplet $a^4D-z^6D^0$, which arises from the same upper level; whether this is really the case or whether it is of instrumental origin is hard to ascertain.

TABLE 4

Intensities of the *Fe* II Lines λ 3938.27 and λ 3938.97 in Bright-Line Stars

	CI Cyg	AX Per	Z And		BF Cyg	AG Peg
3938.29.....	4	1	1–2	3–4	5	2
3938.97.....	Absent	Absent	Absent	Absent	Absent	Absent

[*Fe II*].—The forbidden transitions of *Fe* II observed in η Carinae have been described by P. W. Merrill,[18] H. Spencer Jones,[19] and especially I. S. Bowen.[20] They consist of the

[18] *Ap. J.*, **67**, 391, 1928. [19] *M.N.*, **91**, 794, 1931. [20] *Rev. Mod. Phys.*, **8**, 80, 1936.

following multiplets: a^6D-b^4P, b^4F, a^6S; and a^4F-b^4P, a^4H, b^4F, a^4G. Our investigations of the spectra of WY Geminorum and B 1985[21] have added the following transitions, which appear in the ultraviolet: a^6D-b^4D (weak), a^6D-b^2F (somewhat uncertain), a^6D-b^2G (uncertain), a^4F-b^4D (fairly strong), a^4F-c^2G (very weak), a^4D-b^2D (fairly strong), a^4D-c^2D (weak), a^4D-a^2S (somewhat uncertain).

Besides, two faint emission lines of B 1985 and WY Gem have been observed at λ 4114.4 and λ 4249.1 and have been identified as $a^4F_{4½}-b^2H_{5½}$ (λ_{pred} 4114.5) and $a^4D_{3½}-b^4D_{3½}$ (λ_{pred} 4249.1).

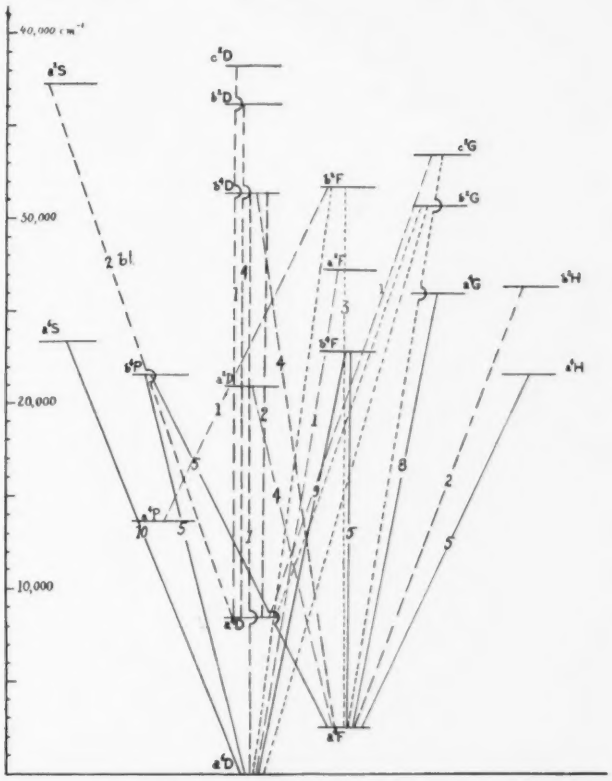

FIG. 1.—Forbidden lines of *Fe* II. Full-drawn lines: forbidden transitions observed in η Carinae; dashed lines: new observed lines; dotted lines: transitions probably present.

Spectrograms of peculiar stars, which have recently been obtained, especially of BF Cygni, provide additional data on the [*Fe* II] spectrum. New components have been found in some of the previously known multiplets, and five new transitions have been observed in spectral regions which had not been thoroughly investigated before. The region λ > 5600 is still practically unknown, and we plan to investigate it in the near future.

The following additional components of the multiplet a^4F-a^4H have been found in BF Cygni:

a^4F-a^4H ..... $4\frac{1}{2}-5\frac{1}{2}$, λ 5111.64 (int. 1)
a^4F-a^4H ..... $3\frac{1}{2}-4\frac{1}{2}$, λ 5220.07 (int. 1)
a^4F-a^4H ..... $2\frac{1}{2}-3\frac{1}{2}$, λ 5296.85 (int. 0–1 bl.)

[21] *Ap. J.*, **91**, 546 (Table 25), 1940; *Ap. J.*, **93**, 455 (Table 2), 1941.

The newly found multiplets are[22] a^6D-a^2F; a^4F-a^2D; a^4D-b^2G, c^2G; and a^4P-b^2F. The observations are given in Table 5.

We may say that a^6D-a^2F is weak but fairly certain; that a^4F-a^2D is certain, with at least one strong component; that a^4D-c^2G is weak but certain; that a^4D-b^2G is extremely weak and rather doubtful; and that a^4P-b^2F, although weak, is fairly certain. The line λ 5527.3 ($a^4F_{3½}-a^2D_{2½}$) is a conspicuous feature, immediately to the blue of the *Fe* II line, λ 5534.86 (lab. int. 4). In BF Cygni, λ 5527 is only slightly weaker than λ 5535; together they constitute a very characteristic pair of lines.

In the section on CI Cygni the presence of the new multiplet a^4F-b^2F has been suggested as probable, although still provisional, pending additional observations.

TABLE 5

NEW [*Fe* II] MULTIPLETS OBSERVED IN BF CYGNI

Transition	λ Pred.	Ex. Pot.	Int. in BF Cyg	Notes
a^6D-a^2F $3\frac{1}{2}-3\frac{1}{2}$	3712.3	0.05–3.37	bl.	1
$2\frac{1}{2}-2\frac{1}{2}$	3709.1	0.08–3.41	1	2
$1\frac{1}{2}-2\frac{1}{2}$	3736.8	0.11–3.41	bl.	3
$1\frac{1}{2}-3\frac{1}{2}$	3779.3	0.11–3.37	0–1	
$2\frac{1}{2}-3\frac{1}{2}$	3751.7	0.08–3.37	bl.	4
$\frac{1}{2}-2\frac{1}{2}$	3752.2	0.12–3.37		
a^4F-a^2D $4\frac{1}{2}-2\frac{1}{2}$	5362.1	0.23–2.53	bl.	5
$3\frac{1}{2}-2\frac{1}{2}$	5527.3	0.30–2.53	4	
$2\frac{1}{2}-2\frac{1}{2}$	5654.9	0.35–2.53	.....	6
$1\frac{1}{2}-2\frac{1}{2}$	5745.7	0.38–2.53	.....	
$3\frac{1}{2}-1\frac{1}{2}$	5295.7	0.30–2.63	0–1	7
$2\frac{1}{2}-1\frac{1}{2}$	5412.6	0.35–2.63	1–2	8
$1\frac{1}{2}-1\frac{1}{2}$	5495.8	0.38–2.63	.....	
a^4D-c^2G $3\frac{1}{2}-4\frac{1}{2}$	3918.7	0.98–4.13	0–1	
$2\frac{1}{2}-4\frac{1}{2}$	3987.0	1.04–4.13	1–0	9
$3\frac{1}{2}-3\frac{1}{2}$	3913.4	0.98–4.14	4 bl.	10
$2\frac{1}{2}-3\frac{1}{2}$	3981.5	1.04–4.14	2	11
$1\frac{1}{2}-3\frac{1}{2}$	4027.7	1.07–4.14	bl.	12
a^4D-b^2G $2\frac{1}{2}-4\frac{1}{2}$	4544.9	1.04–3.75	0	13
a^4P-b^2F $2\frac{1}{2}-3\frac{1}{2}$	5396.7	1.66–3.95	1	

NOTES TO TABLE 5

1. Blended with H_{15}.
2. Slightly blended by *Fe* I 3709.25 (600).
3. Blended with *Ca* II 36.90 (50), *Fe* I 37.13 (1000), *Cr* II 37.55 (10).
4. Blended with H_{12}.
5. Blended with *Fe* II 5362.85 (5).
6. Region not covered by our spectrograms of sufficient dispersion.
7. Blended with new [*Fe* II] line $a^4F_{2½}-a^4H_{3½}$ (λ pred. 5296.85).
8. Blended with *He* II 5411.55 (50) and [*Fe* III] 5411.98.
9. Possibly weakly blended by [*Fe* II] λ pred. 3986.4 ($a^6D_{½}-a^4G_{2½}$).
10. Blended with *Fe* II 3914.48 (2) and *Ti* II 3913.46 (70).
11. Possibly weakly blended by *Fe* II 3981.61 (pred.).
12. Blended with *He* I.
13. Weakly blended by *Ti* II 4545.14 (15).

[22] A weak contribution of a^6D-a^4G is also probable; but practically all the components are blended with ordinary lines.

[Fe III] and [Fe V].—[*Fe* III] is strong in RY Scuti, but the continuous background is also very intense in this star. In other objects, like MWC 17, MWC 349, R Aquarii, AG Pegasi, either [*Fe* III] is not so well developed, or the object is too faint, or other features mask an important part of [*Fe* III]. As for the novae, which at certain stages reveal strong [*Fe* III] lines (RT Serpentis, DO Aquilae, DQ Herculis, RR Pictoris, etc.), the complex or broad structure of the emission features renders the analysis difficult. The object best adapted to a discussion of [*Fe* III] is, at present, BF Cygni; yet even in this star several blends are present. We may use RY Scuti[23] and the Orion nebula[5] to supplement the data.

As for [*Fe* V], the situation is still less favorable because of more numerous possibilities of blends. The novae are not at the present time suitable for such a discussion. The best object is AX Persei, as it appeared around January, 1942.

Table 6 and the accompanying notes summarize the essentials of the discussion. The following results should be added:

a) Long exposures on BF Cygni and the Orion nebula, in the region of the forbidden [*Fe* III] multiplets $3d^5D-3d^3D$ (λλ3239–3368) and $3d^5D-4s^7S$ (λλ 3322–3429), fail to reveal any trace of these transitions. The absence of $^5D-^3D$ is especially striking, in view of the strength of $^5D-^3P$ and $^5D-^3F$.

b) In RY Scuti two faint lines measured at λ 4985.6 (1) and λ 5032.2 (0) have been attributed[23] to the $^5D-^3H$ transition of [*Fe* III]. Wyse[5] also observed two faint lines at the same wave lengths in the Orion nebula. Yet, since no line is observed at these wave lengths in BF Cygni and since the corresponding [*Fe* V] transitions are not found in AX Persei, the identification of $^5D-^3H$ transition needs confirmation.

c) The $^5D-^3G$ transition of [*Fe* V] is present, although very weak in AX Persei. The fact that the corresponding transition of [*Fe* III] is not definitely observed in BF Cygni may be due to blends or to the proximity of strong lines. It should be searched for when other [*Fe* III] stars with less complex spectra become known.

II. OBSERVATIONS OF ABSORPTION SHELLS

Previous papers of this series have helped to elucidate the properties of a very remarkable group of objects, which we have designated as "absorption shells" in order to distinguish them from other types of nebulous masses surrounding certain stars. These formations are usually associated with stars having exceptionally rapid projected components of equatorial rotation and are, therefore, believed to be ringlike structures located predominantly in the equatorial planes of the stars.[24] They are often variable in the

[23] Swings and Struve, *Ap. J.*, **91**, 546 (Tables 16 and 17), 1940.

[24] The argument runs as follows: Ordinary B-type stars show a statistical distribution of observed rotational velocities which is completely at variance with the relation $W(V)dV = V/\sqrt{1-V^2} \cdot dV/V_0$ (Unsöld, *Physik der Sternatmosphären*, p. 325, Berlin, 1938), which predicts the distribution of projected velocities, V, for an assembly of stars, all of which rotate with the equatorial velocity V_0 and whose axes are distributed at random. The departure is in the sense of a large excess of small velocities, which proves that V_0 is not constant. If we pick out from the entire material those B stars which have emission lines and especially if we, in addition, exclude the supergiants, we obtain an assembly which agrees quite closely with the predicted distribution for a value of V_0 of the order of 250 km/sec. Finally, if we consider only those Be stars which have well-developed shells, we find that all have large rotational velocities, of the order of 250 km/sec or more. We conclude that, as a first approximation, the main-sequence Be stars may be regarded as a group of stars all members of which have intrinsically large rotations and whose axes are distributed at random. The shells form a still more restricted group, namely, not only one whose members are characterized by large rotations, but one whose axes are distributed approximately at right angles to the line of sight. Since the absorption features come from a mass of gas in which dilution of radiation plays an appreciable role, we conclude that the shells are ringlike structures concentrated in the equatorial planes of the stars, whose diameters are often of the order of three times the radii of the stars. This chain of arguments depends upon several important observational steps which have been derived from a relatively small amount of material. The correlation between rotation and presence of emission is well established. But heretofore only some two or three dozen stars with shells have been investigated.

TABLE 6

[*Fe* III] AND [*Fe* V] SPECTRA IN PECULIAR STARS

Transition		[*Fe* III] λ Pred.	[*Fe* III] Int. in BF Cyg	[*Fe* III] Int. in RY Scu	[*Fe* III] Int. in Orion Neb.	[*Fe* III] Notes	[*Fe* V] λ Pred.	[*Fe* V] λ in Ax Per.	[*Fe* V] Int. in Ax Per.	[*Fe* V] Notes
$^5D-{}^3F$	4–2	4573.87	abs.	0?	0.3		3923.5	?	?	12
	4–3	4607.03	0?	0	0.5		3911.1	abs.	abs.	
	4–4	4658.05	8	5	1.5		3891.8	3891.4	3–4	
	3–2	4667.01	3–4 bl.	0	0.4	1	3850.8	3851.8	0 bl.	13
	3–3	4701.54	5	3	0.8		3838.9	3839.3	2 bl.	14
	2–2	4733.91	3	1	0.6		3794.6	.....	bl.	15
	3–4	4754.69	3	1	0.9		3820.2	.....	bl.	16
	2–3	4769.43	2	1	0.8		3782.9	3784.2	1–2	
	1–2	4777.69	1–2	0	0.7		3755.5	3754.8	2 bl.	17
	0–2	4799.45	1	.....	.....		3735.2	3736.7	1	
	1–3	4813.87	5 bl.	.....	0.8 bl.	2	3744.1	abs.	abs.	
	2–4	4824.14	abs.	abs.	abs.		3764.8	abs.	abs.	
$^5D-{}^3P$	2–0	4883.93	abs.	abs.	0.7		4229.8	abs.	abs.	
	1–0	4930.54	1	.....	0.5		4181.4	4180.6	1	
	3–1	4936.36	abs.	abs.			4136.4	abs.	abs.	
	2–1	5011.26	2	1	.....	3	4071.5	4071.4	2	
	1–1	5060.35	2	0	0.8		4026.6	bl.	bl.	16
	0–1	5084.77	abs.	abs.	abs.		4003.2	4003.7	1–0 bl.	18
	4–2	5151.93	abs.	abs.	abs.		3970.1	bl.	bl.	19
	3–2	5270.41	7	5	1.0		3895.7	3895.4	3	
	2–2	5355.88	abs.	abs.	abs.		3838.1	bl.	bl.	20
	1–2	5411.98	1–2 bl.	abs.	.....	4	3798.2	bl.	bl.	21
	0–2	5439.93	abs.	abs.	abs.		3777.4	abs.	abs.	
$^5D-{}^3G$	4–3	3976.22	abs.	.....	0.4?		3503.5	abs.	abs.	
	4–4	4008.35	3 bl.	.....	bl.	5	3463.4	abs.	abs.	
	3–3	4046.43	1 bl.	.....	abs.	6	3445.4	bl.	bl.	22
	4–5	4070.72	2 bl.	.....	bl.	7	3430.3	3430.4	1–0	
	3–4	4079.70	abs.	.....	abs.		3406.6	3405.8	1–0	23
	2–3	4096.62	bl.	.....	bl.	8	3400.3	3403.1	0	23
	1–3	4129.35	3 bl.	.....	0.2 bl.	9	3368.9	abs.	abs.	
	2–4	4130.73	1 bl.	.....	0.3 bl.	10	3362.5	abs.	abs.	
	3–5	4144.32	3 bl.	.....	0.7 bl.	11	3374.6	abs.	abs.	

NOTES TO TABLE 6

1. In BF Cygni, blend with *Fe* II 4666.75 (lab. int. 2).
2. In BF Cygni and in the Orion nebula, blend with [*Fe* II] 4814.56 ($a^4F_{4½}-b^4F_{4½}$).
3. In the Orion nebula, the line is unobservable in the red wing of the intense [*O* III] line.
4. Blend with *He* II and [*Fe* II] 5412.6 ($a^4F_{2½}-a^2D_{1½}$) (see Table 5).
5. Blend with *He* I.
6. Blend with *Fe* I 4045.81 (lab. int. 400).
7. In BF Cygni, blend with *Fe* I 4071.74 (lab. int. 300), *Cr* II 4070.90 (10), *O* II 4072.16 (300). In the Orion nebula, blend with *O* II.
8. Too near *N* III 4097.31.
9. In BF Cygni, blend with *Fe* II 4128.73 (3) and *Si* II 4128.05 (20); [*Fe* III] is probably a contributor. In the Orion nebula the line is due to *Si* II and [*Fe* III].
10. In BF Cygni the line is mainly due to *Si* II; in the Orion nebula it is due to *Si* II and *O* II.
11. In BF Cygni, blend with *He* I 4143.76 and *Fe* I 4143.87 (400); in the Orion nebula, mainly *He* I.
12. Near *He* I 3926.53.
13. Weakly blended by [*Fe* VI] 3849 ($^4F_{2½}-{}^2P_{½}$).

14. Blended by a weaker line of [*Fe* v] ($^5D_2-{}^3P_2$).
15. Blended with H_{10}. From the behavior of [*Fe* III] we may expect this [*Fe* v] line to play a role in [*Fe* v] stages of novae or peculiar stars whenever the *H* lines are weak.
16. Blended with *He* I 4026.19. May be expected in [*Fe* v] objects when the *He* I lines are weak.
17. For a discussion of this blend see paragraph on CI Cygni.
18. From the behavior of [*Fe* III] we may deduce that the line λ 4003.7 of Ax Per is not entirely due to [*Fe* v].
19. Blended by $H\epsilon$. From the behavior of [*Fe* III], we deduce that the [*Fe* v] transition is extremely weak.
20. Blend with a much stronger line of [*Fe* v] ($^5D_3-{}^3F_3$).
21. Blend with H_{10}.
22. Blend with O III 3444.10 (fluorescence line).
23. Difficult measures.

intensity of their absorption lines, in radial velocity, and in ionization but are almost always present only in stars which at the same time have bright lines.

Since the recognition that these features originate in more or less detached shells or rings is of fairly recent origin, there is at present little observational material available for their discussion.[25] In order to secure additional data we started in the summer of 1942 on a program of observations covering all Be, Ae, and Fe stars catalogued by Merrill and Burwell,[26] which are within reach of our Cassegrain spectrograph, equipped with quartz prisms and 500-mm camera (dispersion 50 A/mm at λ 4045, limiting photographic magnitude about 11.0). The purpose of this work was as follows: (1) to discover whether any of Merrill's Be stars, not identifiable as absorption shells from his descriptions, have developed features similar to those which in recent years have appeared in Pleione and γ Cas and have disappeared in β Mon A and in γ Cas; (2) to investigate whether some of his Ae stars, or late Be stars, are in reality objects similar to the present condition of Pleione or 48 Librae; (3) to record changes in the bright lines; (4) to gather material for a test of the relation between rotational broadening of the absorption lines and the widths of the emission lines; and (5) to separate, wherever possible, genuine supergiant Be stars from shells which often mimic a supergiant spectrum, though in reality the exciting stars may be of relatively low luminosity.

The observations are still in progress and a complete discussion will be deferred until later. The succeeding paragraphs give descriptions of four Be stars which we believe to possess absorption shells. A fifth, MWC 335 = HD 192954, has been turned over for discussion to Mr. Arthur Broyles of the McDonald Observatory.

MWC 346 = HD 195407.[27]—The spectrum of this star was described by Merrill,[28] who found in 1921 and 1924 that the *H* lines had variable bright components, which were thought to be somewhat similar to those of φ Persei. Lines of helium and iron, presumably in absorption, were "very weak and seldom measured." Several spectrograms taken by us at the McDonald Observatory in July, 1942, showed a remarkably strong shell-absorption spectrum of *H* and *He* I (see Pl. XXIII). The sharp *H* lines can be seen to H_{29} or H_{30}. The *He* I line, λ 3965 ($2^1S-4^1P^0$), whose lower level is metastable, is very strong and sharp. In addition, the members of the triplet series ($2^3P^0-n^3D$), λλ 4472, 4026, 3820, etc., are very sharp and strong, though the higher members of this series look as though they were superposed over broad and diffuse *He* I lines, presumably originating in the reversing layer. The corresponding singlet lines ($2^1P^0-n^1D$) λλ 4388, 4144, 4009, etc., are extremely weak and probably greatly broadened. There is some indication of very broad and weak lines of *O* II and of fairly sharp, weak lines of *Fe* III. *Ca* II K is strong and sharp and may be of interstellar origin.[29] The appearance of this kind of

[25] Struve, *Ap. J.*, **95**, 134, 1942.

[26] *Ap. J.*, **78**, 87, 1933, and later lists.

[27] $\alpha = 20^h26^m.0$; $\delta = 36°39'$ (1900), mag. 7.1; Sp. B3e.

[28] *Ap. J.*, **72**, 108, 1930.

[29] *Ibid.*

shell is a relatively rare occurrence, since the conditions for bringing out the *He* I triplets ($2^3P^0-n^3D$), but not the singlets ($2^1P^0-n^1D$), are rather delicate. The abnormal stage of the spectrum of ϕ Persei and certain stages of the development of the shell spectrum of γ Cassiopeiae were of this nature. The radial velocities from the absorption lines, reduced to the sun, are given in Table 7. Merrill's result was -74 km/sec. The difference in velocity between *H* and *He* is probably real. The spectral type of the underlying star is probably B1 or B2, because broad *O* II undoubtedly comes from the reversing layer and its rotational velocity is exceptionally large. The shell is not quite so early in type as that of γ Cas in February, 1940, because the lines of *Fe* III are very weak in the shell of MWC 346. No lines of *Fe* II are clearly visible in the shell at the present time. Hence it is certain that the spectrum has undergone a marked change since 1920–24. The bright lines of *H* agree closely with Merrill's description. The underlying wings of the *H* lines

TABLE 7

RADIAL VELOCITY OF MWC 346 FROM FOUR PLATES TAKEN JULY 16 AND 29, 1942

Element	No. of Lines	Velocity	Element	No. of Lines	Velocity
		km/sec			km/sec
H	22	−82	*Si* III	1	−75
He I	7	−93	*Ca* II (interstellar)	1	−31

are weak but very broad. The Stark effect is conspicuous, and the star is of relatively low luminosity.

MWC 303 = HD 172694.[30]—According to Merrill,[31] *Hβ* and *Hγ* have sharply defined absorption lines with emission on the violet edge. Several spectrograms taken at the McDonald Observatory in July, 1942, show that this star is a representative of an interesting class of absorption shells for which we have been searching for a long time. The shell lines of *H* are weak; only *Hβ*, Hγ, and *Hδ* show them (see Pl. XXIV). The broad underlying *H* wings are strong and show conspicuous Stark broadening. The star is of moderate luminosity and is certainly not a supergiant. The *He* I lines ($2^3P^0-n^3D$), ($2^1P^0-n^1D$), and ($2^1S-4^1P^0$) are broadened by rapid rotation and belong to the B3 star. These lines show no sharp components. But the blend of *Hζ* and *He* I 3889 ($2^3S-3^3P^0$) has a conspicuous sharp central component. This is clearly the *He* I line which originates in the metastable level 2^3S. In most shells this line is indistinguishable from the shell line of *Hζ*. It is only in those rare shells in which *H* is highly ionized that the sensitive *He* I line becomes a useful indicator of the presence of an absorption shell. The next member of the series, λ 3188 ($2^3S-4^3P^0$), is not often covered by the spectrograph but should, of course, be available even when *H* is strong in the shell. Since the type of the exciting star is B3 and since *He* I 3889 is the only conspicuous shell line, we conclude that the density of the shell must be much lower than that of the shells of such stars as ϕ Per, ζ Tau, and γ Cas (February, 1940), all of which showed conspicuous shell lines of *H*. Heretofore the absence of strong *H* lines has been observed only in shells whose exciting stars are of relatively low temperature (14 Com). It is also clear that, while in general the shells form a definite sequence whose ionization runs parallel to, though lower than, that of the main spectral sequence of the exciting stars, there must be a large dispersion in the ionizations of individual shells, which undoubtedly corresponds to a large dispersion in the densities of the shells.

According to Merrill, the radial velocity from *H*, *He* I, and *Fe* II was $+56$ km/sec in

[30] $\alpha = 18^h36^m5$; $\delta = -15°57'$ (1900), mag. 8.3; Sp. Bpe.

[31] *Ap. J.*, **72**, 105, 1930.

the interval 1921–25. Two plates taken on July 29 and 30, 1942, gave the following values:

H (sharp)	+26 km/sec	*He* I (broad, λ 4026)	+ 6 km/sec
He I (sharp, λ 3889)	+26 km/sec	*Ca* II (interstellar)	+ 8 km/sec

The large departure from Merrill's value is probably significant.

MWC 253 = HD 155851.[32]—This spectrum has been briefly described by Merrill,[33] who finds that "the dark lines are very weak and the type is uncertain." Our plate, taken on July 17, 1942, shows a sharp and fairly strong absorption core at λ 3889. The star is thus similar to HD 172694. The *He* I line must originate in a shell, since the rotational broadening of the triplet *He* I lines ($2^3P^0-n^3D$) is exceptionally great. The higher members of the *H* lines, beginning with $H\epsilon$, show very weak absorption lines which are greatly broadened by Stark effect and rotation. The star is of relatively low luminosity. Our measures give: *He* I (λ 3889), −1 km/sec; *Ca* II (interstellar), −23 km/sec.

TABLE 8

RADIAL VELOCITY OF MWC 321

Element	July 4, 1942	July 10, 1942	August 9, 1942	Element	July 4, 1942	July 10, 1942	August 9, 1942
H	−60 (7)	−64 (3)	−71 (3)	*Ca* II	+19 (1)	+20 (1)	+10 (1)
He I		+33 (3)	+18 (1)	*Si* II ?	+62 (2)		
Mg II		+20 (1)					

MWC 321 = HD 187399.[34]—This remarkable star has very sharp metallic absorption lines. $H\beta$ is very strong in emission and fairly sharp. The *He* I lines are somewhat broadened, but not excessively so. The most interesting feature of the spectrum is a set of strong, sharp *H* components displaced toward the violet against the broad underlying *H* wings produced by Stark effect. This feature resembles the appearance of the *H* lines in 17 Leporis,[35] and we consider it very probable that the star has an expanding shell, which gives rise to these displaced lines. Our plates were obtained on July 4 and 10, 1942. In addition, we had at our disposal a plate taken on August 9, 1942, at the Lick Observatory, which was kindly sent to us by Dr. Neubauer. It should be noted that bright $H\beta$ is much weaker, relative to the adjoining continuous spectrum on the Lick plate, than on the earlier McDonald plates. The variation is almost certainly real. The results of our measurements are as shown in Table 8.

III. OBSERVATIONS OF Be STARS

The normal Be stars which we have observed at the McDonald Observatory and a few unusual stars, for which more material will be required are described in this section. The data should be used in connection with the earlier descriptions by Merrill and his collaborators.[36] When we record "no change" we do not mean to imply that the emission features are constant, but only that there has been no significant change since Merrill's

[32] $\alpha = 17^h9^m0$; $\delta = -32°34'$ (1900), mag. 8.0, Sp. B0ne.

[33] *Ap. J.*, **76**, 180, 1932.

[34] $\alpha = 19^h44^m7$; $\delta = +29°10'$ (1900), mag. 7.7; Sp. B9eβ. Dr. Merrill has informed us that recent measurement of a plate taken at Mount Wilson on April 19, 1924, gives −66 km/sec for the mean of $H\gamma$ and $H\delta$ and −13 km/sec for the other elements. The plate was slightly out of focus and the individual settings were not very accurate. But it shows that the negative *H* velocity was definitely present in 1924.

[35] *Ap. J.*, **95**, 468, 1942.

[36] Esp. *Ap. J.*, **61**, 389, 1925; **76**, 156, 1933; **78**, 87, 1933.

last published description. It will be noted that there have been many changes, though only few have been spectacular. In several cases our plates allowed us to improve the spectral classification. Nearly all such cases consist in the addition of the designation "n." It is most remarkable that the correlation between the existence of bright lines and rotational broadening of the absorption lines is even stronger than had been expected. This is due not only to the increased number of stars designated as "n" but also to the fact that several of the few remaining "s" stars are really supergiants. The number of main-sequence "s" stars with emission lines is very small, which is in good agreement with the hypothesis that all main-sequence Be stars have rapid rotations and that their "s" and "n" character depends mostly upon the orientation of the star's axis. A detailed numerical study of this interesting phenomenon will be postponed until more observations have been secured.

Pending this discussion, it is already possible to state that the correlation between emission-line widths and rotational line-of-sight components derived from the absorption lines is not perfect. This was already apparent from a study of the brighter Be stars,[37] and it is again confirmed in the present work. Rapid rotation is apparently required to produce the outer mass which gives rise to emission lines. These lines also show rotational Doppler broadening, but the amount of the broadening depends not only upon the rotation of the star and the inclination of its axis but also upon other factors, such as the size of the shell.

One other result may be mentioned at this time. The number of stars having very broad and shallow high, ultraviolet members of the Balmer series is unexpectedly large. These lines are usually much broader than the lines of *He* I, and the broadening must, therefore, be ascribed to excessive Stark effect.

Our plates do not cover the region of $H\alpha$. Hence absence of emission usually refers to $H\beta$. The great extension of our quartz spectrograms into the ultraviolet region gave us an opportunity to record the behavior of the higher members of the Balmer series and to notice the surprising weakness of these lines in many Be stars.

IV. MAIN CHARACTERISTICS AND EVOLUTION OF SHELLS

A wide variety of gaseous shells have been observed recently,[38] and a general understanding of their excitation mechanism has been reached.[39] Additional information provided by more recent observations will be mentioned in this section. As is well known, there are found shells which show exclusively absorption features, others show only emission lines, and still others combine emission and absorption to different extents. These differences may be attributed to the properties of the underlying radiation. A recombination spectrum requires that the atoms considered be ionized by the underlying radiation. In stars like 17 Leporis or Pleione the continuous absorption in the star, beyond λ 912, must deplete the stellar radiation so that practically all the hydrogen atoms in the shell are neutral. Similarly, the ions Fe^+, Ti^+, Mn^+, Cr^+, and V^+ will not be ionized a second time even at very low densities, because their second ionization potentials are slightly higher than that of hydrogen. The question arises why we do not observe strong recombination spectra of *Fe* I and the other neutral metals. Unless such emissions by recombination are very frequent, each individual line must be weak, because the total intensity is distributed among a very large number of lines.

The density in shells is always low enough for the fluorescence mechanism to be active. The resulting emission will depend on the quality of the radiation received by the atoms considered. In other words, the velocities of the atoms in the shell, relative to the reversing layer, are of considerable importance. Let us consider, for example, hydrogen.

[37] *Ap. J.*, **73**, 94, 1931.

[38] Swings and Struve, *Ap. J.*, **96**, 254, 1942.

[39] Struve, *Ap. J.*, **95**, 134, 1942; Swings, *Ap. J.*, **95**, 112, 1942; also previous reports mentioned in these papers.

TABLE 9

DESCRIPTION OF Be SPECTRA

Star	Dates of Observation	Description
MWC 2	7.24; 8.1	No change; no emission at $H\beta$
3	11.26	$H\delta$ is clearly visible as a bright line, but $H\epsilon$ is in absorption only; the higher members of the Balmer series in absorption are extremely faint, broad, and diffuse; probably no change
4	7.24	No change; no emission at $H\beta$, but absorption abnormally weak; absorption lines of *He* I, *Si* II, *Fe* II quite narrow, but *H* lines broader than in β Ori or α Cyg; probably not a supergiant; the last Balmer line is H_{21}, suggesting $M = -1$
5	7.25	Type Bose; $H\beta$ almost continuous; $H\gamma$ and $H\delta$ fairly sharp cores on broad absorption background; the *Ca* II lines are very strong; $H\zeta$ is not appreciably enhanced by *He* I in the shell; Merrill describes $H\beta$ as emission and $H\gamma$, $H\delta$ as continuous
6	7.29	The absorption lines are exceptionally broad; $H\beta$ is a fairly strong single emission, $H\gamma$ is a very broad absorption; Merrill described $H\beta$ as continuous
9	7.3	γ Cas appeared in 1942 as a B0n star with very weak indication of emission at $H\beta$; numerous observations have been made at Yerkes Observatory
10	7.30	No emission seen at $H\beta$; the *H* absorption lines are exceptionally strong and broad; the *He* I lines are moderately broadened by rotation
12	7.30; 8.1	Probably no change; the emission lines of *H* are strong and are seen as far as $H\zeta$; the higher members of the Balmer series are very broad and shallow
13	7.30	$H\beta$ in absorption; *Ca* II is very strong; *He* I 4472 is much stronger than *Mg* II 4481; our plates suggest that the type is B3s
14	11.23	Probably no change; the plate is underexposed at $H\beta$
15	11.23	$H\beta$ appears to be in absorption, perhaps with a trace of narrow emission in the center
19	11.23	$H\beta$ and $H\gamma$ are in emission; otherwise the spectrum is nearly continuous, with very weak and broad lines of *He* I and of the higher nembers of the Balmer series
20	11.23	No change; the type is B3ne, but the rotational broadening is not excessive; the higher Balmer lines are broad and weak
21	7.31	Probably no change; the emission at $H\beta$ and $H\gamma$ is very weak
22	11.23	Probably no change
23	11.23; 11.24	This star shows a remarkable shell spectrum of *H*, but the *He* I lines are all broad, with the exception of λ 3888, which shows a slight enhancement as compared with neighboring members of the Balmer series; one plate shows a suspicion of a sharp *He* I line at λ 3965; $H\beta$ shows a very narrow, weak absorption line with a fairly strong emission line on the red side and a weaker emission line on the violet side; $H\gamma$ shows only a strong, sharp absorption line; the other *H* lines have sharp absorption cores superposed over very broad wings produced by Stark effect; rotational broadening in the *He* I lines is large; the luminosity of this star is not great, as judged by the *H* wings
24	11.24	No change; the higher members of the Balmer series are of normal intensity and width, in absorption
62	11.27	Emission at $H\beta$ and $H\gamma$; type probably B3ne
64	11.26	No emission
66	11.27	No change
136	11.25	Probably no change; $H\beta$ is a strong absorption line with a very weak emission line in the center
139	11.25	Probably no change; the bright line at $H\beta$ is narrow and strong, superposed over a broad absorption line; $H\gamma$ is in absorption only; the line spectrum of *H* and *He* I is unusually strong for a Be star, and the rotational broadening, though noticeable, is relatively small

TABLE 9—*Continued*

Star	Dates of Observation	Description
MWC 140.....	11.25	No change; $H\beta$ is in emission; $H\gamma$ is continuous; the higher members of the Balmer series are in absorption and are exceptionally weak, broad, and diffuse; the rotational broadening of the *He* I lines is very large
164.....	11.25	No change
166.....	11.25	No change; the *He* I lines are narrower than in most Be stars, though Merrill's designation B1ne is probably correct
168.....	11.25	Probably no change, although our plate does not show emission at $H\gamma$
205.....	11.24	No change
221.....	7.31	Our plate shows no emission at $H\beta$
222.....	7.3; 7.5; 7.6	κ Dra; B5ne; our plates show no emission at $H\beta$
237.....	7.4	No change
249.....	7.17	No change
252.....	7.17	Probably no change
254.....	7.17	No change
278.....	7.4	$H\beta$ nearly continuous; $H\gamma$ weak absorption
279.....	7.3; 7.4	B9ne; very weak, broad emission at $H\beta$
291.....	7.30	No change
292.....	7.3	B5se; no emission on our plate
294.....	7.24	$H\beta$ and $H\gamma$ in emission
296.....	7.28	No change
301.....	7.29	No change
304.....	7.24	Fairly strong, single emission at $H\beta$; weak emission at $H\gamma$; $H\delta$ absorption only
305.....	7.3	$H\beta$ strong absorption; Merrill describes it as double(?) emission, int. 1
307.....	7.24; 7.29	No change
308.....	7.8; 7.10	$H\beta$ strong absorption; Merrill describes it as double emission, int. 1
309.....	7.24	$H\beta$ emission very weak
310.....	7.3	$H\beta$ almost continuous; $H\gamma$ and $H\delta$ have sharp absorption components over very broad absorption line
311.....	7.24	No emission at $H\beta$, but absorption line somewhat weak
312.....	7.3	B3ne; $H\beta$ fairly strong emission; $H\gamma$ shows a sharp absorption component over a broad absorption line, with an indication of weak double emission
316.....	7.12	Probably no change; the *H* emission lines are very strong
317.....	7.3	Supergiant B9se; $H\beta$ weak emission
318.....	7.8; 7.10; 7.12; 7.13	$H\delta$, $H\gamma$ moderately strong emissions
319.....	7.8; 7.10	B3n; our plates show only absorption at $H\beta$; the *H* and *He* I lines are broad and of normal intensity; the star must have possessed a shell when Merrill observed it to have narrow *H* absorption lines and very intense *He* I 4472, but the shell has completely disappeared
320.....	7.13	No change
322.....	7.8; 7.10; 7.16	No change
323.....	7.8; 7.10; 7.12	$H\beta$ in absorption, but there is a suspicion of widely spaced emission components, producing a shoulder in each wing
324.....	7.13	$H\gamma$ is very strong and broad absorption; $H\beta$ underexposed
326.....	7.8; 7.10; 7.16	Remarkable supergiant spectrum; $H\beta$ probably of P Cygni type; $H\zeta$ is strengthened and deepened by *He* I 3889, but, since all *He* I lines are sharp, it is impossible to decide whether there is a shell in addition to the normal supergiant reversing layer; the presence of *Mg* II 4481 suggests that there is no appreciable dilution
327.....	11.24	$H\beta$, $H\gamma$, $H\delta$, and possibly $H\epsilon$ are in emission; the rest of the spectrum is continuous with the exception of the interstellar *Ca* II lines

TABLE 9—*Continued*

Star	Dates of Observation	Description
MWC 328	7.13	No change
329	7.10; 7.25; 7.29	No emission at $H\beta$ or $H\gamma$
330	11.24	No change; $H\gamma$ may have a weak absorption core between broad emission components; all higher members of the Balmer series are continuous; the *He* I lines are also nearly continuous, except perhaps λ 4472, which shows very broad and weak absorption
331	7.10; 11.24	$H\beta$ emission fairly strong; probably no change
332	7.16; 7.29	Emission at $H\beta$ strong, at $H\gamma$ weak; $H\delta$ is in absorption; the higher Balmer lines are very broad and shallow
333	7.30	B3ne; no emission at $H\beta$
336	7.16; 7.24	No change; the *H* absorption lines are exceptionally broad and shallow
339	7.16	$H\beta$ in absorption only
340	8.1	No change
341	7.10; 7.24	No change
342	11.24; 11.25; 11.27	This is an exceptionally interesting star; the *H* lines consist of strong, double emission components, the intensity of the red component being two or three times greater than that of the violet; between the emission components are sharp, narrow absorption components, characteristic of shells; the emission components can be traced to about H_{12} or H_{13}, while the sharp shell absorption lines extend at least to H_{14} or H_{15}, where they are lost because of underexposure; in addition, there are strong permitted emission lines of *Fe* II, all of which are somewhat diffuse but show no duplicity; the strongest *Fe* II lines have sharp absorption lines on the violet sides and therefore resemble P Cygni lines; the line *Fe* II 4232 is of about the same intensity as the stronger component of $H\delta$; there is a weak emission line of *Mg* II 4481 and a suspicion of the *Si* II group at λ 3860; but the *Si* II pair λ 4128, λ 4130 is absent; there are no absorption lines other than those mentioned, excepting only a relatively weak, interstellar line of *Ca* II K; considering that the photographic magnitude is 10.8, the small intensity of *Ca* II K suggests a relatively low luminosity; the most important emission lines are as follows:

	Intensity			Intensity	
	Star	Lab.		Star	Lab.
Si II 3856	1−0	8	*Mg* II 4481	2	100
Si II 3863	1−0	6	*Fe* II 4489	3	4
H_8	1+2	60	*Fe* II 4491		5
$H\epsilon$	2+3	80	*Fe* II 4508	3	8
$H\delta$	4+6	100	*Fe* II 4515	4	7
Fe II 4173	2	8	*Fe* II 4520	5n	7
Fe II 4179	2	8	*Fe* II 4523		9
Fe II 4233	6	11	*Fe* II 4549	3	10
[*Fe* II] 4244	1−0	.....	*Fe* II 4556	3	8
[*Fe* II] 4277	1−0	.....	*Fe* II 4584	5	11
[*Fe* II] 4287	1−2	.....	*Fe* II 4621	1−0	3
Fe II 4297	1−0	6	*Fe* II 4629	4	7
Fe II 4303	1	8	$H\beta$	15	500
$H\gamma$	5+10	200			
Fe II 4352	5	9			
[*Fe* II] 4359	1	.....			
Fe II 4385	2	7			
[*Fe* II] 4414 / [*Fe* II] 4416	2n	.....			
Fe II 4417		7			
He I 4471	Trace	100			

TABLE 9—*Continued*

Star	Dates of Observation	Description
MWC 343.....	7.10; 7.24; 7.25	$H\beta$, $H\gamma$, and $H\delta$ show faint, sharp absorption cores superposed over very broad and shallow H lines; in $H\beta$ two widely spaced emission components are just discernible
345.....	7.17; 7.24	Emission is strong at $H\beta$ and fairly strong at $H\gamma$; $H\delta$ is in absorption only; Merrill describes $H\gamma$ as absorption
347.....	7.17	Supergiant; the appearance of $H\beta$ suggests P Cygni structure, with weak emission; the H lines are relatively weak; the last Balmer line is H_{17}, which would suggest $M = -3.8$ if the type is B1; however, the appearance of the other lines, notably the great strength and sharpness of *Si* IV and *N* III, imply a higher luminosity; it is probable that H is intrinsically weak
348.....	7.16; 7.29	Emission is strong and can be seen to $H\epsilon$ or $H\zeta$; it is fairly prominent in $H\delta$
350.....	7.24; 7.29	$H\beta$ emission; the *Ca* II line is very weak for type B9ne or B8ne
352.....	7.25	No emission at $H\gamma$; plate underexposed at $H\beta$
353.....	7.30	55 Cyg; no emission at $H\beta$; supergiant
354.....	7.17	Strong emission, visible as far as $H\delta$; the higher members of the Balmer series and the *He* I lines are very weak, broad, and shallow
355.....	7.17	B2ne; $H\beta$ is continuous; $H\gamma$ shows only weak absorption; Merrill describes $H\beta$ and $H\gamma$ as strong emission lines
356.....	7.17	No change; the emission components of $H\beta$ are very widely spaced
357.....	7.24; 7.26	No change; the higher members of the Balmer series are exceptionally broad, shallow, and weak
358.....	7.24; 7.26	Supergiant; no emission at $H\beta$
359.....	7.25; 7.29; 7.30	Weak emission at $H\beta$ and a suggestion of weak, sharp absorption core at $H\gamma$; the higher members of the Balmer series are very weak, broad, and shallow
Mt.W. 243 HD 236940 ...	11.26	Very weak emission is suspected at $H\gamma$ and $H\delta$ in the centers of broad and diffuse absorption lines; the plate is underexposed at $H\beta$

If the underlying star has strong, deep Lyman absorption lines and if the shell is stationary or expanding or contracting slowly, only a small part of the H atoms in the shell will be raised to the levels $n = 3, 4, \ldots$. If the shell is expanding or contracting rapidly, the absorption lines of the atoms in the shell may be shifted by the Doppler effect outside the absorption lines of the star, and fluorescence will operate. In such a case emission lines must be expected. Their intensity will depend essentially on the velocity and density distributions in the shell.

Evidently, if the underlying radiation is not depleted in those wave-length ranges which may be absorbed by atoms of the shell, fluorescence and recombination, excited by underlying radiation, will operate. This is the case, for example, in opaque shells containing their own photosphere, such as in P Cygni or in Wolf-Rayet stars. Yet, here also, care should be exercised because of stratification effects.

It may be pointed out that, since the fluorescence excitation in the shell depends on the velocities of the atoms, different shell lines of a specified atom (also lines belonging to different atoms) may give different profiles and radial velocities, both of the absorption and of the emission components. Actually, the physical interpretation of the profiles and of the measured line displacements is a matter of extreme complexity in shell stars. For example, the radial velocities of the *He* I triplets may be different from those of the singlets; such differences have been measured by Merrill[40] in AG Pegasi.

The essential cause of ejection is not yet clear in any type of shell (even Wolf-Rayet

[40] *Ap. J.*, **95**, 386, 1942.

stars or novae), although the rather safe assumption may be made that radiation pressure is an important factor. In the course of the evolution of a shell a slight change in density or velocity distribution or in the "quality" of the exciting radiation may appear, which enhances the fluorescence excitation. As a consequence, the selective radiation pressure in the resonance lines will increase, and a more or less sudden ejective outburst will result, owing to the fact that the increased velocity of the shell, relative to the reversing layer, displaces the shell absorption lines outside the depleted stellar regions. This explains the more or less sudden appearance of bright lines excited by fluorescence. The expansion will eventually slow down in the lower levels of the shell because of the radiation pressure from the Lyman α flux of the outer shell. Whereas a shell outburst is more or less sudden, the subsequent evolution will be much slower.

That turbulence and axial rotation play an important role in the fluorescence excitation is obvious. Let us consider the simple case of a nonexpanding shell surrounding a star with strong Balmer absorption lines. If the system does not rotate, or if it rotates as a solid body, the radiation reaching the shell will be considerably depleted in the wave lengths needed for the excitation of the hydrogen lines through Lyman line absorption. On the other hand, if the shell rotates with an angular velocity different from that of the central star, the underlying radiation reaching a specific point in the shell will be shifted by Doppler effect, and part of the exciting radiation may be able to excite the hydrogen atoms. Hence, axial rotation should be considered not only as a dynamical agent in the formation of a shell but also as a mechanism influencing the fluorescence excitation and the expansion which might possibly result from the corresponding radiation pressure.

These considerations may help in answering some of the puzzling questions concerning the formation and evolution of shells and the essential characteristics of their spectra. An extreme case which illustrates clearly the phenomena is that of the "nitrogen flaring stages" of novae. These stages in Nova Geminorum (1912) were described by W. H. Wright.[41] The following general description is quoted from Wright:

> The "4640" stage is produced by the development of the enhanced nitrogen radiations into broad nebulous bands, while the "ordinary" lines—assuming their behavior to be indicated by that of 3995 A—retain the normal structure. The phenomenon is accompanied by the complete or partial extinction of the "enhanced helium" radiation at 4686 A, and that of the emission, which sometimes accompanies it in the spectra of the nebulae, in position 3445 A. The "4640" stage, while it has generally been regarded as antecedent to the "nebular" stage, has been found to occur for short intervals of time during a long period after the latter stage has become established. It develops with great suddenness, and the transformation appears to be associated with marked fluctuations of the star.[42]

Bowen has suggested[43] that the concentration of the *N* III 452 line emitted at the end of the fluorescence transitions of *O* III and *N* III may become very large. "It may be this high radiation density of the resonance lines of *N* III that causes the nitrogen to appear to 'blow up' at certain stages of the development of the novae, as indicated by the very sudden and marked widening of the nitrogen lines."

We want to discuss this hypothesis and its spectroscopic consequences in the case of an expanding atmosphere. Before attempting this, the following considerations regarding the forbidden and permitted lines arising in a nebulous envelope which is growing outward and dissipating itself must be mentioned.

1. There exists in the deep layers of novae a general physical stratification which more or less resembles that of Wolf-Rayet stars, while in the outer layers the stratification is of the nebular type. The spatial distribution of the atoms emitting a specific line depends

[41] *Lick Obs. Pub.*, **14**, Part II, 90, 1925. Important observational information on this problem was kindly given to one of us (P. S.) by Dr. W. H. Wright, of the Lick Observatory; this help is gratefully acknowledged.

[42] *M.N.* **81**, 412, 1921.

[43] *Ap. J.*, **81**, 1, 1935.

on the excitation mechanism of the line, on the required ionization, and on the transition probabilities. For example, from the observations of widths, as well as from the relative values of the ionization potentials of He^+ (54.14 v.) and N^{++} (47.2 v.), we should expect the *He* II recombination spectrum to be emitted in deeper layers than the *N* III recombination spectrum. A recent investigation of the spectrum of Nova Herculis showed that the velocities of expansion measured for different atoms of the nebulosity are different, which also suggests stratification.[44]

2. Nova shells are often characterized by a lack of spherical symmetry in the distribution of expanding matter. In Nova Aquilae 1918, which grew into a visible disk, the different maxima of the bright bands came from different regions of the disk. Outbursts of *N* III radiation were observed only in the central portion of Nova Aquilae; they were accompanied by a temporary fading of the *He* II line λ 4686 in the center of the disk, while the λ 4686 radiation remained unaffected in the outer regions.

3. Any change in the exciting radiation will require a "relaxation time" to influence to a given extent the emission of a specific line in a specific region of the nebulosity.[45] As a consequence of these facts, a change in the exciting source will, at a given time, affect in a different way the total intensities and the profiles of the lines arising in the nova atmosphere.

The relative importance of the recombination and of Bowen's fluorescence mechanism in the emission of *O* III and *N* III lines has been discussed in a previous paper.[46] A sudden increase in selective radiation pressure due to the absorption of accumulated *N* III 452 photons may arise from a sudden variation in velocity gradient or in stratification such as would result from a variation in the amount of matter ejected per unit time. Such modification can evidently be expected in the course of the evolution of a nova in the nebular stage. When the ejection of nitrogen has become a predominant feature, the velocity and stratification conditions, which were favorable to Bowen's fluorescence, are destroyed. As a result the selective radiation pressure disappears, and after a rather short time the deep layers resume their more quiescent state. Bowen's hypothesis, combined with the considerations of velocity and stratification outlined here, may thus explain, at least qualitatively, sudden and temporary nitrogen outbursts.

The spectroscopic effects of a nitrogen outburst are evidently different for the following three categories of lines, differing with respect to the location of the corresponding emitting atoms: (1) the outer parts of the atmosphere, lying outside the regions where *N* III is emitted; (2) the *N* III emitting layers; and (3) the inner parts of the Wolf-Rayet layers, lying inside the regions of *N* III emission.

In the *N* III layers the enhancement of the incomplete fluorescence multiplets of *N* III must disappear and give place to a pure recombination spectrum, plus possibly a fluorescence excited by the "continuous" underlying radiation. Once the doubly ionized atoms have been ejected, their ionization may be modified, and we may thus also expect broad bands of *N* IV and probably of *N* II. Other chemical elements may be dragged with the nitrogen, especially the very abundant hydrogen, and this would explain the faint, broad bands of hydrogen that have been observed. If the emission of *N* II, III, or IV is also partly excited by the underlying radiation, together with the recombination mechanism, we may expect certain selectivities of the types discussed in previous papers.[47] While no such selectivity is conspicuous in Nova Geminorum 1912 for *N* III and *N* IV, it may help in explaining the observed behavior of *N* II.[48]

[44] Swings and Struve, *Ap. J.*, **96**, 468, 1942.

[45] In the case of the nebular shell of Z Andromedae, the calculated value of the relaxation time for the hydrogen emission was three or four weeks (*Ap. J.*, **93**, 356, 1941).

[46] *Ap. J.*, **96**, 254, 1942. [47] *Ap. J.*, **96**, 254, 1942.

[48] *N* II 3995 ($3s^1P^0-3p^1P$, exc. pot. 18.4 and 21.5 v.) persists undisturbed, in striking contrast to the *N* III lines. On the other hand, the *N* II lines, λ 5667 and λ 5680 ($3s^3P^0-3p^3D$, exc. pot. 18.4 and 20.6 v.), "sometimes follow the behavior of λ 4640 by becoming hazy when it flares and sometimes remain un-

The emission arising from the deepest Wolf-Rayet layers will be reduced by the continuous absorption of the flaring layers. The opacity associated with outer shells has been investigated recently;[49] it is probably the reason for the disappearance of the bright lines of *O* III and *He* II. The replacement of the emission of λ 4686 by an absorption feature is not surprising, since this absorption requires singly ionized atoms which may be present on the outskirts of the nucleus, whereas the recombination line λ 4686 requires He^{++} ions, which are more abundant in the deepest layers.

Summarizing, we may say that, when an adequate variation of the velocity gradient or stratification in the nova shells or of the quality of the underlying radiation appears, Bowen's fluorescence mechanism of *He* II, *O* III, and *N* III may become prominent. The selective radiation pressure by the accumulating quanta *N* III 452 may expel suddenly the N^{++} atoms (Bowen's suggestion), thus giving rise to very broad *N* III and *N* IV bands. Since this abnormal ejection destroys the conditions required for Bowen's fluorescence mechanism, the outburst is only temporary. Its spectroscopic effects depend on the location of the atoms considered. The variation in the exciting nucleus reacts on the intensities and profiles of the nebular lines arising from the outer nebulosity. The resulting line modifications depend on the distribution of matter and physical conditions in the nebulosity and on the various relaxation times. The most striking changes appear in the lines arising in the deepest Wolf-Rayet layers, which are completely removed by the continuous absorption of the flaring shell; the *He* II emission line arising in the inner Wolf-Rayet layers may even be replaced by an *He* II absorption line arising in the outskirts of the Wolf-Rayet "nucleus."

Eventually, this mechanism may possibly help in explaining the formation of peculiar associations such as have been observed in BD+30°3639, HD 167362,[50] and NGC 40, in which a pure carbon nucleus WC is surrounded by a nebulosity rich in nitrogen (characterized by strong [*N* II] lines). It is known that other planetary nuclei containing both carbon and nitrogen are also surrounded by a nebulosity showing strong [*N* II] lines (e.g., IC 418, IC 4997, NGC 6572, NGC 6210).

The general analogy of the nitrogen flaring stages of novae with the less spectacular variations observed in the Of, P Cygni, and Be stars is obvious.

---

altered" (Wright). The relative intensities and the profiles of the *N* II emission lines arising in the outer regions will not be very disturbed but the part arising from the flaring regions may reveal peculiar selectivity effects, due to a fluorescence excited by the underlying radiation.

[49] Struve, *Proc. Nat. Acad.*, **26**, 117, 1940; Swings and Struve, *Ap. J.*, **94**, 291, 1941; Baldwin, *Ap. J.*, **94**, 283, 1941.

[50] Better spectrograms than hitherto available have been obtained recently for the stellar planetary HD 167362 (see Pl. XXV). Besides the lines listed in our first report on this object (*Proc. Nat. Acad.*, **26**, 454, 1940), the following lines are observed: *C* II: 4267.2 (int. 2); *C* III: 4325.7 (2) and 5272.6 (1); *He* I: 3964.7 (1), 4713.1 (1), 4921.9 (1), and 5015.7 (2); *O* III: 3961.6 (1–0).

BD+14°3887, A PECULIAR Be STAR SHOWING EMISSION LINES OF *Na* I, [*Fe* III], AND *He* I; WITH A NOTE ON THE SPECTRUM OF CD–27°11944*

J. W. SWENSSON
McDonald and Yerkes Observatories
Received January 4, 1943

ABSTRACT

The peculiar Be star, BD+14°3887, shows emission lines of *H*, *He* I, *Fe* II, [*Fe* II], [*Fe* III], *Cr* II, *Mg* I, *Mg* II, and *Na* I. The combination of bright [*Fe* III], *He* I, and *Na* I lines is unusual. The absolute magnitude of the star, the mechanisms of excitation of the emission lines, and the properties of the shell are discussed.

New lines are found in the P Cygni star, CD−27°11944. Among these are the two permitted *Fe* III multiplets, $a^5P - 4p^5P^0$ and $a^5D - 4p^5P^0$, which are sensitive to dilution effects.

Merrill[1] has called attention to the presence of bright lines of hydrogen and ionized iron in the spectrum of BD+14°3887.[2] A more extensive study based on spectrograms obtained at the McDonald Observatory reveals many interesting features which constitute the object of the present paper. Seven spectrograms were taken between July 3 and July 27, 1942; they cover the region λλ 3370–6600, with various dispersions ranging from 40 to 100A/mm at λ 3933; the exposures varied between 1^h40^m and 7^h20^m.

An enlargement of the spectrogram obtained on July 27 is reproduced in Plate XXVI. The measured absorption and emission lines, reduced to the sun, are collected in Table 1. The laboratory wave lengths and intensities were taken from the usual tables.[3] Owing to the disparity of the radial velocities given by the different elements, the wave lengths have not been corrected for the motion of the star. In order to settle the question as to whether or not the object belongs to the same class of binaries as RW Hya, Z And, AX Per, CI Cyg, T CBr, RS Oph, BF Cyg, R Aqr, etc., a search for the bands of *TiO*, C_2, and *CN* was made by comparing our low-dispersion spectrograms with the spectra of typical late-type stars. No late-type absorption features were present in July, 1942. The interstellar H and K lines, as well as the broad, unidentified interstellar band around λ 4430 are present; but the H line of *Ca* II is blended with the P Cygni absorption component of *Hε*. A line measured at λ 6280 is probably Merrill's unidentified, diffuse interstellar line at λ 6284. The interstellar D lines have not been observed, but this may be due to the very low dispersion of our spectrogram covering the yellow region.

The spectra show lines due to *H*, *He* I, *Fe* II, [*Fe* II], [*Fe* III], *Cr* II, *Mg* I, *Mg* II, and *Na* I. Comparisons between our spectrograms covering a period of three weeks reveal differences which appear to be real; it is planned to investigate these spectral variations at some later time. The object is not listed as a variable star.

H.—The Balmer series is observed in emission to H_8. *Hδ* has a faint violet-absorption component. The P Cygni absorption component of *Hε* is blended with the neighboring interstellar line of *Ca* II. H_8 is blended with *He* I 3889. H_9 and H_{10} appear essentially in absorption, but H_9 may have a faint emission on its red side. No appreciable Balmer continuum is observed on our spectrogram extending to λ 3370.

* *Contributions from the McDonald Observatory, University of Texas*, No. 65.

[1] *Ap. J.*, **65**, 292, 1927.

[2] MWC 314; α (1900) = 19^h17^m0; δ (1900) = +14°42′; m_{vis} = 9.5 (in BD cat.); spectrum Bep.

[3] *Fe* II: J. C. Dobbie, *Ann. Solar Phys. Obs.*, **5**, Part I, 1938; *Fe* III: B. Edlén and P. Swings, *Ap. J.* **95**, 532, 1942; all other elements: C. E. Moore, *A Multiplet Table of Astrophysical Interest*.

PLATE XXVI

(*a*) BD +14°3887; (*b*) CD −27°11944

UNIV. OF MICH.

TABLE 1

LINES IN BD+14°3887

λ	Int.*	N†	Identification			Note
			Element	λ	Int.	
3795.5	0A	1	H_{10}	3797.90	.....	1
3818.7	1A	1	He I	3819.61	4	
3835.2	0A	1	H_9	3835.39	.....	2
3889.6	3E	4	He I	3888.65	10	3
			H_8	3889.05	.....	
3933.6	4A	4	Ca II	3933.68	400	
3965.7	2E	1	He I	3964.73	4	4
3968.8	4A	4	Ca II	3968.49	350	
			$H\epsilon$	3970.08	.....	
3970.3	4E	3	$H\epsilon$	3970.08	.....	5
4100.6	1–2A	1				
4102.5	5E	4	$H\delta$	4101.75	.....	6
4179.4	0E	2	Fe II	4178.86	8	
4234.1	2E	3	Fe II	4233.17	11	
4287	0–1E	1	[Fe II]	4287.40	.....	
4313.6	1E	3	Fe II	4314.29	4	7
4341.2	7E	5	$H\gamma$	4340.48	.....	
4351.6	3E	3	Fe II	4351.76	9	
4359.2	2E	2	(Fe II	4357.57)	4	
			[Fe II]	4359.34	.....	
4384.8	3E	3	Fe II	4385.38	7	7
			He I	4387.93	3	
4416.7	2E	3	Fe II	4416.82	7	7
4472.1	4E	3	He I	4471.48	6	
4482.0	0–1E	2	Mg II	4481.14	100	7
				4481.34		
4491.3	3E	4	Fe II	4489.19	4	7
				4491.40	5	
4508.1	3E	3	Fe II	4508.28	8	7
4515.6	3E	3	Fe II	4515.34	7	7
4522.0	3E	3	Fe II	4520.23	7	7
				4522.63	9	
4550.4	1–2E	4	Fe II	4549.47	10	7
4556.8	2–3E	4	Fe II	4555.89	8	
4583.7	3E	4	Fe II	4583.83	11	
4620.4	3E	2	(Cr II	4618.79)	10	
			Fe II	4620.51	3	
4630.4	3E	3	Fe II	4629.34	7	
4658.0	2E	2	[Fe III]	4658.05	.....	
4824	1–0E	1	Cr II	4824.14	10	
4848.4	2E	2	Cr II	4848.26	8	8
4862.6	10E	4	$H\beta$	4861.34	.....	
4923.0	6E	2	He I	4921.93	4	
			Fe II	4923.92	12	
5016.8	7–8E	1	He I	5015.68	6	
			Fe II	5018.43	12	

* A and E designate absorption and emission features, respectively. The intensities are eye estimates based on a scale of 0–12, 0 indicating a very faint feature. Unidentified lines of intensity 0 have not been included in the table. For lines appearing on more than one spectrogram the average of the independent intensity estimates is given.

† *N* designates the number of spectrograms from which measures were taken in determining the average wave length.

TABLE 1—*Continued*

λ	Int.*	N†	Identification			Note
			Element	λ	Int.	
5167.2	7–8E	1	*Fe* II	5169.03	12	
5182.0	2E	1	*Mg* I	5183.62	125	
5196.3	2E	1	*Fe* II	5197.57	6	
5234.4	3E	1	*Fe* II	5234.63	7	
5262.1	1E	1	*Fe* II	5260.33	5	
5273.7	2?E	1	[*Fe* III]	5270.41	.....	
			Fe II	5275.99	7	
5315.4	3E	1	*Fe* II	5316.61	8	
				5316.78	4	
5365.0	2?E	1	*Fe* II	5362.86	5	
5876.4	7E	1	*He* I	5875.62	10	
5900	3–4E	1	*Na* I	5889.98	8	
				5895.94	10	
6280	2A	1	.....	.....	.....	
6561.7	12E	1	*Hα*	6562.82	.....	

NOTES TO TABLE 1

1. Pure absorption.

2. Faint P Cygni emission also present.

3. On July 27, 1942, this line was due to *He* I only, since *Hε* was absent or extremely weak.

4. Observed on only one spectrogram; however, it seems to be real.

5. On July 27, 1942, *Hε* was very weak or absent, whereas it was strong on the other spectrograms (see n. 3).

6. Measure difficult. A faint P Cygni absorption component is present on the four spectrograms of highest dispersion.

7. Measure difficult.

8. This line is one of the strongest, unblended *Cr* II lines in RS Ophiuchi (in emission, Swings and Struve, *Ap. J.*, **97**, 194, 1943) and in α Cygni (in absorption, Struve and Swings, *Ap. J.*, **94**, 344, 1941).

He I *triplets.*—λ 3889($2s^3S - 3p^3P^0$) is blended with H_8. The $2p^3P^0 - md^3D$ series is represented by λ 5876 ($2p^3P^0 - 3d^3D$) and λ 4471($2p^3P^0 - 4d^3D$) in emission and by λ 3820 ($2p^3P^0 - 6d^3D$) in absorption; λ 4026 ($2p^3P^0 - 5d^3D$) seems to be absent.

Singlets.—The following singlets are blended with *Fe* II lines: λλ 4922 ($2p^1P^0 - 4d^1D$), 4388 ($2p^1P^0 - 5d^1D$), 5016 ($2s^1S - 3p^1P^0$). The line λ 3965 ($2s^1S - 4p^1P^0$), which is unblended, is found on only one spectrogram.

Intensity ratio of the triplets and singlets.—This is difficult to estimate because of blends. But the triplets are certainly much stronger than the singlets of corresponding spectroscopic notation.

Fe II.—The observed lines of *Fe* II are rather broad and diffuse. The line intensities are given in Table 2. In so far as the intensities are only eye estimates, differences among the spectrograms may or may not be real; but the following markedly anomalous intensities are to be noted: the weakness of the λ 4233 line in comparison to the other members of the $b^4P - z^4D^0$ multiplet, the extreme weakness or absence of the λ 4303(lab. int. 8) line of the same multiplet, and the great strength of λλ4924, 5018, 5169 of the $a^6S - z^6P^0$ multiplet. The intensity of the first two lines is explained at least in part by blends with *He* I 4922 and *He* I 5016, respectively. The line λ 5169 appears slightly too strong for its

TABLE 2

OBSERVED EMISSION LINES OF *Fe* II

MULTIPLET (LOW E.P.–HIGH E.P.)	TRANSITION	λ (DOBBIE)	INT. (DOBBIE)	OBSERVED INTENSITY*				NOTE
				July 3	July 5	July 12	July 27	
$b^4P-z^4P^0$								
(2.6 v.–5.5 v.)	$2\frac{1}{2}-3\frac{1}{2}$	4178.86	8	.....	.....	0	0	
$b^4P-z^4D^0$								
(2.6–5.5)	$2\frac{1}{2}-3\frac{1}{2}$	4233.17	11	.....	3	2	0	1
(2.7–5.5)	$1\frac{1}{2}-2\frac{1}{2}$	4351.76	9	4	4	2	2	
(2.8–5.6)	$\frac{1}{2}-\frac{1}{2}$	4385.38	7	.....	3	3	3	2
(2.8–5.6)	$\frac{1}{2}-1\frac{1}{2}$	4416.82	7	2	.....	1	2	
.....	.....	4314.29	4	.....	.....	1	1	
.....	.....	4357.57	4	2	3	.....	.....	3
$b^4F-z^4F^0$								
(2.8–5.6)	$3\frac{1}{2}-2\frac{1}{2}$	4489.19	4	3	2	0	3	
	$1\frac{1}{2}-1\frac{1}{2}$	4491.40	5					
(2.8–5.6)	$2\frac{1}{2}-2\frac{1}{2}$	4515.34	7	3	3	1	3	
(2.8–5.5)	$4\frac{1}{2}-3\frac{1}{2}$	4520.23	7	3	3	1	3	4
(2.8–5.5)	$3\frac{1}{2}-3\frac{1}{2}$	4555.89	8	3	3	1?	2	5
(2.8–5.5)	$4\frac{1}{2}-4\frac{1}{2}$	4629.34	7	5	3	2	3	6
$b^4F-z^4D^0$								
(2.8–5.6)	$1\frac{1}{2}-\frac{1}{2}$	4508.28	8	3	3	1	3	
(2.8–5.6)	$2\frac{1}{2}-1\frac{1}{2}$	4522.63	9	3	3	1	3	4
(2.8–5.5)	$3\frac{1}{2}-2\frac{1}{2}$	4549.47	10	1	2	1?	2	7
(2.8–5.5)	$4\frac{1}{2}-3\frac{1}{2}$	4583.83	11	5	3	3	3	8
(2.8–5.5)	$3\frac{1}{2}-3\frac{1}{2}$	4620.51	3	5	3	.....	.....	9
$a^6S-z^6P^0$								
(2.9–5.4)	$2\frac{1}{2}-1\frac{1}{2}$	4923.92	12	.....	6	6	.....	10
(2.9–5.3)	$2\frac{1}{2}-2\frac{1}{2}$	5018.43	12	.....	7	8	.....	11
(2.9–5.3)	$2\frac{1}{2}-3\frac{1}{2}$	5169.03	12	.....	7	8	.....	
$a^4G-z^4F^0$								
(3.2–5.6)	$2\frac{1}{2}-1\frac{1}{2}$	5197.57	6	.....	.....	2	2	
(3.2–5.6)	$3\frac{1}{2}-2\frac{1}{2}$	5234.62	7	.....	.....	3	3	
(3.2–5.5)	$4\frac{1}{2}-3\frac{1}{2}$	5275.99	7	.....	.....	2?	.....	
.....	.....	5260.33	5	.....	.....	1	.....	
$a^4G-z^4F^0$								
(3.1–5.5)	$5\frac{1}{2}-4\frac{1}{2}$	5316.61	8	.....	.....	3	3	
$a^4G-z^4D^0$								
(3.2–5.5)	$3\frac{1}{2}-2\frac{1}{2}$	5316.78	4					
(3.2–5.5)	$4\frac{1}{2}-3\frac{1}{2}$	5362.86	5	.....	.....	1	1	

* When no intensity is given, the line was not measured or observed.

NOTES TO TABLE 2

1. The line is abnormally weak.
2. The line is probably a blend with *He* I 4388.
3. The observed line is rather strong for Dobbie's intensity. Its identification with [*Fe* II] is discussed under [*Fe* II].
4. The lines are blended.
5. This line, as a blend with *Cr* II 4558.65(20), is considered under *Cr* II.
6. This line, as a blend with *Cr* II 4634.08(10), is considered under *Cr* II.

7. The line is a little weak for its laboratory intensity.

8. This line, as a blend with *Cr* II 4588.21(15), is considered under *Cr* II.

9. The observed line is abnormally strong for the laboratory intensity 3. It is considered as a blend with *Cr* II 4619 under *Cr* II.

10. The line is a blend with *He* I 4922.

11. The line is a blend with *He* I 5016.

laboratory intensity in Z Canis Majoris[4] also. No absorption components are found for the members of this sextet as in Z Canis Majoris.[5] Aside from the anomalies here mentioned, the intensities agree well with those found in the laboratory.

[*Fe* II].—The line measured at λ 4359 is identified as a blend of [*Fe* II] 4359 and *Fe* II 4358. The role played by the permitted transition in this blend, if any, is probably minor. *Fe* II 4358 (unclassified in Dobbie) is probably a high-level line, since most of the low-level lines have been classified. Since the observed *Fe* II lines all arise from low levels and since the permitted line λ 4358 is absent in bright-line stars having strong *Fe* II lines, it seems very improbable that the permitted transition could play a significant role in the blend. [*Fe* II] 4287 appears also as a faint line on the spectrogram of July 5.

[*Fe* III].—The strongest line, λ 4658($^5D_4 - {}^3F_4$), is observed on our spectrograms of July 12 and 27. The line λ 5270.4 ($^5D_3 - {}^3P_2$) is blended with *Fe* II 5276.

Cr II.—The stellar line measured at λ 4620.4 is much too strong to be attributed to *Fe* II 4621 (lab. int. 3) only; *Cr* II 4619 must contribute appreciably. However, the line λ 4621 also appears abnormally strong in Z Canis Majoris,[6] a star in which *Cr* II has not been definitely identified. The line measured at λ 4848.4 is due to *Cr* II; it is one of the strongest *Cr* II lines in all stellar spectra in which *Cr* II is observed. The contributions of the *Cr* II lines λλ 4559, 4588, 4634 to blends with *Fe* II are probably minor, since the estimated stellar intensities agree fairly well with Dobbie's values. *Cr* II 4824 is found on our spectrogram of July 27.

Mg I.—λ 5184 is present in emission.

Mg II.—A faint emission line at λ 4482 was measured on two of the spectrograms.

Na I.—The blended D lines are present in emission. HD 190073, CD–27°11944, and γ Cassiopeiae are the only other stars, aside from the novae, known to the author to have $D_{1,2}$ in emission.

Radial velocities.—The values obtained have little accuracy owing to the great width of the lines. The emission lines give the following results:

$$H\beta, \gamma, \delta\text{: } v_{rad} = +53 \text{ km/sec}^{7}, \qquad He \text{ I } 4472\text{: } v_{rad} = +34 \text{ km/sec},$$

$$He \text{ I } 3965\text{: } v_{rad} = +72 \text{ km/sec},$$

$$Fe \text{ II (from λλ 4629, 4584, 4549, 4515, 4233, 4179)}\text{: } v_{rad} = +54(\pm 30) \text{ km/sec}.$$

From the absorption lines we obtain the following ejection velocities:

$$H\delta\text{: } v_{ej} = -140 \text{ km/sec},$$

$$He \text{ I } 3820 \text{ (abs.) compared with } He \text{ I } 4472 \text{ (em.)}\text{: } v_{ej} = -104 \text{ km/sec}.$$

Absolute magnitude of the star.—The star is located on the edge of the great rift in Aquila,[8] a region known for its high obscuration. That a considerable amount of redden-

[4] P. Swings and O. Struve, *Ap. J.*, **96**, 259, 1942. [5] *Ibid.*, p. 258. [6] *Ibid.*, p. 259.

[7] Merrill finds +33 km/sec from *Hβ* and *Hγ* (*loc. cit.*). Our value obtained from *Hβ*, γ, δ is much more accurate than the value from the *Fe* II lines.

[8] See F. E. Ross and M. R. Calvert, *Atlas of the Milky Way*, Pl. XIII; 142 mm from the left edge and 169 mm from the top edge.

ing takes place is indicated by the weakness of the ultraviolet region of the spectrum of this hot star.

In a peculiar object, such as the present one, determinations of distance based on the interstellar K line[9] are subject to considerable doubt, since it is possible that absorption in the shell contributes to some extent to the intensity and position of the observed line. From the example of HD 190073,[10] it is clear that great caution has to be exercised in interpreting the *Ca* II profiles in shells.

Careful measurements of the radial velocity from the K line give a value of −7 km/sec, which, interpreted on the basis of pure galactic rotation, would indicate a distance of about 1300 parsecs. Besides the uncertainty residing in the pure application of the galactic-rotation formula, the measured radial velocity may be in error by several km/sec, so that the distance is rather uncertain, even assuming that the shell does not contribute to the line.

Two microphotometric measurements of the equivalent width of K give 0.8 and 1.0 A, with possible errors of 10–20 per cent. Adopting a minimum value of the equivalent width of 0.6 A, the stellar distance on the basis of Evans' formula[11] is of the order of 1800 parsecs. This determination is also subject to considerable uncertainty.

A more reliable value of the distance has been obtained by the following method: By comparing the distribution of light in the continuum of BD+14°3887 with that in the spectra of late-type stars taken with the same spectrograph and emulsion, a color about equal to that of a gG2–3 or dG4–5 star is indicated, whereas the excitation is about that of a B2 star, yielding a color excess of roughly 1.3 mag.[12]

An apparent photographic magnitude of 10.9 ± 0.3 is obtained by comparing the star on the Franklin-Adams charts with stars in a neighboring region, for which accurate magnitudes have been determined by H. Weaver.[13] A rough photovisual magnitude of 10.4 ± 0.2 determined by comparing two plates taken by G. Van Biesbroeck with the 24-inch reflector of the Yerkes Observatory, one of the star and the other of the neighboring field studied by Weaver,[13] gives a color index of 0.5 mag. and a color excess of 1.1 mag.,[14] agreeing, within the errors of the determination, with the above value of 1.3 mag.

Using a value of 4 for the ratio of the general absorption to the color excess and a value of 1.2 mag. for the color excess, the absorption is found to be 4.8 mag.

An inspection of the Ross and Calvert *Atlas of the Milky Way* shows that this star is probably in the same cloud as was studied by Weaver[13] (a small region about 6° south of the star). An absorption-curve constructed by him for this region indicates that the absorption of 4.8 mag. given above corresponds to a distance of 890 parsecs.

This distance may have to be reduced, owing to reddening in the immediate vicinity of the star itself. Sherman and Morgan[15] find a reddening in the shell of P Cygni amounting to about 0.5 mag. If a color excess of as much as 0.5 mag. originated in the shell of the present star, the absorption due to interstellar reddening alone would be 2.8 mag., assuming that the ratio of the absorption to the color excess is still 4 in the envelope of the star. This corresponds to a distance of 590 parsecs.

[9] The H line is excluded altogether, because of the blending effect of the P Cygni absorption component of $H\epsilon$.

[10] C. S. Beals, *J.R.A.S. Canada*, **36**, 145 and 201, 1942; O. Struve and P. Swings, *Ap. J.*, **96**, 475, 1942.

[11] *Ap. J.*, **93**, 275, 1941.

[12] CE of the star = CI of a gG2–3 star − CI of a B2 star = 0.7 − (−0.6) = 1.3.

[13] Unpublished.

[14] Assuming, still, that we are dealing with a B2 star of color index −0.6.

[15] *Ap. J.*, **89**, 509, 1939.

An absolute photographic magnitude of -3.6 is found by using $m_{pg} = 0.9$, $A = 4.8$ mag., and $r = 890$ parsecs. The value of the absolute photographic magnitude is very uncertain, however, since we do not know how much of the color excess is produced in the immediate vicinity of the star itself. Using a value of 2.8 mag. for the absorption (A) and the corresponding distance of 590 parsecs, we get an absolute photographic magnitude of -0.8, giving us a rather wide range on the absolute-magnitude scale and a probable distance of 700–900 parsecs.

The photospheric layer.—Other than the interstellar absorption features, the only absorption lines measured are the P Cygni absorption component of *H* δ, *He* I 3820, and two very faint features identified as H_9 and H_{10}. The latter three features all have negative velocity displacements and are considered to be P Cygni absorption components arising in the shell of the star.

The members of the Balmer series appear as rather narrow emissions, apparently without any underlying, broad-winged absorption, which in normal B stars would be attributed to absorption in the reversing layer of the underlying star. Hence it is apparent that we are dealing with a star like P Cygni, RY Scuti, Z Canis Majoris, or CD–27° 11944,[16] in which the opacity of the shell is large. Only the spectrum of the shell is observed, and all possible features arising in the underlying star are obscured, owing to the great optical thickness of the envelope, which is absorbing and emitting a continuous spectrum of its own.

The shell.—From the great relative intensity of the *He* I triplets compared to the singlets,[17] we may conclude that the *He* I emission is for the major part due to the recombination mechanism. Such a mechanism is also at least partly responsible for the *Fe* II emission, since the presence of *Fe* III implies the existence of Fe^{++} ions, hence the possibility of electron captures by Fe^{++}. Yet collisional excitation may also be in operation for the *Fe* II spectrum, owing to the small energies of the excited *Fe* II levels concerned. Such a collisional mechanism is precluded for the *H* or *He* I spectrum, however, since the excited states of *H* and *He* I have potentials far in excess of the energies of electrons at reasonable electron temperatures.

The intensity of [*Fe* III] 4658 appears to be about equal to or a little greater than that of the strongest [*Fe* II] line. In this connection it is of interest to place the shell in a sequence of shells having decreasing excitation, using the intensity ratio [*Fe* II]/[*Fe* III] as a criterion of the excitation.[18] Thus we have RY Scuti[19] (strong [*Fe* III], no [*Fe* II]), BF Cygni[20] (strong [*Fe* III], intermediate [*Fe* II]), DO Aquilae 1925[21] (strong [*Fe* III], strong [*Fe* II]), MWC 349[22] (weak [*Fe* III], weaker [*Fe* II]), BD+14°3887 (weak [*Fe* III], weak [*Fe* II]), MWC 17[23] (strong [*Fe* II], weak [*Fe* III]), CD−27°11944[24] (very weak [*Fe* II] only), and η Carinae[25] (strong [*Fe* II] only).

The first ionization potentials of *Na* and *Mg* are, respectively, 5.1 and 7.6 volts. Hence practically all the *Na* and *Mg* atoms must be ionized, and the observed *Na* I and *Mg* I lines are emitted essentially by the recombination mechanism. Since the second ionization potential of *Na* is 47.0 volts, practically all the *Na* atoms will be in the singly ionized state in all parts of the shell. *Mg* II 4481 has a fairly high excitation potential (11.6 volts),

[16] For a description of the spectra of these objects see P. Swings and O. Struve, *Ap. J.*, **91**, 546, 1940, and **96**, 254, 1942.

[17] P. Swings and O. Struve, *Ap. J.*, **96**, 260, 1942.

[18] *Ibid.*, **93**, 351, 1941. [19] *Ibid.*, **91**, 546, 1940. [20] *Ibid.*, **97**, 194, 1943.

[21] B. Vorontsov-Velyaminov, *Ap. J.*, **92**, 283, 1940.

[22] Swings and Struve, *Ap. J.*, **95**, 159, 1942.

[23] *Ibid.*, **93**, 349, 1941. [24] *Ibid.*, p. 352.

[25] J. H. Moore and R. F. Sanford, *Lick Obs. Bull.*, **8**, 55, 1913; P. W. Merrill, *Ap. J.*, **67**, 391, 1928; H. Spencer Jones, *M.N.*, **91**, 794, 1931; and esp. I. S. Bowen, *Rev. Mod. Phys.*, **8**, 55, 1936 (esp. pp. 80–81).

so that excitation by electron collisions is definitely excluded. The second ionization potential of *Mg* being only 15 volts, we may expect the *Mg* II line to be due mostly to the recombination mechanism, although optical excitation by the underlying radiation is not altogether excluded. Since the third ionization of *Mg* is approximately 80 volts, no *Mg* atoms will be more than doubly ionized in the shell.

Note on the spectrum of CD–27°11944.—An excellent spectrogram of this star, showing the region $\lambda < 5600$, was obtained at the McDonald Observatory on July 24, 1942. It reveals the following lines in addition to those listed by Swings and Struve (Pl. XXVI):[26]

Fe II: 4508(1–2E), 4515(1–2E), *Mg* II: 4481(1A, 2E),

Fe III: 5127(1A, 2E), 5156(1A, 2E) (very close to [*Fe* II] 5159),

4420(1–2E) (very close to *Fe* II 4417 and [*Fe* II] 4416).

Several emission lines which did not show any trace of absorption companions in 1940 have now acquired such components. The spectrum of this star is definitely variable.

It should be noticed that the observed *Fe* III lines belong to the two multiplets $a^5D - 4p^5P^0$ and $a^5P - 4p^5P^0$. As has been shown previously,[27] these two multiplets, whose lower levels are metastable,[28] are especially sensitive to dilution effects. None of the other *Fe* III lines, which are much stronger in the laboratory but which connect high nonmetastable levels, is found in this star. This means that the observed *Fe* III lines are not emitted by the recombination mechanism. Since collisional excitation is excluded for λλ 5127, 5156, and 4420 because of the high energy of $4p^5P^0$(11.0 volts), these lines must then be excited in Rosseland fluorescence cycles excited by the underlying radiation.[29]

As far as *Fe* III is concerned, CD–27°11944 is indeed very similar to P Cygni, and the dilution factor must also be at least 0.1. But the excitation is much lower in CD–27°11944 than in P Cygni, as is shown by the *Fe* II emission; CD–27°11944 also differs from P Cygni in that the former shows faint [*Fe* II] lines.

My thanks are due to Drs. O. Struve, P. Swings, and H. Weaver for fruitful discussions and advice.

[26] *Ap. J.*, **93**, 352, 1941.

[27] Edlén and Swings, *loc. cit.*

[28] Actually these are the lowest metastable *Fe* III levels observable by permitted lines in the astronomical region.

[29] Edlén and Swings, *loc. cit.*

THE SPECTRUM OF HD 192954*

ARTHUR A. BROYLES[1]
McDonald Observatory
Received January 31, 1943

ABSTRACT

The star HD 192954 was given a spectral classification B9 in the *Henry Draper Catalogue* and A2e by P. W. Merrill. This raises the question of the presence of a shell. Since the contours of the hydrogen lines show very narrow and deep central cores with broad shallow wings to each side, it is evident that part of the absorption takes place in a dense layer corresponding to a star of the main sequence and part in a layer of very low pressure. The weakening of *Mg* II and of *Si* II lines indicates further that dilution takes place in the outer layer and that therefore the layer is probably a shell of the type of Pleione. The presence of helium, together with other facts, indicates that the star itself is of type B9n. The radial velocity is about +15 km/sec. A list of lines measured in the spectrum of HD 192954 from λ 3321 to λ 5479 is given in Table 2.

1. The star HD 192954[2] = MWC 335 was announced by Merrill[3] to have a strong bright line at $H\alpha$ and a weak double bright line at $H\beta$. Earlier observations by Humason confirmed the character of $H\beta$. Since the spectral type is given as A2e by Merrill and as B9 by Miss Cannon, the following questions arise: (1) Is the star a supergiant, or has it

TABLE 1

OBSERVATIONS OF HD 192954

Plate	Date	U.T.	Emulsion	Exposure (Min.)
CQ 1554.....	1942, July 13	9^h37^m	103a0	34
1576.....	17	5 45	103a0	15
1582.....	18	3 27	103a0	15
1583.....	18	3 49	103a0	8
1586.....	24	5 36	Plenachrome	15
1803.....	Dec. 26	1 30	103a0	35
1825.....	30	1 15	103a0	35
1835.....	31	1 14	103a0	60

a moderate luminosity? (2) Does the relatively late spectral type signify that it is a representative of the group of stars designated as "shell stars" (similar to Pleione in its present stage)? (3) Does the difference in spectral type between Harvard and Mount Wilson signify that the spectrum is variable and that the metallic lines have increased gradually in intensity while the *He* I lines have disappeared?

2. The material available consisted of several plates of the spectrum taken with the Cassegrain quartz spectrograph and the 500-mm camera at the McDonald Observatory. These are listed in Table 1. Plates CQ 1582, 1583, 1803, 1825, and 1835 were used only for the measurement of radial velocities. Plate CQ 1554 was measured in the ultraviolet region from λ 3321 to λ 3727; plate CQ 1576 was measured from λ 3662 to λ 4667, and

* *Contributions from the McDonald Observatory, University of Texas*, No. 66.

[1] Mr. Broyles has left the observatory in order to join the Armed Forces.

[2] MWC 335; $\alpha = 20^h12^m6$; $\delta = +15°33'$ (1900); magnitude, 7.3; spectrum, A2e (Merrill), B9 (HDC).

[3] *Ap. J.*, **78**, 107, 1933.

plate CQ 1586 was measured from λ 4729 to λ 5478. The contrast of plate CQ 1586 is inferior to that of the other two plates, so that intensities assigned to lines in the visual region are not comparable with those in the ultraviolet region. However, an attempt was made to keep the intensities consistent on plates CQ 1554 and CQ 1576.

3. A list of the absorption lines found on the plates with wave lengths reduced for radial velocity is given in Table 2. Almost all the lines were identified with the aid of tables of lines in α Cygni.[4] This was done because α Cygni is an A2 star and the lines are much stronger in it. The lines in HD 192954 were, therefore, identified (with few exceptions) with those in α Cygni, and the identifications of the α Cygni lines were then used. The intensities in α Cygni are given in the third column. Since the ultraviolet region (λλ 3321–3938) of α Cygni was investigated with the Cassegrain quartz spectrograph (CQ) and the visual region (λλ 3865–5479) with the coudé spectrograph, the intensities of the two α Cygni tables are not comparable. Because plate CQ 1576 was underexposed and plate 1586 overexposed in the region around $H\beta$, some lines may have been omitted that would otherwise have appeared. Lines of HD 192954 with intensities of zero are considered questionable or extremely weak, while higher intensities are indicated by the numbers 1, 2, 3, etc. The source of the laboratory intensities is listed as follows:

H I.....M.I.T.*	*Mn* II...Moore‡	*Cr* II....Moore‡
Fe I....M.I.T.*	*Ca* II...Moore†	*Ni* II...Moore‡
Ni I....M.I.T.*	*He* I....M.I.T.*	*V* II....Meggers & Moore‖
S II.....M.I.T.*	*Mg* I....Moore‡	*Lu* II...Moore†
Cr I....M.I.T.*	*Al* I....Moore†	*Y* II....Moore†
Mg II...Moore†	*Al* II....Moore†	*Cl* II....M.I.T.*
Si II....Moore†	*Ca* I....Moore†	*Zr* II....M.I.T.*
Ti II....Moore†	*Yb*.....Moore†	*A* I.....M.I.T.*
Sc II....Moore†	*Fe* II....Dobbie§	*K*.....M.I.T.*

* *Massachusetts Institute of Technology Wavelength Tables.*
† Charlotte E. Moore, *A Multiplet Table of Astrophysical Interest.*
‡ Charlotte Moore Sitterly's unpublished material.
§ J. C. Dobbie, *Annals of the Solar Physics Observatory*, Vol. **5**, Part 1.
‖ National Bureau of Standards, *Research Paper RP 1317.*

In order better to compare the intensities of various elements in the two stars, Table 3 gives certain lines of HD 192954 by elements. Only those lines were chosen which are unblended or very slightly blended.

4. The star has now an absorption spectrum of approximately type A2. Since none of the plates at hand extends to $H\alpha$, this line could not be investigated; but $H\beta$ seems to have weak emission lines on each side, with the one toward the violet most distinct. The rest of the hydrogen lines are in strong absorption.

Underexposed plates show very broad hydrogen lines, while overexposed plates show, in addition, deep, narrow cores. This indicates that the lines have broad shallow wings with sharp deep cores in the middle. The broad wings are caused by the Stark effect and indicate that they originate in a dense layer. The star cannot, therefore, be a supergiant but must be of relatively low luminosity. The narrow lines of great absorption in the centers, however, must come from a much less dense outer layer. Since these cores coincide with the centers of the broad wings, this layer must be stationary with respect to the star.

Upon comparison of the *Mg* II and *Si* II lines in α Cygni and HD 192954, it becomes apparent that these lines are weakened in HD 192954. The line *Mg* II 4481.39 shows this clearly and by direct comparison to the line *Fe* II 4416.80. The *Si* II line λ 3856.14 was found to be much weaker in HD 192954 than the *Mg* I line 3838.29, while the reverse is true in α Cygni. Line λ 3862.61 of *Si* II is quite strong in α Cygni ($I = 6$) but is not strong enough to be measured in HD 192954. The *Si* II lines λ 4128.13 and λ 4131.26

[4] Struve, *Ap. J.*, **90**, 699, 1939; Struve and Swings, *Ap. J.*, **94**, 344, 1941.

are also quite strong in α Cygni (I = 8) but are barely visible in HD 192954 ($I = 0$). This shows unquestionably that geometrical dilution is having effect. The lines of these elements are not appreciably broader than those of *Fe* II and *Ti* II and give no indication of rapid rotation. They may originate in the deeper strata of the shell.

The proof of the existence of *He* I is rendered difficult by the presence of strong metallic lines near by. Both lines, λ 4025.48 and λ 4472.28, were found to be nebulous on plate CQ 1576, and other plates confirm this. The line λ 4472.28 appeared to be made up of two components 1.76 A apart on a plate of greater exposure. These two components must be λ 4471.48 of *He* I and λ 4472.92 of *Fe* II. In the same way it was found that line λ 4025.48 was made up of two components 1.30 A apart. One component must be due to *Ti* II, and the other to *He* I. From the nebulous appearance of the *He* I lines we conclude that the observed equatorial rotation of the star is of the order of 150–200 km/sec. The spectral type of the star itself must be about B8.

The different atoms and ions shown in the spectrum are arranged below in the order of decreasing ratio: HD 192954/α Cygni. This list is comparable to the one by Struve and Swings[5] for Pleione:

Mn II, *Fe* I, *Mg* I, *Cr* II, *Ti* II, *Sc* II, *Ni* II, *V* II, *Fe* II, *Ca* II, *Mg* II, *Al* I, *Si* II.

It is interesting to note that *Fe* I and *Mg* I are relatively strong in HD 192954. Only one line of *Al* I is available, so that its position cannot be determined accurately in this list. Since only two lines were available for *Mn* II, its position is also uncertain.

5. The radial velocity of HD 192954 was determined as follows:

Date	Vel. (Km/Sec)	Qual.	Date	Vel. (Km/Sec)	Qual.
1942, July 13.....	+17.8	good	1942, July 18.....	− 5.1	poor
1942, July 17.....	15.1	good	1942, July 24.....	+ 4.3	poor
1942, July 18.....	+ 6.5	poor	1942, Dec. 31.....	+25.2	good

The observations give no indication of a variation in velocity during the short interval covered by the observations.

I am indebted to Dr. O. Struve and Dr. P. Swings for numerous suggestions in connection with this work and for part of the spectrographic material.

[5] *Ap. J.*, **93**, 446, 1941.

PLATE XXVII

THE SPECTRUM OF HD 192954

(*a*) Short exposure; (*b*) long exposure. The line labeled *Fe* II 4178 in the upper spectrum is really *Si* II 4131

TABLE 2

ABSORPTION LINES IN HD 192954

λ	Int.	Int. (α Cyg)	Identification		
			Elem.	λ (Lab.)	Int. (Lab.)
3321.81	0	3	*V* II	3321.54	150
			Ti II	3321.71	25
3323.05	0	6	*Cr* II	3322.69	12
			Ti II +	3322.93	75
			Fe II +	3323.07	8
			Ti II	3323.40	pr
3335.28	1	6	*Ti* II	{3335.17 3335.22}	40
			Cr II	3335.28	40
			Cr II	3335.46	30
3336.20	1	5	*Cr* II	3336.32	40
3340.03	2	7	*Cr* II +	3339.80	50
			Si II	3339.84	3
			Cr II	3339.90	20
			Ti II +	{3340.33 3340.39}	35
3342.57	1	5	*Cr* II	3342.51	50
3347.94	0	5	*Cr* II	3347.83	40
3349.21	2	10	*Ti* II	3348.91	10?
			Ti II +	3349.00	75
			Cr II	3349.34	6
			Ti II +	{3349.39 3349.47}	125
3357.55	0n	2	*Cr* II	3357.40	40
3360.24	0	4	*Fe* II	3360.10	3
			Cr II +	3360.30	100
3368.27	1	7	*Cr* II	3367.42	12
			Cr II +	3368.05	150
3393.12	2	3	*V* II	3392.66	50
			Cr II +	3393.00	35
3422.69	1	7	*Cr* II	3422.74	125
3425.38	0	2	*Fe* II	3425.58	3
3442.03	0	8	*Mn* II +	3441.98	100
			Fe II	3442.24	3
3444.03	0	4	*Ti* II	3444.33	30
3468.87	1	4	*Fe* II	3468.68	8
3471.33	1	4	*Fe* II	3470.24	1
			Ni II +	3471.35	2
			Cr II +	3472.07	25

TABLE 2—*Continued*

λ	Int.	Int. (α Cyg)	Identification		
			Elem.	λ (Lab.)	Int. (Lab.)
3493.40	2	8	*V* II	3493.16	150
			Fe II +	3493.47	10
3511.69	1	3	*Cr* II	3511.84	35
3514.07	2	5	*Cr* II	3513.03	10
			Fe I	3513.82	400
			Ni II +	3513.94	8
3520.11	0	3	*V* II	3520.02	120
			Ti II +	3520.26	20
3555.35	0	1	(*Lu* II)	3554.45	200
			Fe I +	3554.93	400
			Fe II	3555.08	pr
3559.21	0	M	*Fe* II	3559.40	pr
3576.80	2	7	*Sc* II	{3576.33 3576.39}	30
			Ni II +	3576.76	3
3585.26	2–3	10	*Cr* II +	3585.31	60
			Cr II	3585.54	40
3595.82	0	3	*Ti* II	3596.06	60
3603.53	0–1	6	*Cr* II	3603.61	20
			Cr II +	3603.80	40
			Cr II	3603.86	20
3621.35	1	5	*V* II	3621.20	150
			Fe II +	3621.27	6
3652.14	0	1	*Cr* II	3651.68	12
3657.90	0	0–1	*Cr* II	3658.19	20
3659.66	0	2	*Ti* II	3659.76	60
3662.42	1	2	*Ti* II	3662.24	40
			H 30 +	3662.26	.....
3663.58	0	1	*H* 29	3663.40	.....
3664.57	0–1	2	*H* 28 +	3664.68	.....
			Cr II	3664.95	30
3665.97	1	2	*H* 27	3666.10	.....
3667.65	1	2	*H* 26	3667.68	.....
3669.51	2	4	*V* II	3669.41	300
			H 25 +	3669.47	.....
3671.48	2	4	*H* 24	3671.48	.....
3673.77	3	6	*H* 23	3673.76	.....

TABLE 2—*Continued*

λ	Int.	Int. (α Cyg)	Identification		
			Elem.	λ (Lab.)	Int. (Lab.)
3676.24	3	5	*H* 22	3676.36	.....
3677.63	1	4	*Cr* II +	3677.69	40
			Cr II +	3677.86	50
			Cr II	3677.93	30
3679.40	4	6	*H* 21	3679.36	.....
3682.78	4	8	*H* 20	3682.81	.....
3685.30	1	5	*Ti* II	3685.20	250
3686.65	5	9	*H* 19	3686.83	.....
3691.48	5	10	*H* 18	3691.56	.....
3694.02	0	0–1	*Fe* I	3694.03	400
			Yb II	3694.20	200
3697.13	6	12	*H* 17	3697.15	3
3703.82	7	15	*H* 16	3703.86	4
3705.68	2	M 6	*Fe* I +	3705.57	700
			Ca II	3706.04	10
			Ti II	3706.22	20
3709.56	0n	2n	*Fe* I	3709.25	600
			V II	3709.34	40
			V II	3710.29	500
3712.08	8n	15	*H* 15	3711.97	(5)
3715.40	2n	5	*Cr* II	3715.19	20
			Cr II	3715.45	20
			V II	3715.48	1200
3719.85	1	3	*Fe* I +	3719.94	1000R
			Fe II	3720.17	pr
3721.99	9	15	*H* 14	3721.94	6
3727.71	1n	4	*V* II	3727.35	.....
			Cr II	3727.37	40
			Fe I	3727.62	200
3734.31	9	15	*H* 13 +	3734.37	8
			Fe I	3734.87	1000
3736.95	0	6	*Ca* II +	3736.92	11
			Fe I	3737.14	1000
3745.69	1n	4	*Fe* II	3745.36	pr
			Fe I	3745.56	500
			V II	3745.81	800
3748.49	2	6	*Ti* II	3748.00	10
			Fe I	3748.26	500
			Cr II	3748.68	7

TABLE 2—*Continued*

λ	Int.	Int. (α Cyg)	Identification		
			Elem.	λ (Lab.)	Int. (Lab.)
3750.09	9	15	*H* 12 +	3750.15	10
			V II	3750.88	600
3751.29	2	M	*Cr* II	3750.56	12
3754.14	1	4	*Cr* II	3754.59	20
3759.19	2nv	6	*Ti* II +	3759.30	200
			Fe II	3759.46	6
3761.41	2	6	*Ti* II +	3761.32	200
			Cr II	3761.69	7
			Ti II	3761.88	15
			Cr II	3761.90	8
3763.85	0	4	*Fe* I	3763.79	500
			Fe II	3764.11	pr
3770.41	10nv	5	*Ni* II	3769.46	5
			H 11	3770.63	15
			V II	3770.97	400
3775.55	0	2	*Ti* II	3776.06	6
3794.98	1n	1	*V* II	3794.37	50
			Fe I +	3795.01	500
3797.84	11	20	*H* 10	3797.90	20
3805.20	1	M	*Fe* I	3805.35	400
3814.59	1n	4	*Fe* II +	3814.12	4
			Ti II	3814.60	4
			V II	3815.38	200
			Fe I	3815.84	700
3820.97	3n	M	*He* I	3819.60	50
			He I	3819.76	4
		4	*Fe* I	3820.43	800
		3	*Fe* II	3821.97	pr
3825.13	2	4	*Fe* II	3824.91	4
		3	*Fe* I	3825.88	500
3827.75	1	3	*Fe* II	3827.08	4
			Fe II	3827.69	pr
			Fe I	3827.83	200
3832.63	1	4	*Mg* I	3832.31	15
3835.37	12	20	*H* 9	3835.39	40
3838.29	3	5	*Fe* II	3838.04	2?
			Mg I +	3838.30	25
3841.40	0	3	*Fe* I +	3840.45	400
			Fe I +	3841.05	500
			Fe II	3841.36	pr

TABLE 2—*Continued*

λ	Int.	Int. (α Cyg)	Identification		
			Elem.	λ (Lab.)	Int. (Lab.)
3850.03	1n	3	*Fe* I	3849.97	500
3856.14	2n	5	*Si* II	3856.03	8
			Fe I	3856.37	500
3859.40	1n	3	*Fe* I +	3859.91	1000r
			Fe II	3860.11	pr
3865.36	1n	2	*Fe* I	3865.53	600
			Cr II +	3865.59	75
3872.89	1	4	*Fe* II	3872.76	pr
			Fe I	3872.51	300
3878.56	2n	4n	*Fe* I	3878.58	300
			V II	3878.72	300
3881.83	1	2	*Ni* II	3881.92	1
			Mn II	3883.28	3
3885.56	1	1	*Fe* I	3886.28	600
3889.02	12	20	*H* 8	3889.05	60
3900.86	1n	5	*Ti* II	3900.54	70
3903.01	1	2	*V* II	3903.28	250
3906.08	2	4	*Cr* II	3905.64	25
			Fe II	3906.04	5
3913.82	2n	5	*Ti* II	3913.47	60
3930.33	0	3	*Fe* I	3930.30	600
3933.64	4	20	*Ca* II	3933.68	400
3938.84	0	6	*Fe* II	3938.29	2
			Fe II	3938.97	4
3958.17	1	1	*Cr* II	3958.07	20
			Zr II	3958.22	500
3961.32	0	3	*Al* I	3961.53	10
3969.84	12	20	*Hε*	3970.08	80
3973.85	2	1	*V* II	3973.64	300
3979.34	1	4	*Cr* II	3979.51	20
3985.57	1	M	*Fe* I	3985.39	125
4012.32	2	6	*Ti* II	4012.39	4
			Fe II	4012.47	1
			Cr II	4012.50	30
4024.54	1n	5	*Fe* II	4024.55	5

TABLE 2—*Continued*

λ	Int.	Int. (α Cyg)	Identification		
			Elem.	λ (Lab.)	Int. (Lab.)
4025.48	1n	2	*Ti* II	4025.14	2
		2n	*He* I	4026.19	70
4028.56	1	5	*Ti* II	4028.35	7
4044.86	1n	2	*Fe* II	4044.01	pr
		5	*Fe* I	4045.82	400
4053.77	0	3	*Ti* II	4053.83	(3)
4063.56	1	3	*Fe* I	4063.60	400
4093.66	1	1	*Fe* II	4093.24	0
4095.95	0	M	*Fe* I	4095.97	80
4099.03	0	1	(*N* I)	4099.94	150
			(*S* II)	4099.44	8
4101.63	13	20	*Hδ*	4101.74	100
4122.94	1	5	*Fe* II	4122.64	4
		1	*Fe* I	4123.74	80
4128.13	0	8	*Si* II	4128.05	8
4131.26	0	8	*Si* II +	4130.88	10
		0	*Fe* I	4132.06	300
4144.46	0	2	*He* I	4143.76	15
			Fe I	4143.87	400
		1	*S* II	4145.10	250
4147.79	0	0	*Fe* I	4147.67	200
4163.66	2	5	*Ti* II	4163.66	40
4173.22	3	8	*Fe* II	4173.45	8
4178.78	3	8	*Fe* II	4178.85	8
4226.15	0	1	*Ca* I	4226.73	500
			Al II	4226.81	6
4233.25	3+	12	*Fe* II	4233.17	11
4238.65	1	1	*Fe* I	4238.82	200
4241.87	0	0	*Cl* II	4241.38	60
		7	*Cr* II	4242.38	30
4247.05	2	6	*Sc* II	4246.83	100
4253.82	1n	3	*Cr* II	4252.62	10
		0	*Cr* II	4253.51	75
		2	*Cr* I	4254.35	5000
4258.31	1	4	*Fe* II	4258.15	3

TABLE 2—*Continued*

λ	Int.	Int. (α Cyg)	Identification		
			Elem.	λ (Lab.)	Int. (Lab.)
4262.29	1–2	5	*Cr* II	4261.92	20
4272.07	1n	2	*Fe* I	4271.76	1000
		5	*Fe* II	4273.32	3
4283.81	0n	3	*Cr* II	4284.21	10
4289.86	2	5	*Ti* II	4290.23	50
			Cr I	4289.72	3000
4297.01	0	7	*Fe* II	4296.58	6
4298.67	0	1	*Fe* I	4299.24	500
4302.84	2	9	*Fe* II	4303.17	8
4308.52	1	4	*Ti* II	4307.90	40
			Fe I	4307.91	1000
4314.27	3	4	*Fe* II	4314.29	4
			Sc II	4314.08	30
4325.86	1n	3	*Fe* I	4325.76	1000
4340.44	13	20	*Hγ*	4340.46	200
4351.50	3n	10	*Fe* II	4351.76	9
			(*Mg* I)	4351.92	5Nd?
4358.29	1n	0	*Fe* I	4358.50	70
4367.85	1	2	*Ti* II	4367.68	15
4374.88	1	2	*Sc* II	4374.47	30
			Ti II	4374.82	1
4379.82	1	0	*Mn* II	4379.74	1
4385.10	2n	6	*Mg* II	4384.64	8
			Fe II	4384.33	pr
		8	*Fe* II	4385.38	7
4390.07	1	3	*Mg* II	4390.58	10
4399.76	1	4	*Ti* II	4399.77	35
4404.38	1	3	*Fe* I	4404.75	1000
4412.38	1	M	*Ti* II	4411.94	15
4416.80	3	6	*Fe* II	4416.82	7
4444.24	2	7	*Ti* II	4443.81	50
4450.07	2	4	*Ti* II	4450.49	10
4454.98	0	3	*Fe* II	4455.26	3

TABLE 2—*Continued*

λ	Int.	Int. (α Cyg)	Identification		
			Elem.	λ (Lab.)	Int. (Lab.)
4459.36	0	M	*Fe* I	4459.12	400
4464.23	1	2	*Ti* II	4464.46	1
			V II	4464.32	40
4469.01	2n	5	*Ti* II	4468.50	50
		0	*Ti* II	4469.16	tr
			Fe I	4469.38	200
4472.28	0n	2	*He* I	4471.48	100
			He I	4471.68	7
		3	*Fe* II	4472.92	2
4481.39	2	16	*Mg* II	4481.33	100
4490.08	2n	5	*Fe* II	4489.19	4
		6	*Fe* II	4491.40	5
4500.51	1n	5	*Ti* II	4501.28	40
4508.69	2n	7	*Fe* II	4508.28	8
4515.80	1	7	*Fe* II	4515.34	7
4521.75	2	6	*Fe* II	4520.22	7
		7	*Fe* II	4522.63	9
4528.99	2+	0	*Fe* I	4528.62	600
			V II	4528.51	300
		1	*Ti* II	4529.49	1
4533.66	1	7	*Ti* II	4533.97	30
			Fe II	4534.17	2
			Mg II	4534.26	(4)
4541.14	1	4	*Fe* II	4541.52	4
4549.24	3	15	*Fe* II	4549.47	10
			Ti II	4549.63	60n
			Fe II	4549.21	4
4555.20	1–2	4	*Cr* II	4555.02	20
		6	*Fe* II	4555.89	8
4557.88	1	6	*Cr* II	4558.66	100
4563.88	1	5	*Ti* II	4563.77	30
4574.47	2	0	(*Fe* I)	4574.72	12
			Zr II	4574.50	2
4575.61	1	4	*Fe* II	4576.33	4
4583.30	3	4	*Fe* II	4582.83	3
		9	*Fe* II	4583.83	11
4588.66	1	5	*Cr* II	4588.22	75
			Ti II	4589.95	2
			Cr II	4589.89	3

TABLE 2—*Continued*

λ	Int.	Int. (α Cyg)	Identification		
			Elem.	λ (Lab.)	Int. (Lab.)
4591.55	1	0	*Cr* II	4591.39	tr
		4	*Cr* II	4592.09	20
4595.76	1	3	*Fe* II	4595.68	pr
			A I	4596.10	1000
4601.69	0	0	*Fe* II	4601.34	pr
			Cl I	4601.00	20
4619.59	1n	6	*Cr* II	4618.83	35
		4	*Fe* II	4620.51	3
4629.11	2	9	*Fe* II	4629.34	7
		5	*Cr* II	4634.11	25
4634.65	1	4	*Fe* II	4635.33	5
4656.22	0n	4	*Fe* II	4656.97	1
			Ti II	4657.21	(tr)
4667.78	0	3	*Fe* II	4666.75	2
		0	*Fe* I	4668.14	125
			S II	4668.58	50
4729.74	0	6	*Fe* II	4731.44	3
4755.01	0	0	(*Mn* II)	4755.73	0n
4804.62	1	2	*Ti* II	4805.10	2
4821.46	1	M	.....	.....	.....
4825.79	0	8	*Cr* II	4824.13	75
4855.91	1	1	*Cr* II	4856.19	20
4861.26	5	15	*Hβ*	4861.33	[500]
4893.00	1	M	.....	.....	.....
4904.53	1	M	.....	.....	.....
4924.30	3	10	*Fe* II	4923.92	12
4992.36	1	1	*Fe* II	4993.35	1
5019.18	3	10	*Fe* II	5018.43	12
5061.51	0	1	*Fe* II	5061.79	1
5127.43	1	0–1	*Fe* II	5127.87	1
5169.17	1n	8	*Fe* II	5169.03	12
5184.54	1	4	*Mg* I	5183.62	30
		2	*Ti* II	5185.90 (1)	(2)
5198.15	0	7	*Fe* II	5197.57	6

TABLE 2—*Continued*

λ	Int.	Int. (α Cyg)	Identification		
			Elem.	λ (Lab.)	Int. (Lab.)
5216.35	0	2	*Fe* II	5216.93	3
5226.72	0	2	*Ti* II	5226.60	5
		1	*Fe* (II?)	5227.0	.....
			Fe I	5227.19	400
5233.67	1	1	*Fe* I	5232.94	800
			Cr II	5232.50	15
		7	*Fe* II	5234.62	7
5264.72	0	1	*Fe* II	5264.23	1
			Mg II	5264.14	5
		3	*Fe* II	5264.80	2
5276.56	1	6	*Fe* II	5275.99	7
5283.81	0	4	*Fe* II	5284.09	3
5316.12	0	8	*Fe* II	5316.61	8
			Fe II	5316.78	1
5363.73	1	6	*Fe* II	5362.86	5
5478.57	1	2	*Cr* II	5478.35	15

TABLE 3

UNBLENDED AND SLIGHTLY BLENDED LINES IN HD 192954

λ	Int. (HD 192954)	Int. (α Cyg) CQ Plate	Int. (α Cyg) Coudé Plate	λ (Lab.)	Int. (Lab.)
	H				
3662.42	1	2	.....	3662.26	.....
3663.58	0	1	.....	3663.40	.....
3664.57	0–1	2	.....	3664.68	.....
3665.97	1	2	.....	3666.10	.....
3667.65	1	2	.....	3667.68	.....
3669.51	2	4	.....	3669.47	.....
3671.48	2	4	.....	3671.48	.....
3673.77	3	6	.....	3673.76	.....
3676.24	3	5	.....	3676.36	.....
3679.40	4	6	.....	3679.36	.....
3682.78	4	8	.....	3682.81	.....
3686.65	5	9	.....	3686.83	.....
3691.48	5	10	.....	3691.56	.....
3697.13	6	12	.....	3697.15	3
3703.82	7	15	.....	3703.86	4
3712.08	8n	15	.....	3711.97	5
3721.99	9	15	.....	3721.94	6
3734.31	9	15	.....	3734.372	8
3750.09	9	15	.....	3750.152	10
3770.41	10nv	5	.....	3770.63	15
3797.84	11	20	.....	3797.90	20
3835.37	12	20	.....	3835.39	40
3889.02	12	20	20	3889.05	60
3969.84	12	.....	20	3970.08	80
4340.44	13	.....	20	4340.46	200
4861.26	5	.....	15	4861.33	500
	Fe II				
3425.38	0	2	.....	3425.58	3
3468.87	1	4	.....	3468.68	8
3493.40	2	8	.....	3493.47	10
3559.21	0	M	.....	3559.40	pr
3621.35	1	5	.....	3621.27	6
4024.54	1n	.....	5	4024.55	5
4093.66	1	.....	1	4093.24	0
4173.22	3	.....	8	4173.45	8
4178.78	3	.....	8	4178.85	8
4233.25	3–4	.....	12	4233.17	11
4258.31	1	.....	4	4258.15	3
4297.01	0	.....	7	4296.58	6
4302.84	2	.....	9	4303.17	8
4351.50	3n	.....	10	4351.76	9
4416.80	3	.....	6	4416.82	7
4454.98	0	.....	3	4455.26	3
4508.69	2n	.....	7	4508.28	8
4515.80	1	.....	7	4515.34	7
4521.75	2	.....	6	4520.22	7
4521.75	.....	.....	7	4522.63	9
4541.14	1	.....	4	4541.52	4
4575.61	1	.....	4	4576.33	4

TABLE 3—*Continued*

λ	Int. (HD 192954)	Int. (α Cyg) CQ Plate	Int. (α Cyg) Coudé Plate	λ (Lab.)	Int. (Lab.)
	Fe II—*Continued*				
4729.74	0	.....	6	4731.44	3
4924.30	3	.....	10	4923.92	12
4992.36	1	.....	1	4993.35	1
5019.18	3	.....	10	5018.43	12
5061.51	0	.....	1	5061.79	1
5127.43	1	.....	0–1	5127.87	1
5169.17	1n	.....	8	5169.03	12
5198.15	0	.....	7	5197.57	6
5216.35	0	.....	2	5216.93	3
5276.56	1	.....	6	5275.99	7
5283.81	0	.....	4	5284.09	3
5363.73	1	.....	6	5362.86	5
	Fe I				
3555.35	0	1	.....	3554.93	400
3694.02	0	0–1	.....	3694.03	400
3705.68	2	M	.....	3705.57	700
3719.85	1	3	.....	3719.94	1000
3763.85	0	4	.....	3763.79	500
3794.98	1n	1	.....	3795.01	500
3805.20	1	M	.....	3805.35	400
3850.03	1n	3	.....	3849.97	500
3872.89	1	4	7	3872.51	300
3885.56	1	1	1	3886.28	600
3930.33	0	3	4	3930.30	600
3985.57	1	.....	M	3985.39	125
4063.56	1	.....	3	4063.60	400
4095.95	0	.....	M	4095.47	80
4147.79	0	.....	0	4147.67	200
4238.65	1	.....	1	4238.82	200
4298.67	0	.....	1	4299.24	500
4325.86	1n	.....	3	4325.76	1000
4358.29	1n	.....	0	4358.50	70
4404.38	1	.....	3	4404.75	1000
4459.36	0	.....	M	4459.12	400
	Mg II				
4390.07	1	.....	3	4390.58	10
4481.39	2	.....	16	4481.33	100
	Mg I				
3838.29	3	.....	5	3838.30	25
3832.63	1	.....	4	3832.31	15

TABLE 3—*Continued*

λ	Int. (HD 192954)	Int. (α Cyg) CQ Plate	Int. (α Cyg) Coudé Plate	λ (Lab.)	Int. (Lab.)
			Si II		
4128.13	0	.....	8	4128.05	8
4131.26	0	.....	8	4130.88	10
			Ti II		
3444.03	0	4	.....	3444.33	30
3520.11	0	3	.....	3520.26	20
3595.82	0	3	.....	3596.06	60
3659.66	0	2	.....	3659.76	60
3685.30	1	5	.....	3685.20	250
3761.41	2	6	.....	3761.32	200
3775.55	0	2	.....	3776.06	6
3900.86	1n	5	.....	3900.54	70
3913.82	2n	5	10	3913.47	60
4028.56	1	.....	5	4028.35	7
4053.77	0	.....	3	4053.83	3
4163.66	2	.....	5	4163.66	40
4308.00	1	.....	4	4307.90	40
4367.85	1	.....	2	4367.68	15
4399.76	1	.....	4	4399.77	35
4412.38	1	.....	M	4411.94	15
4444.24	2	.....	7	4443.81	50
4450.07	2	.....	4	4450.49	10
4500.51	1n	.....	5	4501.27	40
4563.88	1	.....	5	4563.77	30
4804.62	1	.....	2	4805.10	2
			V II		
3903.01	1	2	1	3903.28	250
3973.85	2	.....	1	3973.64	300
			Sc II		
4247.05	2	.....	6	4246.83	100
			Ni II		
3576.80	2	7	.....	3576.76	3
			Mn II		
4379.82	1	.....	0	4379.74	1
4755.01	0	.....	0	4755.73	0n

TABLE 3—*Continued*

λ	Int. (HD 192954)	Int. (α Cyg) CQ Plate	Int. (α Cyg) Coudé Plate	λ (Lab.)	Int. (Lab.)
			Ca II		
3933.64	4	15	20 15	3933.68	400
			Al I		
3961.32	0	.....	3	3961.53	10
			Cr II		
3336.20	1	5	.....	3336.32	40
3342.57	1	5	.....	3342.51	50
3347.94	0	5	.....	3347.83	40
3357.55	0n	2	.....	3357.40	40
3368.27	1	7	.....	3368.05	150
3393.12	2	3	.....	3393.00	35
3422.69	1	7	.....	3422.74	125
3511.69	1	3	.....	3511.84	35
3652.14	0	1	.....	3651.68	12
3657.90	0	0–1	.....	3658.19	20
3751.29	2	M	.....	3750.56	12
3754.14	1	4	.....	3754.59	20
3979.34	1	.....	4	3979.51	20
4262.29	1–2	.....	5	4261.92	20
4283.81	0n	.....	3	4284.21	10
4557.88	1	.....	6	4558.66	100
4588.66	1	.....	5	4588.22	75
4591.55	1	.....	4	4592.09	20
4825.79	0	.....	8	4824.13	75
4855.91	1	.....	1	4856.19	20
5478.57	1	.....	2	5478.35	15

NOTES TO TABLE 3

1. The intensities in HD 192954 and the corresponding smoothed-out intensities of α Cygni on the Cassegrain quartz plate and the coudé plate are as follows:

Elem.	MWC 335 Int.	α Cyg CQ Plate Int.	α Cyg Coudé Int.	Elem.	MWC 335 Int.	α Cyg CQ Plate Int.	α Cyg Coudé Int.
Fe II	0	2	1.5	*Ni* II	2	6	.....
	1	4.5	4				
	2	8	7.5	*V* II	2	.....	1
	3	.....	10.5				
	3–4	.....	12	*Fe* I	0	2	1
					1	2	2
Mg I	1	.....	4				
	3	.....	5	*Ca* II	4	15	17
Cr II		1.5	3	*Mg* II	1	.....	3
	1	4	4		.....	2	16
	2	5.5	.....				
	3	6.5	.....	*Al* I	0	.....	3
	4	7	.....				
				Si II	0	8	8
Ti II	0	3	2.5				
	1	5	3.5	*Mn* II	0	.....	0
	2	5.5	5		1	.....	0
Sc II	2	.....	6				

2. *He* I: Present but blended with other lines.

3. *Cr* I: The line λ 4253.82 appears to be made up of two lines about 1.40 A apart, one of which is probably *Cr* I.

THE SPECTRUM OF υ SAGITTARII IN THE VISUAL REGION

JESSE L. GREENSTEIN
Yerkes Observatory
Received January 13, 1943

ABSTRACT

The visual region of the spectrum of υ Sgr is marked by the strength of lines of nitrogen and neon. Estimates of the abundances of the lighter elements show high abundance of neon and an abnormal abundance of nitrogen with respect to oxygen.

The spectrum of υ Sgr, HD 181615–6, has already been investigated in the ultraviolet[1] and photographic regions.[2,3] A preliminary report by Merrill,[4] indicating abnormal strength of *Ne* I lines, was the origin of the present investigation. The four spectrograms measured in the visual region were obtained in July and September, 1940, with the Yerkes autocollimating grating spectrograph; the dispersion is 27.1 A/mm. The visual region is as crowded with lines as are the other regions of this complex spectrum. Some

TABLE 1

ELEMENTS IDENTIFIED IN υ SGR, VISUAL REGION

H	Weak; *Hα* emission	*Al* II	Present
He I	Strong	*Si* II	Strong
C II	Present	*P* II	Present
N I	Strong	*S* II	Strong
N II	Possibly present	*Ti* II	Present
O I	Weak	*V* II	Weak
Ne I	Strong	*Cr* II	Present
Na I	Present	*Mn* II	Present
Mg II	Present	*Fe* II	Strong

five hundred lines were measured in the region λ 4900 to λ 6700. The resolving power of the equipment is insufficient for a definitive list of lines; the following note is concerned only with the identification of those lines measured on two or more good plates (the average number of plates per line is three). Even the sharpest lines proved to be considerably blended in many cases.

Table 1 contains a list of elements identified in the visual region. No elements in high stages of ionization are found, but elements with lines arising from highly excited normal or metastable levels are present in great strength. The appearance of *N* I had hitherto been noted only in the infrared. The *He* I and *Ne* I lines are among the strongest in the visual region; the lines of these elements represent excitation potentials from 11 to 21 volts. The hydrogen lines are relatively weak, and *Hα* is a complex emission band.

In the following discussion the conditions of ionization and excitation were assumed

[1] Greenstein, *Ap. J.*, **91**, 438, 1940. In the discussion of the ionization equilibria of *He*, the ionization of *He* II was neglected. A recomputation has shown this to be unsafe. The data for log (He^*) in Table 6 should consequently be corrected to read: for $g_e = 1$, $\theta_e = 0.39$, 16.1, for $\theta_e = 0.33$, 16.0; for $g_e = 10$, $\theta_e = 0.39$, 16.2, for $\theta_e = 0.33$, 16.5; for $g_e = 100$, $\theta_e = 0.33$, 16.8. The derived results for $(He^*)'$ in Table 12 are changed only slightly: $g_e = 100$, $\theta_e = 0.33$, 17.0; $g_e = 10$, $\theta_e = 0.39$, 16.7. The conclusions are not affected by these changes.

[2] J. S. Plaskett, *Pub. Dom. Ap. Obs. Victoria*, **4**, No. 1, 1928.

[3] W. W. Morgan, *Pub. Yerkes Obs.*, VII, Part III, 1935.

[4] *Pub. A.S.P.*, **51**, 218, 1939.

to be those in an unstratified atmosphere, with effective temperature equal to the excitation temperature, 10,500°, and with electron pressure 25 bar.[1] The abundances so derived are quite rough; if stratification were included, the abundances of the metals and of elements with low excitation potentials would be slightly higher than those derived.

H.—$H\beta$ is a moderately strong absorption line; no structure can be observed, since it is at the limit of the plate. At $H\alpha$ a very broad, weak emission band, roughly 8 A in width, can be seen. On the violet side of the latter is superposed a narrow strong emission; no absorption component is certainly visible. After correcting measured wave lengths for the orbital motion given by the absorption lines of other elements, the mean position of the broad emission is near λ 6566.0, and that of the narrow emission near

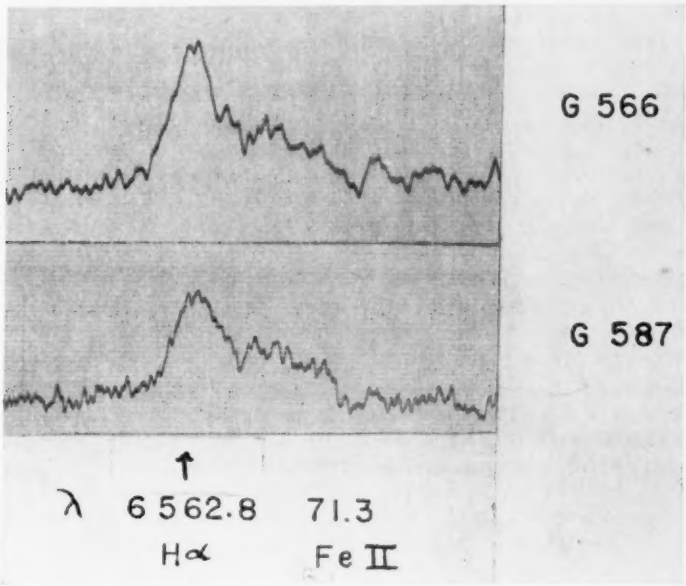

FIG. 1.—Microphotometer tracings of the $H\alpha$ emission bands in v Sgr. The normal position of $H\alpha$ is indicated.

λ 6562.8. It would be extremely important to observe this structure for variability during the orbital cycle. Figure 1 gives a reproduction of two microphotometer tracings of plates G 566, July 4, 1940, and G 587, September 16, 1940. The shift of the structure to the red and the differing sharpness of the two components make it clear that the emission is of an unusual type. The appearance of the bands is complicated by the line λ 6565.4 (unidentified) and λ 6571.3 (*Fe* II).

He I.—All helium lines are present and strong. The line λ 5016, arising from the metastable 2^1S level, does not show any structure or enhancement.

N I.—An extremely strong line (I = 12), apparently double, is seen at λ 6483.8. It can be identified[5] with λ 6482.74 and λ 6484.88 of *N* I. This line is not present on any available visual spectra of B or A stars and was not measured by Marshall.[6] The lines of *N* I observed in the infrared[7] have excitation potentials lower by one volt. About thirty unblended lines, besides other partly blended lines, may be identified as *N* I; they arise from the levels $3p(^4S^0, ^4D^0, ^4P^0, ^2S^0)$. The laboratory and stellar intensities

[5] Duffendack and Wolfe, *Phys. Rev.*, **34**, 409, 1929.

[6] *Ap. J.*, **82**, 97, 1935.

[7] Merrill, *Ap. J.*, **79**, 183, 1934.

agree for most of the quartet lines. The doublet lines λ 5999.47 and λ 6008.48 are as strong in the laboratory as λ 6482.74 and λ 6484.88, but they are weak and blended in the star (I = 1n). Similarly, the $3s^2P-4p^2S^0$ transitions at λ 4914.90 and λ 4935.03 are absent from Morgan's list;[3] they lie in a poor spectral region, however, for prism spectrographs. Metastability cannot be involved, and the parent ions for doublets and quartets are the same. However, theoretical intensities computed from supermultiplet intensity rules suggest that the strongest $^4D^0-{}^4F$ lines should be about eight times as strong as the strongest $^2S^0-{}^2P$ lines for equal numbers of atoms. Further, the statistical weight of the strongest lines, at λ 6483, is seven times greater than that of the doublets, so that a total factor of about 50 between quartets and doublets may be expected. It seems very possible that some anomalous excitation is responsible for the high laboratory intensities of the doublet lines.

N II.—The lines may be weakly present, as should be expected for excitation potential 18 to 21 volts.

C II.—The lines arise from the level, E = 14.4 volts, that produces λ 4267. The absence of *C* I lines in the visual and in the photographic region[3] is rather unexpected, since the ionization and excitation conditions lead to roughly equal numbers of atoms of excited *C* I and *C* II; possibly the transition probabilities are low for the *C* I lines, and stratification effects can enhance *C* II.

O I.—The lines are weak compared to *N* I, in spite of the fact that a larger fraction of *O* atoms are in neutral excited states than *N* atoms. Apparently the abundance is lower. The lines of *O* II, at 23 to 28 volts, are not to be expected. The abundances of the elements may be estimated to be in the order $N > C > O$. This order is in disagreement with the results of Unsöld for τ Scorpii[8] and of Menzel for the sun;[9] it is probably also contradicted by the greater strength of *O* I lines than *N* I lines in the infrared spectrum[7] of α Cygni.

Ne I.—The lines of *Ne* I are strong; *Ne* II is absent because of high value of E = 27 volts. The strongest *Ne* I lines have intensities somewhat smaller than that of λ 5876 of *He* I; if the standard ionization conditions are adopted, and if the transition probabilities for the strongest *Ne* I lines are of the same order as that of λ 5876, we can estimate the abundance ratio of *He* to *Ne* as 100:1 or perhaps slightly less. This is to be preferred to an earlier estimate,[1] which was near 1000:1. The abundance of *Ne* is certainly greater than that of *N*, *C*, or *O;* the ratio of *Ne* to *C* should not exceed 10:1. These abundances for the lighter elements are in general agreement with those determined for normal stars, except in the case of *N*. With more knowledge of the actual transition probabilities it should be possible to ascertain whether the abnormally low abundance of *H* in υ Sgr is accompanied by an abnormal abundance of *N*.

The other ionized elements are those to be expected in a high-temperature A or late B star. The strength of *S* II and *P* II is greater than in normal stars[6] and must find its origin in the low opacity. The ionized iron-group metals are relatively inconspicuous, an effect due to greater ionization and low abundance but also the result of the poverty of observational data on the laboratory spectra of these elements in the visual region. *Na* I is partly stellar and partly interstellar.

[8] *Zs. f. Ap.*, **20**, 311, 1941; **21**, 1, 1941. Proof received before publication.

[9] *Astr. Symposium Western Reserve University*, p. 89, 1938.

DYNAMICAL FRICTION

I. GENERAL CONSIDERATIONS: THE COEFFICIENT OF DYNAMICAL FRICTION

S. CHANDRASEKHAR
Yerkes Observatory
Received January 7, 1943

ABSTRACT

In this paper it is shown that a star must experience *dynamical friction*, i.e., it must suffer from a systematic tendency to be decelerated in the direction of its motion. This dynamical friction which stars experience is one of the direct consequences of the fluctuating force acting on a star due to the varying complexion of the near neighbors. From considerations of a very general nature it is concluded that the *coefficient of dynamical friction*, η, must be of the order of the reciprocal of the time of relaxation of the system. Further, an independent discussion based on the two-body approximation for stellar encounters leads to the following explicit formula for the coefficient of dynamical friction:

$$\eta = 4\pi m_1 (m_1 + m_2) \frac{G^2}{v^3} \log_e \left[\frac{D_0 \overline{|u|^2}}{G(m_1 + m_2)} \right] \int_0^v N(v_1) dv_1 ,$$

where m_1 and m_2 denote the masses of the field star and the star under consideration, respectively; G, the constant of gravitation; D_0, the average distance between the stars; $\overline{|u|^2}$, the mean square velocity of the stars; $N(v_1)\,dv_1$, the number of field stars with velocities between v_1 and $v_1 + dv_1$; and, finally, v, the velocity of the star under consideration. It is shown that the foregoing formula for η is in agreement with the conclusions reached on the basis of the general considerations. Finally, some remarks are made concerning the further development of these ideas on the basis of a proper statistical theory.

1. *General considerations.*—In a first approximative discussion[1] of the fluctuating part of the gravitational field acting on a star we may conveniently describe it in terms of two functions: a function $W(\boldsymbol{F})$, which governs the probability of occurrence of a force $\boldsymbol{F}$ per unit mass acting on a star, and a function $T(|\boldsymbol{F}|)$, which gives the average time during which such a force acts. On this assumption we can properly visualize the motion of the representative point in the velocity space as follows: The representative point suffers random displacements in a manner that can be described in terms of the theory of random flights.[2] More specifically, the star may be assumed to suffer a large number of discrete increments in velocity of amounts $|\boldsymbol{F}|T(|\boldsymbol{F}|)$ occurring in random directions. The mean square increase in velocity which the star may be expected to suffer in a time t (large compared to the mean periods of the elementary fluctuations in $\boldsymbol{F}$) is then given by

$$\overline{|\Delta \boldsymbol{u}|^2} = \overline{|\boldsymbol{F}|^2 T(|\boldsymbol{F}|)}\, t . \tag{1}$$

Equivalently, we may describe the same situation by asserting that the probability function $W(\boldsymbol{u}, t)$, governing the occurrence of the velocity $\boldsymbol{u}$ at time t, satisfies the *diffusion equation*

$$\frac{\partial W}{\partial t} = q \nabla_u^2 W , \tag{2}$$

[1] S. Chandrasekhar, *Ap. J.*, **94**, 511, 1941.

[2] For a general discussion of this and related theories see a forthcoming article by the writer in the *Reviews of Modern Physics*.

where the *diffusion coefficient* q has the value

$$q = \tfrac{1}{6}\overline{|\boldsymbol{F}|^2 T}\,. \tag{3}$$

If the star has a velocity $\boldsymbol{u}_0$ at time $t = 0$, then the solution of the diffusion equation (2) which will be appropriate for describing the distribution of $\boldsymbol{u}$ at later times is clearly

$$W(\boldsymbol{u}, t; \boldsymbol{u}_0) = \frac{1}{(4\pi q t)^{3/2}}\, e^{-|\boldsymbol{u}-\boldsymbol{u}_0|^2/4qt}\,. \tag{4}$$

It is now seen that formula (1) is an immediate consequence of the foregoing solution for W.

We shall now indicate why the considerations of the preceding paragraph can be valid only for times which are short compared to $\overline{|\boldsymbol{u}|^2}/\overline{|\boldsymbol{F}|^2 T}$, where $\overline{|\boldsymbol{u}|^2}$ denotes the mean square velocity of the stars in an appropriately chosen local standard of rest. For, if $W(\boldsymbol{u}, t; \boldsymbol{u}_0)$ according to equation (4), described the stochastic variations of $\boldsymbol{u}$ for all times, then the probability for a star to suffer any assigned arbitrarily large acceleration can be made as close to unity as we may choose by allowing t to be sufficiently large. This conclusion is, however, contrary to what we should expect on quite general grounds, namely, that $W(\boldsymbol{u}, t; \boldsymbol{u}_0)$ tends to a Maxwellian distribution, independently of $\boldsymbol{u}_0$ as $t \to \infty$. Expressed somewhat differently, we should strictly suppose that the stochastic variations in the velocity which a star suffers must be such as to leave an initial Maxwellian distribution of the velocities invariant. Defining, now, a stochastic process as *conservative* if it leaves a Maxwellian distribution unchanged, it is clear that the process described by equation (2) is *nonconservative*. Consequently, equation (2) is suitable for describing the underlying physical situation only for times t which satisfy the inequality

$$t \ll \frac{\overline{|\boldsymbol{u}|^2}}{\overline{|\boldsymbol{F}|^2 T}}\,. \tag{5}$$

The question now arises as to how our earlier approximate considerations can be modified so as to make the underlying stochastic process conservative. Now, as has been made familiar in the physical theories of Brownian motion by Ornstein, Uhlenbeck, and others,[3] this can be achieved by the introduction of *dynamical friction*. More particularly, we suppose that the acceleration, $\Delta\boldsymbol{u}$, which a star suffers in a time Δt, which is short compared to the time intervals during which $\boldsymbol{u}$ may change appreciably but long compared to the periods of the elementary fluctuations in $\boldsymbol{F}$, can be expressed as the sum of two terms in the form

$$\Delta\boldsymbol{u} = \delta\boldsymbol{u}(\Delta t) - \eta\boldsymbol{u}\Delta t\,, \tag{6}$$

where the first term on the right-hand side is governed by the probability distribution (cf. eq. [4])

$$\psi(\delta\boldsymbol{u}[\Delta t]) = \frac{1}{(4\pi q \Delta t)^{3/2}}\, e^{-|\delta\boldsymbol{u}-\mathrm{grad}_{\boldsymbol{u}} q\Delta t|^2/4q\Delta t} \tag{7}$$

and where the second term represents a *deceleration* of the star in the direction of its motion by an amount proportional to $|\boldsymbol{u}|$. The constant of proportionality, η, can therefore be properly defined as the *coefficient of dynamical friction*.

With the underlying stochastic process defined as in equation (6) the distribution

[3] See the article quoted in n. 2 for further amplifications of what follows in the text.

function $W(\mathbf{u}, t + \Delta t)$ at time $t + \Delta t$ can be derived from the distribution $W(\mathbf{u}, t)$ at the earlier time t by means of the integral equation

$$W(\mathbf{u}, t+\Delta t) = \int_{-\infty}^{+\infty} W(\mathbf{u}-\Delta\mathbf{u}, t)\, \psi(\mathbf{u}-\Delta\mathbf{u}; \Delta\mathbf{u})\, d(\Delta\mathbf{u}) , \tag{8}$$

where $\psi(\mathbf{u}; \Delta\mathbf{u})$ denotes the *transition probability* (cf. eqs. [6] and [7])

$$\psi(\mathbf{u}; \Delta\mathbf{u}) = \frac{1}{(4\pi q \Delta t)^{3/2}}\, e^{-|\Delta\mathbf{u} - \operatorname{grad}_{\mathbf{u}} q\Delta t + \eta \mathbf{u}\Delta t|^2/4q\Delta t} . \tag{9}$$

Expanding $W(\mathbf{u}, t + \Delta t)$, $W(\mathbf{u} - \Delta\mathbf{u}, t)$, and $\psi(\mathbf{u} - \Delta\mathbf{u}; \Delta\mathbf{u})$, which occur in equation (8) in the form of Taylor series, evaluating the various moments of $\Delta\mathbf{u}$ according to the distribution (9), and passing finally to the limit $\Delta t = 0$, we obtain the following equation, which is of the Fokker-Planck type:

$$\frac{\partial W}{\partial t} = \operatorname{div}_{\mathbf{u}} (q \operatorname{grad}_{\mathbf{u}} W) + \operatorname{div}_{\mathbf{u}} (\eta W \mathbf{u}) . \tag{10}$$

At this point we may explicitly draw attention to the fact that the foregoing equation is valid also when q and η are functions of $\mathbf{u}$.

Finally, the condition that the Maxwellian distribution

$$\left(\frac{3}{2\pi\overline{|\mathbf{u}|^2}}\right)^{3/2} e^{-3|\mathbf{u}|^2/2\overline{|\mathbf{u}|^2}} \tag{11}$$

satisfy equation (10) *identically* requires that q and η be related according to

$$\frac{q}{\eta} = \tfrac{1}{3}\overline{|\mathbf{u}|^2} = \text{constant} . \tag{12}$$

Now the solution of equation (10) appropriate for describing the distribution of the velocities at time t, given that $\mathbf{u} = \mathbf{u}_0$ at time $t = 0$, is

$$W(\mathbf{u}, t; \mathbf{u}_0) = \left[\frac{3}{2\pi\overline{|\mathbf{u}|^2}(1 - e^{-2\eta t})}\right]^{3/2} e^{-3|\mathbf{u} - \mathbf{u}_0 e^{-\eta t}|^2/2\overline{|\mathbf{u}|^2}(1-e^{-2\eta t})} . \tag{13}$$

In writing down the foregoing solution we have assumed that q and η are constants. We readily verify that $W(\mathbf{u}, t; \mathbf{u}_0)$, according to equation (13), tends to our earlier solution (4) for $t \ll \eta^{-1}$ in virtue of the relation (12); moreover, it tends to the Maxwellian distribution (11) as $t \to \infty$. Accordingly, η^{-1} can be taken as a measure of the *time of relaxation* of the system. Combining equations (3) and (12), we have

$$\frac{1}{\eta} = 2\,\frac{\overline{|\mathbf{u}|^2}}{\overline{|\mathbf{F}|^2}T} , \tag{14}$$

which agrees with the customary definition of the time of relaxation except for a factor 2.[4]

Summarizing the conclusions reached, we may say that *general considerations such as the invariance of the Maxwellian distribution to the underlying stochastic process require that stars experience dynamical friction during their motion and that the coefficient of dynamical friction be of the order of the reciprocal of the time of relaxation of the system.*

2. *An elementary derivation of the coefficient of dynamical friction on the two-body approximation for stellar encounters.*—In the preceding section we have seen how the exist-

[4] Cf. Chandrasekhar, *Ap. J.*, **94**, 511, 1941 (see particularly §§ 7, 8, and 9).

ence of dynamical friction can be inferred on quite general grounds. We shall now show how the operation of such a force can also be derived from a direct analysis of the fluctuating force acting on a star. It is perhaps simplest and most instructive to examine the problem on an approximation in which the fluctuations in $\boldsymbol{F}$ are analyzed in terms of single stellar encounters each idealized as a two-body problem. On this approximation the increments in velocity, $\Delta v_{||}$ and $\Delta v_{\perp}$,which a star with velocity $v_2 = |\boldsymbol{v}_2|$ and mass m_2 suffers as the result of an encounter in directions which are respectively parallel to and perpendicular to the direction of motion are[5]

$$\Delta v_{||} = -\frac{2m_1}{m_1+m_2}\,[\,(v_2 - v_1\cos\theta)\cos\psi + v_1\sin\theta\cos\Theta\sin\psi\,]\cos\psi \qquad (15)$$

and

$$\left.\begin{aligned}\Delta v_{\perp} = \pm\frac{2m_1}{m_1+m_2}[\,v_1^2+v_2^2-2v_1v_2\cos\theta - \{\,(v_2-v_1\cos\theta)\cos\psi \\ + v_1\sin\theta\cos\Theta\sin\psi\}^2]^{1/2}\cos\psi\,,\end{aligned}\right\} \qquad (16)$$

where m_1 and v_1 denote the mass and the velocity of a typical field star and the rest of the symbols have the same meanings as in *Stellar Dynamics*, chapter ii (see, particularly, pp. 51–64).

According to equation (16), and as can, indeed, be expected on general symmetry grounds, $\Delta v_{\perp}$, when summed over a large number of encounters, vanishes identically. But this is not the case with $\Delta v_{||}$, for the net increase in the velocity which the star suffers in the direction of its motion during a time Δt (long compared to the periods of the elementary fluctuations but short compared to the time intervals during which v_2 may be expected to change appreciably) is given by

$$\Sigma\Delta v_{||} = \Delta t\int_0^{\infty} dv_1\int_0^{\pi} d\theta\int_0^{2\pi} d\varphi\int_0^{D_0} dD\int_0^{2\pi}\frac{d\Theta}{2\pi}\{2\pi N(v_1,\,\theta,\,\varphi)\,V\,D\Delta v_{||}\}\,, \qquad (17)$$

where the various integrations are, with respect to the different parameters, defining the single encounters. The integration over Θ, the inclination of the orbital plane to the fundamental plane containing the vectors $\boldsymbol{v}_1$ and $\boldsymbol{v}_2$, is readily effected, and we are left with

$$\left.\begin{aligned}\Sigma\Delta v_{||} = -4\pi\frac{m_1}{m_1+m_2}\Delta t\int_0^{\infty} dv_1\int_0^{\pi} d\theta\int_0^{2\pi} d\varphi\int_0^{D_0} dD\,N(v_1,\,\theta,\,\varphi) \\ \times V(v_2-v_1\cos\theta)\frac{D}{1+\dfrac{D^2V^4}{G^2(m_1+m_2)^2}}\,,\end{aligned}\right\} \qquad (18)$$

where we have substituted for $\cos^2\psi$ from *Stellar Dynamics*, equation (2.301). The integral over the impact parameter D when extended from 0 to ∞ diverges; but for reasons explained in *Stellar Dynamics*, page 56, we allow for D only a finite range of integration, namely, from 0 to D_0, where D_0 is of the order of the average distance between the stars. Performing, now, the integration over D, we obtain

$$\left.\begin{aligned}\Sigma\Delta v_{||} = -2\pi m_1(m_1+m_2)G^2\Delta t\int_0^{\infty} dv_1\int_0^{\pi} d\theta\int_0^{2\pi} d\varphi N(v_1,\,\theta,\,\varphi)\frac{1}{V^3} \\ \times(v_2-v_1\cos\theta)\log(1+\mathscr{G}^2V^4)\,,\end{aligned}\right\} \qquad (19)$$

[5] Cf. S. Chandrasekhar, *Principles of Stellar Dynamics*, p. 229 (eq. [5.721]), University of Chicago Press, 1942. This monograph will be referred to hereafter as "*Stellar Dynamics*."

where we have written

$$\vartheta = \frac{D_0}{G(m_1 + m_2)}. \tag{20}$$

If we now assume that the distribution of the velocities v_1 is spherical, then $N(v_1, \theta, \varphi)$ has the form (cf. *Stellar Dynamics*, eq. [2.336])

$$N(v_1, \theta, \varphi) = N(v_1)\frac{1}{4\pi}\sin\theta. \tag{21}$$

Substituting the foregoing form for $N(v_1, \theta, \varphi)$ in equation (19) and performing the integration over φ, we obtain

$$\left.\begin{aligned}\Sigma\Delta v_{||} = -\pi m_1(m_1 + m_2)G^2\Delta t\int_0^\infty dv_1 N(v_1)\int_0^\pi d\theta\,\frac{\sin\theta}{V^3} \\ \times (v_2 - v_1\cos\theta)\log(1+\vartheta^2V^4).\end{aligned}\right\} \tag{22}$$

To effect the integration over θ, we shall use the relative velocity V as the variable of integration instead of θ. Since

$$V^2 = v_1^2 + v_2^2 - 2v_1v_2\cos\theta, \tag{23}$$

we have

$$\left.\begin{aligned}V\,dV &= v_1v_2\sin\theta\,d\theta, \\ v_2 - v_1\cos\theta &= \frac{1}{2v_2}(V^2 + v_2^2 - v_1^2).\end{aligned}\right\} \tag{24}$$

Using relations (24), we find that equation (22) can be reduced to the form

$$\Sigma\Delta v_{||} = -\tfrac{1}{2}\pi m_1(m_1 + m_2)\frac{G^2}{v_2^2}\Delta t\int_0^\infty \frac{1}{v_1}N(v_1)J\,dv_1, \tag{25}$$

where we have used J to denote

$$J = \int_{|v_1 - v_2|}^{(v_1+v_2)}\left(1 + \frac{v_2^2 - v_1^2}{V^2}\right)\log(1+\vartheta^2V^4)\,dV. \tag{26}$$

After an integration by parts the expression for J becomes

$$\left.\begin{aligned}J = \left(V - \frac{v_2^2 - v_1^2}{V}\right)\log(1+\vartheta^2V^4)\Big|_{|v_1-v_2|}^{(v_1+v_2)} \\ - 4\int_{|v_1-v_2|}^{(v_1+v_2)}\left(1 - \frac{v_2^2 - v_1^2}{V^2}\right)\frac{\vartheta^2V^4}{1+\vartheta^2V^4}\,dV.\end{aligned}\right\} \tag{27}$$

Now, under most conditions of practical interest ϑ^2V^4 is generally very large compared to unity (cf. *Stellar Dynamics*, eqs. [2.323] and [2.347]; also eq. [5.215]). Hence, to a sufficient accuracy we have

$$J = \left[\left(V - \frac{v_2^2 - v_1^2}{V}\right)\log(1+\vartheta^2V^4) - 4\left(V + \frac{v_2^2 - v_1^2}{V}\right)\right]_{|v_1-v_2|}^{(v_1+v_2)}. \tag{28}$$

After some further reductions we find that the foregoing equation becomes

$$J=\begin{cases} 2v_1\log\left(1+\mathcal{G}^2[v_1+v_2]^4\right)\left(1+\mathcal{G}^2[v_1-v_2]^4\right) & (v_1<v_2), \\ 2v_1\log\left(1+16\mathcal{G}^2v_1^4\right)-8v_1 & (v_1=v_2), \\ 2v_1\log\dfrac{1+\mathcal{G}^2(v_1+v_2)^4}{1+\mathcal{G}^2(v_1-v_2)^4}-16v_2 & (v_1>v_2). \end{cases} \tag{29}$$

Again, since $\mathcal{G}^2(v_1+v_2)^4$ and $\mathcal{G}^2(v_1-v_2)^4$ are also generally very large compared to unity, we can further simplify equation (29) to

$$J=\begin{cases} 8v_1\log\mathcal{G}\,(v_2^2-v_1^2) & (v_1<v_2), \\ 4v_1\log 4\mathcal{G}v_1^2-8v_1 & (v_1=v_2), \\ 8v_1\log\dfrac{v_1+v_2}{v_1-v_2}-16v_2 & (v_1>v_2). \end{cases} \tag{30}$$

The foregoing formula for J shows that in an approximation in which we retain only the "dominant term" (cf. *Stellar Dynamics*, pp. 62–64) we have

$$J=\begin{cases} 8v_1\log\mathcal{G}\,\overline{|\boldsymbol{u}|^2} & (v_1<v_2), \\ 0 & (v_1>v_2), \end{cases} \tag{31}$$

where $\overline{|\boldsymbol{u}|^2}$ may be taken to denote the mean square velocity of the stars in the system. According to equations (30) and (31), we have the remarkable result that *to a sufficient accuracy only stars with velocities less than the one under consideration contribute to* $\Sigma\Delta v_{||}$. As we shall see presently, it is precisely on this account that dynamical friction appears on our present analysis.

Combining equations (25) and (31), we have

$$\Sigma\Delta v_{||}=-4\pi m_1(m_1+m_2)\frac{G^2}{v_2^2}\log\left(\mathcal{G}\,\overline{|\boldsymbol{u}|^2}\right)\Delta t\int_0^{v_2}N(v_1)\,dv_1. \tag{32}$$

Finally, if we assume that the velocities $\boldsymbol{v}_1$ are distributed according to Maxwell's law, then

$$\int_0^{v_2}N(v_1)\,dv_1=\frac{4j^3}{\pi^{1/2}}N\int_0^{v_2}e^{-j^2v_1^2}v_1^2dv_1, \tag{33}$$

where N denotes the number of stars per unit volume and j is a parameter which measures the dispersion of the velocities in the system. Expressing the integral on the right-hand side of equation (33) in terms of the error integral

$$\Phi(x)=\frac{2}{\pi^{1/2}}\int_0^x e^{-x^2}dx, \tag{34}$$

and substituting the result in equation (32), we find that

$$\Sigma\Delta v_{||}=-4\pi Nm_1(m_1+m_2)\frac{G^2}{v_2^2}\log\left(\mathcal{G}\,\overline{|\boldsymbol{u}|^2}\right)\Delta t\left[\Phi(x_0)-x_0\Phi'(x_0)\right], \tag{35}$$

where we have written $x_0=jv_2$.

Equation (35) shows that the star does, in fact, experience dynamical friction and that the coefficient of dynamical friction has the value

$$\eta = 4\pi N m_1 (m_1 + m_2) \frac{G^2}{v_2^3} \log (\gamma \overline{|u|^2}) \, [\Phi(x_0) - x_0 \Phi'(x_0)] \, . \tag{36}$$

It is now of interest to see that with the coefficient of dynamical friction defined as in equation (36) we can directly verify the existence of a relation of the form (12). For, according to equations (2.356) and (5.724) in *Stellar Dynamics*, we have

$$\Sigma \Delta v_{||}^2 = \tfrac{8}{3} \pi N m_1^2 \frac{G^2}{v_2^3} \overline{|u|^2} \log (\gamma \overline{|u|^2}) \, \Delta t \, [\Phi(x_0) - x_0 \Phi'(x_0)] \, . \tag{37}$$

Hence,

$$\frac{\Sigma \Delta v_{||}^2}{\eta \Delta t} = \frac{2}{3} \frac{m_1}{m_1 + m_2} \overline{|u|^2} \, , \tag{38}$$

which is to be compared with equation (12). It is thus seen that a detailed analysis of the fluctuating field of the near-by stars in terms of individual stellar encounters idealized as two-body problems fully confirms the conclusions reached in § 1 on the basis of certain general principles.

3. *Dynamical friction as a consequence of the statistical properties of the fluctuating gravitational field of a random distribution of stars.*—The discussion of dynamical friction in § 1, while sufficiently general for a first orientation in the subject, suffers, nevertheless, from certain drawbacks. For example, in writing down the probability distribution for $\delta \boldsymbol{u}(\Delta t)$ (eq. [7]) we have assumed that it has spherical symmetry. However, to be entirely general we should rather suppose that $\psi(\delta \boldsymbol{u}[\Delta t])$ has the form

$$\psi(\delta \boldsymbol{u}[\Delta t]) = \frac{1}{\pi^{3/2}} \begin{vmatrix} a_{11} & a_{12} & a_{13} \\ a_{21} & a_{22} & a_{23} \\ a_{31} & a_{32} & a_{33} \end{vmatrix} e^{-(a_{11}\delta u_1^2 + a_{22}\delta u_2^2 + a_{33}\delta u_3^2 + 2a_{12}\delta u_1 \delta u_2 + 2a_{23}\delta u_2 \delta u_3 + 2a_{31}\delta u_3 \delta u_1)/\Delta t} \, , \tag{39}$$

where $\delta \boldsymbol{u} = (\delta u_1, \delta u_2, \delta u_3)$ and $(a_{\mu\nu})$ is a symmetric tensor of the second rank. The components of $(a_{\mu\nu})$ can very well depend on $\boldsymbol{u}$. While it would not be difficult to write down for the correspondingly more general form of the transition probability the appropriate generalization of equation (10), we should not be able to make much practical use of such an equation without some direct knowledge concerning $(a_{\mu\nu})$. In other words, a detailed statistical analysis of the fluctuating part of the gravitational field acting on a star must precede a discussion of the necessary generalization of equation (10). A start in this direction has recently been made by Chandrasekhar and von Neumann in two papers.[6] Particularly in their second paper, where all the first and the second moments of $\dot{\boldsymbol{F}}$ for given $\boldsymbol{F}$ and $\boldsymbol{v}$ have been evaluated, a direct indication for the existence of dynamical friction on the statistical theory has indeed been found. However, a complete solution of the problem will require a more far reaching discussion than has yet been undertaken. But the general outlines of such a theory are not difficult to foresee. For, the essential information which is needed is, of course, the average force, $\overline{\boldsymbol{F}_t}$, per unit mass acting on a star at time t when a force $\boldsymbol{F}_0$ acted at time $t = 0$. The statistical problem is thus merely one of finding the joint distribution $W(\boldsymbol{F}_0, \boldsymbol{F}_t)$ of $\boldsymbol{F}_0$ and $\boldsymbol{F}_t$, where

$$\boldsymbol{F}_0 = G \sum_i M_i \frac{\boldsymbol{r}_i}{|\boldsymbol{r}_i|^3} \tag{40}$$

[6] *Ap. J.*, **95**, 489, 1942, and **97**, 1, 1943.

and

$$\boldsymbol{F}_t = G\sum_i M_i \frac{\boldsymbol{r}_i + \boldsymbol{V}_i t}{|\boldsymbol{r}_i + \boldsymbol{V}_i t|^3}. \tag{41}$$

In equations (40) and (41) $\boldsymbol{r}_i$ and $\boldsymbol{V}_i$ denote, respectively, the position and the velocity of a typical field star *relative* to the one under consideration. By an application of Markoff's method (cf. the papers of Chandrasekhar and von Neumann) we readily find that the required distribution is formally given by

$$W(\boldsymbol{F}_0, \boldsymbol{F}_t) = \frac{1}{64\pi^6}\int_{-\infty}^{+\infty}\int_{-\infty}^{+\infty} e^{-i(\boldsymbol{\rho}\cdot\boldsymbol{F}_0 + \boldsymbol{\sigma}\cdot\boldsymbol{F}_t)} A(\boldsymbol{\rho}, \boldsymbol{\sigma})\, d\boldsymbol{\rho} d\boldsymbol{\sigma}, \tag{42}$$

where $\boldsymbol{\rho}$ and $\boldsymbol{\sigma}$ are two auxiliary vectors and

$$A(\boldsymbol{\rho}, \boldsymbol{\sigma}) = e^{-NC(\boldsymbol{\rho}, \boldsymbol{\sigma})} \tag{43}$$

and where

$$C(\boldsymbol{\rho}, \boldsymbol{\sigma}) = \int_{-\infty}^{\infty}\int_{-\infty}^{\infty}\int_{0}^{\infty}\left[1 - e^{iGM\left\{\frac{\boldsymbol{r}\cdot\boldsymbol{\rho}}{r^3} + \frac{(\boldsymbol{r}+\boldsymbol{V}t)}{|\boldsymbol{r}+\boldsymbol{V}t|^3}\cdot\boldsymbol{\sigma}\right\}}\right]\tau(\boldsymbol{V}, M)\, dM\, d\boldsymbol{r} d\boldsymbol{V}. \tag{44}$$

In equation (44) $\tau(\boldsymbol{V}, M)$ governs the probability of occurrence of a star with a relative velocity $\boldsymbol{V}$ and with a mass M.

For our purposes it would, however, be sufficient to know the first moment of $\boldsymbol{F}_t$ for given $\boldsymbol{F}$ and v, in which case we shall need only the behavior of $C(\boldsymbol{\rho}, \boldsymbol{\sigma})$ for $|\boldsymbol{\sigma}| \to 0$. It is not difficult to push the formal theory a little further, but without going into these developments here it is clear that in terms of $\overline{\boldsymbol{F}_t}(\boldsymbol{F}_0, v)$ we shall be able to solve the entire problem of the stochastic variation of $\boldsymbol{F}$ acting on a star. More particularly the consideration of the integral

$$\int_0^{\infty} \overline{\boldsymbol{F}_t}(\boldsymbol{F}_0, v)\, dt \tag{45}$$

will not only provide us with the means of giving a precise meaning to the notion of the mean life of $\boldsymbol{F}$ but will also disclose in a direct manner the existence of dynamical friction on the statistical theory. We shall return to the development of the theory along these lines on a later occasion.

4. *General remarks.*—To avoid misunderstandings we shall make some remarks (which are otherwise obvious) concerning the reasons for introducing the new notion of dynamical friction and avoiding the usage of the term "viscosity." First, the physical ideas underlying the concepts of dynamical friction and viscosity are quite distinct: thus, while the "coefficient of dynamical friction" refers to the systematic deceleration which *individual* stars experience during their motion, "viscosity," as commonly understood, refers to the sheering force exerted by one *element of gas* on another. Second, dynamical friction is an exact notion expressing the systematic decelerating effect of the fluctuating field of force acting on a star *in motion*, in contrast to viscosity, which, as a concept, is valid only when averaged over times which are long compared to the time of relaxation of the system and over spatial dimensions which are large compared to the mean free paths of the individual molecules. Thus, while the introduction of dynamical friction in stellar dynamics presents no difficulty, the circumstances are very different for a rational introduction of "viscosity" in the subject (cf. *Stellar Dynamics*, pp. 76–78 and 184).

DYNAMICAL FRICTION

II. THE RATE OF ESCAPE OF STARS FROM CLUSTERS AND THE EVIDENCE FOR THE OPERATION OF DYNAMICAL FRICTION

S. CHANDRASEKHAR
Yerkes Observatory
Received January 7, 1943

ABSTRACT

In this paper a general method is described for determining the rate of escape of stars from galactic and globular clusters which is based on certain general statistical principles. Essentially the method consists in reducing the problem to a boundary-value problem in partial differential equations and in making use of the interpretation of the stochastic process in the velocity space as a diffusion process of a rather general type.

The rate of escape has been evaluated, first, ignoring dynamical friction, and, second, making due allowance for it. It appears that the rate of escape of stars predicted on the first basis is too rapid to be compatible with a life for galactic clusters even of the order of 5×10^8 years. However, the rates of escape are drastically reduced when dynamical friction is allowed for and permits a time scale of the order of 3×10^9 years. It is concluded that in the very existence of galactic clusters like the Pleiades we can look for direct evidence for the operation of dynamical friction which was predicted on theoretical grounds in the preceding paper.

1. *Introduction.*—In the preceding paper[1] we have shown that stars must experience dynamical friction during their motion. This conclusion, first reached on the basis of certain very general considerations, was later confirmed by a more direct analysis of the fluctuating force acting on a star in terms of the two-body approximation for stellar encounters. In this paper we propose to draw attention to certain facts of stellar dynamics which provide direct evidence for the operation of dynamical friction.

Since the coefficient of dynamical friction is of the order of the reciprocal of the time of relaxation of the system (cf. I, eq. [14]), it is evident that it is only during times of the order of the time of relaxation itself that dynamical friction will have a chance to become an effective agent. Consequently, the effects of dynamical friction will be apparent only in stellar systems with relatively short times of relaxation. Such systems are provided by galactic clusters like the Pleiades, which are characterized by times of relaxation of the order of 6×10^7 years.[2] Since the times of relaxation of the galactic clusters are of this order of magnitude, it is clear that an important factor in their evolution must be the escape of stars from them.[3] For, in times of the order of the time of relaxation, the probability that a star will, on account of accidental fluctuations, acquire a velocity equal to or greater than the velocity of escape must be appreciable. And, if this should happen, we can reasonably expect the star to escape from the cluster. The question now arises as to the rate at which stars will thus leave the cluster. In this paper we shall show how this rate can be evaluated on the basis of certain general statistical principles and how

[1] Referred to hereafter as "I."

[2] Cf. S. Chandrasekhar, *Principles of Stellar Dynamics*, chap. v, University of Chicago Press, 1942. This monograph will be referred to hereafter as "*Stellar Dynamics*."

In *Stellar Dynamics* (p. 202) the time of relaxation of the Pleiades is given as 2.9×10^7 years. However, in view of the fact that in a sufficient approximation η^{-1} is equal to *twice* the time of relaxation as defined in *Stellar Dynamics* (cf. the remarks in I following eq. [14]), and since for our present purposes η^{-1} provides a better unit for measuring time, we have quoted in the text a value which is twice that given in *Stellar Dynamics*.

[3] This fact was first clearly recognized by Ambarzumian and Spitzer. For references to these papers and for a general discussion of the related ideas see *Stellar Dynamics*, chap v, §§ 5.2–5.4.

precisely in this rate of escape we can look for evidence for the operation of dynamical friction.

2. *A general method for estimating the rate of escape of stars from galactic and globular clusters.*—In the preceding paper we have shown that, when the diffusion coefficient, q, and the coefficient of dynamical friction, η, are functions of $\boldsymbol{u}$, the equation which governs the distribution $W(\boldsymbol{u}, t)$ of $\boldsymbol{u}$ at time t is

$$\frac{\partial W}{\partial t} = \operatorname{div}_{\boldsymbol{u}} (q \operatorname{grad}_{\boldsymbol{u}} W + \eta W \boldsymbol{u}) , \tag{1}$$

where q and η are further related according to

$$\frac{q}{\eta} = \tfrac{1}{3} \overline{|\boldsymbol{u}|^2} = \text{constant} . \tag{2}$$

This differential equation for W leads to an important interpretation of the stochastic process which takes place in the velocity space. For, according to equation (1), we can visualize the motion of the representative points in the velocity space as a *process of diffusion* in which the rate of flow across an element of surface $d\sigma$ is given by

$$-(q \operatorname{grad}_{\boldsymbol{u}} W + \eta W \boldsymbol{u}) \cdot \mathbf{1}_{d\sigma} d\sigma , \tag{3}$$

where $\mathbf{1}_{d\sigma}$ is a unit vector which is normal to the element of surface considered. With this interpretation of the stochastic process in mind, the following method for finding the rate at which a star may be expected to acquire a given velocity naturally suggests itself.

First, we find the probability, $p(v_0, t)\, dt$, that a star with an initial velocity $|\boldsymbol{u}| = v_0$ will acquire for the *first time* a certain preassigned velocity, $|\boldsymbol{u}| = v_\infty$, say, between t and $t + dt$. We then integrate $p(v_0, t)$ over t from 0 to t, to obtain the total probability, $Q(v_0, t)$, that the star will have acquired the velocity v_∞ during the entire interval from 0 to t. Finally, we average $Q(v_0, t)$ over the relevant range of the initial velocities v_0, to obtain the *expectation*, $Q(t)$, that a star will have acquired the velocity v_∞ during a time t.

The advantage of formulating the problem in the manner described is that the function $p(v_0, t)$ can be determined in terms of a spherically symmetric solution of equation (1) which satisfies the boundary conditions

$$W(|\boldsymbol{u}|, t) = 0 \qquad \text{for} \qquad |\boldsymbol{u}| = v_\infty \text{ for all } t > 0 \tag{4}$$

and

$$W(|\boldsymbol{u}|, t) \to \frac{1}{4\pi v_0^2} \delta(|\boldsymbol{u}| - v_0) \text{ as } t \to 0 , \tag{5}$$

where δ stands for Dirac's δ-function. If W is such a solution, the required probability function $p(v_0, t)$ is given by (cf. the interpretation of eq. [1] in an earlier paragraph)

$$p(v_0, t) = -\left(4\pi q |\boldsymbol{u}|^2 \frac{\partial W(|\boldsymbol{u}|, t)}{\partial |\boldsymbol{u}|}\right)_{|\boldsymbol{u}| = v_\infty} \tag{6}$$

The probability $Q(v_0, t)$ that a star having an initial velocity v_0 will have acquired the velocity v_∞ during a time t is then given by

$$Q(v_0, t) = \int_0^t p(v_0, t)\, dt . \tag{7}$$

And, finally, the expectation $Q(t)$ that a star will have acquired the velocity v_∞ during a time t is given by

$$Q(t) = \int_0^{v_\infty} Q(v_0, t)\, f(v_0)\, dv_0 , \tag{8}$$

where $f(v_0)$ governs the frequency of occurrence of an initial velocity v_0.

Now the coefficient of dynamical friction η, as derived on the basis of the two-body approximation for stellar encounters, is (cf. I, eq. [32] for the case $m_1 = m_2 = m$)

$$\eta = 8\pi N m^2 G^2 \log\left[\frac{D_0\overline{|\boldsymbol{u}|^2}}{2Gm}\right] \frac{1}{|\boldsymbol{u}|^3} \int_0^{|\boldsymbol{u}|} f(v)\, dv . \tag{9}$$

According to this formula, η tends to a constant limiting value as $|\boldsymbol{u}| \to 0$. But, as $|\boldsymbol{u}| \to \infty$, $\eta \to 0$; however, according to the relation (2), q also tends to zero simultaneously with η. Consequently, by allowing q and η to be constants and equal to their respective average values, we shall be compensating for the overestimation of η for large values of $|\boldsymbol{u}|$ by a corresponding overestimation in the diffusion coefficient q. In this paper we shall accordingly restrict ourselves, for the sake of simplicity, to the case where q and η are constants. In a later paper we shall present the results of a similar calculation in which due allowance will be made for the dependence of q and η on $|\boldsymbol{u}|$.

3. *The rate of escape of stars from galactic clusters.*—For the reasons explained toward the end of the last section we shall suppose in this investigation that q and η are both constants and independent of $|\boldsymbol{u}|$. Equation (1) can then be re-written as (cf. eq. [2])

$$\frac{\partial W}{\partial t} = \tfrac{1}{3}\overline{|\boldsymbol{u}|^2}\eta \nabla_{\boldsymbol{u}}^2 W + \eta \operatorname{div}_{\boldsymbol{u}} (W\boldsymbol{u}) . \tag{10}$$

Let

$$\eta t = \tau ; \qquad \boldsymbol{u} = (\tfrac{2}{3}\overline{|\boldsymbol{u}|^2})^{1/2}\boldsymbol{\rho} ; \tag{11}$$

or, in words, τ measures the time in units of the time of relaxation; and, if a Gaussian distribution of the velocities

$$\frac{j^3}{\pi^{3/2}}\, e^{-j^2|\boldsymbol{u}|^2} d\boldsymbol{u} \tag{12}$$

be assumed, $\boldsymbol{\rho}$ measures the velocity $\boldsymbol{u}$ in units of j^{-1}. With the transformation of the variables (11) equation (10) becomes

$$\frac{\partial W}{\partial \tau} = \tfrac{1}{2}\nabla_{\boldsymbol{\rho}}^2 W + \operatorname{div}_{\boldsymbol{\rho}} (W\boldsymbol{\rho}) . \tag{13}$$

It should be noted that in our present choice of the units the diffusion coefficient has the value $\frac{1}{2}$.

For a spherically symmetric solution, equation (12) reduces to

$$\frac{\partial W}{\partial \tau} = \frac{1}{2\rho^2}\frac{\partial}{\partial \rho}\left(\rho^2 \frac{\partial W}{\partial \rho}\right) + \left(3W + \rho \frac{\partial W}{\partial \rho}\right), \tag{14}$$

where we have used ρ to denote $|\boldsymbol{\rho}|$. And, according to our remarks in § 2, we have to seek a solution of equation (14) which satisfies the boundary conditions

$$W(\rho, \tau) = 0 \qquad \text{for} \qquad \rho_0 = \rho_\infty \text{ (say) for } \tau > 0 \tag{15}$$

and

$$W(\rho, \tau) \to \frac{1}{4\pi\rho_0^2}\, \delta(\rho - \rho_0) \text{ as } \tau \to 0 . \tag{16}$$

i) *The rate of escape of stars from clusters when dynamical friction is ignored.*—When dynamical friction is ignored, equation (14) further simplifies to

$$\frac{\partial W}{\partial \tau} = \frac{1}{2\rho^2}\frac{\partial}{\partial \rho}\left(\rho^2 \frac{\partial W}{\partial \rho}\right), \tag{17}$$

and the solution of this equation satisfying the boundary conditions (15) and (16) is[4]

$$W = \frac{1}{2\pi\rho\rho_\infty\rho_0}\sum_{n=1}^{\infty} e^{-n^2\pi^2\tau/2\rho_\infty^2} \sin\left(\frac{n\pi}{\rho_\infty}\rho\right)\sin\left(\frac{n\pi}{\rho_\infty}\rho_0\right). \tag{18}$$

In terms of the foregoing solution we can determine the probability $p(\rho_0, \tau)\, d\tau$ that a star with an initial velocity corresponding to ρ_0 will acquire for the first time a velocity corresponding to ρ_∞ during τ and $\tau + d\tau$. Remembering that in our present units the coefficient of diffusion has the value $\frac{1}{2}$, we have (cf. eq. [6])

$$p(\rho_0, \tau) = -2\pi\rho_\infty^2\left(\frac{\partial W}{\partial \rho}\right)_{\rho=\rho_\infty}; \tag{19}$$

or, using the solution (18), we have

$$p(\rho_0, \tau) = \frac{\pi}{\rho_0\rho_\infty}\sum_{n=1}^{\infty} n(-1)^{n+1} e^{-n^2\pi^2\tau/2\rho_\infty^2} \sin\left(\frac{n\pi}{\rho_\infty}\rho_0\right). \tag{20}$$

The total probability $Q(\rho_0, \tau)$ that the star would have acquired the velocity ρ_∞ during the interval $(0, \tau)$ is therefore given by

$$Q(\rho_0, \tau) = \int_0^\tau p(\rho_0, \tau)\, d\tau = \frac{2\rho_\infty}{\pi\rho_0}\sum_{n=1}^{\infty}\frac{(-1)^{n+1}}{n}\left(1 - e^{-n^2\pi^2\tau/2\rho_\infty^2}\right)\sin\left(\frac{n\pi}{\rho_\infty}\rho_0\right). \tag{21}$$

Finally, to obtain the expectation that an "average" star will have acquired the velocity ρ_∞ in a time τ, we must average the foregoing expression over all ρ_0. For this purpose we shall use for the distribution over ρ_0 the radial Gaussian function

$$\frac{4}{\pi^{1/2}} e^{-\rho_0^2}\rho_0^2 \tag{22}$$[5]

and extend the range of integration from 0 to ∞. Strictly speaking, this is not a valid procedure, particularly the extending of the range of integration beyond ρ_∞. However, for the values of ρ_∞ we shall be normally interested in (cf. eqs. [25] and [26], below), the number of stars with $\rho > \rho_\infty$ forms a negligible fraction of the total number (see, e.g., *Stellar Dynamics*, p. 207, eq. [5.311]). With this understanding, the averaging of $Q(\rho_0, \tau)$ over ρ_0 leads to the formula

$$Q(\tau) = 2\sum_{n=1}^{\infty}(-1)^{n+1}\left(1 - e^{-n^2\pi^2\tau/2\rho_\infty^2}\right) e^{-n^2\pi^2/4\rho_\infty^2}. \tag{23}$$

[4] See, e.g., H. S. Carslaw and J. C. Jaeger, *Operational Methods in Applied Mathematics*, p. 235 (Ex. 16), Oxford, England, 1941.

[5] Remembering that in our present choice of the units $j = 1$.

Now, in a star cluster we have the following relation between the mean square velocity of escape and the mean square velocity of the stars in the system (cf. *ibid.*, pp. 206–207, eqs. [5.306] and [5.311])

$$\overline{v_\infty^2} = 4\overline{|u|^2}\,; \tag{24}$$

or, in our present choice of the units (cf. eq. [11]), we have

$$\overline{\rho_\infty^2} = 6\,. \tag{25}$$

However, in view of the circumstance that a star acquiring a velocity $2(\overline{|u|^2})^{1/2}$ does not necessarily imply its leaving the cluster unless it acquires a somewhat higher velocity (cf. *ibid.*, pp. 208–209), we shall suppose that

$$\rho_\infty^2 = 8\,, \tag{26}$$

to allow a reasonable margin. Table 1 gives the values of $Q(\tau)$ both for $\rho_\infty = \sqrt{6}$ and for $\rho_\infty = \sqrt{8}$.

TABLE 1

THE EXPECTATION $Q(\tau)$ FOR A STAR TO ESCAPE FROM A CLUSTER DURING A TIME τ (MEASURED IN UNITS OF THE TIME OF RELAXATION) WHEN DYNAMICAL FRICTION IS IGNORED

τ	$Q(\tau)$		τ	$Q(\tau)$	
	$\rho_\infty^2 = 6$	$\rho_\infty^2 = 8$		$\rho_\infty^2 = 6$	$\rho_\infty^2 = 8$
0.25	0.069	0.023	2.5	0.82	0.68
0.5	.19	.081	3.0	.87	.77
1.0	.42	.25	4.0	.94	.87
1.5	.60	.43	5.0	0.97	0.93
2.0	0.73	0.57			

Remembering that the time of relaxation of galactic clusters is of the order of 6×10^7 years, an examination of Table 1 reveals that the rates of escape predicted (when dynamical friction is ignored) are far too rapid to be compatible even with lives for these clusters of the order of 3×10^8 years. This can also be seen directly from equation (23). For, according to this equation,

$$Q(\tau) \sim 2e^{-\pi^2/4\rho_\infty^2}\,(1 - e^{-\pi^2\tau/2\rho_\infty^2}) \qquad (\tau \gtrsim 1)\,; \tag{27}$$

or, for $\rho_\infty^2 = 6$, respectively 8, we have the approximate formulae

$$\left.\begin{aligned} Q(\tau) &\sim 1.3\,(1 - e^{-0.82\tau}) \qquad (\rho_\infty^2 = 6)\,, \\ Q(\tau) &\sim 1.5\,(1 - e^{-0.62\tau}) \qquad (\rho_\infty^2 = 8)\,. \end{aligned}\right\} \tag{28}$$

However, as we shall presently see, the rates of escape are drastically reduced from what we have just now found when proper allowance is made for dynamical friction.

ii) *The rate of escape of stars from clusters when allowance is made for dynamical friction.*—Passing now to the case when dynamical friction is not ignored, we have to solve equation (14), together with the boundary conditions (15) and (16). Introducing the variable

$$w = W\rho\,, \tag{29}$$

equation (14) simplifies to

$$\frac{\partial w}{\partial \tau} = \frac{1}{2}\frac{\partial^2 w}{\partial \rho^2} + 2w + \rho\frac{\partial w}{\partial \rho}. \tag{30}$$

The boundary conditions (15) and (16) now become

$$w(\rho, \tau) = 0 \text{ for both } \rho = \rho_\infty \quad \textit{and} \quad \rho = 0 \text{ for all } \tau > 0 \tag{31}$$

and

$$w(\rho, \tau) \to \frac{1}{4\pi\rho_0}\,\delta(\rho - \rho_0) \text{ as } \tau \to 0. \tag{32}$$

We shall now show how the solution of equation (30), together with the boundary conditions (31), can be reduced to a problem in characteristic values.

First we notice that a separation of the variables can be effected by the substitution

$$w = e^{-\lambda\tau}\phi(\rho), \tag{33}$$

where λ is, for the present, an unspecified constant. Equation (30) now leads to the differential equation

$$\frac{d^2\phi}{d\rho^2} + 2\rho\frac{d\phi}{d\rho} + (2\lambda + 4)\phi = 0. \tag{34}$$

Again, writing

$$\phi = e^{-\rho^2/2}\psi, \tag{35}$$

we have for ψ the differential equation

$$\frac{d^2\psi}{d\rho^2} + (2\lambda + 3 - \rho^2)\psi = 0; \tag{36}$$

or, putting

$$\lambda = \mu - 1, \tag{37}$$

we have

$$\frac{d^2\psi}{d\rho^2} + (2\mu + 1 - \rho^2)\psi = 0. \tag{38}$$

It is seen that the differential equation (38) for ψ is the same as the familiar wave equation for a simple harmonic oscillator. However, the boundary conditions with which we have now to solve equation (38) are different from those customary in solving the problem of the simple harmonic oscillator in the quantum theory, for the solution we are now looking for must satisfy the boundary conditions

$$\psi = 0 \quad \text{for} \quad \rho = 0 \quad \text{and also for} \quad \rho = \rho_\infty. \tag{39}$$

In other words, the ψ's of our problem are the characteristic functions of a simple harmonic oscillator bounded at the origin and at $\rho = \rho_\infty$, i.e., an oscillator in a "box." It is, therefore, clear that the ψ's which satisfy the boundary conditions (39) form a complete set of orthogonal functions which can be further normalized.

Let

$$\psi_1, \psi_2, \ldots, \psi_n, \ldots \tag{40}$$

represent the normalized characteristic functions of our problem belonging respectively to the characteristic values

$$\mu_1, \mu_2, \ldots, \mu_n, \ldots \tag{41}$$

The general solution of equation (30) satisfying the boundary conditions (31) can therefore be expressed in the form

$$w = \sum_{n=1}^{\infty} A_n e^{-(\mu_n - 1)\tau} e^{-\rho^2/2} \psi_n(\rho) , \tag{42}$$

where the A_n's are certain constants which should be so chosen that the boundary condition for $\tau = 0$ is satisfied.

Now, since a δ-function can always be built up from any complete set of normalized orthogonal functions according to

$$\delta(\rho - \rho_0) = \sum_{n=1}^{\infty} \psi_n(\rho)\, \psi_n(\rho_0) , \tag{43}$$

it follows that the solution which satisfies the boundary conditions (31) *and* (32) is

$$w = \frac{e^{-(\rho^2 - \rho_0^2)/2}}{4\pi\rho_0} \sum_{n=1}^{\infty} e^{-(\mu_n - 1)\tau} \psi_n(\rho)\, \psi_n(\rho_0) . \tag{44}$$

Thus our solution for W takes the form

$$W = \frac{e^{-(\rho^2 - \rho_0^2)/2}}{4\pi\rho\rho_0} \sum_{n=1}^{\infty} e^{-(\mu_n - 1)\tau} \psi_n(\rho)\, \psi_n(\rho_0) . \tag{45}$$

Using the foregoing solution for W, we find that (cf. eq. [67])

$$p(\rho_0, \tau) = \frac{\rho_\infty}{2\rho_0} e^{-(\rho_\infty^2 - \rho_0^2)/2} \sum_{n=1}^{\infty} e^{-(\mu_n - 1)\tau} \left(-\frac{d\psi_n}{d\rho} \right)_{\rho = \rho_\infty} \psi_n(\rho_0) ; \tag{46}$$

or, for the probability $Q(\rho_0, \tau)$, we have

$$Q(\rho_0, \tau) = \frac{\rho_\infty}{2\rho_0} e^{-(\rho_\infty^2 - \rho_0^2)/2} \sum_{n=1}^{\infty} \frac{1}{\mu_n - 1} \left[1 - e^{-(\mu_n - 1)\tau} \right] \left(-\frac{d\psi_n}{d\rho} \right)_{\rho = \rho_\infty} \psi_n(\rho_0) . \tag{47}$$

Finally, to obtain $Q(\tau)$ we must further average the foregoing expression over the relevant range of ρ_0. With this we have formally solved the problem. To make the solution explicit, it remains only to specify the characteristic functions ψ_n and the corresponding characteristic values μ_n.

The nature of the dependence of the characteristic values μ_n on the length of the "box" ρ_∞ can be obtained by following a procedure developed by Sommerfeld in his studies of the Kepler problem and the problem of the rotator in the quantum theory with "artificial" boundary conditions.[6]

First, it is clear that when

$$\rho_\infty \to \infty , \qquad \mu_n \to n \qquad (n = 1, 3, 5, \ldots) . \tag{48}$$

(Only the odd integral values of n need concern us here, since the wave function has to vanish at the origin.) It is further evident that the functions

$$\Psi_n = e^{-\rho^2/2} H_n(\rho) , \tag{49}$$

where the H_n's are the various Hermite polynomials, formally solve equation (38) with $\mu_n = n$; and, if n is an odd integer, these functions Ψ_n satisfy also the boundary condition

[6] A. Sommerfeld and H. Welker, *Ann. d. Phys.*, **32**, 56, 1938, and A. Sommerfeld and H. Hartmann, *Ann. d. Phys.*, **37**, 333, 1940.

at the origin. If it should now happen that ρ_∞ coincides with a zero of one of the odd Hermite polynomials, then the corresponding wave function ψ_n will satisfy the boundary condition at ρ_∞ as well. Thus,

$$H_3 = 8\rho^3 - 12\rho \tag{50}$$

has a zero at $\rho = (1.5)^{1/2}$. Accordingly, if $\rho_\infty = (1.5)^{1/2}$, $\mu = 3$ is a characteristic value of our problem, and Ψ_3 for $\rho \leqslant (1.5)^{1/2}$ is the characteristic function which belongs to it. This represents, then, a special solution to our problem. Similarly, the higher-order Hermite polynomials will further provide such special solutions. The advantage in obtaining these special solutions is that by plotting the zeros of the various Hermite polynomials in a (μ, ρ_∞) diagram (as in Fig. 1) we obtain at once a general indication of how the various characteristic values are modified by the "artificial" boundary condition at $\rho = \rho_\infty$.

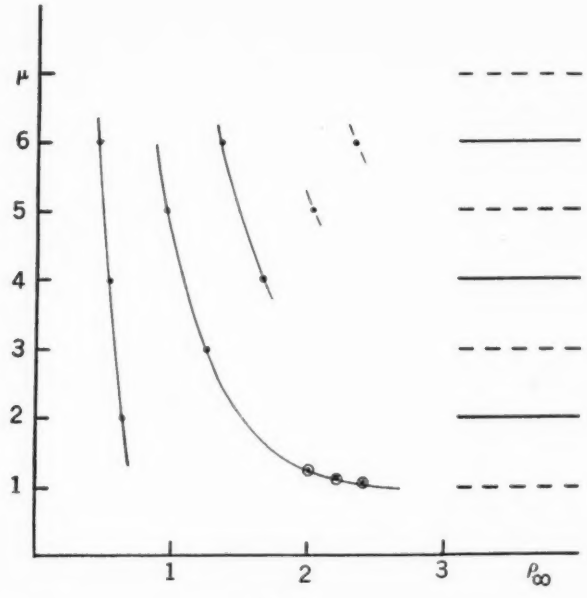

FIG. 1

Now an examination of Figure 1 shows that for $\rho_\infty > 2$ the first characteristic value of our problem must be extremely close to unity, so that $\mu_1 - 1$ must be a very small quantity. On the other hand, the higher characteristic values will lead to values of $(\mu_n - 1) \sim (n - 1)$ $(n > 1$, but an odd integer). Accordingly, for values of τ of the order of unity and greater, the first term in the series on the right-hand side of equation (47) will provide ample accuracy. Thus,

$$\left.\begin{aligned} &Q(\rho_0, \tau) \\ &\simeq \frac{\rho_\infty}{2\rho_0(\mu_1 - 1)}\, e^{-(\rho_\infty^2 - \rho_0^2)/2}\,[1 - e^{-(\mu_1 - 1)\tau}]\left(-\frac{d\psi_1}{d\rho}\right)_{\rho=\rho_\infty} \psi_1(\rho_0) \quad (\tau \gtrsim 1)\,. \end{aligned}\right\} \tag{51}$$

Finally, to determine $(\mu_1 - 1)$ corresponding to the "lowest state" of our artificially limited simple harmonic oscillator, we proceed as follows:

Writing

$$\psi = e^{-\rho^2/2} f \tag{52}$$

in equation (38), we obtain the differential equation

$$\frac{d^2f}{d\rho^2} - 2\rho\frac{df}{d\rho} + 2\mu f = 0 . \tag{53}$$

Substituting for f the series

$$f = \Sigma c_s \rho^s , \tag{54}$$

where s runs through all the odd integers, we obtain the recursion formula

$$c_{s+2} = -\frac{2(\mu - s)}{(s+2)(s+1)} . \tag{55}$$

We already know that the particular characteristic value we are interested in must be very close to unity. Accordingly, writing

$$\mu_1 = 1 + \epsilon \tag{56}$$

and treating ϵ as a small quantity, we find that all the coefficients $c_3, c_5, \ldots$, contain ϵ as a factor. Retaining only the first-order terms in ϵ and letting $c_1 = 1$, we readily find that we can write f in the form

$$f = \rho(1 - \epsilon\chi) , \tag{57}$$

where

$$\chi = \tfrac{1}{3}\rho^2 + \tfrac{1}{15}\rho^4 + \tfrac{4}{315}\rho^6 + \tfrac{2}{945}\rho^8 + \ldots . \tag{58}$$

The condition that f has to vanish at some specified ρ_∞ will determine ϵ. Thus it was found that

$$\left.\begin{aligned} \epsilon &= 0.059 \qquad (\rho_\infty^2 = 6) , \\ \epsilon &= 0.013 \qquad (\rho_\infty^2 = 8) ; \end{aligned}\right\} \tag{59}$$

and, as was expected, ϵ is in fact a very small quantity.

In a first approximation ψ_1 can therefore be written as

$$\psi_1 = \alpha e^{-\rho^2/2}\rho(1 - \epsilon\chi) , \tag{60}$$

where α denotes the normalizing factor, which can be determined numerically in any given case.

Substituting for ψ_1 from equation (60) in equation (51), we obtain

$$\left.\begin{aligned} &Q(\rho_0, \tau) \\ &\simeq \frac{\alpha^2\rho_\infty e^{-\rho_\infty^2}}{2\epsilon}\left[-\frac{d}{d\rho}(\rho - \epsilon\rho\chi)\right]_{\rho=\rho_\infty}[1 - \epsilon\chi(\rho_0)](1 - e^{-\epsilon\tau}) \qquad (\tau \gtrsim 1) . \end{aligned}\right\} \tag{61}$$

It is found that for the cases $\rho_\infty^2 = 6$, respectively 8, the foregoing equation (after averaging over ρ_0) takes the simple numerical forms

$$\left.\begin{aligned} Q(\tau) &\simeq (1 - e^{-0.059\tau}) \qquad (\rho_\infty^2 = 6;\ \tau \gtrsim 1) , \\ Q(\tau) &\simeq (1 - e^{-0.013\tau}) \qquad (\rho_\infty^2 = 8;\ \tau \gtrsim 1) . \end{aligned}\right\} \tag{62}$$

Comparing the formulae (28) and (62), we see that when allowance is made for dynamical friction the mean life of a cluster is increased by factors ranging from 15 ($\rho_\infty \sim 2.5$) to 50 ($\rho_\infty \sim 2.8$). More particularly, the rates of escape given in Table 2 should be compared with those of Table 1.

It is seen that the rates of escape are sufficiently reduced to be compatible with a time scale of the order of 3×10^9 years. Physically, this drastic reduction in the rates of escape

when dynamical friction is allowed for is readily understood, for dynamical friction operates essentially in the direction of preventing a star from being accelerated by too large amounts with any appreciable probability (cf. the remarks in I, § 1), and it is clearly on this account that the probability that a star will acquire the necessary high velocities for escape is so small. Further, it is to be noticed that in the mathematical analysis this reduction is brought about by the small numerical values of $(\mu_1 - 1)$, where μ_1 corresponds to the lowest quantum state of an artificially restricted simple harmonic oscillator; and, as we have seen (cf. Fig. 1) for the values of ρ_∞ which come under discussion, $(\mu_1 - 1)$ is not only a small quantity but it also depends very sensitively on the precise value of ρ_∞ (cf. the values of $[\mu_1 - 1]$ for the cases $\rho_\infty^2 = 6$ and $\rho_\infty^2 = 8$ given in eq. [62]). We may

TABLE 2

THE EXPECTATION $Q(\tau)$ FOR A STAR TO ESCAPE FROM A CLUSTER DURING A TIME τ (MEASURED IN UNITS OF THE TIME OF RELAXATION) WHEN ALLOWANCE IS MADE FOR DYNAMICAL FRICTION

τ	$Q(\tau)$		τ	$Q(\tau)$	
	$\rho_\infty^2 = 6$	$\rho_\infty^2 = 8$		$\rho_\infty^2 = 6$	$\rho_\infty^2 = 8$
5	0.26	0.064	20	0.95	0.23
10	0.44	0.12	100	.....	0.73

therefore conclude that dynamical friction provides exactly the right kind of agency for preventing too rapid a disintegration of an isolated cluster; and thus, in the very existence of galactic clusters like the Pleiades, we can look for evidence not only for the operation of dynamical friction but also for the now generally adopted time scale of the order of 3×10^9 years.

4. *Remarks on further developments.*—Our discussion of the rate of escape of stars from clusters has shown that dynamical friction must be a dominating factor in the dynamics of these systems. The question now arises as to how we can incorporate in a rational system of dynamics the stochastic variations in the velocity which a star suffers on account of the fluctuating force acting on it. It is evident that to build such a system of dynamics what we need is essentially a differential equation which will be appropriate for discussing the probability distribution in *phase space* in contrast to equations of the Fokker-Planck type, which describe the situation only in the velocity space. In other words, we need a proper generalization of Liouville's equation of classical dynamics to include terms corresponding to the stochastic variations in $\boldsymbol{u}$. Such a generalized Liouville equation can be readily found.

Quite generally we may write (cf. I, eq. [6])

$$\left.\begin{aligned} \Delta\boldsymbol{u} &= \boldsymbol{K}\Delta t + \delta\boldsymbol{u}\,(\Delta t) - \eta\boldsymbol{u}\Delta t\,, \\ \Delta\boldsymbol{r} &= \boldsymbol{u}\Delta t\,, \end{aligned}\right\} \tag{63}$$

where $\boldsymbol{K}$ denotes the external force per unit mass acting on a star and the rest of the symbols have the same meanings as in I, § 1. Also, analogous to the integral equation in the velocity space (I, eq. [8]), we now have

$$\left.\begin{aligned} &W(\boldsymbol{r}, \boldsymbol{u}, t+\Delta t) \\ &\quad = \int_{-\infty}^{+\infty}\int_{-\infty}^{+\infty} W(\boldsymbol{r}-\Delta\boldsymbol{r}, \boldsymbol{u}-\Delta\boldsymbol{u}, t)\Psi(\boldsymbol{r}-\Delta\boldsymbol{r}, \boldsymbol{u}-\Delta\boldsymbol{u}; \Delta\boldsymbol{r}, \Delta\boldsymbol{u})\,d(\Delta\boldsymbol{r})\,d(\Delta\boldsymbol{u})\,, \end{aligned}\right\} \tag{64}$$

where $\Psi(\boldsymbol{r}, \boldsymbol{u}; \Delta\boldsymbol{r}, \Delta\boldsymbol{u})$ denotes the transition probability in the phase space. We have (cf. I, eq. [9])

$$\left.\begin{aligned}\Psi(\boldsymbol{r}, \boldsymbol{u}; \Delta\boldsymbol{r}, \Delta\boldsymbol{u}) = \frac{1}{(4\pi q\Delta t)^{3/2}}\, e^{-|\Delta\boldsymbol{u}-\operatorname{grad}_{\boldsymbol{u}} q\Delta t+\eta\boldsymbol{u}\Delta t-\boldsymbol{K}\Delta t|^2/4q\Delta t} \\ \times \delta(\Delta x - u_x\Delta t)\, \delta(\Delta y - u_y\Delta t)\, \delta(\Delta z - u_z\Delta t)\,.\end{aligned}\right\} \tag{65}$$

Expanding the various terms in equation (64) in the form of Taylor series and proceeding as in usual deviation of the Fokker-Planck equation, we obtain[7]

$$\frac{\partial W}{\partial t} + \boldsymbol{u}\cdot\operatorname{grad}_{\boldsymbol{r}} W + \boldsymbol{K}\cdot\operatorname{grad}_{\boldsymbol{u}} W = \operatorname{div}_{\boldsymbol{u}}\,(q\operatorname{grad}_{\boldsymbol{u}} W + \eta W\boldsymbol{u})\,. \tag{66}$$

In the foregoing equation q and η can be functions of $\boldsymbol{r}$ and $\boldsymbol{u}$; they should, however, be related according to

$$\frac{q}{\eta} = \tfrac{1}{3}\overline{|\boldsymbol{u}|^2} \tag{67}$$

at all points of the phase space.

Equation (66) is the required generalization of Liouville's equation of classical dynamics, and it is on the basis of this equation that the dynamics of the galactic and the globular clusters should be developed. We shall return to these further developments on a future occasion.

[7] For details of the derivation see a forthcoming article by the writer in the *Reviews of Modern Physics*.

NOTES

NOTE ON ALGOL

In a recent article Kopal[1] attempts to explain discrepancies in the observed rotation effect of Algol by assuming that the primary's rotation axis makes an angle of about 15° with the perpendicular to the orbital plane and that it precesses in a period of about 3.6 years. He appears to have overlooked the fact that if such a precession takes place, the fundamental plane of reference will be an invariable plane of the system and that the orbital plane itself must then also regress on this invariable plane. This question has been treated before by Shajn,[2] who considered it as nodal regression of the orbital plane on the plane of the primary's equator, and it has been fully discussed by the writer;[3] no reference to either of these papers is made by Kopal. If m_1 and m_2 and r_1 and r_2 are masses and radii, respectively, of the components of the eclipsing system, a the radius of the orbit, ω the angular velocity of rotation and revolution, assumed to be synchronous (it is also assumed that the primary and secondary rotate as rigid bodies with no change in angular velocity with decreasing distance from the center), and k a constant depending upon the internal constitution of the stars, then the values for the angular momenta are

$$\text{Orbital } \Omega_0 = \frac{m_1 m_2}{m_1 + m_2}\, a^2\omega\,,$$

$$\text{Primary's Rotational } \Omega_1 = \tfrac{2}{5} m_1 \left(\frac{r_1}{a}\right)^2 k_1 a^2\omega\,,$$

$$\text{Secondary's Rotational } \Omega_2 = \tfrac{2}{5} m_2 \left(\frac{r_2}{a}\right)^2 k_2 a^2\omega\,.$$

Using the numerical values derived by Kopal, viz., $m_1 = 2.3$, $m_2 = 0.61$, $r_1/a = 0.22$, and $r_2/a = 0.246$ and adopting $k = 0.3$, a reasonable value, we obtain: $\Omega_0 = 0.48\ a^2\omega$, $\Omega_1 = 0.015\ a^2\omega$, and $\Omega_2 = 0.005\ a^2\omega$. If, therefore, the rotation axis of the primary makes an angle of 15° with the perpendicular to the invariable plane, then the orbital plane will possess an inclination of the order of half a degree relative to this invariable plane, and the *observed* inclination should fluctuate by this amount on either side of the mean value. If the mean inclination is 82°.1, the extreme values should be 81°.6 and 82°.6; the area of the primary occulted during primary minimum should then range from 0.65 to 0.70, and a difference of fully 0.1 mag. may be expected in the depth of primary minimum. Kopal claims a period of 3.6 years for the precessional motion but finds perfect agreement between the photoelectric curves of Stebbins and Smart. The mean dates of observation for these two series of observations are 1919.9 and 1935.3, respectively—too far apart to enable us to draw any definite conclusions. It seems evident, however, that the same conclusion which I stated previously is justified, viz., that if precession and nodal regression take place, it would seem most profitable to look for their effects in precise observations of the depth of primary minimum rather than in spectroscopic observations of rotational velocities.

W. J. Luyten

[1] *Ap. J.*, **96**, 399, 1942.

[2] *Ap. J.*, **57**, 129, 1923.

[3] *Zs. f. Ap.*, **15**, 97, 1938.

NOTES ON PROPER-MOTION STARS. V*

ABSTRACT

Two new white dwarfs, as well as six new binaries with large proper motion, are announced; for three known binaries large parallaxes are found.

The first two stars in Table 1 are new white dwarfs. The northerly star is of the 40 Eridani type, to which 25 white dwarfs were previously known to belong.[1] The other object was found by Luyten[2] to share the motion of BD−0°4234. Two spectra of low dispersion show it to be very blue; the spectrum may be continuous although it is possible that H and K are weakly present. The classification on the basis of these preliminary observations is therefore either *Con* or *wF*.[1] The primary, BD−0°4234, was found to be $9^m.7$ K2, making the spectral parallax of the system about $0''.023$. The resulting absolute magnitude of the companion, about $10^m.5$, is somewhat puzzling. The relative position was measured with the micrometer: 1942.66 29°.6 $133''.86$ 1*n*.

TABLE 1

Star	α (1900) δ	*m*(v)	Sp.	μ	θ	*p* (Sp.)	Remarks
AC 73°8031	21^h27^m +73° 12′	12.5	wA	$0''.32$	172°	.....	
−0°4234 B	21 27.0 − 0 13	13.7	Con:	0.46	89	(23)	$134''$, 30°
Karpov 9A	0 18.4 + 9 14	12.9	M1	0.37	207	22	
Karpov 9B		14.0	M3	.....	.....	22	$4''.0$, 148°
−12°2918AB	9 26.5 −13 03	10.2	M4	0.75	92	130	$0''.60$, 59°
Furuhj. 31 A	11 05.8 +43 58	11.6	M4	0.75	234	91	
Furuhj. 31 B		11.9	M3+	.....	.....	66	$4''$, 70°
−15°5584 A	20 07.8 −15 44	8.7	K1	0.44	232	32	
−15°5584 B		13.5:	M2	.....	.....	22:	$9''$, 347°
−19°5899 A	20 37.2 −19 18	10.4	M1	1.10	144	69	$2''$, 240°, $14^m.0$
−17°6769(A)	23 27.6 −17 23	8.7	K6	0.37	126	72	
−17°6768(BC)	23 27.6 −17 22	10.6	M4	0.40	125	100	Close, $\Delta m=0$
LDS 65A	1 57.7 −27.03	13.1	M6	0.30	147	110	$3''$, 60°
LDS 65B		13.4	M6	0.30	147		
LDS 78A	2 41.3 −44 09	12.2	M5+	0.37	168	180	$43''$, 60°
LDS 78B		12.5	M6+	0.37	168		
+19°5116A	23 26.7 +19 23	10.3	M4	0.52	89	180	$3''.6$, 180°
+19°5116B		12.8	M6+	0.52	89		

Of the binaries, BD−12°2918 is of special interest. Because of the poor agreement between the spectral parallax and the trigonometric parallax it had been concluded[3] that the star might be an unresolved binary. This conclusion has now been confirmed, though the discrepancy between the parallaxes has not been fully removed. On previous occasions the star was found to be "round," so that the orbit is probably eccentric and the period less than ten years.

For Furuhjelm 31 the corrected position was given by Vyssotsky,[4] who found the

* *Contributions from the McDonald Observatory, University of Texas*, No. 67. Earlier notes: *Ap. J.*, **96**, 315, 1942, and references there given.

[1] *Pub. A.S.P.*, **53**, 248, 1941; *Ap. J.*, **96**, 315, 1942.

[2] *Pub. Astr. Obs. Minnesota*, **3**, No. 3, 1941. [3] *Ap. J.*, **95**, 206 (n. 92), 1942. [4] *Ap. J.*, **97**, 77, 1943.

spectral type dM2. BD−17°6768 was found to be a close pair at the Lick Observatory in 1934 ($d = \frac{3}{4}''$, $\Delta m = 0.0$). The star became of interest when Luyten[2] found it to have common proper motion with BD−17°6769. Recent micrometer observations show the orbital motion to be rapid. All three objects just mentioned promise to be of importance for the mass-luminosity relation; a fourth star, −19°5899, may prove to be too difficult for that purpose.

Two more objects for which mass determinations may be expected are LDS 65 and +19°5116; the latter star was found to be double by Wirtanen.[5] Photographic observations of these two pairs and of Furuhjelm 31 will be of interest.

One doubtful pair included in an earlier list,[6] CoD−34°4160, at 7^h54^m9 −34°41′ (1900) is now regarded as optical, as shown by additional observations. Two doubtful pairs in Russell and Moore's General Catalogue of Dynamical Parallaxes,[7] ADS 466 and 2818, are also optical; the spectral types of the two companions are gM5 and G2, respectively.

G. P. KUIPER

YERKES OBSERVATORY
March 1943

REVIEWS

Nicholas Copernicus, 1543–1943. By STEPHEN P. MIZWA. New York: Kosciuszko Foundation, 1943. Pp. 88. $0.75.

The Kosciuszko Foundation of New York, whose main objective during the last three years has been "to help preserve the brains of Poland by helping Polish scholars to survive," has issued this brochure with an appeal to American colleges and universities to organize this spring an appropriate celebration or tribute to Copernicus on the occasion of the quadricentennial of his death and of the publication of the *De revolutionibus orbium coelestium*. Mr. Mizwa has contributed two chapters: "The Life-Story of Copernicus" and "Sarmaticus Astronomus." While they contain no essentially new information and present the astronomical work of Copernicus in the most elementary terms, they are interesting because of the large number of little-known illustrations, including a photograph of the copy of a self-portrait of Copernicus made by Tobias Stimmer in 1571 on the astronomical clock tower of the cathedral of Strasbourg. The cover design is a modern painting of Copernicus, reproduced in color, by the well-known refugee Polish artist, Arthur Szyk.

Because the purpose of the book is to create interest in the Copernicus quadricentennial, it is appropriate to record that Mr. Mizwa has approached with moderation and dignity the puzzling and controversial question of the nationality of Copernicus' ancestors. He points out that "Copernicus lived in an age when there was no clear-cut conception of nationality in the modern sense and loyalties and patriotism—in contradistinction to universal intellectual interests—were chiefly local . . . ."; and he answers the question "Why are the Poles proud of Copernicus?" by saying that "he was born and raised on the soil they love . . . . , he received his first instruction and inspiration . . . . in the University of Krakow . . . . " and he "fought that enemy which they had been fighting for centuries before and have been fighting all these centuries since."

However, not all passages are equally moderate. Thus, it sounds strange when, in defense of the church which, according to the author, "overlooked the revolutionary importance of *De revolutionibus* and did not put it on the *Index* till 1616," he says: "It should however be observed here, to the credit of his Church, that although it was slower in accepting the Copernican system as established scientific truth, it neither persecuted its creator nor exposed him to ridicule."

Astronomers will welcome the initiative of the Kosciuszko Foundation in organizing a national celebration for Copernicus in New York on May 24, 1943, under the chairmanship of Professor Harlow Shapley. The name of Copernicus—whom two nations claim as their own but who, perhaps better than any other personality, illustrates the universality of science which "recognizes no political boundaries, pays no attention to nationalities"—is a symbol of a better world than the one we are living in.

O. STRUVE

[5] *Pub. A.S.P.*, **53**, 340, 1941. [6] *Ap. J.*, **96**, 315, 1942.

[7] *The Masses of the Stars* ("Astrophysical Monographs"), 1940.